



SOLUTION AND SOLID-STATE STUDIES OF
SOME BLEACHABLE SEMI-CONDUCTING PHOTOGRAPHIC DYES

by

DOUGLAS JAMES EDWARDS

A THESIS

presented for the degree of

DOCTOR OF PHILOSOPHY

in the Faculty of Science

UNIVERSITY OF LONDON

Bedford College, London

March, 1987

ProQuest Number: 10098968

All rights reserved

INFORMATION TO ALL USERS

The quality of this reproduction is dependent upon the quality of the copy submitted.

In the unlikely event that the author did not send a complete manuscript and there are missing pages, these will be noted. Also, if material had to be removed, a note will indicate the deletion.



ProQuest 10098968

Published by ProQuest LLC(2016). Copyright of the Dissertation is held by the Author.

All rights reserved.

This work is protected against unauthorized copying under Title 17, United States Code.
Microform Edition © ProQuest LLC.

ProQuest LLC
789 East Eisenhower Parkway
P.O. Box 1346
Ann Arbor, MI 48106-1346

ACKNOWLEDGEMENTS

I would like to thank a number of people, they include:

The Science and Engineering Research Council for the CASE Studentship.

My supervisor Dr. M.C. Grossel for his guidance, enthusiasm and friendship.

Professor A.K. Cheetham and Dr. M.M. Eddy, Chemical Crystallography, Oxford University, for their help and patience with me while working within their research group at Oxford.

Professor R.M. Hill and Dr. C. Pickup, Solid State Physics, Chelsea College, University of London, whom, like Chem. Chryst found it difficult to get rid of me.

Dr. T.C. Webb, Dr. S.R. Postle and Dr. W.E. Long, Ilford Ltd., for their ideas, expertise and the job.

Dr. R. Bolton, Bedford College, University of London for always being willing to talk chemistry.

Mrs. D. Storey for the typing.

ABSTRACT

A number of monomeric and oligomeric hydroxypyridone mono- and poly-methine bridged oxonol and merocyanine dyes have been prepared and their solution and solid-state properties have been investigated.

One particular and commercially important feature of the solution chemistry of the oxonol dyes is the reaction with sulphite ion leading to bleaching of the dye. The mechanism of this process has not previously been investigated. A detailed kinetic and spectroscopic study supports the previously proposed mechanism in which the nucleophile adds to the methine bridge in a Michael-type fashion. The reaction intermediates have been detected spectroscopically for several nucleophiles but in general are too unstable to be isolated.

Oxonol and merocyanine dyes readily undergo molecular aggregation in both solution and the solid-state. One previous X-ray diffraction analysis of an oxonol dye has been carried out which revealed that the anions formed planar molecular stacks. Such an arrangement is well suited to intermolecular charge transfer and hence electronic conduction. The main objective of the current work has been to investigate how this stacking might be influenced by variation of substituents and counter-ions with a view to modifying the conduction properties. X-ray structure studies reveal that variation of the cation leads to three different types of solid-state structure: herringbone; uniform; and dimeric. The electrical properties have been investigated in detail by d.c. conductivity and a.c. dielectric spectroscopy measurements. They suggest that in general, the simple hydroxypyridone trimethine oxonols are

semi-insulating ($10^{-8} < \sigma < 10^{-12} \Omega^{-1} \text{ cm}^{-1}$) though some exceptions have been found. Any observable d.c. conduction is essentially ionic in nature. The merocyanines and pentamethine oxonols are semi-conducting ($10^{-4} < \sigma < 10^{-8} \Omega^{-1} \text{ cm}^{-1}$) as a consequence of added electronic contributions to the conduction mechanism. The most highly conducting oxonol salt, containing the tetrathiafulvalene (TTF) radical cation has a d.c. conductivity, $\sigma \simeq 10^{-3} \Omega^{-1} \text{ cm}^{-1}$ (compacted powder, room temperature). In this case electronic conduction dominates.

CONTENTS

	Page No
CHAPTER 1 Bleachable Dye Photography	
1.1 Bleachable Dyes	14
1.2 Dye Aggregation	22
1.3 Aims and Objectives (Photographically)	24
CHAPTER 2 Syntheses	
2.1 Preparation of Hydroxypyridones	26
2.1.1 Preparation of cyanoacetamides	
2.1.2 Conversion of cyanoacetamides to hydroxy- pyridones	
2.1.3 Preparation of potentially polymerisable hydroxypyridones	
2.2 Intermediates for the Synthesis of Unsymmetrical (Merocyanine) Dyes	29
2.3 An Intermediate in the Preparation of a Radical- Cation Oxonol Dye	30
2.4 Preparation of Dyes	31
2.4.1 Preparation of symmetrical hydroxypyridone methine bridged oxonols	
2.4.2 Preparation of unsymmetrical hydroxypyridone methine bridged oxonols and merocyanines	
2.4.3 Preparation of cationic hydroxypyridone methine bridged oxonols	
CHAPTER 3 Polymeric Dye Systems as Bleachable Antihalation Underlayers	
3.1 Introduction	37
3.2 Chain-Growth Polymerisation	38
3.2.1 Hydroxypyridone oxonol salts of polymerisable cation	
3.2.2 Polymerisable hydroxypyridone methine bridged oxonol anions	
3.3 Step-Growth Polymerisation	44

	Page No.
CHAPTER 4 The Bleaching Reaction	
4.1 Introduction	50
4.2 Sulphite Bleaching	55
4.2.1 Kinetic studies	
4.2.2 N.M.R. studies	
4.3 Other Nucleophiles	64
4.3.1 Qua \ itative studies	
4.3.2 N.M.R. studies	
4.4 Trapping a Bleached Adduct	68
 CHAPTER 5 Electrical Properties of Semi-insulating and Semiconducting Materials	
5.1 Basic Classification	71
5.2 Band Theory	71
5.2.1 Metals	
5.2.2 Insulators	
5.2.3 Intrinsic semiconductors	
5.2.4 Extrinsic semiconductors	
5.3 Distribution of Electrons and Holes in Energy States	77
5.3.1 The Fermi-Dirac distribution function	
5.3.2 Density of energy states	
5.3.3 Intrinsic semiconductor	
5.4 Conduction Mechanisms in Insulating Materials	85
5.4.1 Ionic conduction	
5.4.2 Space charge limited conduction	
5.4.3 Impurity conduction	
5.4.4 Tunnelling	
5.4.5 Schottky Effect	
5.4.6 Poole-Frenkel conduction	
5.5 Organic Semiconductors to Organic Metals	88
5.6 Aims and Objectives (Electrically)	101

	Page No.
CHAPTER 6	Structural Studies in the Solid State
6.1	X-ray Crystal Structure Analyses 104
6.1.1	Introduction
6.1.2	The structure of tetraphenylphosphonium 1-ethyl-3-cyano-6-hydroxy-4-methyl pyrid-2-one trimethine oxonol
6.1.3	The structure of tetrabutylammonium, 1-ethyl- 3-cyano-6-hydroxy-4-methyl pyrid-2-one trimethine oxonol
6.1.4	The structure of dimethylammonium ethyl methacrylate 1-ethyl-3-cyano-6-hydroxy-4- methyl pyrid-2-one trimethine oxonol
6.1.5	Other investigations
6.1.6	Conclusions
6.2	Solid State N.M.R. Spectroscopic Studies 140
6.2.1	Introduction
6.2.2	The Spectra
CHAPTER 7	Electrochemical Investigations: The Design of a Radical Cation Dye Complex
7.1	Introduction 145
7.2	The Electrochemistry of tetrathiafulvalene, TTF 146
7.3	The Electrochemistry of Selection of Oxonol Dye Salts 147
7.4	The Preparation of a TTF-Oxonol Dye Complex 150
7.5	Conclusions 153
CHAPTER 8	D.C. Conductivity and Dielectric Spectroscopic Measurements
8.1	D.C. Conductivity 155
8.2	Dielectric Spectroscopy 155
8.3	The Measurements 157

	Page No.
8.4 Class I Type Material	158
8.4.1 HPT 288	
8.4.2 HPT 299	
8.4.3 HPT 261 and HPT 324	
8.4.4 HPT 289	
8.4.5 HPT 338	
8.4.6 MI 1579	
8.5 Class II Type Material	175
8.6 Class III Type Material	185
8.7 Class IV Type Material	186
8.8 Class V Type Material	194
8.9 Conclusions	194
 CHAPTER 9	
Conclusions	201
 CHAPTER 10	
Experimental	
10.1 Syntheses	206
10.1.1 Instrumentation	
10.1.2 Aluminium isopropoxide	
10.1.3 α -methyl-(m-nitrobenzyl)alcohol	
10.1.4 M-Nitrostyrene	
10.1.5 M-Aminostyrene	
10.1.6 Cyanoacetamide	
10.1.7 <u>N</u> -Ethyl cyanoacetamide	
10.1.8 <u>N</u> -Butyl cyanoacetamide	
10.1.9 <u>N</u> -Phenyl cyanoacetamide	
10.1.10 <u>N</u> -(p-Tolyl)cyanoacetamide	
10.1.11 <u>N</u> -(p-Anisyl)cyanoacetamide	
10.1.12 <u>N,N'</u> -Dicyanoacetyl-1,3-diaminopropane	
10.1.13 <u>N,N'</u> -Dicyanoacetyl-1,4-diaminobutane	
10.1.14 <u>N,N'</u> -Dicyanoacetyl-1,6-diaminohexane	
10.1.15 3-Cyano-2,6-dihydroxy-4-methyl pyridine	
10.1.16 1-Ethyl -3-cyano-6-hydroxy-4-methyl pyrid-2-one	

- 10.1.17 1-Butyl-3-cyano-6-hydroxy-4-methyl
pyrid-2-one
- 10.1.18 1-Phenyl-3-cyano-6-hydroxy-4-methyl
pyrid-2-one
- 10.1.19 1-(p-Tolyl)-3-cyano-6-hydroxy-4-
methyl pyrid-1-one
- 10.1.20 1-(p-Anisyl)-3-cyano-6-hydroxy-4-methyl
pyrid-2-one
- 10.1.21 1-(Dimethylaminopropyl)-3-cyano-6-hydroxy-
4-methyl pyrid-2-one
- 10.1.22 1-Methyl-3-cyano-6-hydroxy-4-methyl
pyrid-2-one
- 10.1.23 1-Hexyl-3-cyano-6-hydroxy-4-methyl
pyrid-2-one
- 10.1.24 1-Ethyl-3-amido-6-hydroxy-4-methyl
pyrid-2-one
- 10.1.25 N,N'-Trimethylene-bis-(3-cyano-6-
hydroxy-4-methyl pyrid-2-one)
- 10.1.26 N,N'-Tetramethylene-bis-(3-cyano-6-
hydroxy-4-methyl pyrid-2-one)
- 10.1.27 N,N'-Hexamethylene-bis-(3-cyano-6-
hydroxy-4-methyl pyrid-2-one)
- 10.1.28 β -Anilinoacrolein anil hydrochloride
- 10.1.29 3-(3'-Acetanilidoallylidiene)-1-ethyl-
4-methyl-5-cyano pyrid-2,6-dione
- 10.1.30 N-(2,4-Dinitrophenyl)pyridinium chloride
- 10.1.31 Glutaconic dialdehyde dianil hydrochloride
- 10.1.32 2-Methyl-3-ethyl benzothiasolium iodide

- 10.1.33 1-Ethyl-2-methyl- β -naphthothiasolium tosylate
- 10.1.34 Ethylene bis-(triphenylphosphonium)bromide
- 10.1.35 Allyl triphenylphosphonium bromide
- 10.1.36 Dibenzotetrathiafulvalene
- 10.1.37 HPM 1/HPT 338
- 10.1.38 HPT 302
- 10.1.39 HPT 339
- 10.1.40 HPT 326
- 10.1.41 HPT 340
- 10.1.42 HPT 261
- 10.1.43 HPT 336
- 10.1.44 HPT 335
- 10.1.45 HPT 334
- 10.1.46 MI 1579
- 10.1.47 HPT 288
- 10.1.48 HPT 289
- 10.1.49 HPT 297
- 10.1.50 HPT 299
- 10.1.51 HPT 327
- 10.1.52 HPT 328
- 10.1.53 HPT 324
- 10.1.54 HPT 314
- 10.1.55 HPT 298
- 10.1.56 HPT 309
- 10.1.57 HPT 182
- 10.1.58 HPT 308
- 10.1.59 HPT 179

	Page No.
10.1.60 HPT	282
10.1.61 HPT	330
10.1.62 HPT	331
10.1.63 HPT	325
10.1.64 HPP	337
10.1.65 HPP	323
10.1.66 HPP	322
10.1.67 HPP	321
10.1.68 HPP	320
10.1.69 HPT	319
10.2 Polymeric Dye Systems as Bleachable Antihalation Underlayers	248
10.2.1 Instrumentation	
10.2.2. Chain-growth polymerisation: Hydroxy pyridone oxonol salts of polymerisable cation	
10.2.3 Step-growth polymerisation	
10.3 The Bleaching Reaction	253
10.3.1 Instrumentation	
10.3.2 Kinetic studies of sulphite bleaching	
10.3.3 Qua\ itative studies	
10.3.4 N.M.R. Studies	
10.3.5 Trapping a bleached adduct	
10.4 Structural Studies on the Solid State	256
10.4.1 X-Ray crystal structure analyses	
10.4.1.1 Instrumentation	
10.4.1.2 The structure of tetraphenyl- phosphonium 1-ethyl-3-cyano-6- hydroxy-4-methyl pyrid-2-one trimethine oxonol	

	Page No.	
10.4.1.3	The structure of tetrabutylammonium 1-ethyl-3-cyano-6-hydroxy-4-methyl pyrid-2-one trimethine oxonol	
10.4.1.4	The structure of dimethylammonium ethyl methacrylate 1-ethyl-3-cyano-6-hydroxy-4-methyl pyrid-2-one trimethine oxonol	
10.4.1.5	<u>N</u> -Methyl morpholinium 1-butyl- 3-cyano-6-hydroxy-4-methyl pyrid-2-one trimethine oxonol	
10.4.1.6	Methyl triphenylphosphonium 1-ethyl-3-cyano-6-hydroxy-4-methyl pyrid-2-one trimethine oxonol	
10.4.2	Solid state N.M.R. spectroscopic studies	
10.5	Electrochemical Investigations:	262
	The Design of a Radical Cation-Dye Complex	
10.5.1	Instrumentation	
10.5.2	Experimental	
10.5.3	The preparation of the TTF-oxonol dye complex	
10.6	D.C. Conductivity and Dielectric Spectroscopic Measurements	264
10.6.1	Sample preparation	
10.6.2	Low temperature measurements	
10.6.3	High temperature measurements	
	10.6.4.1 Instrumentation	
	10.6.4.2 Experimental	
10.6.5	Dielectric measurements	
	10.6.5.1 Instrumentation	
	10.6.5.2 Experimental	

	Page No.	
APPENDIX 1A	X-Ray Structure Determination	
1.1	The CAD4-F Diffractometer	270
1.2	Data Reduction	272
1.3	Fourier Synthesis	273
1.4	The Patterson Function and the Heavy Atom Method	275
1.5	Direct Methods	276
1.6	Completion of the Structure	277
APPENDIX 1B	X-Ray Structure Data	
1.1	The Isotropic Temperature Factors for the Hydrogen Atoms of I(b)	278
1.2	Structure Factors for I(b)	279
1.3	Structure Factors for I(c)	291
1.4	Structure Factors for I(d)	301
APPENDIX 2	Dielectrics	
2.1	Basic Definitions	308
2.2	Time Dependent Dielectric Behaviour	311
2.3	Frequency Dependent Dielectric Behaviour	314
2.4	Time Dependence of Relaxation	317
2.5	Low Frequency Dispersion	320
2.6	Dielectrics of Semiconductrs (DSS)	323
REFERENCES		325

CHAPTER 1

Bleachable Dye Photography

1.1 Bleachable Dyes^{1,2}.

A bleachable dye, in the photographic sense, may be broadly defined as a dyestuff component of a photographic assembly (film, paper, etc.) which is not present in the final version of that assembly, having been removed during one of the processing stages. It does not, therefore, refer to dyes formed during chromogenic development to give colour prints, etc., and also by convention it does not refer to dyestuffs added to sensitise silver halide crystals to light. A simplified picture of a typical photographic assembly, is a colour negative film, shown in figure 1.1. This shows seven basic layers (A-G) and a film base (H). The backing layer (I) is not present in a colour

A	Non-stress and u.v. absorber
B	Blue-sensitive emulsion
C	Yellow filter layer
D	Green-sensitive emulsion
E	Magenta filter layer
F	Red-sensitive emulsion
G	Underlayer
H	Base
I	Backing layer

Figure 1.1

negative film but has been included for the sake of completeness; the use of such a layer will be described shortly. Layer (A) is a mechanically protective coating and may also contain an ultraviolet light absorber. Since all silver halide crystals are activated by ultraviolet light a u.v. absorber is incorporated to prevent incorrect colour rendition (for example, it is essential that the red-sensitive layer should be excited only by red light). Layer (B) is an emulsion sensitive to blue light ($\lambda = 400 - 500 \text{ nm}$). As it is desirable that no blue light reaches the other emulsion layers, layer (C) is inserted. This layer is a yellow filter layer and this absorbs blue light, blue and yellow being complementary colours. Below this are a green-sensitive emulsion (D) ($\lambda = 500 - 600 \text{ nm}$) and associated green-absorbing layer (E), followed by a red-sensitive emulsion (F) ($\lambda = 600 - 700 \text{ nm}$) and an underlayer (G). This latter absorbs all the light that negotiates regions (A) to (F) without absorption. Layer (I) is only present in certain films (microfilms and X-ray films) and performs the same function as layer (G). It may also serve to balance the load of gelatin on either side of the base, thus keeping the film flat (a particular problem in X-ray films).

Bleachable dyes find their uses in the filter layers (C), (E), (G) and (I), all of which require coloured components that must be absent in the final picture. However, unlike the dyes of layers (B) to (F), the dyes of layers (G) and (I) have to cover a much wider range of the visible spectrum, indeed they must cover the whole range to which the film is sensitive.

Probably the main use of dyes in underlayers and backing layers is as antihalation agents. Halation is a phenomenon resulting from reflection of unabsorbed light from the gelatin/base or base/air

interfaces. This results in activation of a number of silver halide crystals, figure 1.2. The result is a foggy edge around what might have

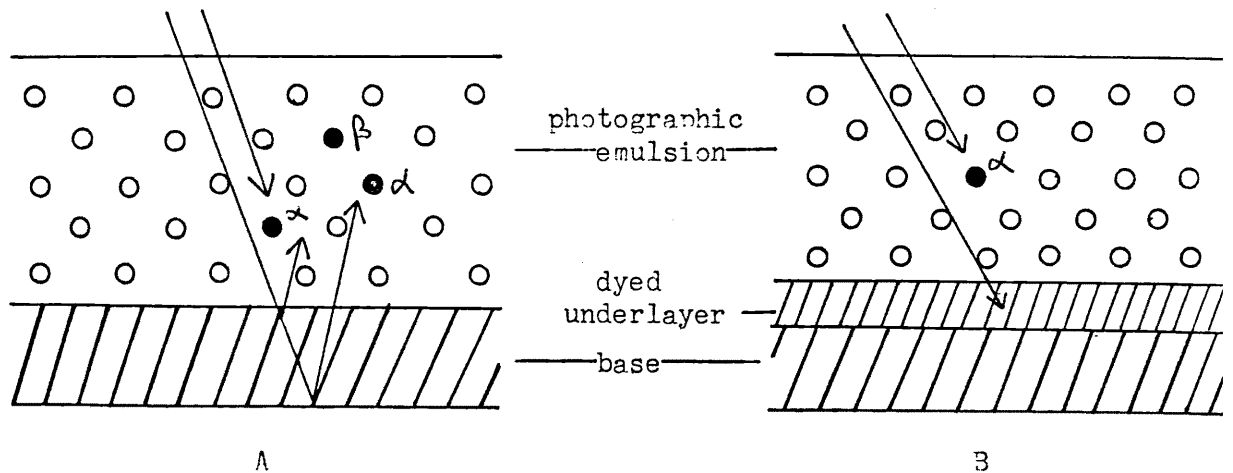


Figure 1.2

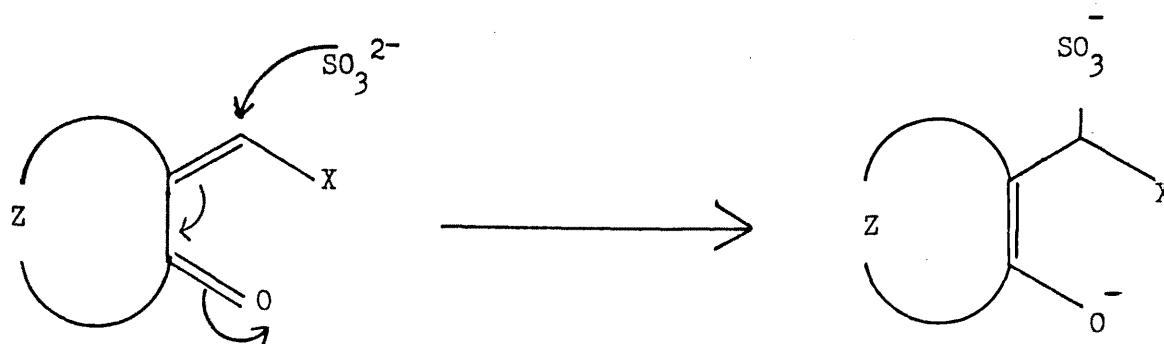
been a sharply defined image, a halo. In (A) light is absorbed directly by silver halide crystal α to give a latent image. Light from the same image source that fails to hit a silver halide crystal reaches the base and may be reflected from either surface, thus activating crystals β and γ . In (B) a dyed underlayer prevents all reflections and a sharper image α is obtained. It can be seen that a backing layer would perform the same function as an underlayer, but less efficiently as now only light that reaches the far side of the base will be absorbed.

It is also possible to eliminate halation by uniformly distributing a dye (known as an acutance dye) throughout the emulsion layer. A disadvantage of this is that light which would normally have reached a silver halide crystal may be absorbed before it finds its target, with the result that a longer exposure is required. Acutance

dyes, to their credit, increase the definition of an image by eliminating the light scattered by the individual silver halide crystals.

One cannot, at random, select a dye from the Colour Index and insert it into a photographic assembly and assume perfect performance. Bleachable dyes must be compatible with all the other components and processes occurring in a photographic assembly. Thus a bleachable dye should not sensitise or desensitise an emulsion. This rules out many cationic dyes. Strictly speaking, an acutance dye has a desensitising effect on the film as a whole, but not specifically on the halide crystals. The dyes should be removable at some point between the end of exposure and the end of processing i.e. the dyes should be "bleachable". As a first approximation, most water-soluble dyes can be used as photographic antihalation dyes, as they, in theory, wash out during aqueous processing. In practice they do not wash out completely, leaving delicately tinted stains, and they turn the processing solutions highly coloured. In practice, therefore, dye destruction is used to complement, or even supplant, dye desorption.

In the majority of cases it is the sulphite of the developer which destroys the bleachable dye, although mechanistic details have, up until now, been lacking. Since the majority of bleachable dyes contain an α,β -unsaturated carbonyl centre, Scheme 1.1, this is available for Michael-type attack, and consequently the chromophore is broken and the leuco-dye is made more water soluble.



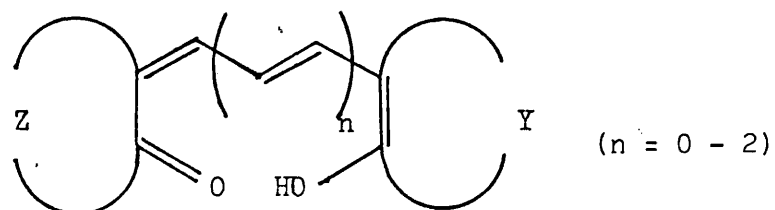
Scheme 1.1

What is not known is the part played by other nucleophiles in the processing brews. The developer often contains thiol-containing moieties which, were they to be present in large enough concentrations, might also add in Michael-type fashion. Hydroxylamine, ethylenediamine and hydrazine are other nucleophiles sometimes present. The fixer consists largely of thiosulphate ion, itself a good, soft nucleophile.

A bleachable dye must also be 'substantive', that is, the dye should stay where it is put. For an acutance dye this means everywhere in the film, and this means that a freely gelatin-soluble (effectively, water soluble) dye can be used, assisting also the bleaching phase. For a filter or antihalation dye, the requirement of layer-specificity (substantivity) is more severe. A first approach to layer-specificity treats the gelatin as a 3-D array of inert strands and designs a dye which is bulky enough to be caught in this "fishing net". This works very well but a dye too bulky to bleed from the gelatin layer in which it is put is often also too bulky to wash out during processing and can regenerate later. It is most difficult to obtain dyes of exactly the right bulk to be layer specific, yet to bleach completely, and other methods of achieving substantivity have been devised. Dyes bristling

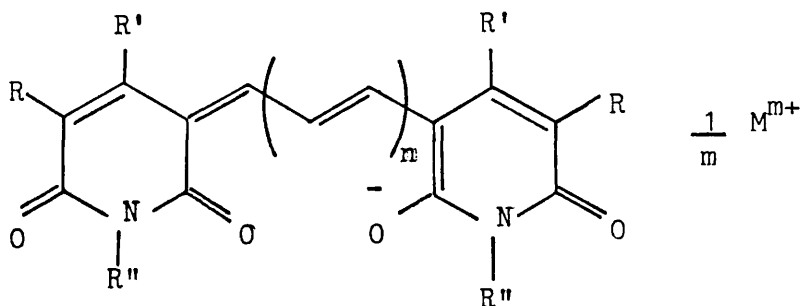
Bleachable dyes used today in photography fall largely into four classes.

(a) Oxonols (1). The dye may be present as a salt, usually



(1)

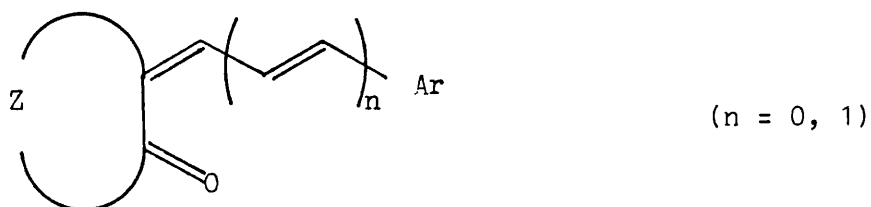
both z and y represent heterocyclic rings, frequently z = y. In the main, the oxonols form the subject of this research project, the hydroxypyridone methine bridged oxonols (2) being of particular interest, where *M* = metallic



(2)

or organometallic cation, $R = \text{CN}, \text{CONH}_2, \text{H}$; $R' = \text{H}, \text{Me}, \text{NH}_2, \text{OH}, \text{CO}_2\text{H}$; $R'' = \text{H}, \text{alkyl}, \text{aryl}$.

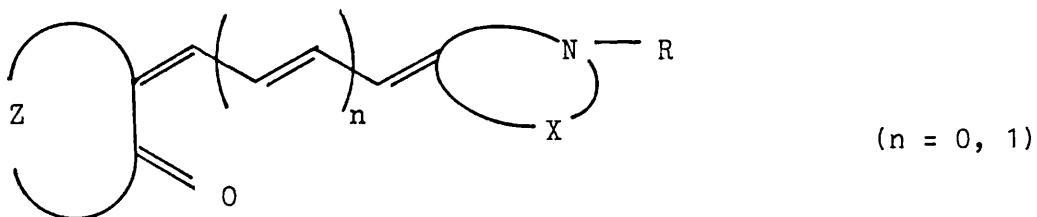
(b) Benzylidene and Cinnamylidenes (3). $Z = \text{heterocyclic}$,



(3)

Ar = NR_2 or a nitrogen containing heterocycle, e.g. 3-indolyl.

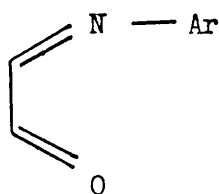
(c) Merocyanines (4). $X, z = \text{heterocyclic rings}$, the first



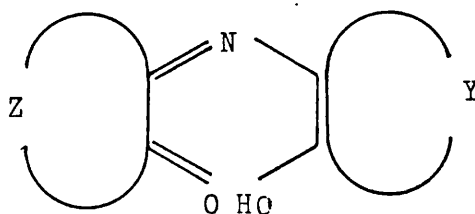
(4)

dye in Scheme 1.2 is an example.

(d) Azamethines (5).



azamethine



azamethine oxonol

(5)

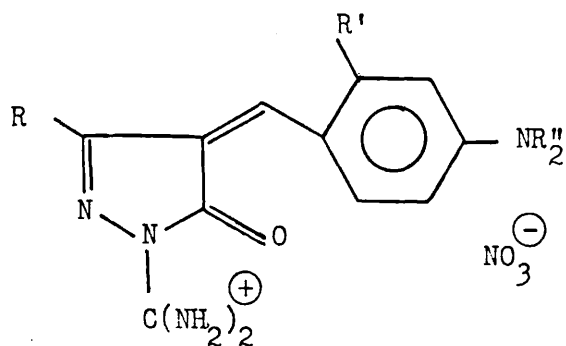
1.2 Dye Aggregation

Most dyes, when present in a concentrated form (solution, coating in gelatin, solid state⁴) form aggregates. Interactions take place between the electron-rich portions of the dye (the chromophoric system) and these lead to electronic transitions which result in new absorption maxima in the visible region. Aggregation may lead to dimers, trimers or oligomers in solution and is, of course, most prevalent in the solid state, in this case, the aggregation is of a different sort⁵. The subject has been well treated for dyes in general^{4,6} including the cyanine dyes used in photography^{7,8}. Polarography^{6,9} has thrown much light on the mode of aggregation, as has X-ray crystallography^{4,8}.

Little, however, is known about the aggregation of bleachable dyes. Bleachable dyes readily form aggregates in solution and in gelatin coatings. This can accelerate to the point of precipitation in the coatings and their visible spectra show D and H-bands corresponding to aggregation. Electronic transitions corresponding to aggregate formation may also be induced by dyes stacked correctly onto polymeric mordant backbones⁶, a phenomenon known as metachromasy.

The advantages of aggregation are twofold in bleachable dyes, provided that it can be controlled. Firstly, the fact that new absorption maxima are obtained means that one dye now covers a rather greater portion of the visible spectrum and secondly, the aggregates formed are inevitably so bulky that they are caught in the gelatin "fishing net" yet revert to leuco-monomers during bleaching.

Amidinium pyrazolones (6) aggregate strongly in concentrated solution or gelatin coating.



(6)

For example, the dye ($R = \text{Me}$, $R' = \text{OCH}_2\text{CO}_2\text{Et}$, $R'' = \text{Et}$) in aqueous solution gives three new species, figure 1.3¹. The monomer (dotted line)

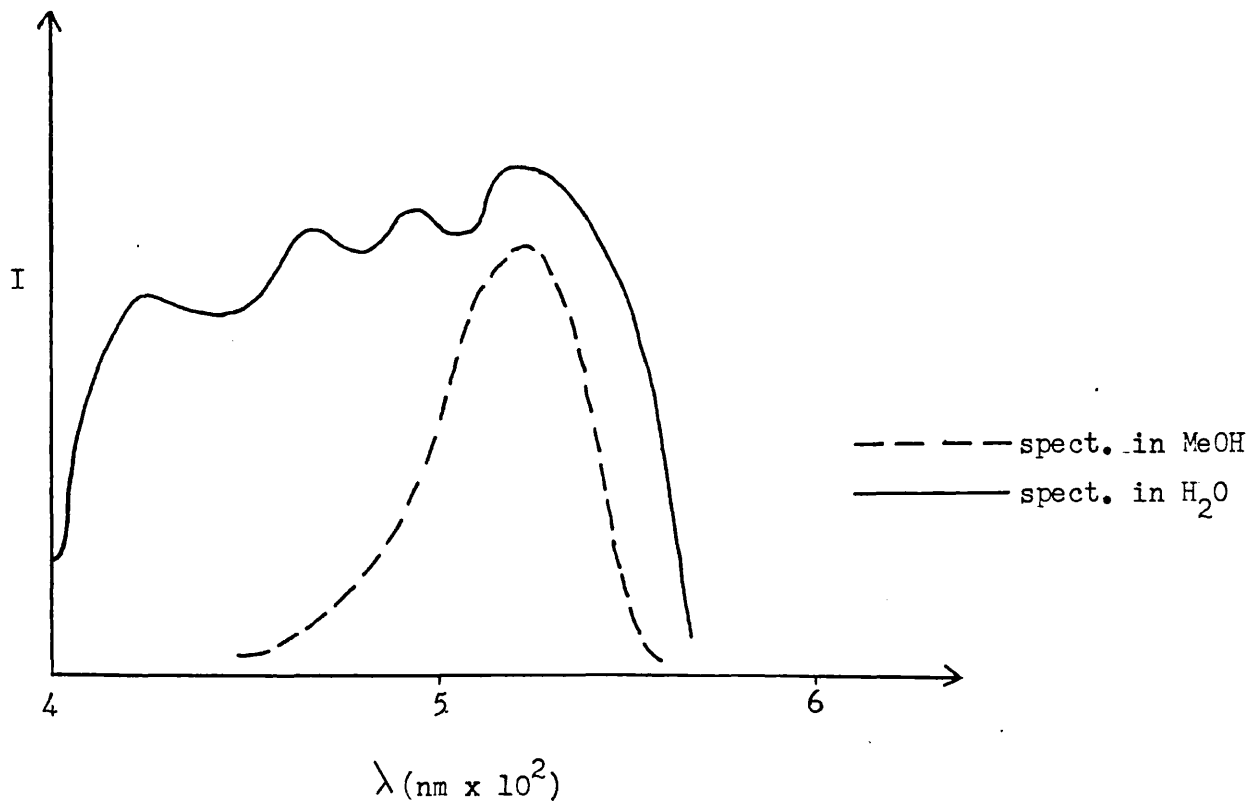


Figure 1.3

has $\lambda_{\max} = 510$ nm and the oligomers (solid lines) at ca. 490 nm, 470 nm and 430 nm. The aggregation of these dyes is influenced by R, R' and R". When R' = H and R" = Me, aggregate peaks occur thus: ca. 475 nm (R = Me), ca. 430 nm and 480 nm (R = P_rⁿ), ca. 455 nm (R = Ph), but for R = Bu^t only the monomer is seen. Hydrophobic interactions are thus seen to be of great significance. The imidinium residue is important, too, for replacing it either by H-, Ph-, -CONH₂ or -C(NHMe)₂⁺ leads to non-aggregating dyes. Furthermore, the anion also affects the aggregate species. Replacement of NO₃⁻ by Cl⁻, for example, gives stronger aggregates and, in the dye of figure 1.3, each aggregate peak may, in turn, be removed by increasing concentrations of anionic wetting agent, and is different for sulphate and sulphonate-type wetting agents. The water content of gelatin coatings is yet a further factor to be considered.

Pigments are the ultimate form of dye aggregates, and a pigment of a water-insoluble dye will, of course, be layer-specific. It has been found that certain bleachable dye types, when used as pigments and possessing base-soluble or "hydrophilicising" groups (e.g. hydroxyl) bleach rapidly enough to be of value. Hydroxypyridone trimethine oxonols are of great interest as pigments and aggregated species.

1.3 Aims and Objectives (Photographically)

(a) To investigate the development of new anti-halation underlayer dye systems. This would take a variety of forms and is the subject of chapter 3.

(b) To make a comprehensive study of the bleaching reaction, being not only concerned with sulphite bleaching but also studying the effects of a whole range of other nucleophiles. This would involve investigation by ^{13}C , ^1H n.m.r. and visible spectroscopy. Attempts would also be made to isolate the bleached adducts. This investigation forms the subject of chapter 4.

(c) To study aggregate formation by concentration - dependent solution spectroscopy. For a wide range of dyes examples can be drawn and a study of H-band appearance with increasing concentration made, again using ^{13}C , ^1H n.m.r. and visible spectroscopy.

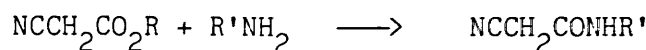
CHAPTER 2

Syntheses

2.1. Preparation of Hydroxypyridones

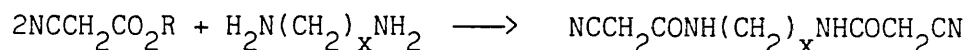
2.1.1. Preparation of cyanoacetamides

In general cyanoacetamides are readily prepared by treatment of an ester of cyanoacetic acid with an amine (Scheme 2.1). In a similar manner



(Scheme 2.1)

bis-amides can be prepared (Scheme 2.2) and these are useful intermediates to oligomeric dyes (see Chapter 3). The basic procedure of Carson, Scott

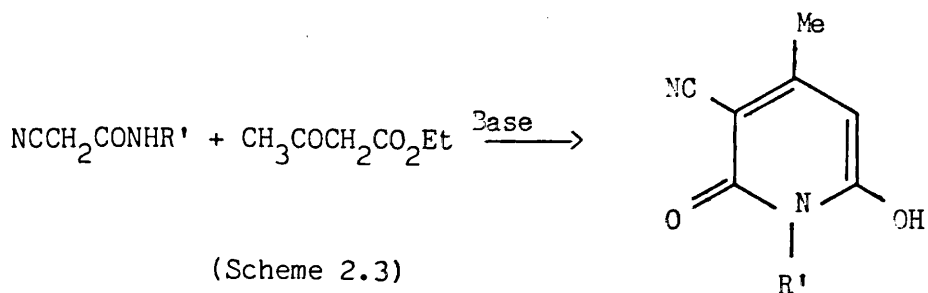


(Scheme 2.2)

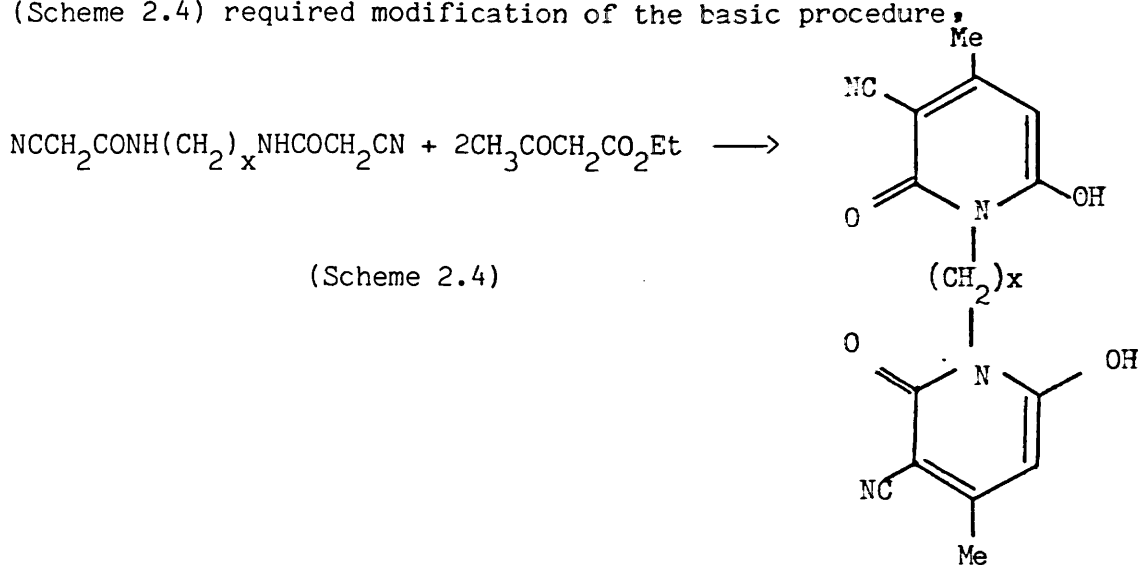
and Vose¹⁰ used (where R' = H, Me, Et) was modified for the preparation of more complex amides (where R' = aryl, styryl; and bis-cyanoacetamides).

2.1.2. Conversion of cyanoacetamides to hydroxypyridones

The procedure followed for the preparation of simple hydroxypyridones (where R' = H, Me, Et) was that of Bobbitt and Scola¹¹ who had investigated the preparation and reactions of 4-methyl-3-substituted pyridines. This involved condensation of the cyanoacetamides with ethyl acetoacetate (Scheme 2.3). The synthesis of more complex



hydroxypyridones (where R' = aryl, styryl) and bis-hydroxypyridones (Scheme 2.4) required modification of the basic procedure,

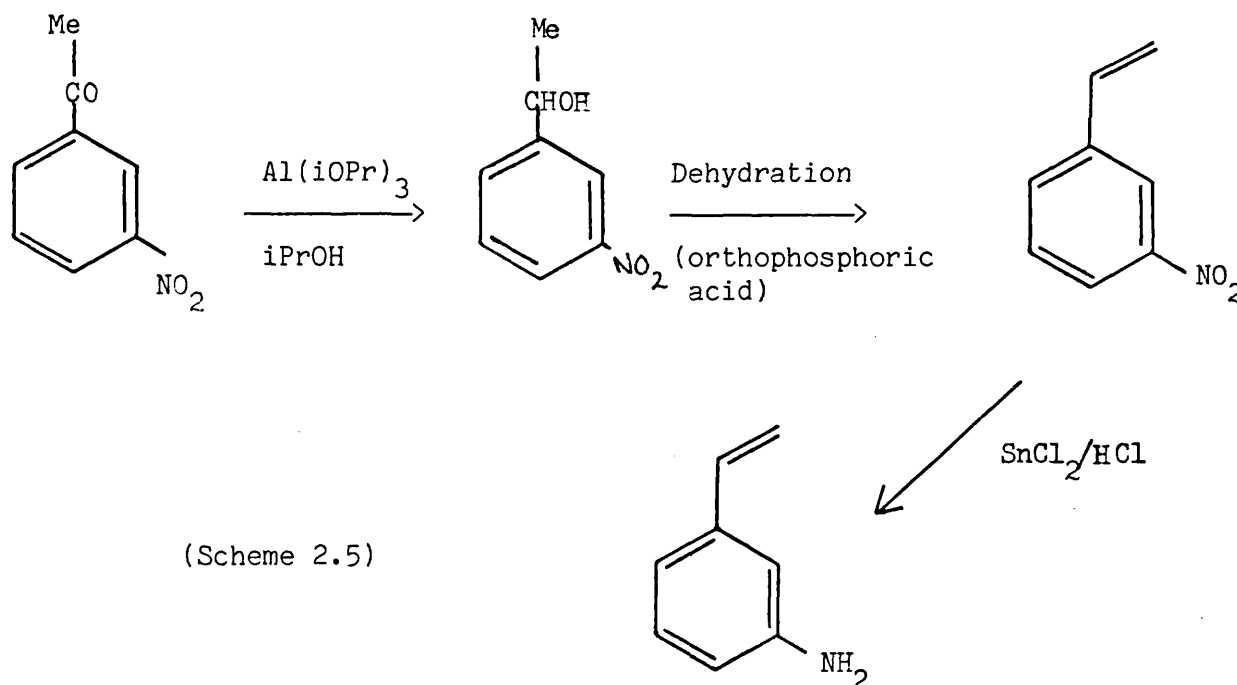


usually involving change of solvent, base (e.g. OH^- , MeO^- , NH_3), mole ratios or reaction time. Hydroxypyridones can also be prepared without isolation of the cyanoacetamide but, in general, we have preferred to purify the synthetic intermediates.

2.1.3. Preparation of potentially polymerisable hydroxypyridones

One important objective of the synthetic work was the preparation of oxonol dyes attached to a polymer chain. Several approaches to this problem were investigated (see Chapter 3). One of these required the synthesis of a hydroxypyridone having an N-styryl substituent. The synthetic approach chosen required the preparation of *m*-aminostyrene

(Scheme 2.5) which could then be converted to its cyanoacetamide and thence to the hydroxypyridone. α -Methyl-(*m*-nitrobenzyl) alcohol was

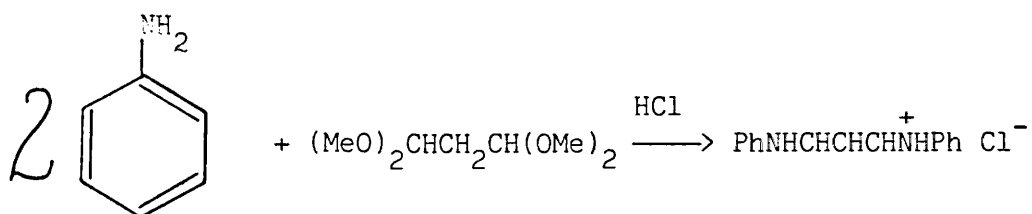


prepared by the method of Lund¹² using the Meerwein-Ponndorf-Verley reduction of *m*-nitroacetophenone. This alcohol was then dehydrated with *o*-phosphoric acid, which is now the method of choice for such dehydrations¹³. The *m*-nitrostyrene so obtained was cleanly reduced to *m*-aminostyrene using stannous chloride and concentrated hydrochloric acid¹⁴.

The conversion of the amine to amide proved to be a difficult process. Meanwhile other more convenient routes to oligomeric oxonol dyes were discovered and time did not permit the further investigation of the syntheses of *N*-styryl oxonol dye salts.

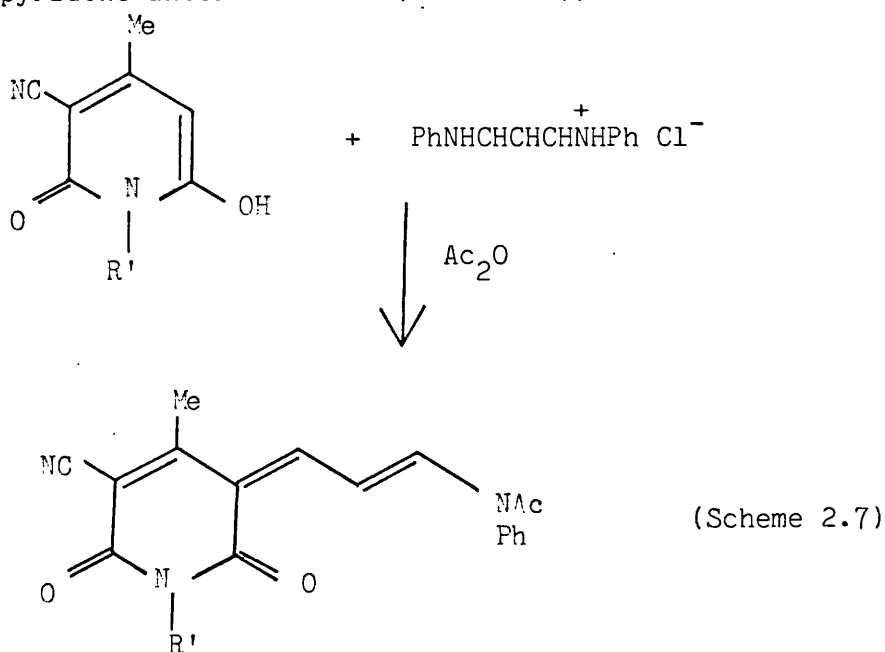
2.2 Intermediates for the synthesis of unsymmetrical (merocyanine) dyes

The standard routes to the symmetrical hydroxypyridone methine bridged oxonols (2.4.1) do not permit efficient preparation of unsymmetrical structures and a step-wise reaction sequence has been devised to circumvent this problem. β -Anilinoacrolein anil hydrochloride which is readily prepared by reaction of two molar equivalents of aniline with 1,1',3,3'-tetramethoxypropane in the presence of concentrated hydrochloric acid¹⁵ (Scheme 2.6) reacts with a hydroxypyridone in the



(Scheme 2.6)

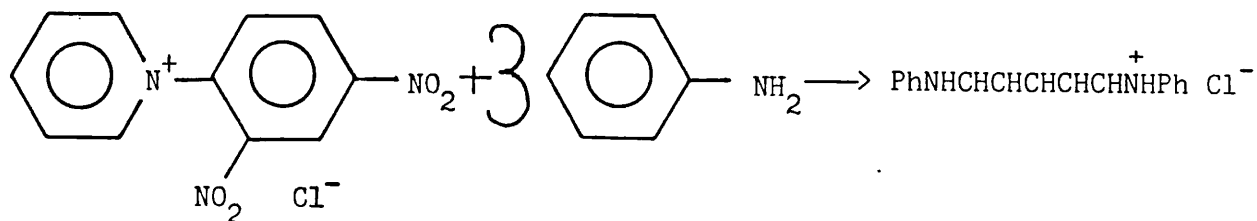
presence of acetic anhydride to form an 3-(3'-acetanilidoallylidiene) hydroxypyridone intermediate¹⁶ (Scheme 2.7) which can be isolated.



(Scheme 2.7)

When this is treated with an active methylene compound, for example, a different hydroxypyridone molecule or a 2-methyl benzothiazolium salt, an unsymmetrical dye is obtained (Scheme 2.11).

Dyes containing an extra bridging double bond may be prepared in a similar manner using glutaconic dialdehyde dianil hydrochloride. This intermediate is derived by reaction of *N*-(2,4-dinitrophenyl) pyridinium chloride with three molar equivalents of aniline¹⁷ (Scheme 2.8) and its

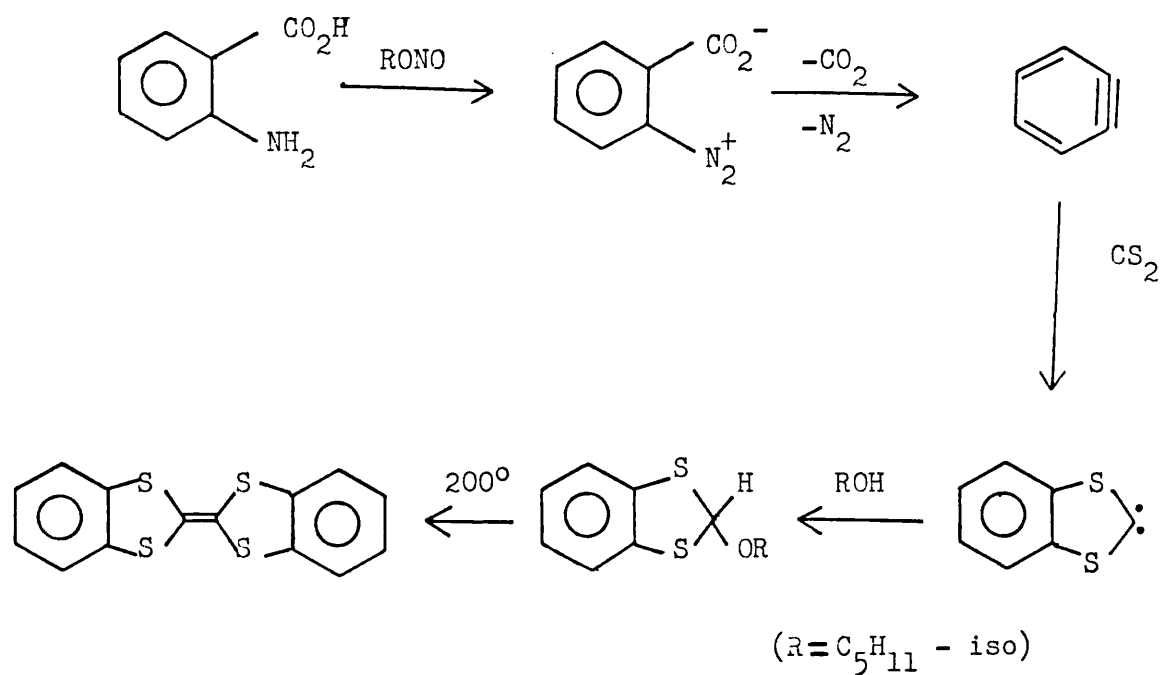


(Scheme 2.8)

subsequent reaction with a hydroxypyridone yields the penta-methine bridged intermediate¹⁶. Glucaconic dialdehyde dianil hydrochloride is also used for the preparation of symmetrical penta-methine bridged oxonol dyes (2.4.1).

2.3. An intermediate in the preparation of a radical-cation oxonol dye

The aprotic diazotisation of anthranilic acid by isopentyl nitrite in the presence of carbon disulphide and isopentyl alcohol in boiling 1,2-dichloroethane yielded 2-isopentoxy-1,3-benzodithiole. Thermal decomposition of the benzodithiole at 200^o produced dibenzotetrathiafulvalene¹⁸ (Scheme 2.9).



2.4. Preparation of dyes

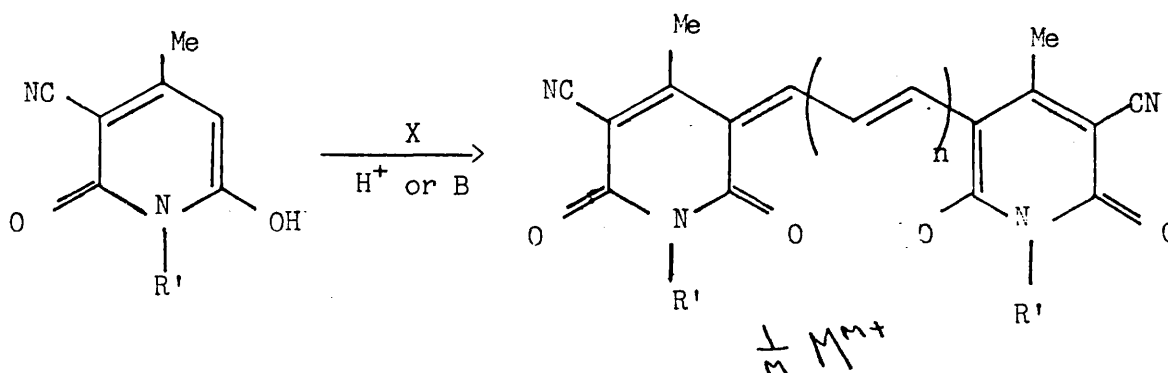
Five general classes of dye have been prepared:

- (a) symmetrical hydroxypyridone mono-, tri-, and penta- methine bridged oxonols;
- (b) unsymmetrical hydroxypyridone methine bridged oxonols and merocyanines;
- (c) cationic hydroxypyridone methine bridged oxonols;
- (d) polymeric and polymerisable hydroxypyridone methine bridged oxonols;
- (e) radical-cation hydroxypyridone methine bridged oxonol salts.

Dyes of type (d) and (e) form the subjects of Chapters 3 and 7, respectively, and hence are not covered here.

2.4.1. Preparation of symmetrical hydroxypyridone methine bridged oxonols¹⁹

The general synthetic route to these materials involves condensation of two moles of hydroxypyridone with one mole of coupling agent in the presence of a base or salt (usually an acetate or halide). For monomethine bridged oxonol salts triethylorthoformate is the coupling agent. For the trimethine analogues 1,1'3,3'-tetramethoxypropane is used and for the pentamethine dyes glutaconic dialdehyde dianil hydrochloride is present. (Scheme 2.10).



(m = 1-4)

- n = 0 X = (EtO)₃CH
- n = 1 X = (MeO)₂CHCH₂CH(OMe)₂
- n = 2 X = PhNHCHCHCHCHNHPH Cl⁻

(Scheme 2.10)

Table 2.1 lists the hydroxypyridone methine bridged oxonols prepared by this method.

Table 2.1.

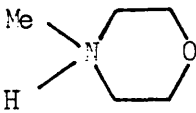
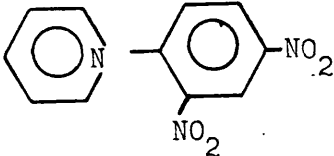
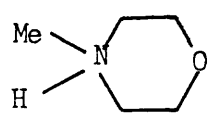
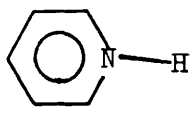
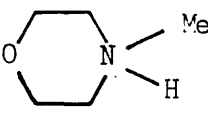
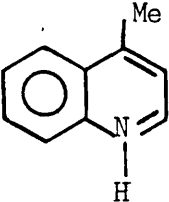
X	R'	M	m
$(\text{EtO})_3\text{CH}$	Et	Et_3NH	1
$(\text{MeO})_2\text{CHCH}_2\text{CH}(\text{OMe})_2$	H	Ca	2
"	Me	Bu_4N	1
"	"	Et_4N	1
"	"	Ph_3MeP	1
"	Et	Ca	2
"	"	Co	2
"	"	Ni	2
"	"	Al	3
"	"	Ag	1
"	"	Et_3NH	1
"	"	Ph_4P	1
"	"	$\text{Ph}_3\text{PCH}_2\text{CH}_2\text{PPh}_3$	2
"	"	$\text{H}_2\text{C}=\text{CHCH}_2\text{PPh}_3$	1
"	"	Bu_4N	1
"	"		1
"	"		1

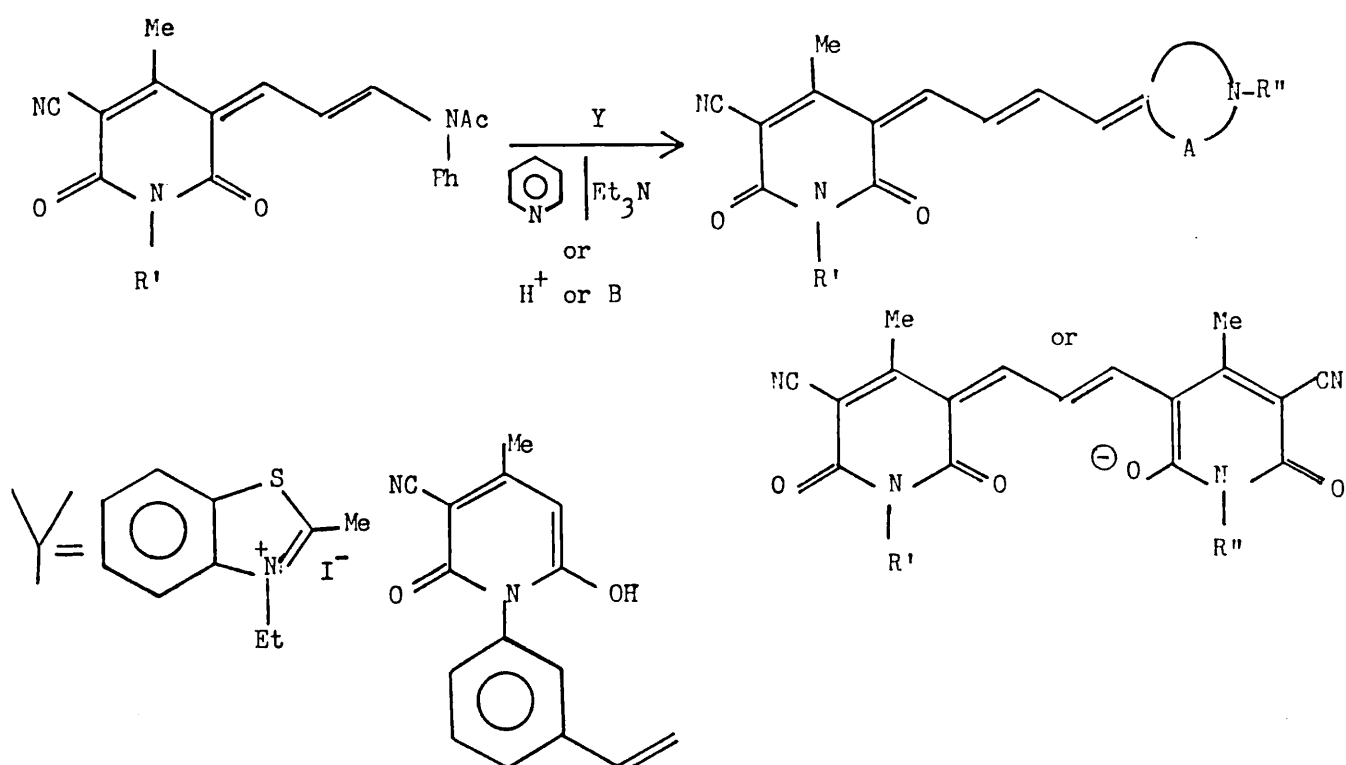
Table 2.1 (continued)

X	R'	M	m
"	"	$\text{H}_2\text{C} = \overset{\text{Me}}{\underset{ }{\text{C}}} - \overset{\text{O}}{\parallel}{\text{C}} - \text{OCH}_2\text{CH}_2\overset{\text{H}}{\underset{ }{\text{N}}}\text{Me}_2$	
"	Bu ⁿ	H	1
"	"	Na	1
"	"	Li	1
"	"		1
"	"	Bu ₄ N	1
"	Hex ⁿ	Bu ₄ N	1
"	Phenyl	H	1
"	Tolyl	Ca	2
"	Anisyl	Ca	2
PhNHCHCHCHCHCHNHPH C ⁻	Et	Et ₃ NH	1
"	"		1
"	"		1
"	"		1

The dye parent acid is obtained from reaction of hydroxypyridone and, for example, 1,1',3,3'-tetramethoxypropane in the presence of acetic acid.

2.4.2. Preparation of unsymmetrical hydroxypyridone methine bridged oxonols and merocyanines.²⁰

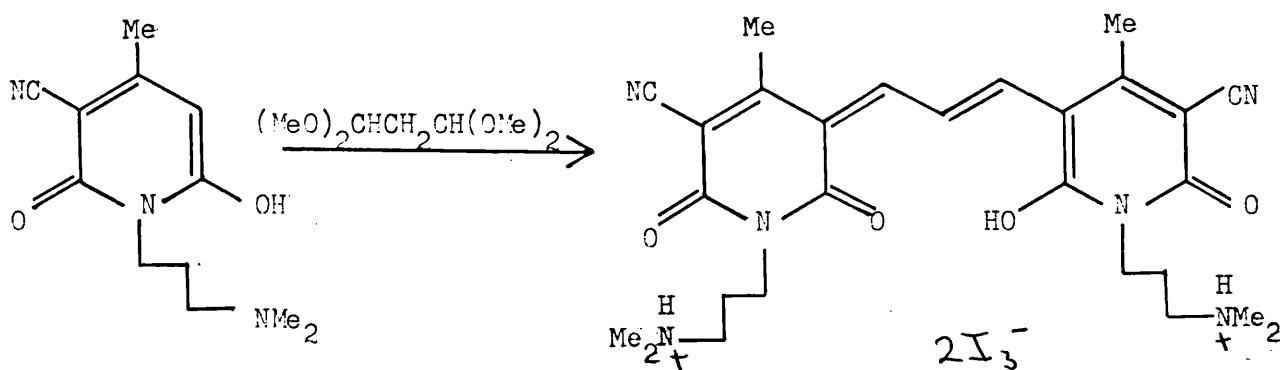
These materials are prepared by the treatment of 3-(3'-acetanilido-allyldiene)hydroxypyridone with active methylene compounds in the presence of pyridine/triethylamine (Scheme 2.11). Where a second mole of a different hydroxypyridone is used unsymmetrical trimethine bridged oxonols result. Tetramethine formally neutral merocyanines result when active heterocycles such as 2-methyl benzothiazolium bromide are present.



(Scheme 2.11)

2.4.3. Preparation of cationic hydroxypyridone methine bridged oxonols ²¹

The only cationic oxonol synthesised was that obtained by reaction of N-dimethylaminopropyl hydroxypyridone with coupling agent 1,1',3,3'-tetramethoxypropane in the presence of hydroiodic acid/iodine (Scheme 2.12).



(Scheme 2.12)

This enabled a cationic oxonol with non-stoichiometric iodine content to be obtained.

CHAPTER 3

Polymeric Dye Systems as Bleachable

Antihalation Underlayers

3.1. It is the function of the antihalation underlayer to prevent any unabsorbed rays of light which have passed through the sensitive film layers from being reflected, thereby preventing "halation". One might assume that making the light which reaches the underlayer of a narrow enough wavelength range could reduce the underlayer composition to a single dye component. For example, in a colour film, a combination of yellow and magenta filter layers, coloured colour forming agents called "masks" and a light-tight camera could reduce the requirement for the underlayer to merely a red light absorbing (cyan) component. In practice, however, the inefficiency of the filter layers to absorb all of the light passing through them and the additional expectancy of the underlayer, in many cases, to also behave as a backing layer (that is to prevent light entering through the back of the assembly) means that it more usually has to deal with a much wider range of the visible spectrum. This is presently achieved by using a combination of up to three separate dyes and relying on dye aggregate formation to provide good overlap of the individual dye absorptions,²² figure 3.1.

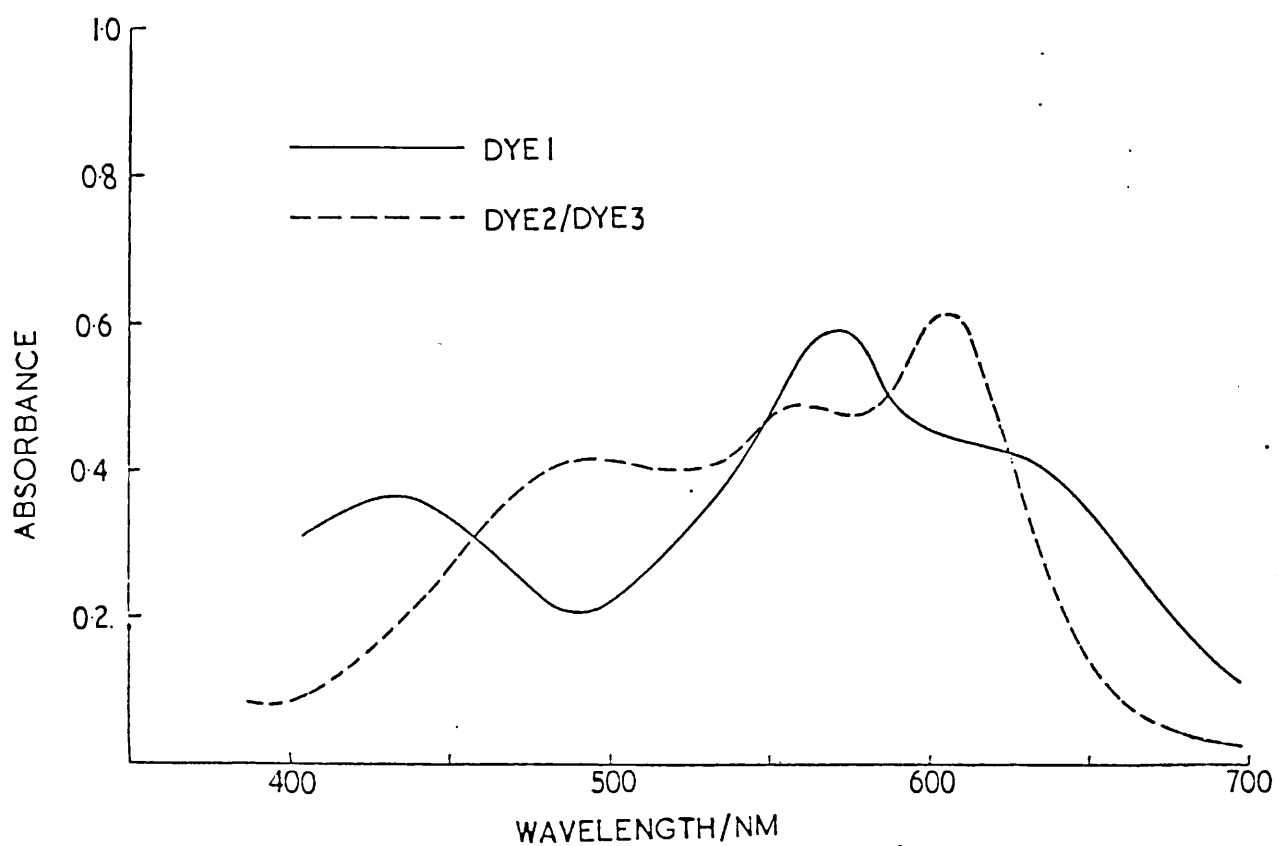


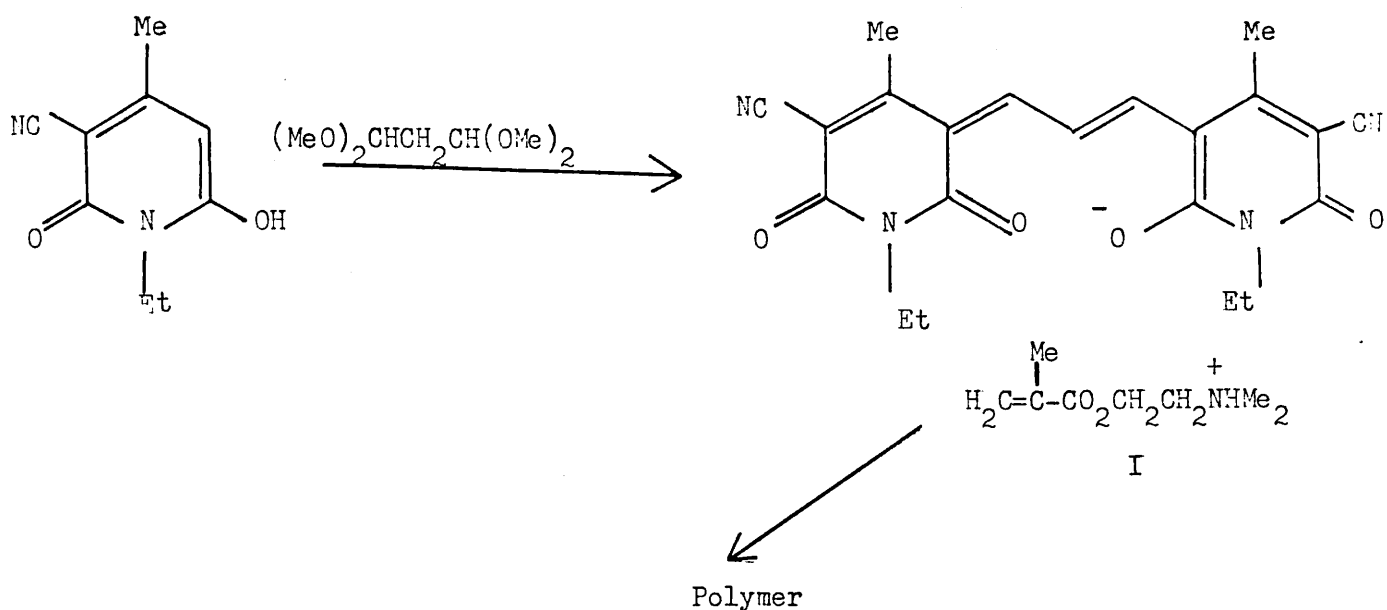
Figure 3.1.

Commercially, underlayer formulation involves separate preparations of the component dyes and polymer, followed by their subsequent co-precipitation. It was our intention to investigate both the simplification of this procedure and other approaches to improving dye substantivity.

3.2. Chain-Growth Polymerisation

3.2.1. Hydroxypyridone oxonol salts of polymerisable cation

We synthesised a monomeric dye-mordant species (I) (Scheme 3.1) which we hoped to polymerise in either solution or the solid state.



Scheme 3.1

Several methods were tried. These included reacting

- (a) a 10% w/w solution of (I) in water, in the presence of 1 mol % of the initiator 4,4'-azobis(4-cyanopentanoic acid (ABCPA) at 60°C overnight,
 - (b) a 20% w/w solution of (I) in absolute ethanol, in the presence of 0.5 mol % azobisisobutyronitrile (AZBN) at 60°C overnight,
 - (c) a 10% w/w solution of (I) in dimethylformamide, in the presence of 0.5 mol % AZBN, at 60°C overnight,
- and
- (d) a 20% w/w solution of (I) in dimethylformamide, in the presence of 0.5 mol % AZBN, at 60°C overnight.

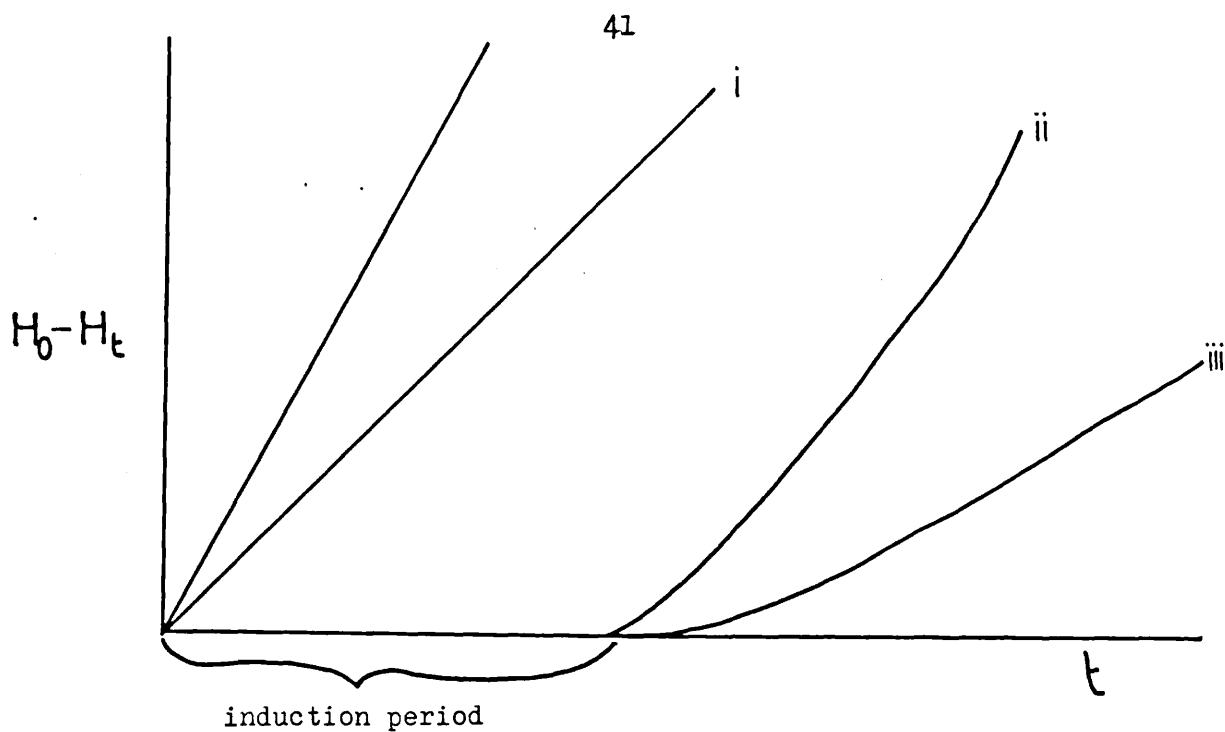
In the solid state, solid (I) was:

- (e) heated at 160°C overnight,
- and
- (f) exposed to ultraviolet radiation ($\lambda = 207 \text{ nm}$) over a weekend.

In every case ^1H n.m.r. spectra indicated that the vinyl group protons remained intact. It was thought that the hydroxypyridone oxonol anion in (I) might be inhibiting the chain-growth polymerisation. Certainly the chromophore was involved in a reaction of sorts during the attempted polymerisation since bleaching was seen to occur. This process was investigated by dilatometric measurements. The progress of a polymerisation can be determined by means of continuous monitoring of the volume contraction. Starkweather and Taylor²³ demonstrated that a linear relationship exists between volume contraction in per cent and the degree of polymerisation. We have compared the polymerisation of methyl methacrylate, using azobisisobutyronitrile, AZBN, as initiator in methyl ethyl ketone at 60°C with and without added (I). In theory, there were three possibilities:

- (a) (I) could be inhibiting the polymerisation,
- (b) (I) could be retarding the polymerisation,
- (c) (I) could be both retarding and inhibiting the polymerisation.

Retarders slow down the rate and inhibitors will completely stop polymerisation. Both types tend to act in the same way and differ only in their efficiency in rendering the growing chains inactive. The effect of the addition of a retarder or an inhibitor to a free-radical polymerisation system is shown in figure 3.2²⁴. Nitrobenzene for example, acts as a retarder for styrene through a chain-transfer reaction. The



- (i) Retardation
- (ii) Inhibition (note the induction time during which the inhibitor is consumed)
- (iii) Inhibition and Retardation (the product from the inhibition reaction is a retarder for the polymerisation)

Figure 3.2

radicals yielded by this reaction are rather inactive and react only slowly with styrene monomer molecules. In this case both the rate and degree of polymerisation are reduced. On the other hand benzoquinone inhibits the polymerisation of styrene by scavenging every polymer radical formed and converting them into unreactive substances. The inhibitor itself is rendered inactive by the reaction and this leads to a phenomenon known as an "induction period" whereby inhibition only takes place for a limited period of time. After all the inhibitor molecules are used up polymerisation proceeds in the normal way²⁴. Figure 3.3 shows the observed effects with (ii) and without (i) added (I) on the polymerisation, clearly demonstrating its inhibiting nature.

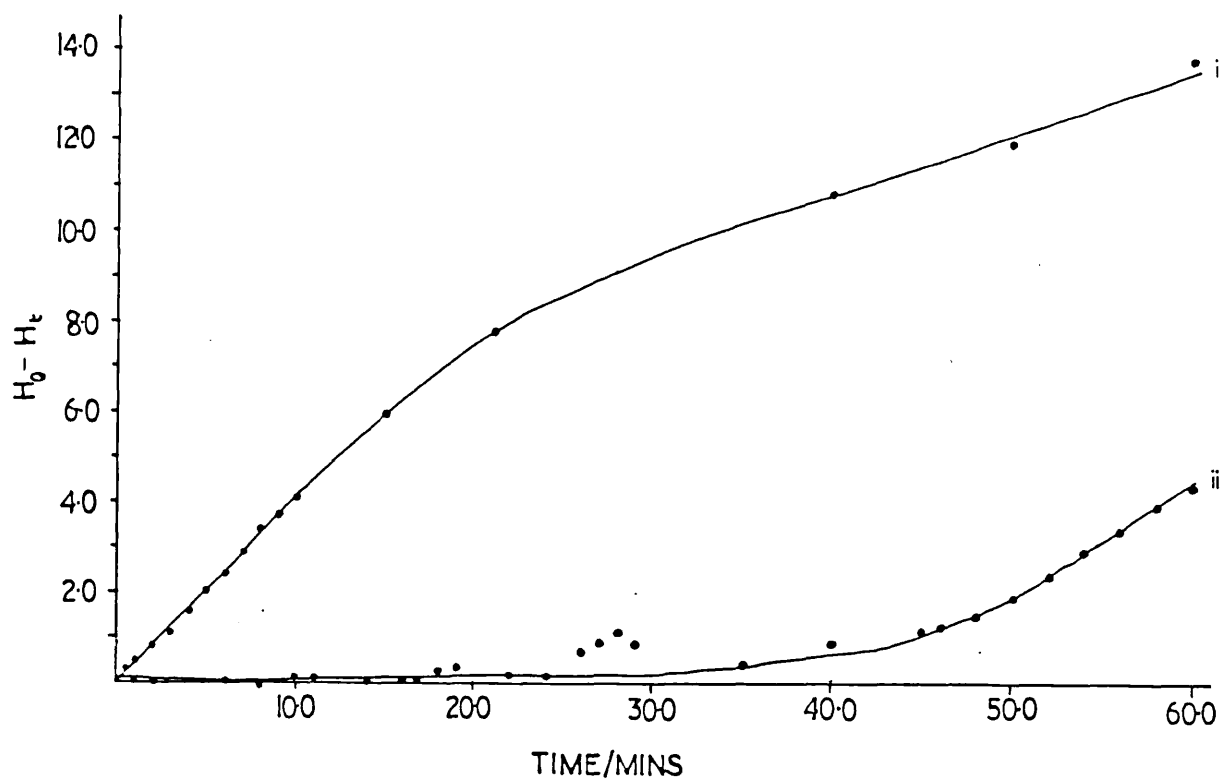


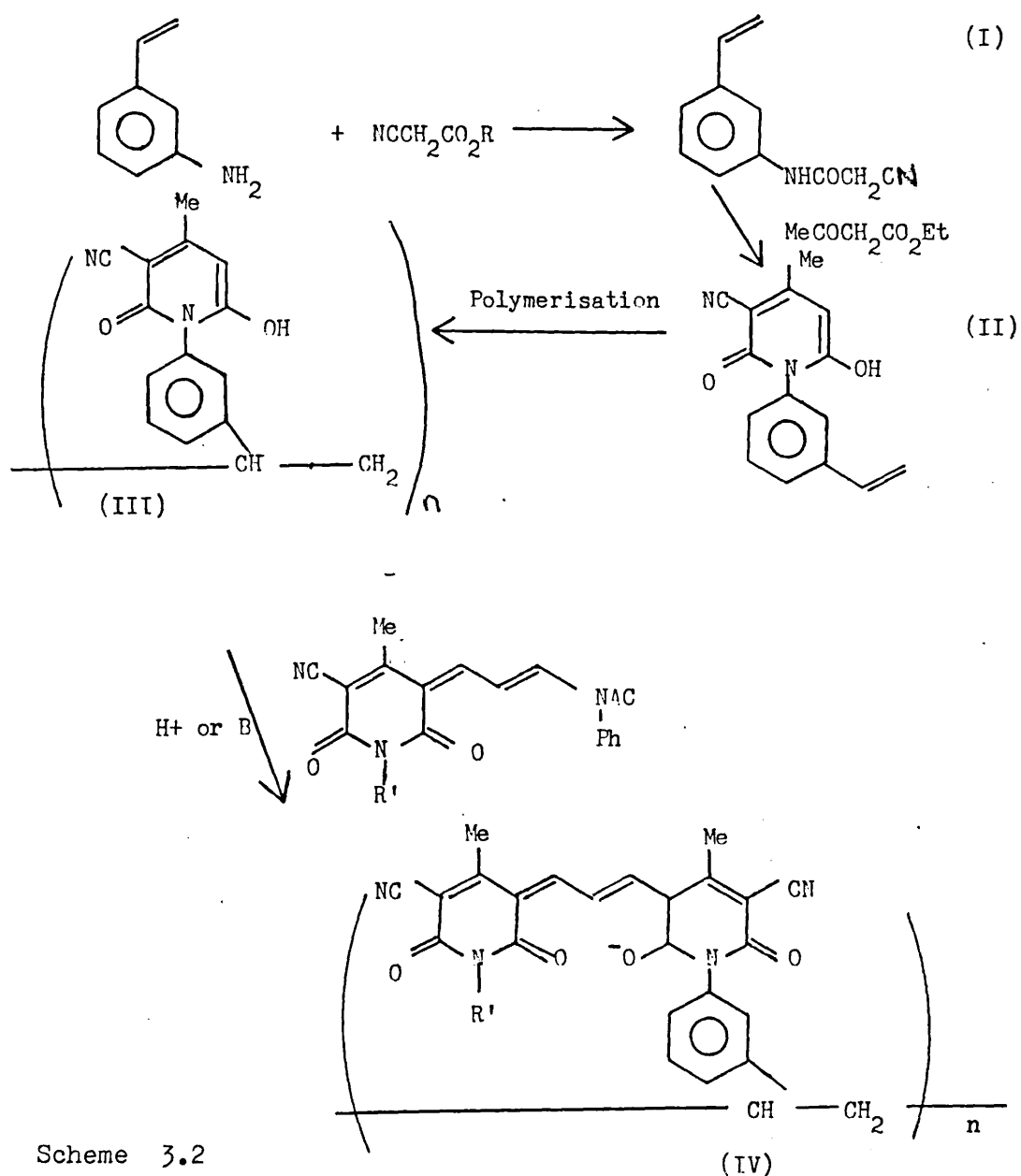
Figure 3.3.

A later X-ray structural study of (I) revealed the closest proximity between the vinyl groups of adjacent cations in the lattice to be 13 \AA (see Chapter 6). It was therefore not surprising that the solid state polymerisation was not successful.

3.2.2. Polymerisable hydroxypyridone methine bridged oxonol anions

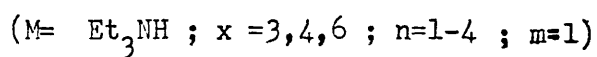
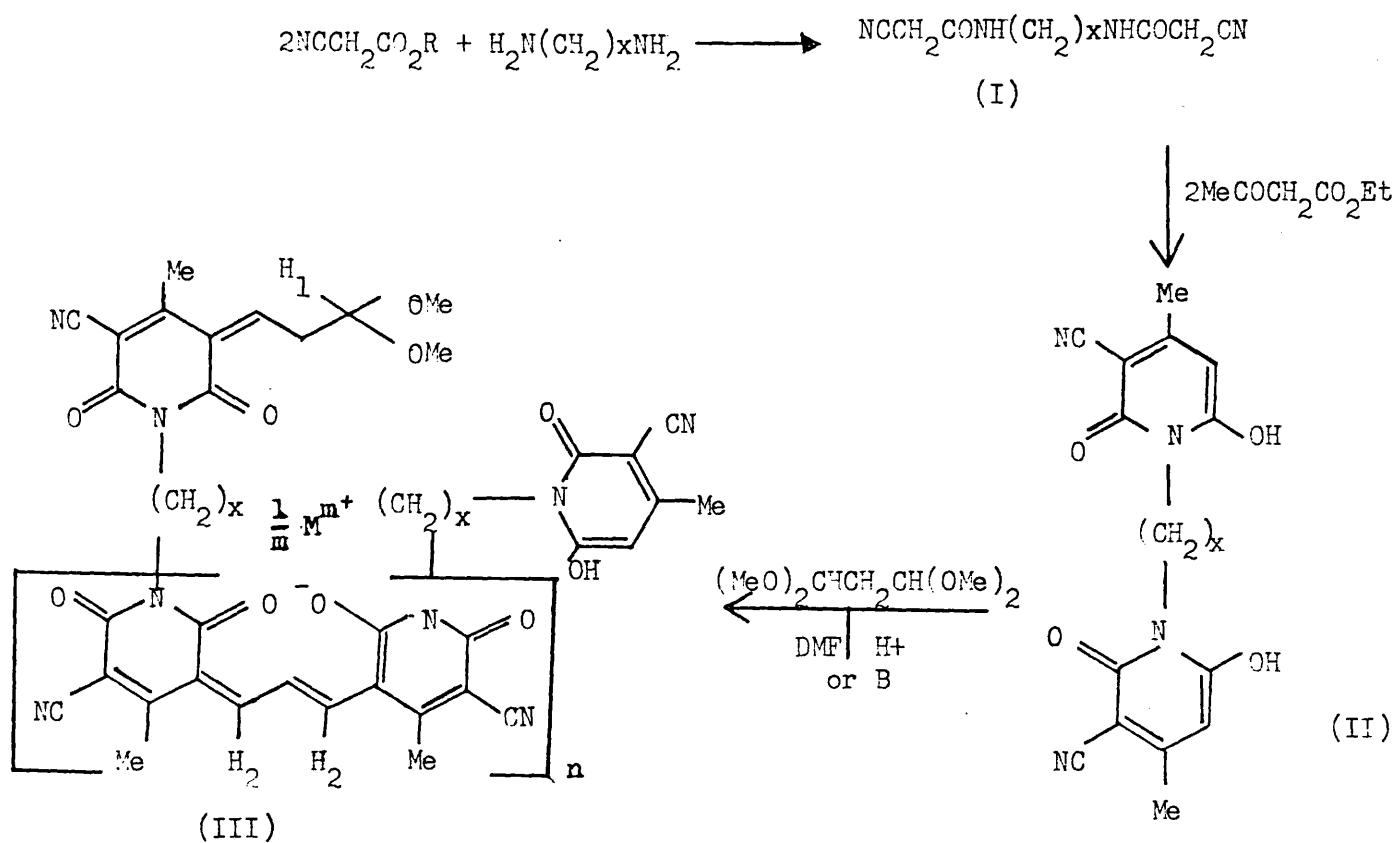
Our initial intention was to introduce a polymerisable N-styryl substituent on to one of the pyridone rings of the oxonol dye anion. However, as a result of the findings of the dilatometric measurements in the previous section we decided that the polymerisation would have to be

carried out at the hydroxypyridone stage, Scheme 3.2, as the evidence tended to suggest that it was the methine bridge of the oxonol dye anion which was responsible for its inhibiting properties. The cyanoacetamide (I) (Scheme 3.2) however, proved difficult to synthesise, and this, coupled with the discovery of a more convenient route to polymeric/oligomeric systems (3.3), meant that no further work was done in this area.



3.3 Step-Growth Polymerisation

This involved the synthesis of symmetrical bis-hydroxypyridones, hence providing two identical sites at which condensation could take place (Scheme 3.3). The subsequent "step-growth" condensation polymerisation reaction with 1,1',3,3'-tetramethoxypropane, yielded oligomeric species III, Scheme 3.3.



Scheme 3.3

The course of the polymerisation where (III, $x = 6$, $M = Et_3NH$ and $m = 1$) was followed with time by removing small aliquots from the reaction mixture (a 40% w/w solution of the bis-hydroxypyridone in dimethyl-formamide with a molar equivalent of 1,1',3,3'-tetramethoxypropane and excess triethylamine) every four hours. These were then reprecipitated from ethyl acetate and characterised using high field 1H and ^{13}C n.m.r. and u.v./visible spectroscopic techniques.

"End-group" analyses by way of the high field 1H n.m.r. spectra provided us with more quantitative results. These analyses were carried out by selecting two peaks in the 1H spectrum of each of the aliquots, one corresponding to one or more equivalent protons of an end-group (H^1 , Scheme 3.3) and the other to one or more equivalent protons of the repeating unit (H^2 , Scheme 3.3). The ratio of their relative integrals provides an estimate of the number of repeating units (n) at any one time (Table 3.1), though it must be borne in mind that one is always dealing with a molecular weight distribution.

Time/Hours	4	8	12	16	21	25	29	45
n	2.30	2.89	3.54	4.08	3.46	3.00	2.39	1.58

Table 3.1

Figure 3.4 shows the absorbances at the λ_{max} values for each of the aliquots (1 mg in 100 cm^3 H_2O). Close examination of these

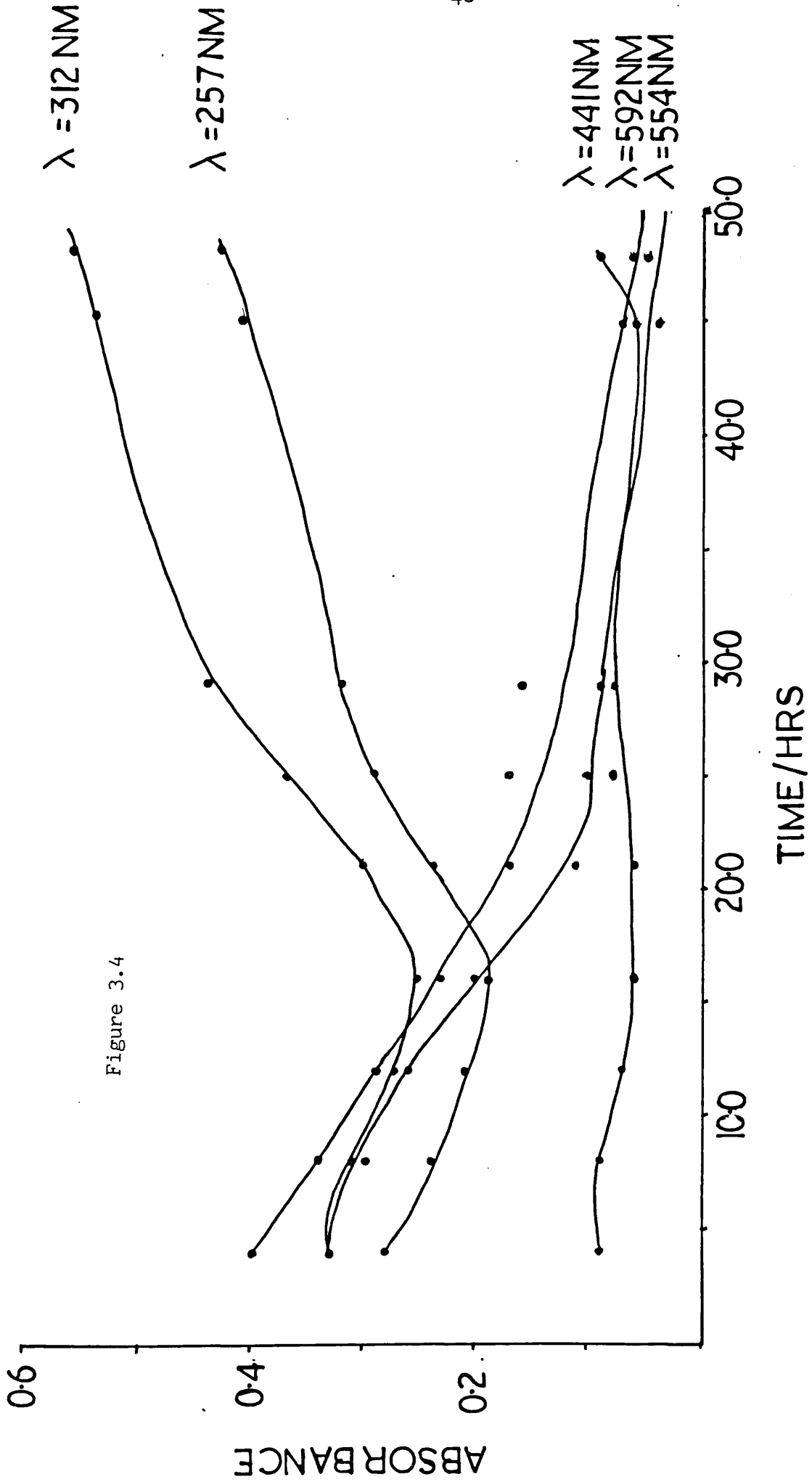


Figure 3.4

results in conjunction with their ^1H n.m.r. spectra shows

(a) 0 - 16 hours; (i) a gradual decrease in absorbances at 592, 554 and 441 nm coupled with a decrease at 312 and 257 nm;

and

(ii) a steady shift to a higher molecular weight distribution.

(b) 16 - 48 hours; (i) a gradual increase in absorbances at 257 and 312 nm coupled with a decrease at 592, 554 and 441 nm.

and

(ii) a steady shift to a lower molecular weight distribution.

The absorbances at 592, 554 and 441 nm are essentially due to the lower molecular weight, water soluble species, monomeric and dimeric material in the main. The absorbances at 257 and 312 nm correspond to the bis-hydroxypyridone (II, Scheme 3.3). The results then suggest that between 0 - 16 hours we are observing a consumption of the bis-hydroxypyridone and the formation of higher molecular weight, water insoluble, material. Between 16 - 48 hours we are seeing an increase in residual bis-hydroxypyridone resulting possibly from the gradual decomposition of oligomeric material.

It thus became apparent that the most promising material was the low molecular weight oligomeric material formed after only four hours. It was water soluble and appeared to aggregate sufficiently well even at this low molecular weight distribution to provide very good spectral coverage, figure 3.5. Gelatin coatings on triacetate base have been made of this material and it has undergone Ilford Ltd's standard evaluation tests for substantivity (a) and bleachability (b) and (c), figure 3.5 (see section 10.2.3). The material is seen to be both highly substantive and bleachable.

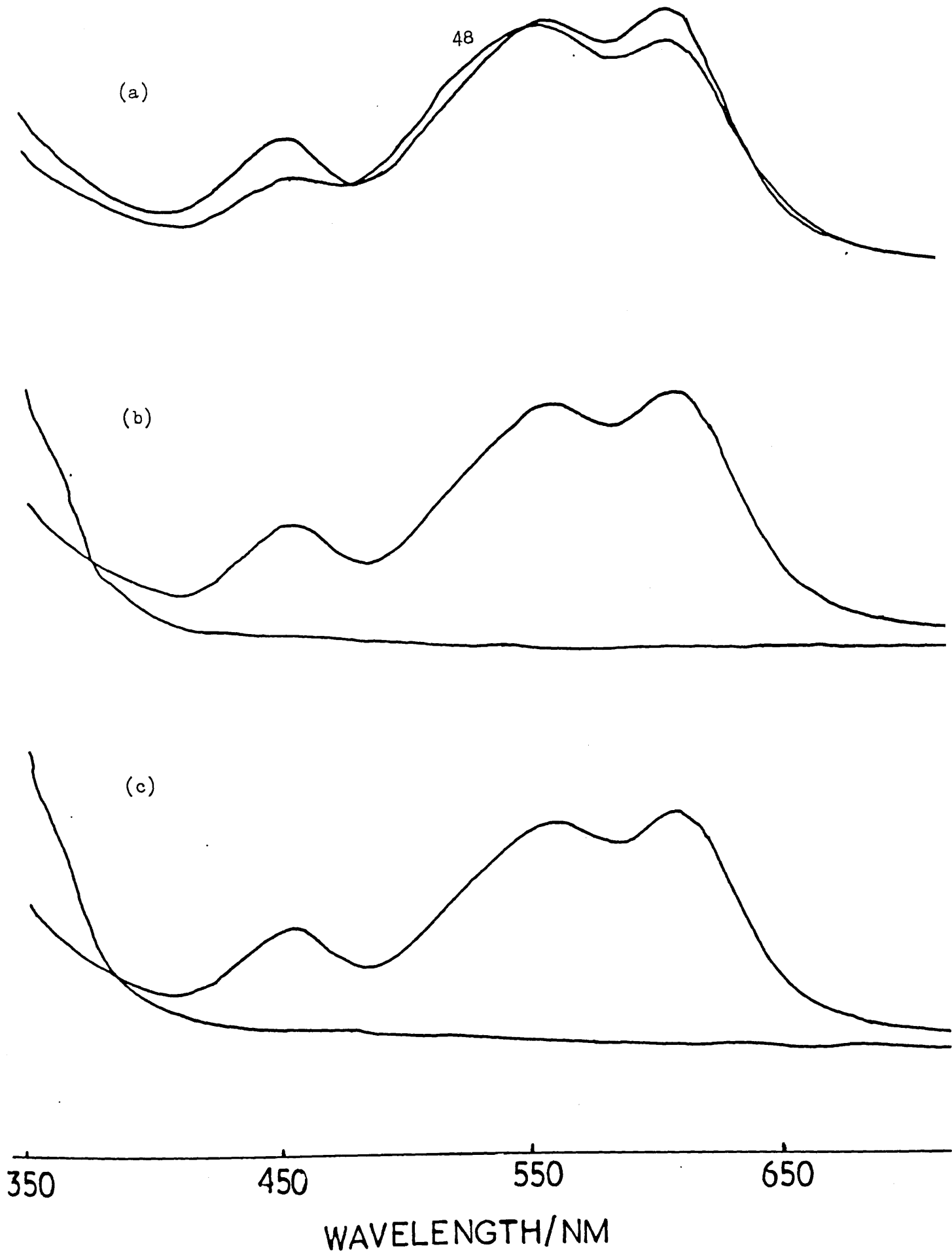


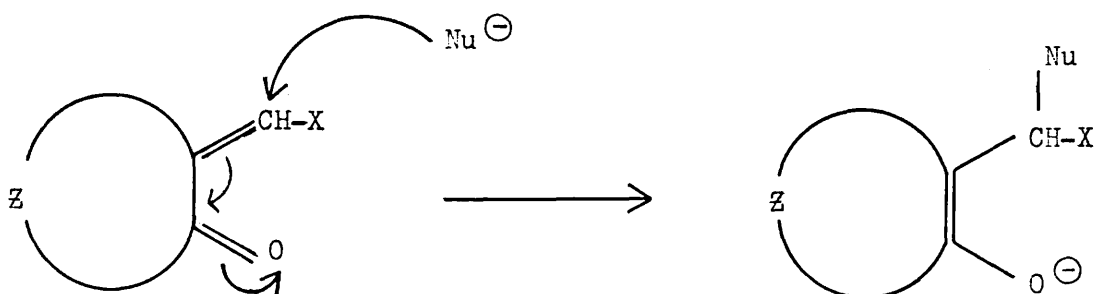
Figure 3.5

Thus, although the long chain "double bond" free-radical polymerised materials are not readily synthesised the oligomers obtained by condensation polymerisation appear to have the desired properties of an anti-halation underlayer and are easily prepared. Indeed the materials described here are currently undergoing further commercial evaluation.

CHAPTER 4

The Bleaching Reaction

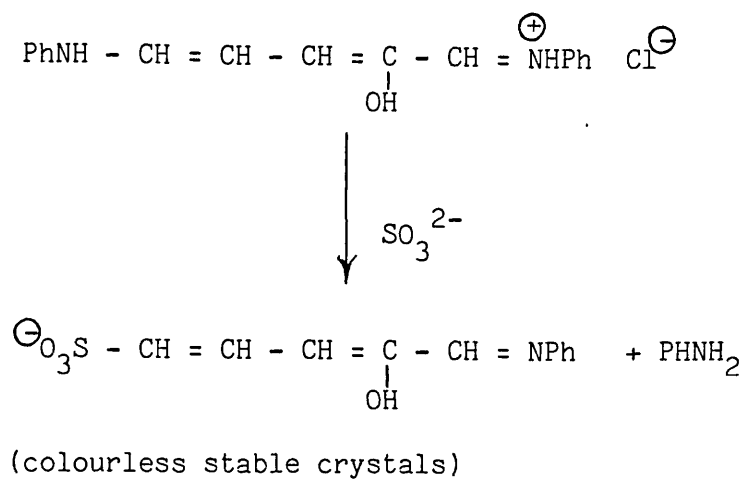
4.1 Most bleachable dyes have the α , β -unsaturated carbonyl residue as part of their chromophore. This is susceptible to a Michael-type conjugate attack at the soft electrophilic centre on the methine bridge, Scheme 4.1.



Scheme 4.1

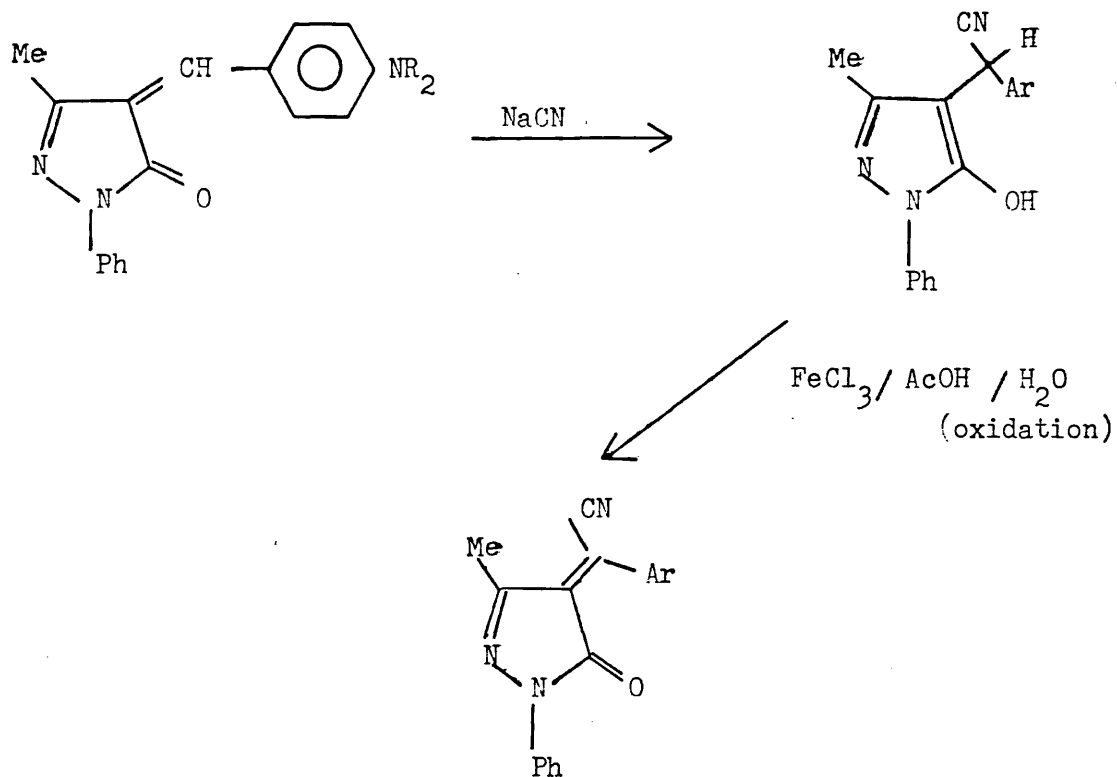
This not only solubilises the dye, assisting its removal by washing out during aqueous processing, but also interrupts the chromophoric system (hence "bleaching" as a term). It may also, in aggregated systems disrupt the aggregand/crystal packing, making the aggregate as a whole less well held in the gelatin "fishing net".

Photographic folklore has always assumed the sulphite of the developer to be the major bleaching agent, but direct evidence for sulphite ion bleaching dyes of this type has been lacking. The so-called Stenhouse dyes have shown to undergo attack by sulphite ions²⁵ as shown in Scheme 4.2. The benzylidene dyes, which are also bleachable, have



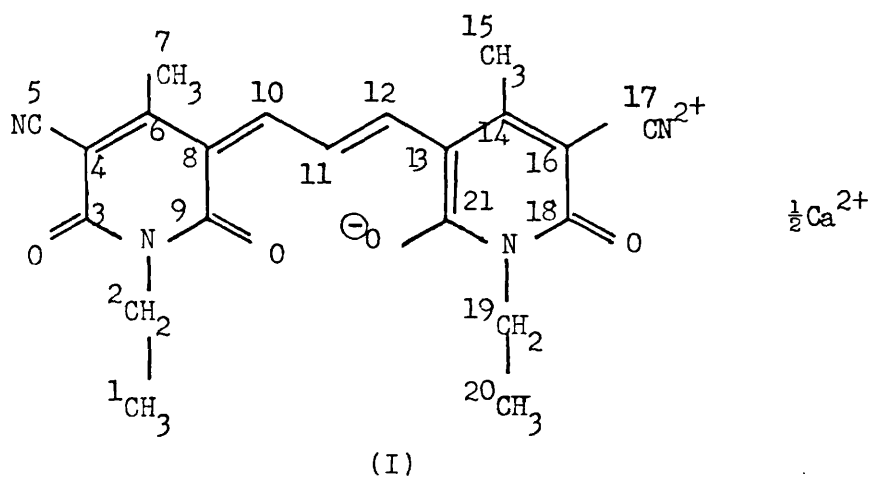
Scheme 4.2

been shown to undergo nucleophilic addition by the cyanide ion in a similar fashion, Scheme 4.3.



Scheme 4.3

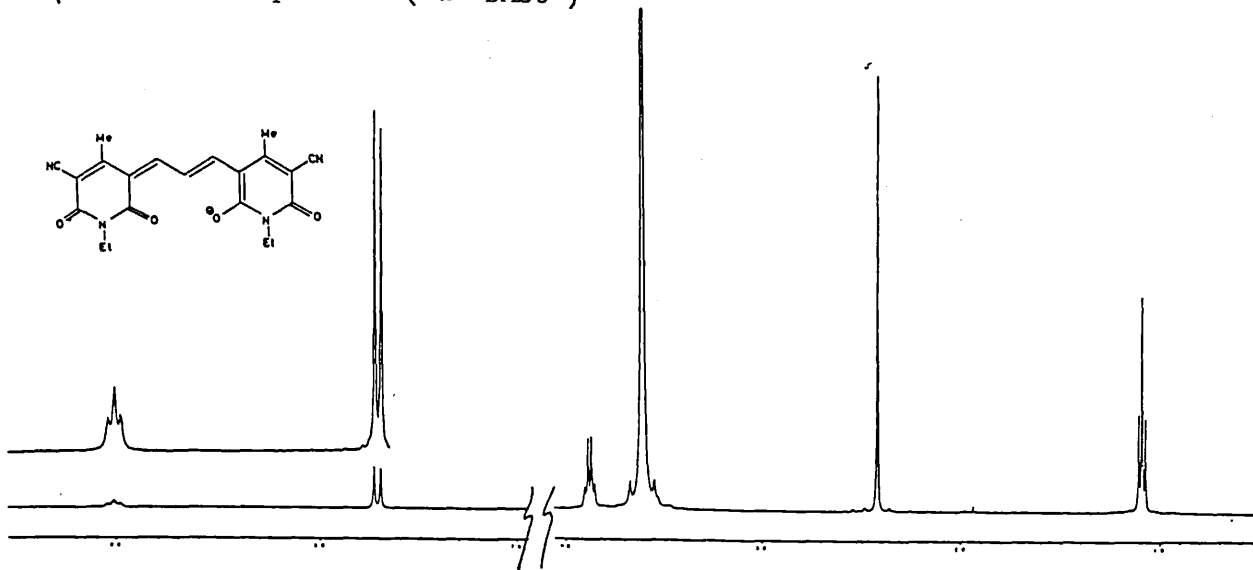
We thus set out to investigate in more depth the bleaching of the hydroxypyridone trimethine oxonols by a variety of nucleophiles using visible and ^1H and ^{13}C n.m.r. spectroscopic techniques. Although the sulphite ion was to be studied most extensively, reactions involving ions such as OH^- , S^{2-} , CN^- , OMe^- , NH_3 and EtNH_2 were also examined. Dye (I) was chosen for our investigations as it had relatively simple ^1H and ^{13}C n.m.r. spectra resulting from its metallic cation and



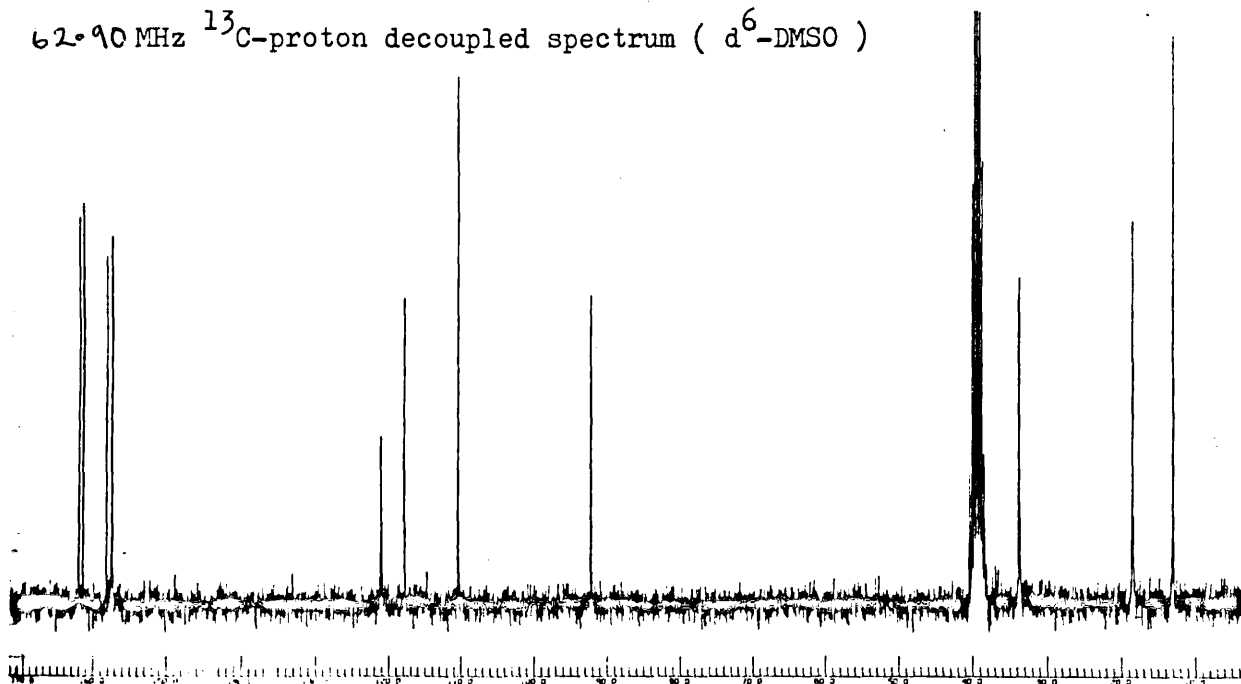
symmetry. Figure 4.1 shows its ^1H , ^{13}C -proton decoupled and ^{13}C fully proton coupled n.m.r. spectra, tables 4.1 and 4.2 their respective assignments.

400.13 MHz ^1H spectrum ($\text{d}^6\text{-DMSO}$)

53



62.90 MHz ^{13}C -proton decoupled spectrum ($\text{d}^6\text{-DMSO}$)



62.90 MHz ^{13}C -fully proton coupled spectrum ($\text{d}^6\text{-DMSO}$)

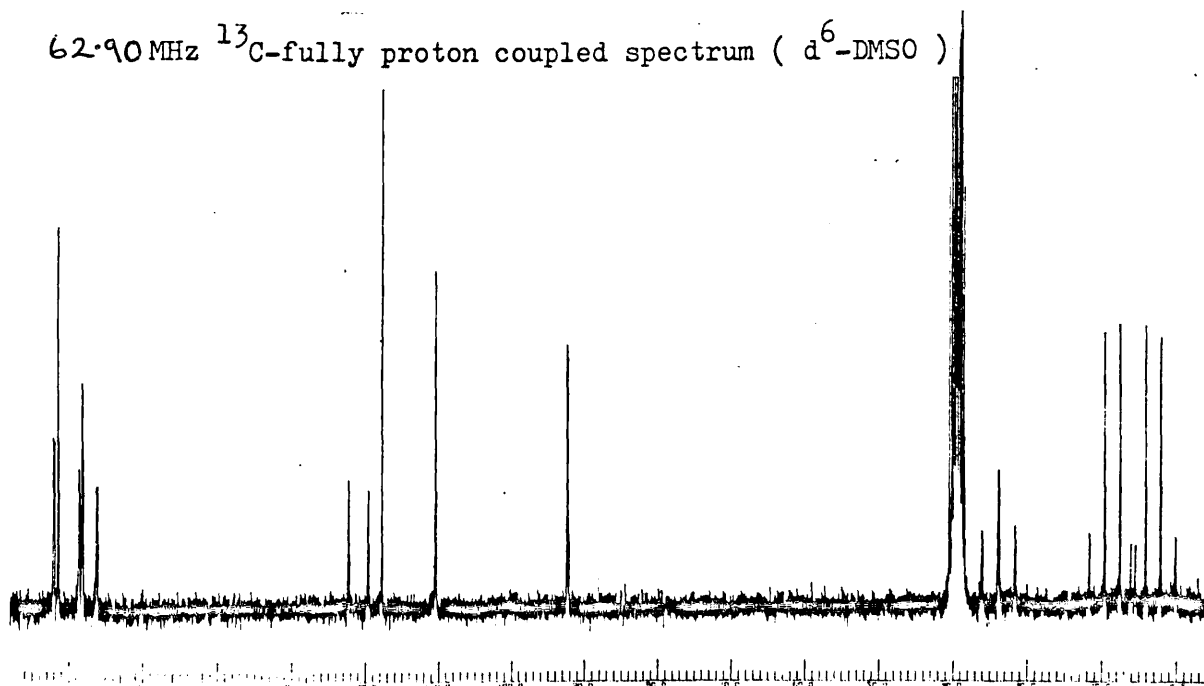


Figure 4.1

Table 4.1

$\delta(d^6\text{-DMSO, ppm})$	J, Hz	Assignment
1.09 (t)	7.0	C ^{1,20} H ₃
2.44 (s)		C ^{7,15} H ₃
3.90(qt)	7.0	C ^{2,19} H ₂
7.71 (d)	13.0	C ^{10,12} H
9.01 (t)	13.0	C ¹¹ H

Table 4.2

$\delta(d^6\text{-DMSO, ppm})$	Assignment
13.08	C(1), C(20)
18.55	C(7), C(15)
33.82	C(2), C(19)
92.21	C(6), C(14)
110.40	C(8), C(13)
117.72	C(5), C(17)
120.93	C(11)
157.36	C(10), C(12)
158.13	C(4), C(16)
161.39 } 161.97 }	C(3), C(9) C(18), C(21)

4.2. Sulphite Bleaching

4.2.1 Kinetic studies

The bleaching of (I) was studied in aqueous solution at 20°C, using large excesses of sodium sulphite ($[\text{SO}_3^{2-}]/[\text{Dye}] > 20$) to simplify the kinetics. Under these conditions (figure 4.2) the consumption of dye was first-order:

$$-d[\text{Dye}]/dt = k_1[\text{Dye}]$$

The pseudo first-order rate constant, k_1 , was also linearly linked with the stoichiometric sulphite ion concentration (Table 4.3, figure 4.3), i.e.

$$-d[\text{Dye}]/dt = k_2[\text{Dye}][\text{SO}_3^{2-}]_{\text{stoich.}}$$

Table 4.3

$[\text{Dye}]_0 = 1.0 \times 10^{-6} \text{M}$

$[\text{SO}_3^{2-}]_0/\text{M}$	k_1/s^{-1}	$\ln[\text{SO}_3^{2-}]$	$\ln k_1$
3.32×10^{-5}	1.43×10^{-2}	-10.31	-4.25
6.62×10^{-5}	3.31×10^{-2}	-9.62	-3.41
1.32×10^{-4}	11.60×10^{-2}	-8.93	-2.15
1.96×10^{-4}	13.30×10^{-2}	-8.54	-2.02
2.60×10^{-4}	22.50×10^{-2}	-8.25	-1.49

$$k_2 = 921 \text{ M}^{-1} \text{ s}^{-1}$$

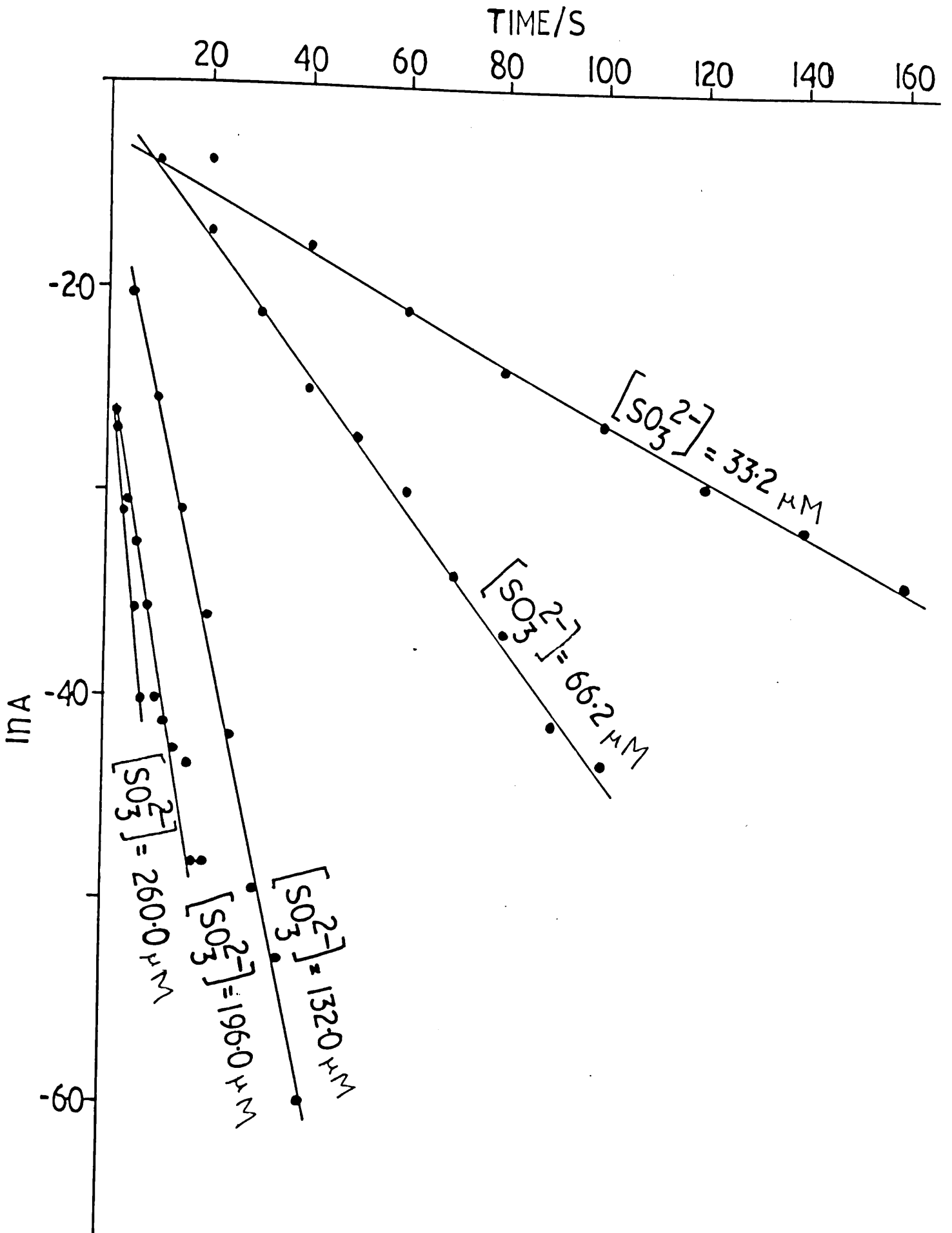


Figure 4.2

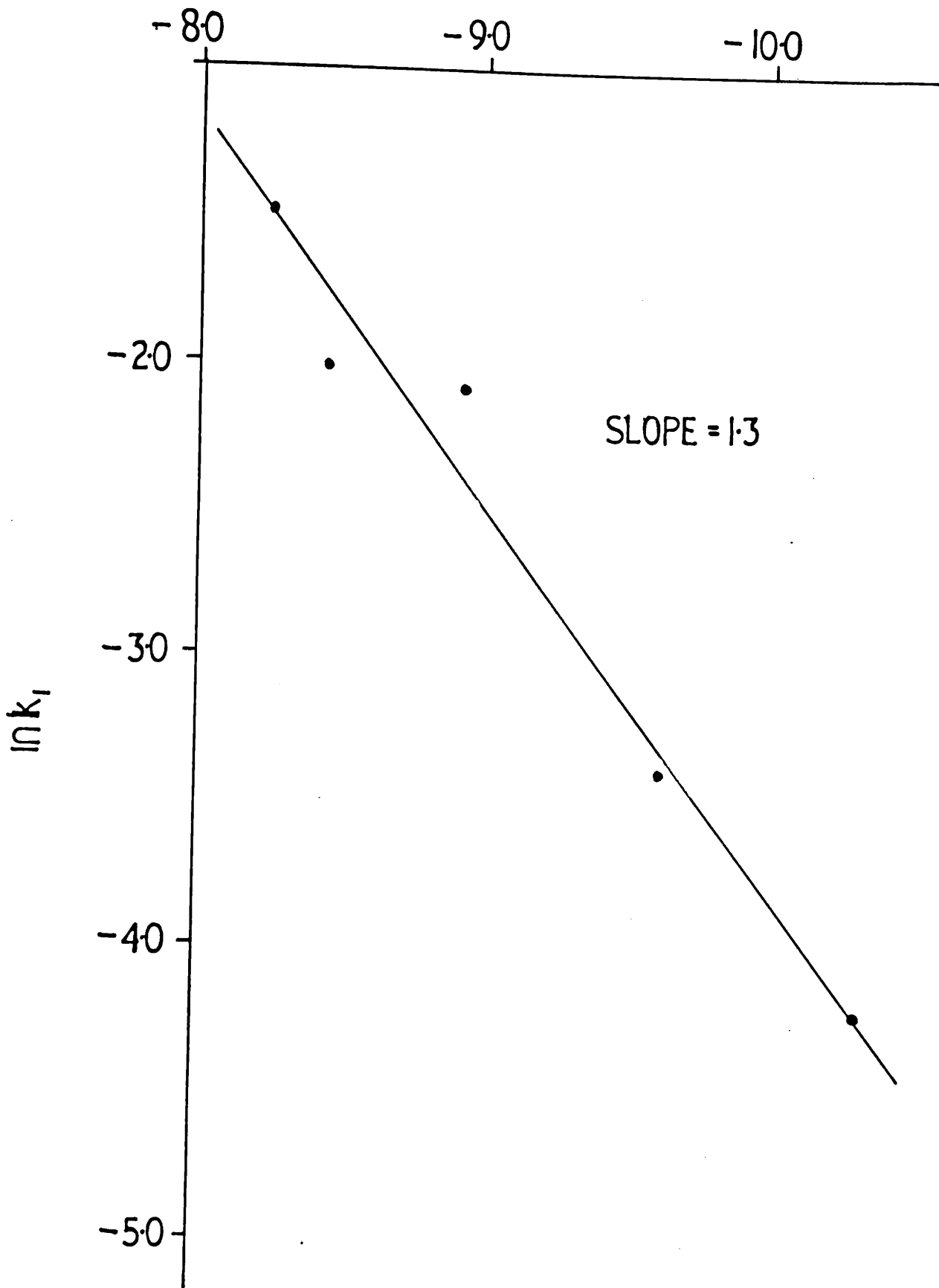
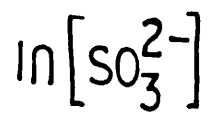


Figure 4.3

The kinetic form with respect of sulphite ion suggests

$$\text{Rate} \propto [\text{SO}_3^{2-}]^{1.3}$$

and this implies two contributions of different kinetic order.

Other possible bleaching reagents in this system included sulphur dioxide, bisulphite ions or even hydroxide ions. The effect of changing the pH of the solution upon the observed rate of reaction (Table 4.4, figure 4.4) shows that neither sulphur dioxide nor hydroxide ions could possibly have been the bleaching reagents. Although the bisulphite ion

Table 4.4

pH	2.13	3.15	4.04
k^1/s^{-1}	2.87×10^{-3}	4.77×10^{-3}	18.82×10^{-3}
$[\text{H}^+]/\text{M}$	7.40×10^{-3}	7.08×10^{-4}	9.12×10^{-5}
$[\text{HSO}_3^-]/\text{M}$	4.22×10^{-3}	5.98×10^{-3}	6.21×10^{-3}
$[\text{SO}_3^{2-}]/\text{M}$	5.80×10^{-8}	8.62×10^{-7}	69.50×10^{-7}
$[\text{SO}_2]/\text{M}$	2.03×10^{-3}	0.82×10^{-3}	0.04×10^{-3}

concentration is seen to increase with increasing pH and observed rate of reaction, the extent to which it increases is very slight. This leaves us then with the most probable bleaching reagent being the sulphite ion.

The reaction can thus be separated into

$$k^1 [\text{Dye}][\text{SO}_3^{2-}] = k_a [\text{Dye}][\text{SO}_3^{2-}] + k_b [\text{Dye}][\text{SO}_3^{2-}]^2$$

$$\Rightarrow k^1 = k_a + k_b [\text{SO}_3^{2-}]$$

thence

$$\frac{-d [\text{Dye}]}{dt} = 2.88 \times 10^{-3} [\text{Dye}][\text{SO}_3^{2-}] + 2100 [\text{Dye}][\text{SO}_3^{2-}]^2$$

in which the kinetic order of the second contribution has not been rigorously defined.

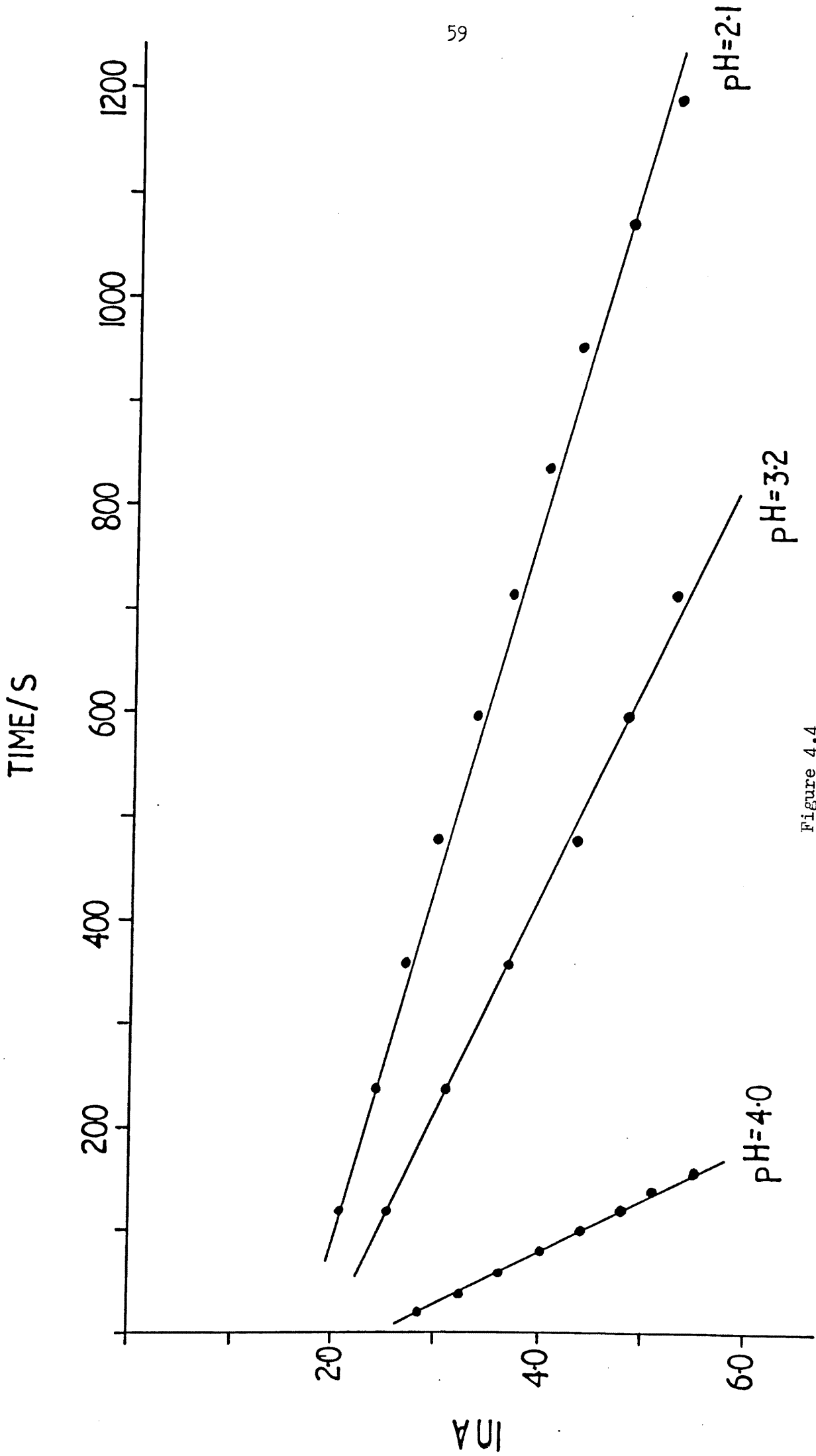


Figure 4.4

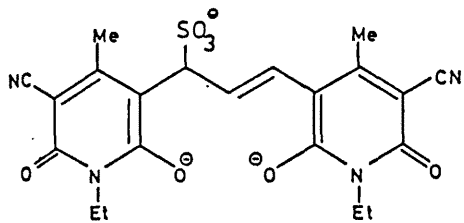
4.2.2. N.m.r. studies

The dissymmetry introduced into the dye molecule by the addition of sulphite ion is reflected in both the ^1H and ^{13}C n.m.r. spectra (figure 4.5).

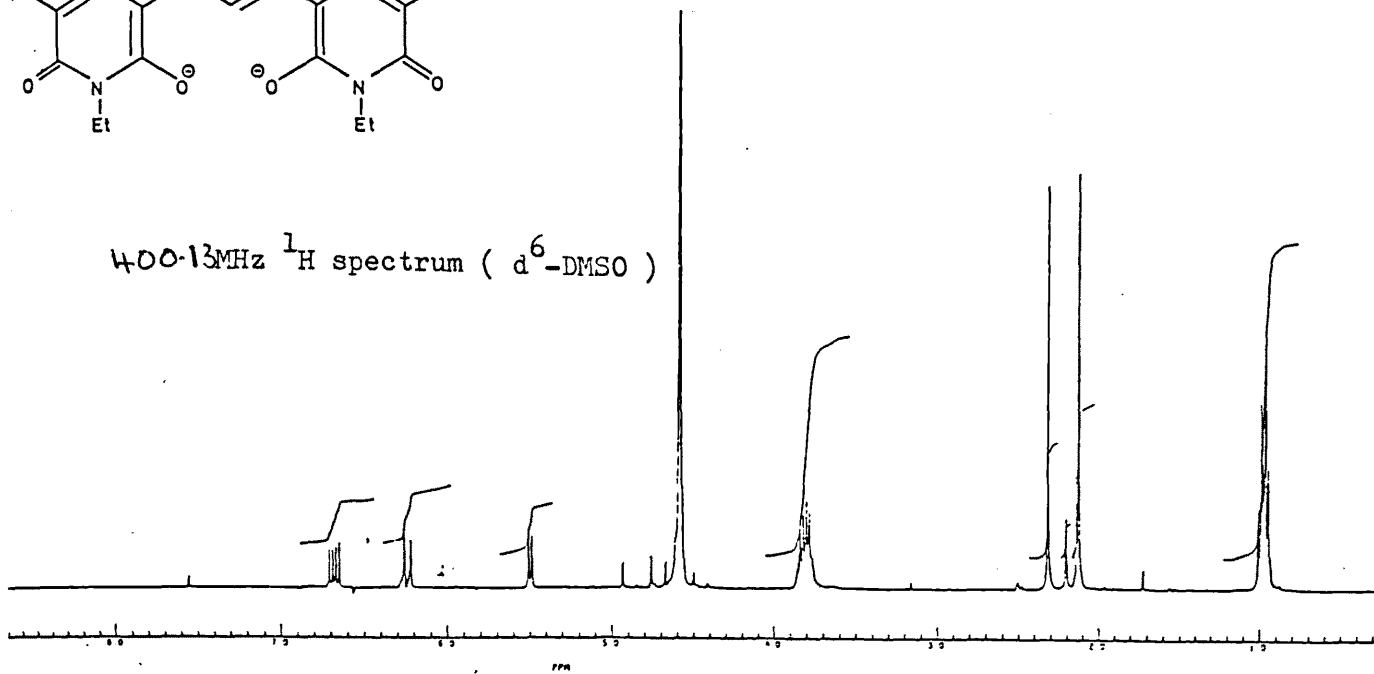
Tables 4.5 and 4.6 show the assignments of the ^1H and ^{13}C n.m.r. spectra, respectively. The double up on signals, the shift in

Table 4.5.

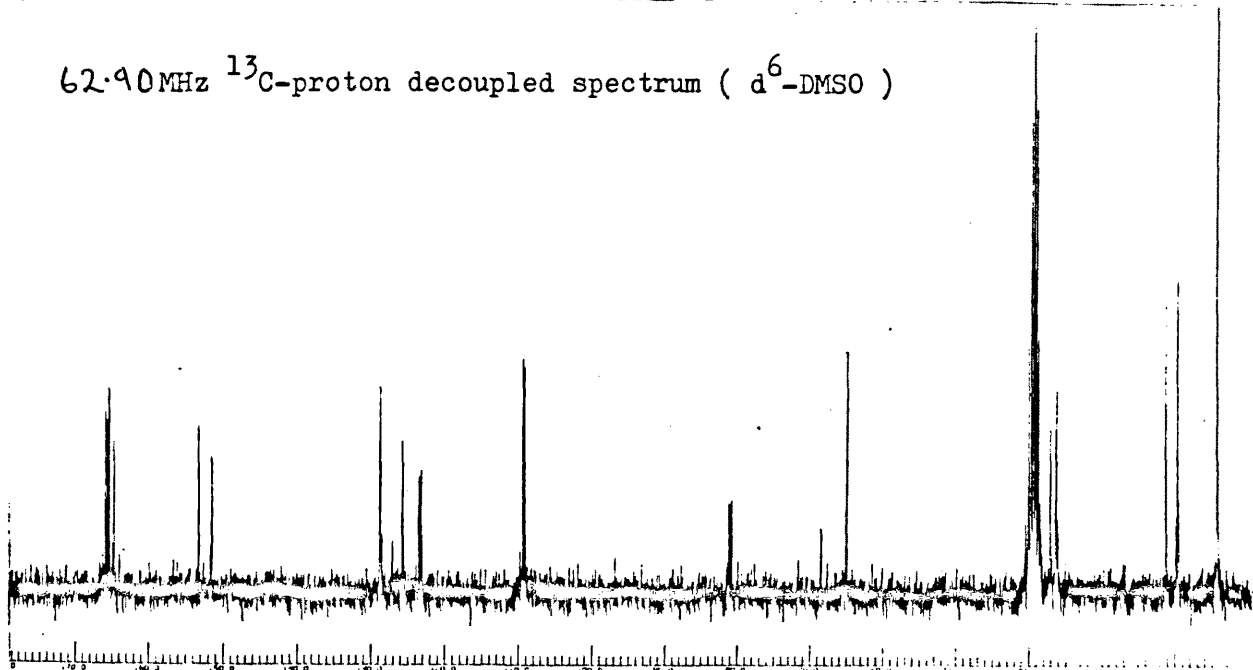
$\delta(\text{d}^6\text{-DMSO/D}_2\text{O, ppm})$	J, Hz	Assignment
0.96 (t)	7.2	C^1H_3
0.99 (t)	7.0	C^{20}H_3
2.12 (s)		C^7H_3
2.31 (s)		C^{15}H_3
3.79 (qt)	7.3	C^2H_2
3.83 (qt)	7.2	C^{19}H_2
5.50 (qt)	1.3	C^{10}H
	8.3	
6.24 (qt)	1.3	C^{12}H
	15.6	
6.68 (qt)	8.3	C^{11}
	15.6	



400.13MHz ^1H spectrum ($\text{d}^6\text{-DMSO}$)



62.90MHz ^{13}C -proton decoupled spectrum ($\text{d}^6\text{-DMSO}$)



62.90 MHz ^{13}C -fully proton coupled spectrum ($\text{d}^6\text{-DMSO}$)

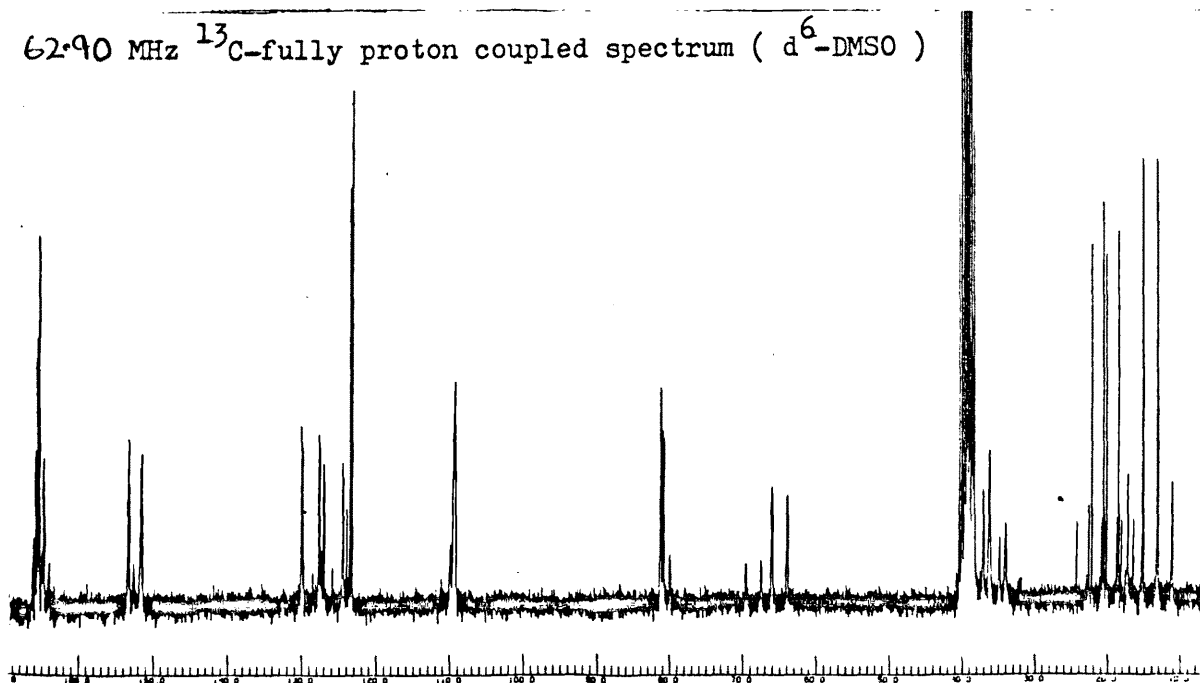


Table 4.6

$\delta(\text{d}^6\text{-DMSO}/\text{D}_2\text{O}, \text{ppm})$	Assignment
14.32	C(1), C(20)
19.69 } 21.31 }	C(7), C(15)
36.34 } 37.15 }	C(2), C(19)
65.02	C(10)
80.88 } 81.18 }	C(6), C(14)
109.26 } 109.44 }	C(5), C(17)
123.27 } 123.53 }	C(8), C(13)
125.79	C(11)
128.79	C(12)
151.55 } 153.29 }	C(4), C(16)
164.74 } 165.41 } 165.60 } 165.88 }	C(3), C(9) C(18), C(21)

position of the C(10) peak from 157.4 to 65.0 ppm and the region of the ^1H spectrum corresponding to the methine bridge protons (shown expanded in figure 4.6) all suggest the existence of a Michael-type adduct.

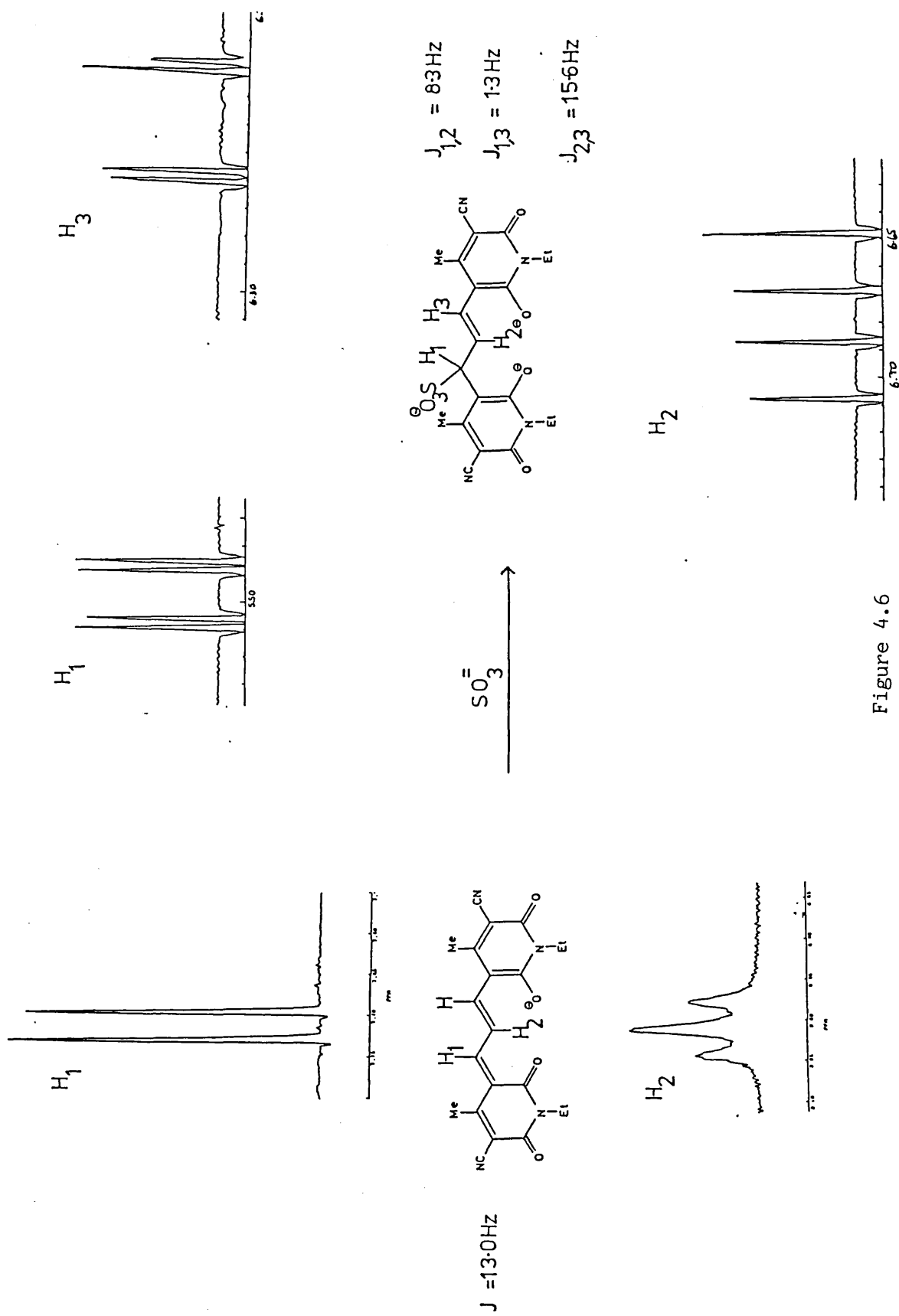


Figure 4.6

4.3 Other Nucleophiles

4.3.1 Initial qualitative studies revealed CN^- , MeO^- , S^{2-} , NH_3 , Et_3N , OH^- , SH^- and EtNH_2 like SO_3^{2-} to be effective in bleaching dye I. The additions of OH^- , SH^- , NH_3 , and EtNH_2 being reversible (that is the acidification of the bleached solution, in each case, regenerated the original dye chromophore, figure 4.7).

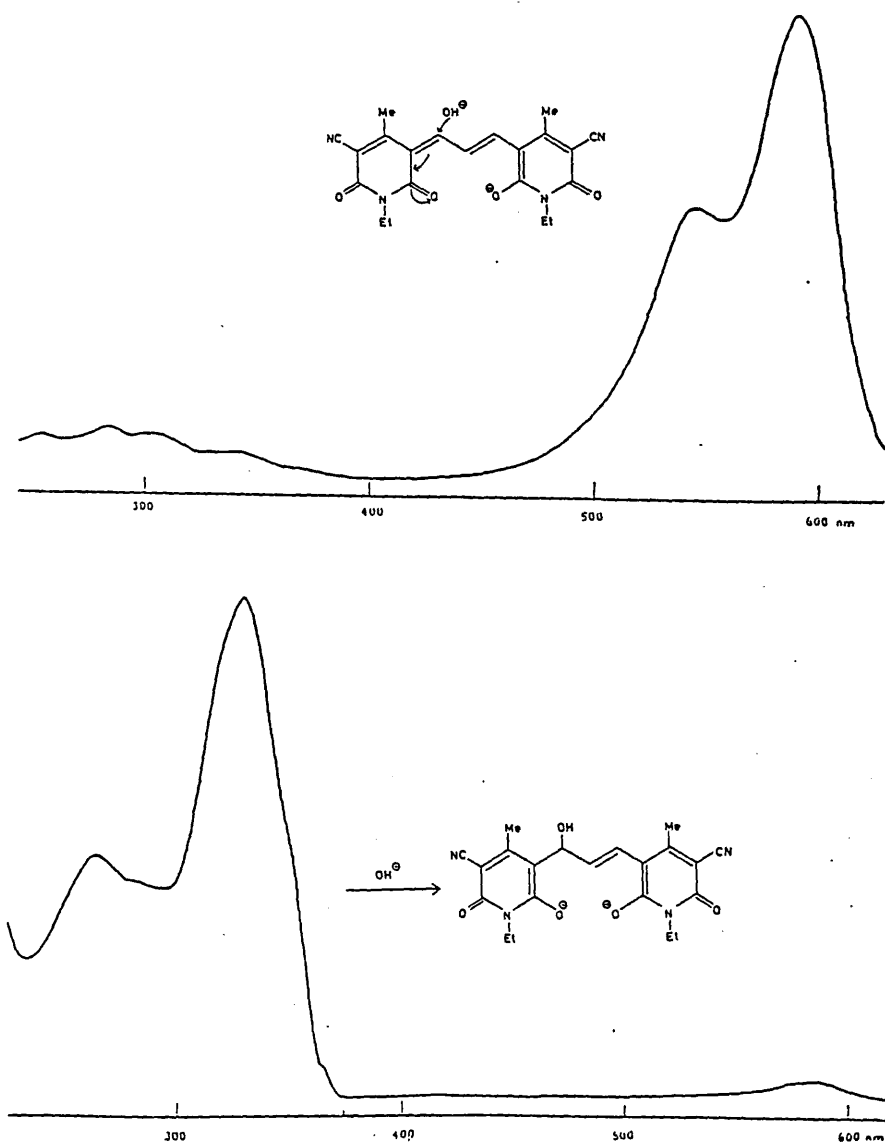


Figure 4.7

Nucleophiles such as N_3^- , PhNH_2 , SCN^- , Ph_3P and $\text{S}_2\text{O}_3^{2-}$ were found to be ineffective bleaching agents.

4.3.2 N.m.r. studies

Of the nucleophiles investigated, the ^1H and ^{13}C n.m.r. spectra of the CD_3O^- , S^{2-} and EtNH_2 bleached adducts resembled most closely those of the SO_3^{2-} case, figure 4.8.

The spectra of the NH_3 bleached adduct were highly complex, figure 4.9 (possibly as a result of the equilibrium;

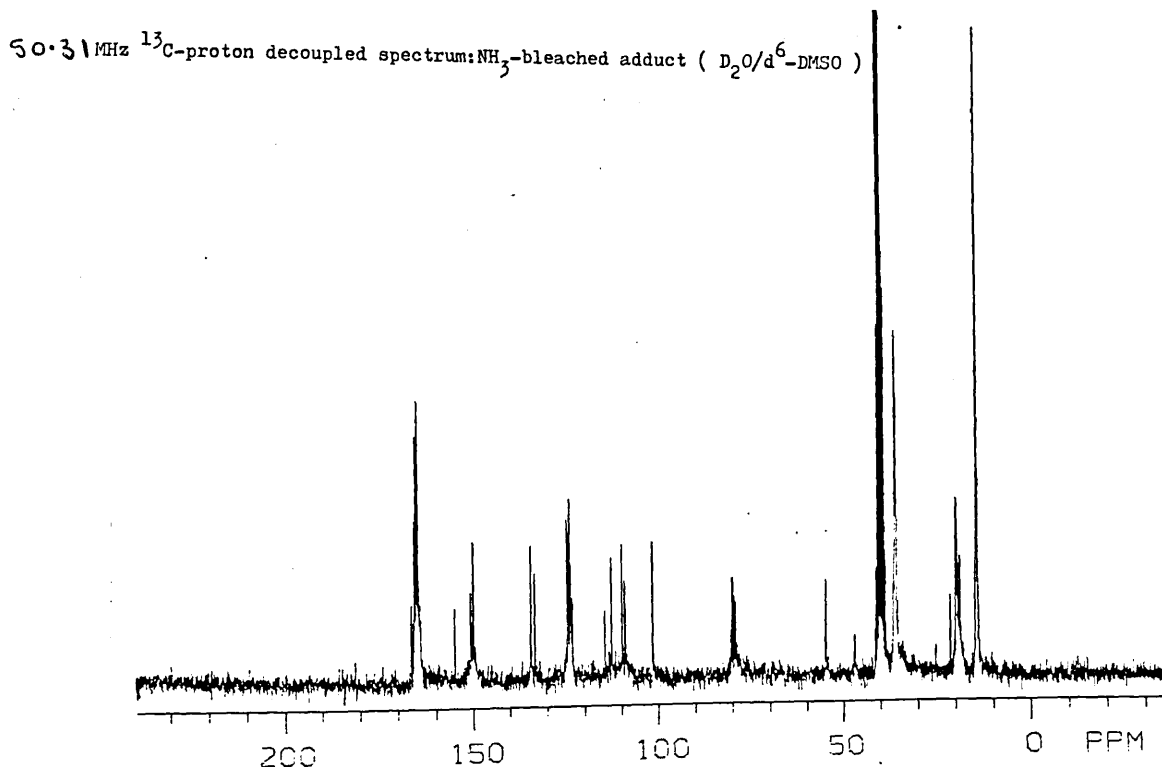
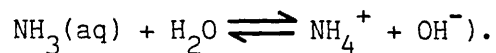
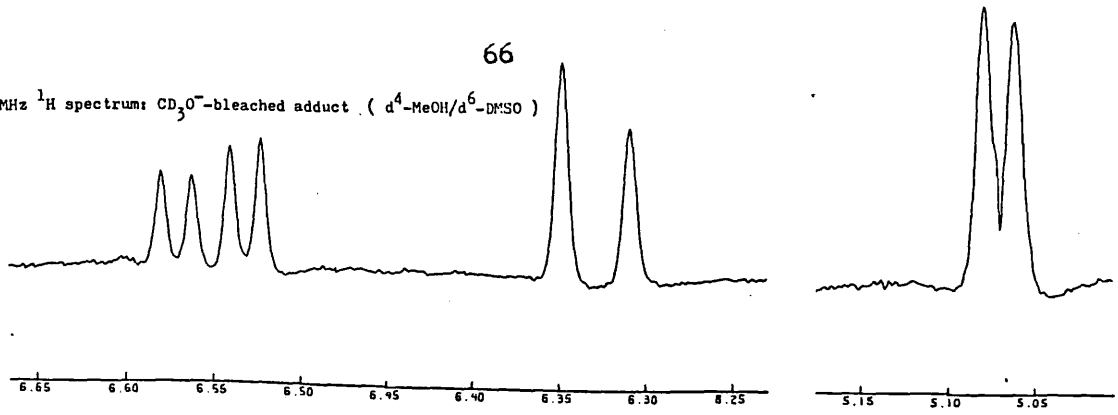


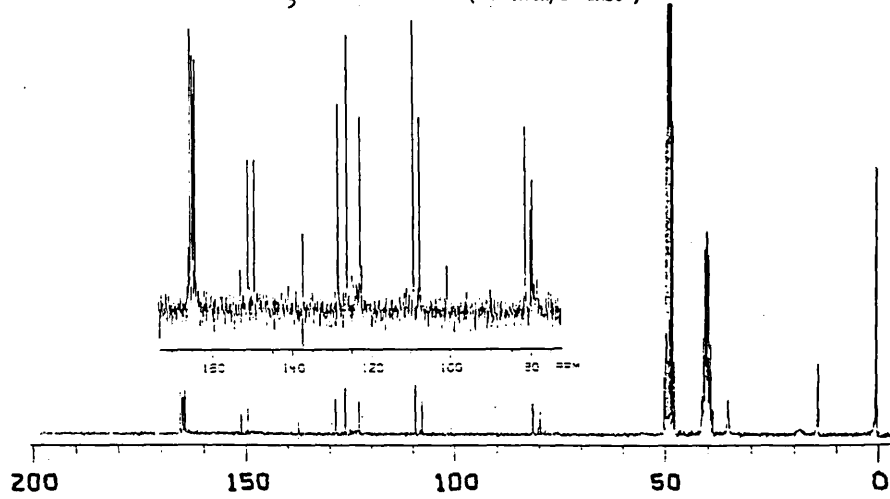
Figure 4.9

66

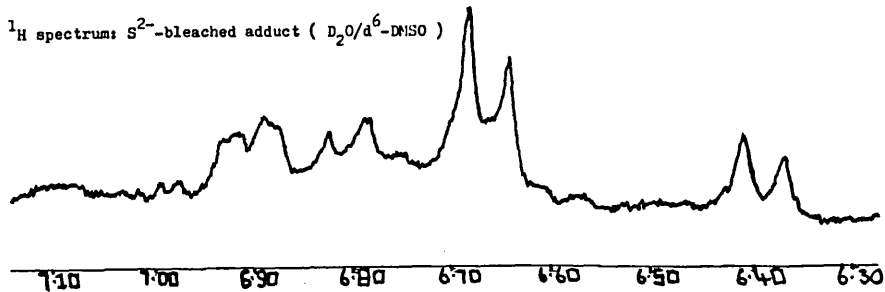
400.13 MHz ^1H spectrum; CD_3O^- -bleached adduct ($\text{d}^4\text{-MeOH/d}^6\text{-DMSO}$)



50.31 MHz ^{13}C -proton decoupled spectrum; CD_3O^- -bleached adduct ($\text{d}^4\text{-MeOH/d}^6\text{-DMSO}$)



400.13 MHz ^1H spectrum; S^{2-} -bleached adduct ($\text{D}_2\text{O/d}^6\text{-DMSO}$)



50.31 MHz ^{13}C -proton decoupled spectrum; EtNH_2 -bleached adduct ($\text{d}^6\text{-DMSO}$)

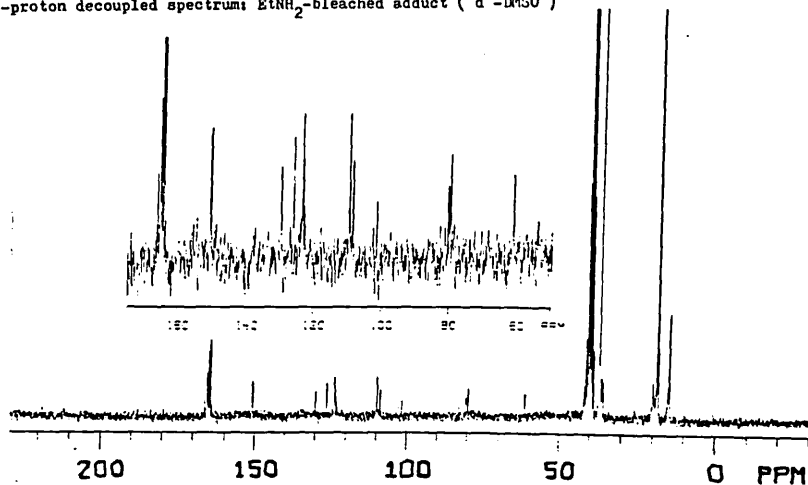
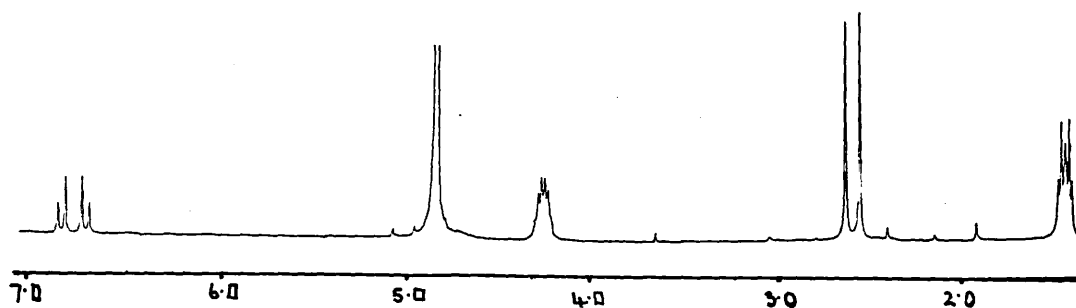


Figure 4.8

For the CN^- case the coupling of the methine bridge protons changed drastically, figure 4.10 (i). The most probable explanation being that the C(10) proton had deuterium exchanged leaving just the two non-equivalent bridge protons on carbons (11) and (12). The carbon-deuterium coupling is, however, not readily identifiable from the ^{13}C -proton decoupled spectrum, figure 4.10 (ii).

400.13 MHz ^1H spectrum: CN^- -bleached adduct ($\text{D}_2\text{O}/\text{d}^6\text{-DMSO}$)



100.60 MHz ^{13}C -proton decoupled spectrum: CN^- -bleached adduct ($\text{D}_2\text{O}/\text{d}^6\text{-DMSO}$)

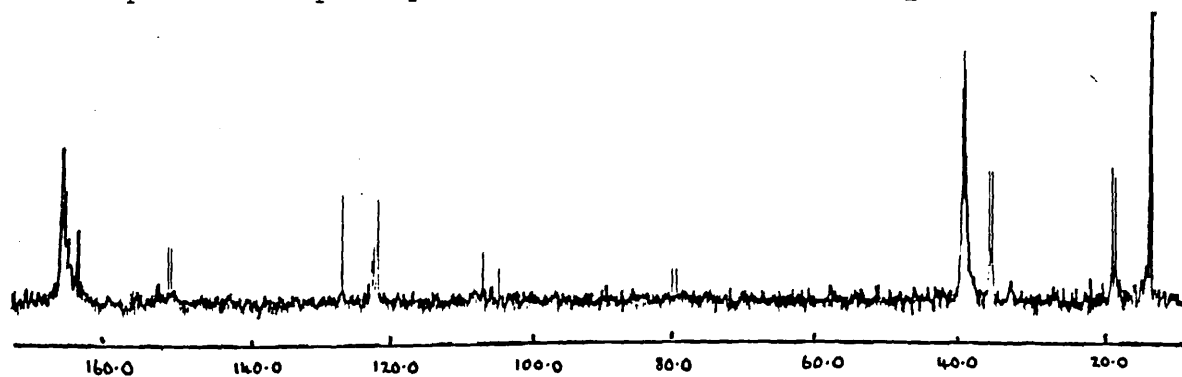
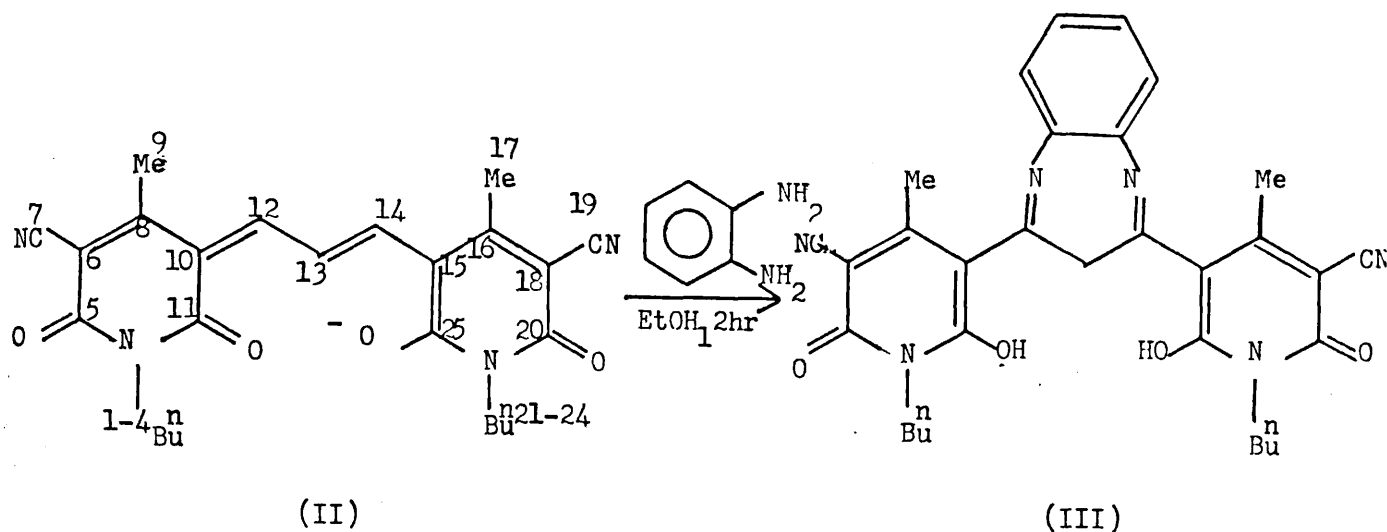


Figure 4.10

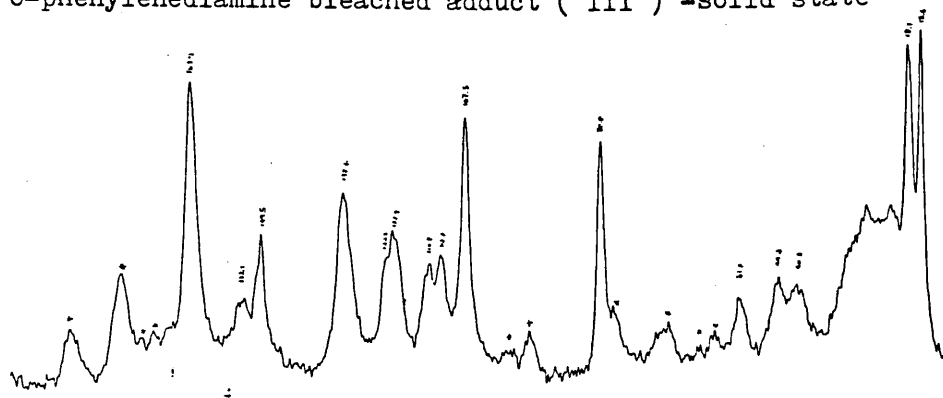
4.4 Trapping a Bleached Adduct

After many different approaches to trapping a bleached adduct we eventually had some success using *o*-phenylenediamine as the attacking nucleophile, Scheme 4.4. The pale blue adduct precipitated from a hot

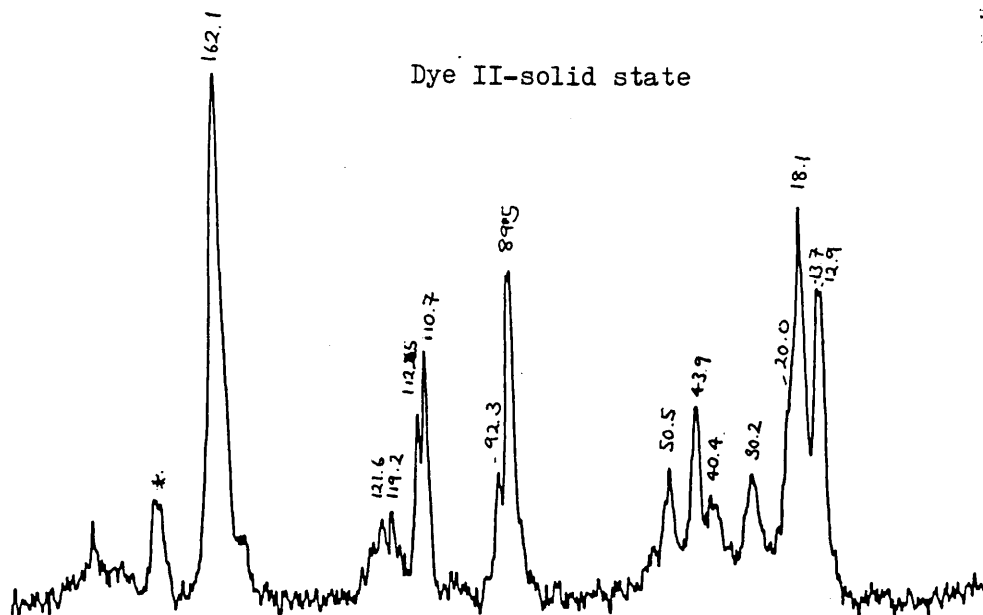


ethanolic solution (see 10.3.5). It was however found to be totally insoluble in all of the available deuterated n.m.r. solvents. Solid-state ^{13}C n.m.r. spectra of dye II and its *o*-phenylenediamine bleached adduct (III) were of limited use, however, addition peaks in the aromatic region are clearly visible, figure 4.11. Table 4.7 lists the assignment of the solution ^{13}C n.m.r. spectrum of dye II. The accurate top mass of 553

O-phenylenediamine bleached adduct (III) -solid state



Dye II-solid state



Dye II-22.5 MHz ^{13}C -proton decoupled spectrum (d^6 -DMSO)

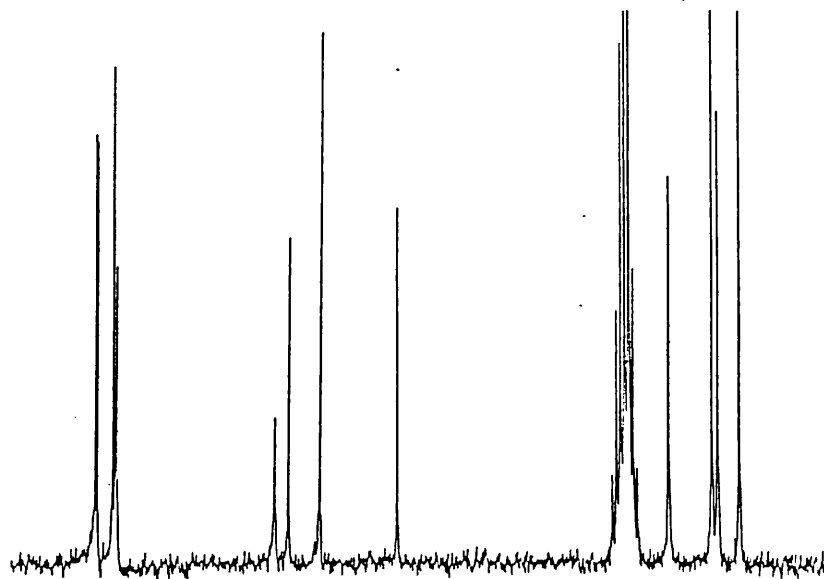


Figure 4.11

Table 4.7

$\delta(d^6\text{-DMSO, ppm})$	Assignment
13.58	C(1), C(24)
18.40	C(9), C(17)
19.76	C(2), C(23)
29.52	C(3), C(22)
38.49	C(4), C(21)
92.08	C(8), C(16)
110.22	C(10), C(15)
117.63	C(7), C(19)
120.82	C(13)
157.24	C(12), C(14)
157.95	C(6), C(18)
161.46	C(5), C(11)
161.92	C(20), C(25)

from mass spectrometry was consistent with a monoprotinated species of III. The elemental analysis was not wholly satisfactory however, attempts to further purify the adduct failed.

Michael-type addition at the methine bridge does appear to be the major process involved in the bleaching of these oxonol dyes. The kinetic and n.m.r. data, however, suggests that to consider this the only process is an over-simplification. A far more detailed investigation is obviously required to give a fuller understanding of this reaction.

CHAPTER 5

Electrical Properties of Semi-insulating and
and Semiconducting Materials5.1 Basic Classification²⁷.

From the electrical standpoint a material may be classified as a metal, a semiconductor or an insulator, depending on its conductivity, although the limits of conductivity which mark the boundaries between these classes are somewhat arbitrary. At room temperature, if the conductivity lies in the range $10^6 - 10^3 \Omega^{-1} \text{ cm}^{-1}$, the material is said to be a metal, and if it is lower than $10^{-12} \Omega^{-1} \text{ cm}^{-1}$ it is an insulator. Semiconductors have conductivities lying in the range $10^3 - 10^{-7} \Omega^{-1} \text{ cm}^{-1}$, although not all materials having conductivities within this range are semiconductors. Substances with conductivities in the range $10^{-7} - 10^{-12} \Omega^{-1} \text{ cm}^{-1}$ may be regarded as "poor" or "semi-insulators".

5.2 Band Theory^{27,28,29}.

To differentiate between various elements and compounds, in respect of their electrical conduction properties one needs only to consider electrons with energies in two bands - the "valence" and "conduction" bands. The valence band is the uppermost band which is filled or partially filled with electrons; the conduction band is the next higher band, which may be either empty or partially filled. Electrons in deeper lying levels, which are normally filled, play no part in the conduction process. Representative energy band diagrams for a metal (a), an insulator (b) and a semiconductor (c) are shown in figure 5.1.

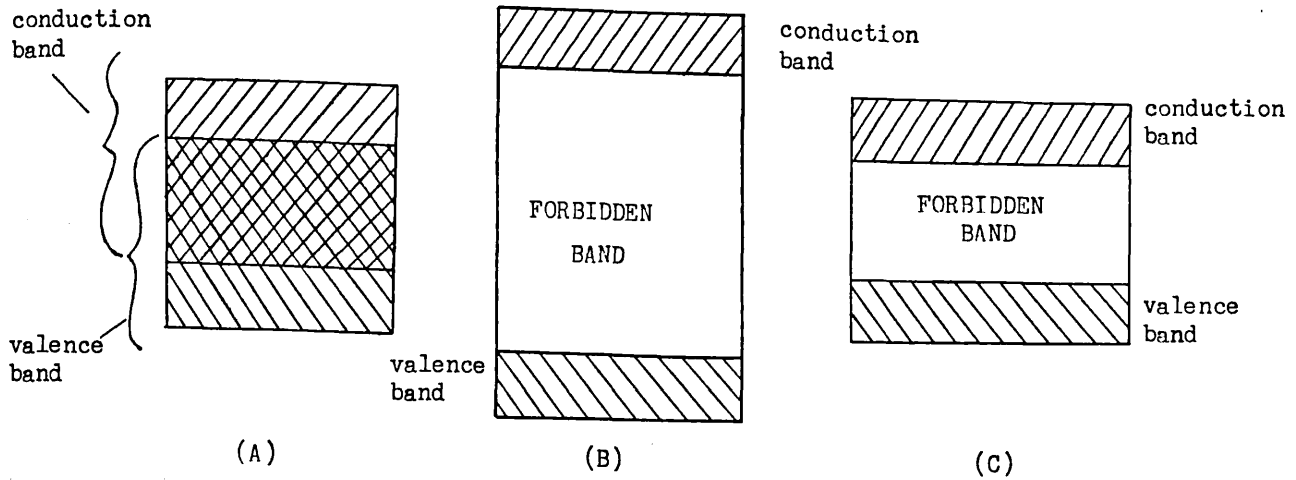


Figure 5.1

5.2.1 Metals

Metals are characterised by an upper energy band which is approximately half-filled. Such a band can originate for two reasons; (i) overlap can occur between the valence and conduction bands; (ii) the atoms may have insufficient valence electrons to fill the available states in the valence band (e.g. alkali metals).

Since vacant electron energy levels exist in close proximity to the levels which are occupied, electrons can be readily excited to higher levels when an electric field is applied and current can flow. The high conductivity of metals arises because of the large number of electrons with energies in the topmost partially filled band (approximately one per atom).

5.2.2 Insulators

If a material has a full valence band and an empty conduction band, which is separated by a forbidden band, then it is either an insulator or a semiconductor. An insulator is characterised by a conduction band which is virtually empty, both in thermal equilibrium and when an electric field is applied. This means that the forbidden gap separating the energy levels of the valence and conduction bands has to be so large that electrons cannot be excited from the valence to the conduction band. Such excitation could arise in thermal equilibrium if the forbidden gap was narrow enough. This is because the atoms of the solid are continually vibrating about their mean positions and some of this thermal vibrational energy is shared by the electrons. In the presence of an electric field valence electrons also absorb energy, but again, if this is less than the energy gap, they cannot be excited to the conduction band.

5.2.3 Intrinsic Semiconductors

If the valence and conduction bands are separated by a narrow forbidden energy gap, then at all temperatures above absolute zero there may be some electrons in the conduction band and some holes in the valence band of a pure crystal in thermal equilibrium i.e. even though no external exciting radiation or electric field is applied. Since the conduction band is then partially filled and the valence band partially empty, further energy can be absorbed from an external electric field by the electrons in the conduction band and the holes in the valence band. For such an "intrinsic" semiconductor the density n_i of electrons in the conduction band is equal to the density of p_i of holes in the valence band and both classes of carrier will contribute to the current.

5.2.4 Extrinsic Semiconductors

The usefulness of semiconductors in electronic devices is ultimately bound up, not with the pure or "intrinsic" type of semiconductor referred to above, but with the modifications brought about in such materials by incorporating relatively small percentages of selected impurities in the host crystal. The resulting material is known as an impurity or "extrinsic" semiconductor. The basic features of extrinsic semiconduction can be simply demonstrated with reference to germanium, which in pure form is an intrinsic semiconductor.



Figure 5.2

Germanium is tetravalent. In single crystal form each germanium atom is surrounded by four nearest neighbours at the corners of a regular tetrahedron. Each of the four valence electrons combines with a similar electron belonging to one of the near-neighbour atoms to form a covalent bond. This arrangement is shown diagrammatically in two dimensions in figure 5.2(a). Each pair of lines represents a covalent bond. In figure 5.2(b) the modification of this diagram is shown when one of the germanium atoms is replaced by a pentavalent atom such as arsenic. Only four of the five valence electrons of the arsenic atom can form covalent bonds, the fifth revolves around the arsenic nucleus in a loosely bound orbit. The microscopic energy band picture in the vicinity of the arsenic atom is illustrated in figure 5.3. A potential well has been

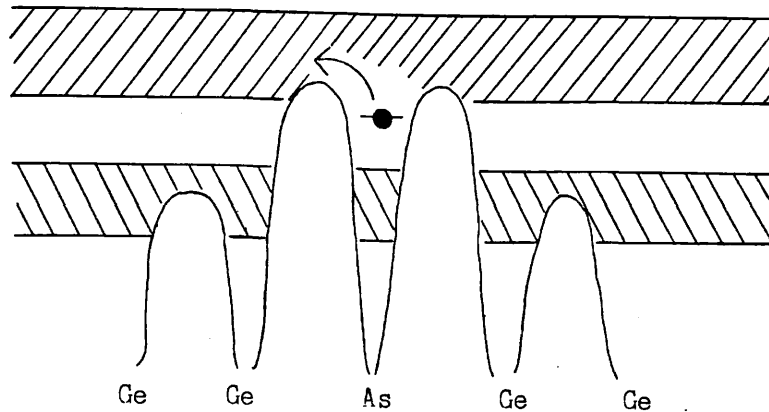


Figure 5.3

shown at the site of the arsenic atom, in which there is a localised electron energy level just below the bottom of the conduction band. At very low temperatures the fifth valence electron will occupy this level. Since the level is very near the bottom of the conduction band, however, only a small amount of thermal energy is required to excite this electron into the conduction band. The arsenic atom is then positively ionised and the liberated electron is free to move through the crystal.

A pentavalent atom like arsenic in the germanium lattice is called a "donor" impurity, since it has in effect donated a conduction electron. The associated name for the conductivity is "n-type" (electrons have a negative charge) with a concentration "n" of free electrons in the conduction band which exceeds the concentration p of holes in the valence band.

Trivalent atoms such as indium replacing germanium atoms produce a concentration of holes in the valence band which exceeds the

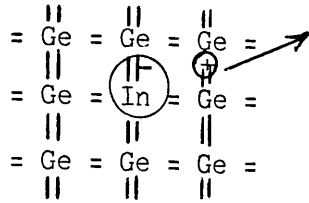


Figure 5.4

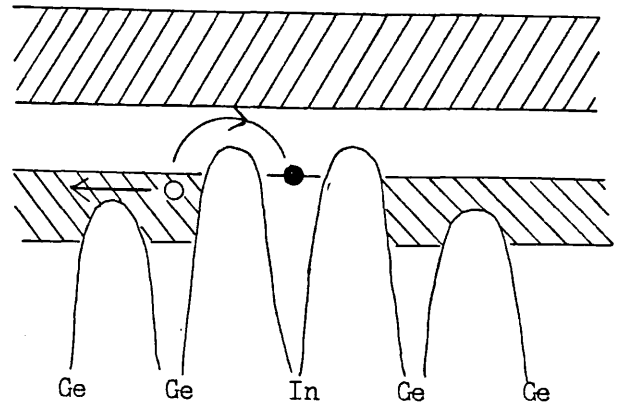


Figure 5.5

concentration of electrons in the conduction band. The resulting conductivity is called "p-type" (holes have positive charge). Such impurities are called "acceptors" since they accept an electron from the valence band in their ionised state. The mechanism is illustrated by figures 5.4 and 5.5.

In any practical semiconductor both donor and acceptor impurities will be present although, by design one impurity type is usually dominant. Since in thermal equilibrium the general tendency is for electrons to occupy the lowest levels, one finds that the acceptors are ionised as far as possible by the extra electrons available from donor atoms. In consequence, as far as impurity carrier density is concerned, this is of a type equivalent to the dominant impurity present. If the densities of donors and acceptors are N_d and N_a respectively then material for which $N_d > N_a$ is n-type and if $N_a > N_d$ it is p-type. If $N_a = N_d$ the material is said to be "compensated" and as far as free carrier densities are concerned will behave like intrinsic material. Its conduction properties will differ from intrinsic material, however, because of the extra scattering of free charges introduced by the ionised donor and acceptor atoms.

5.3 Distribution of Electrons and Holes in Energy States^{27,28}.

5.3.1 The Fermi-Dirac distribution function.

The Fermi-Dirac probability distribution function, $f(\epsilon)$, specifies the probability that an electron energy state at energy ϵ is occupied by an electron. Its form is

$$f(\epsilon) = \frac{1}{1 + \exp \{(\epsilon - \epsilon_F)/kT\}} \quad 5.1$$

where ϵ_F is the "Fermi level"; when $\epsilon = \epsilon_F$, then $f(\epsilon) = \frac{1}{2}$. An alternative interpretation of $f(\epsilon)$ is that the product $f(\epsilon)d\epsilon$ represents the average value of the fraction of all the states in an energy range, between ϵ and $\epsilon + d\epsilon$, which are occupied. The form of the Fermi-Dirac distribution is shown in figure 5.6 for three different temperatures; $T_1 = 0$ and $0 < T_2 < T_3$.

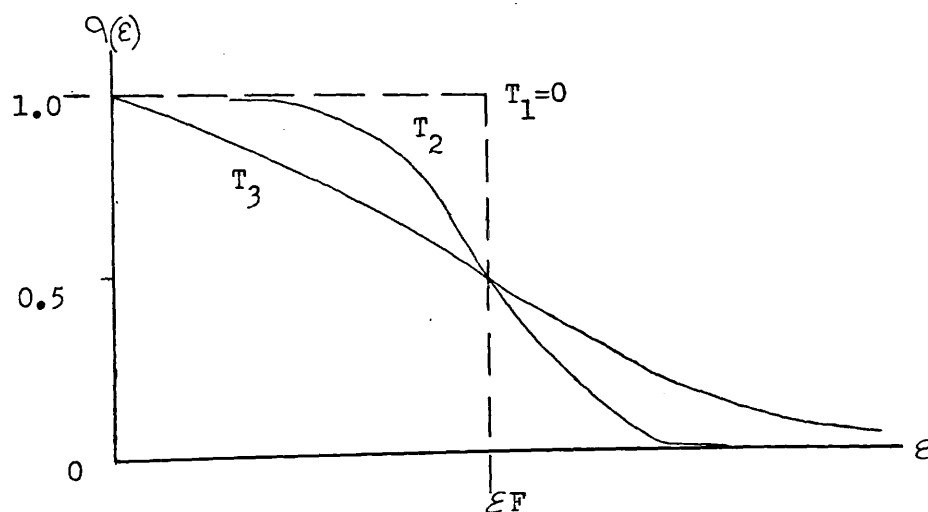


Figure 5.6

If ϵ is larger than ϵ_F by several times kT then the exponential term in the denominator is large compared with unity and $f(\epsilon)$ has the appropriate form

$$f(\epsilon) \approx \exp \{ -(\epsilon - \epsilon_F)/kT \} \quad 5.2$$

This approximate form is the same as the Maxwell-Boltzmann distribution, which applies to a gas. When applied to semiconductors it is referred to as the "classical approximation".

Clearly, if $f(\epsilon)$ is the fraction of quantum states at ϵ occupied by electrons, $1 - f(\epsilon)$ is the fraction left vacant or occupied by holes. Writing this as $f_h(\epsilon)$ one has, from equation 5.1.

$$f_h(\epsilon) = 1 - f(\epsilon) = \frac{1}{1 + \exp \{ (\epsilon_F - \epsilon)/kt \}} \quad 5.3$$

For $\epsilon \ll \epsilon_F$ by several units of kT this reduces to

$$f_h(\epsilon) \approx \exp \{ -(\epsilon_F - \epsilon)/kT \} \quad 5.4$$

The functions $f(\epsilon)$ and $f_h(\epsilon)$ discussed above simply indicate the probabilities that a quantum state at energy ϵ is occupied by an electron or a hole. The actual density of electrons or holes in a range of energy $d\epsilon$ at ϵ is given by the product of the appropriate probability function and the density of states function $N(\epsilon)$ at ϵ .

5.3.2 Density of energy states.

The electrons and holes which contribute significantly to conduction have energies near the bottom of the conduction band and near the top of the valence band, respectively. For most purposes it suffices therefore to determine the density of available states only in the vicinity of the edges of these bands. The energy versus wavenumber (k) relationships in these regions have the form

$$\epsilon_k = \frac{h^2 k^2}{8\pi^2 m} \quad 5.5$$

(where h is the Planck constant and m is the mass of the charge carrier) and are parabolic. If states specifically near the bottom of the conduction band are considered, at which the energy datum is taken as ϵ_c , then one can write

$$\epsilon - \epsilon_c = \frac{h^2 k^2}{8\pi^2 m_e^*} \quad 5.6$$

where m_e^* is the effective electron mass. If the incremental volume of k -space between k -values of k and $k + dk$ is considered; in the first Brillouin zone this is $4\pi k^2 dk$ if spherical symmetry is assumed. Since each electron state (not allowing for spin) occupies $8\pi^3/V$ of k -space where V is the volume of the crystal it follows that the number of energy states in this incremental volume of k -space, per unit volume of the

crystal is given by

$$dN = 2 \times \left\{ \frac{4\pi k^2 dk / (8\pi^3/V)}{V} \right\} = \frac{k^2 dk}{\pi^2} \quad 5.7$$

where the multiplying factor 2 takes account of the two possible directions of spin associated with each state. This equation may be rewritten

$$dN = \frac{k(kdk)}{\pi^2} \quad 5.8$$

and substitutions may be made for k and kdk (by differentiation) from equation 5.6. Hence, one obtains

$$dN = \left(\frac{4\pi}{h^3} \right) (2 e^{*\frac{3}{2}} (\epsilon - \epsilon_c)^{\frac{1}{2}}) d\epsilon \quad 5.9$$

as the number of energy states in the range of energy from ϵ to $\epsilon + d\epsilon$, per unit volume of the crystal. It follows that the number of electron energy states, per unit energy, per unit volume of the crystal can be specified as

$$N(\epsilon) = \frac{dN}{d\epsilon} \quad 5.10$$

so that from equation 5.9

$$N(\epsilon) = \left(\frac{4\pi}{h^3} \right) (2m_e^*)^{\frac{3}{2}} (\epsilon - \epsilon_c)^{\frac{1}{2}} \quad 5.11$$

A similar expression is obtained for the density of available electron states near the top of an energy band starting with

$$\epsilon - \epsilon_v = \frac{-h^2 k^2}{8\pi^2 m_h^*} \quad 5.12$$

and hence,

$$N(\epsilon) = \left(\frac{4\pi}{h^3} \right) (2m_h^*)^{\frac{3}{2}} (\epsilon_v - \epsilon)^{\frac{1}{2}} \quad 5.13$$

Here ϵ_v is the energy at the top of the valence band and m_h^* is the effective mass of a hole.

By combining the results of the two preceding sections it is possible to calculate the densities, i.e. numbers of electrons and holes per unit volume, having energies in the range ϵ to $\epsilon + d\epsilon$. The respective expressions are:

$$n(\epsilon) = f(\epsilon)N(\epsilon)d\epsilon \quad 5.14a$$

$$p(\epsilon) = f_h(\epsilon)N(\epsilon)d\epsilon \quad 5.14b$$

5.3.3 Intrinsic semiconductor

Figure 5.7 shows how, by applying the results of the above sections, the actual density distributions, $n(\epsilon)$ and $p(\epsilon)$, of electrons and holes respectively, can be determined from the Fermi-Dirac distribution function

and the density of states functions. The Fermi-Dirac function is plotted in part (a), the density of state functions in part (b) and the resultant curves, obtained by multiplying these, in part (c). The areas under the upper and lower curves of part (c) give the total electron and hole densities n and p respectively.

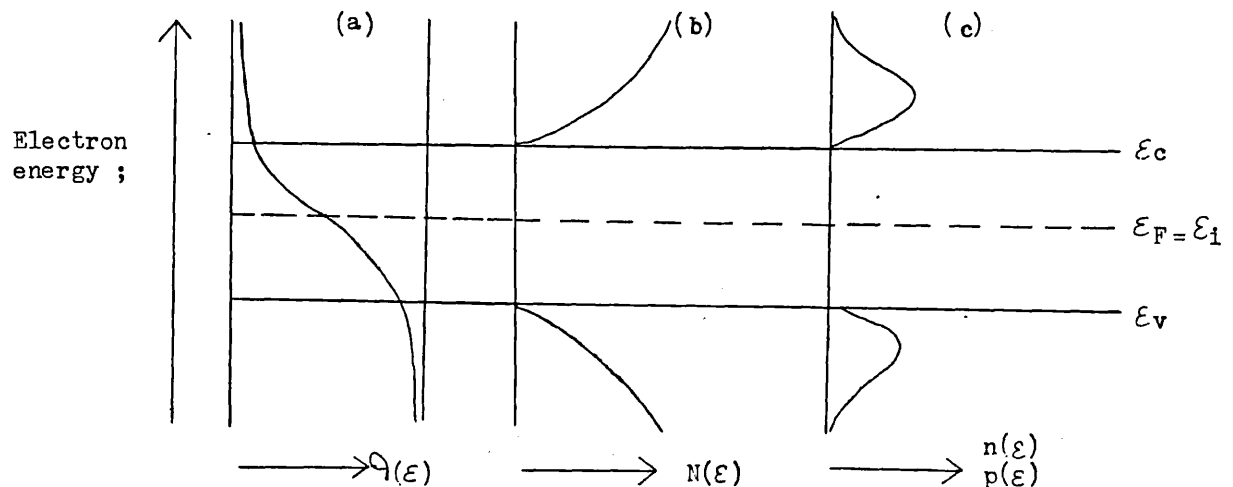


Figure 5.7

Expressions for n and p may be obtained analytically from equations 5.1 and 5.11 and 5.3 and 5.13 by integrating equations 5.14a and 5.14b respectively. Since intrinsic material contains equal densities of electrons and holes it can be assumed that the Fermi level is near the centre of the forbidden gap so that the energies of electrons in the conduction band are several units of kT higher than ϵ_F , provided that the energy gap, $(\epsilon_c - \epsilon_v) \gg kT$. In this case the classical

approximation for $f(\epsilon)$ can be used and

$$\begin{aligned} n_o &= \exp(\epsilon_F/kT) \int_{\epsilon_C}^{\epsilon_2} [4\pi(2m_e^*)^{\frac{3}{2}}/h^3](\epsilon - \epsilon_C)^{\frac{1}{2}} \exp(-\epsilon/kT) d\epsilon \\ &= \left\{ \exp[(\epsilon_F - \epsilon_C)/kT] 4\pi(2m_e^*)^{\frac{3}{2}}/h^3 \right\} \int_0^{\epsilon_2 - \epsilon_C} \exp(-\epsilon_1/kT) \epsilon_1^{\frac{1}{2}} d\epsilon_1 \end{aligned} \quad 5.15$$

where $\epsilon_1 = \epsilon - \epsilon_C$ and ϵ_2 is an energy level in the conduction band several units of kT above ϵ_C , at which the parabolic distribution for $N(\epsilon)$ is still valid and the suffix o is used to indicate the value of a quantity, in thermal equilibrium. The integral converges rapidly, because the exponential term in the integrand is dominant. Physically, this means that the probability of finding an electron in any state decreases rapidly the higher is the energy of the state. Hence $\epsilon_2 - \epsilon_C$ can be replaced by ∞ , whereby it is converted to a standard form, with a value $(\pi kT)^{\frac{1}{2}} kT/2$. Hence

$$n_o = 2(2\pi m_e^* kT/h^2)^{\frac{3}{2}} \exp\{-(\epsilon_C - \epsilon_F)/kT\} \quad 5.16$$

This is frequently written as

$$n_o = N_C \exp\{-(\epsilon_C - \epsilon_F)/kT\} \quad 5.17$$

where

$$N_C = 2(2\pi m_e^* kT/h^2)^{\frac{3}{2}} \quad 5.18$$

N_C is interpreted as the "effective density of states" in the

conduction band. The reason for this becomes clear when it is recognised that $\exp \{-(\epsilon_C - \epsilon_F)/kT\}$ is the value of the Fermi-Dirac function at the bottom of the conduction band. N_C can therefore be regarded as a localised density of states at this level.

A similar calculation may be carried out for hole density, and it is found that

$$p_O = N_V \exp \{-(\epsilon_F - \epsilon_V)/kT\} \quad 5.19$$

where

$$N_V = 2(2\pi m_h^* kT/h^2)^{\frac{3}{2}} \quad 5.20$$

Here N_V is the effective density of states for holes at the top of the valence band.

For intrinsic material $p_O = n_O$ and both are usually represented by the symbol n_i so that, from equations 5.18 and 5.20, one obtains

$$p_O n_O = n_i^2 = N_C N_V \exp \{-(\epsilon_C - \epsilon_V)/kT\} \quad 5.21$$

and therefore

$$n_i = \sqrt{N_C N_V} \exp \{-(\epsilon_C - \epsilon_V)/2kT\} \quad 5.22$$

Now d.c. conductivity (σ_O) for an intrinsic material is given by

$$\sigma_O = n_i e (\mu_e + \mu_h) \quad 5.23$$

where μ_e and μ_h are the mobilities of the electron and hole respectively, and e is the electronic charge.

Thus

$$\sigma_0 = [\sqrt{N_c N_v} e (\mu_e + \mu_h)] \exp \{ -(\epsilon_c - \epsilon_v)/2kT \} \quad 5.24$$

Now [] varies slowly with temperature compared with the exponential term of equation 5.24 and it can be regarded as substantially constant for some purposes. Therefore, in general, for an intrinsic material,

$$\sigma_0 = A \exp \{ - \Delta\epsilon/2kT \} \quad 5.25$$

where $\Delta\epsilon = \epsilon_c - \epsilon_v$ and is referred to as the "activation energy" or "band gap energy" (for an intrinsic material).

5.4 Conduction Mechanisms in Insulating Materials

Sections (5.2) and (5.3) have essentially discussed semiconductor theory and hence electronic conduction. Conduction is, however, neither solely specific to metals, and semiconductors nor restricted to being electronic in nature. A variety of conduction mechanisms exist which could be effective in insulators (dielectrics).

These are of particular interest to us, since many of our materials fall into the semi-insulating class.

5.4.1 Ionic conduction³⁰.

It is known that carriers, in insulators, have an inherently low mobility and move by some form of hopping. Ionic conduction is an extreme form of hopping and it occurs when the carriers (ions) jump through sites which are vacancies.

5.4.2 Space charge limited conduction³¹

Space charge limited conduction arises when the supply of carriers is electrode controlled and a copious injection of charges takes place from an electrode, regardless of the mobility of the charge carriers in the material. Space charge limited conduction can have a pronounced effect on the transport of charge in insulators at room temperature. This is particularly the case in the presence of an ohmic contact which facilitates the injection of charge into the insulator³². SCL conduction is characterised by a quadratic voltage-current response i.e. $I \propto (V^2/d^3)$.

5.4.3 Impurity conduction³⁰.

In impure insulators the wave function of the charge associated with the impurity centre is localised in the region of the centre. The wave functions of electrons of neighbouring impurity atoms overlap if there is a moderate concentration of impurities. In such cases a conduction process is possible in which the electrons move between centres without activation into the conduction band. This is known as impurity conduction.

5.4.4 Tunnelling³³.

There can arise situations when an energy barrier is too large for a charge carrier to surmount. In such cases carriers may prefer to pass through the material without changing their potential energies. This process is called tunnelling and requires the barrier thickness to be of the order of a localised wave function length.

5.4.5 Schottky Effect³⁰.

In the presence of high fields electron emission is possible from an electrode, which has a negative potential into the conduction band of the insulator. The high fields lower the metal-insulator interface barrier such that a thermally activated electron can easily pass over the barrier. The current density for such an emission is given by the Richardson-Schottky equation:

$$J = AT^2 \exp \{-\Phi/kT\} \exp \{\beta_s E^{\frac{1}{2}}/kT\} \quad 5.26$$

where A is a constant, Φ is the barrier height, T is the temperature and β_s is the Schottky barrier lowering coefficient with e the electronic charge.

5.4.6 Poole-Frenkel conduction.

The Poole-Frenkel mechanism is commonly used to explain high field currents in amorphous materials and in impure semiconductors³⁴. The effect is based on the lowering of the effective ionisation energy of a donor by the applied field. For an ionisation energy E_1 , the field-lowered value is $E_1 - \beta F^{\frac{1}{2}}$, where β is called the Poole-Frenkel constant. The current is given by

$$J = J_0 \exp \{(\beta F^{\frac{1}{2}}/kT) - (E_1/kT)\} \quad 5.27$$

Theoretically³⁵,

$$\beta = \left\{ \frac{q^3}{\pi \epsilon_0 \epsilon_r} \right\}^{\frac{1}{2}} \quad 5.28$$

where ϵ_0 is the permittivity of free space and ϵ_r the relative permittivity for low or high frequencies depending on whether the medium surrounding the donor can or cannot polarise within the emission time. At very low temperatures the carriers are emitted at constant energy by direct tunnelling into the conduction band, and at moderate temperatures carriers are emitted by thermally assisted tunnelling through the top of the potential barrier.

The Poole-Frenkel effect requires the presence of donor sites which may co-exist³⁵ with traps present in the forbidden gap. In general it is assumed that the potential surrounding a site is coulombic in nature and does not contain a screening factor, i.e. it falls off as the inverse distance measured from the site under consideration. This assumption gives a decrease in the potential barrier proportional to $E^{\frac{1}{2}}$ in the single site case.

The appearance of a linear region in a $\log I$ vs $V^{\frac{1}{2}}$ (or $E^{\frac{1}{2}}$) graph is considered³⁶ to be evidence for the presence of a Poole-Frenkel mechanism.

5.5 Organic semiconductors to organic metals^{37,38,39,40,41,42}

The electrical conductivity of most organic materials (when purified) is extremely low. However, strong π -molecular donor (D) and acceptor (A) molecules often react to form radical-ion salts (X^+A^-

and D^+X^-) and charge-transfer compounds (DA and D^+A^-) which have considerably higher conductivities. As may be seen in Table 5.1, the conductivities of some of the organic compounds resemble those of metals.

Table 5.1

Material	σ	n	μ
Ag	6.6×10^5	5.8×10^{22}	70
Cu	6.4×10^5	8.5×10^{22}	47
Hg	4.4×10^4	4.2×10^{22}	6.6
InSb	3.5×10^2		6.5×10^4
Si(n-type)	4×10^1	1×10^{18}	240
TCNQ salts	1 - 1000	$\approx 10^{21}$	4
Perylene I ₃	2×10^1	1.3×10^{20}	≈ 1
Anthracene	$\ll 10^{-14}$	$\ll 10^5$	≈ 1
Teflon	$\ll 10^{-14}$		

(All values at room temperature, σ = conductivity in $\Omega^{-1} \text{ cm}^{-1}$, n = density of carriers in cm^{-3} , and μ = mobility in $\text{cm}^2 \text{ V}^{-1} \text{ s}^{-1}$).

Charge-transfer complexes are formed from closed-shell molecules, are neutral in their ground state, and are characterised by weak van der Waals interactions. In the crystalline CT complexes, the donor and acceptor molecules stack in the order DA DA DA DA, as shown in figure 5.8 for perylene-fluoranil⁴³. These stacks are called "mixed" or

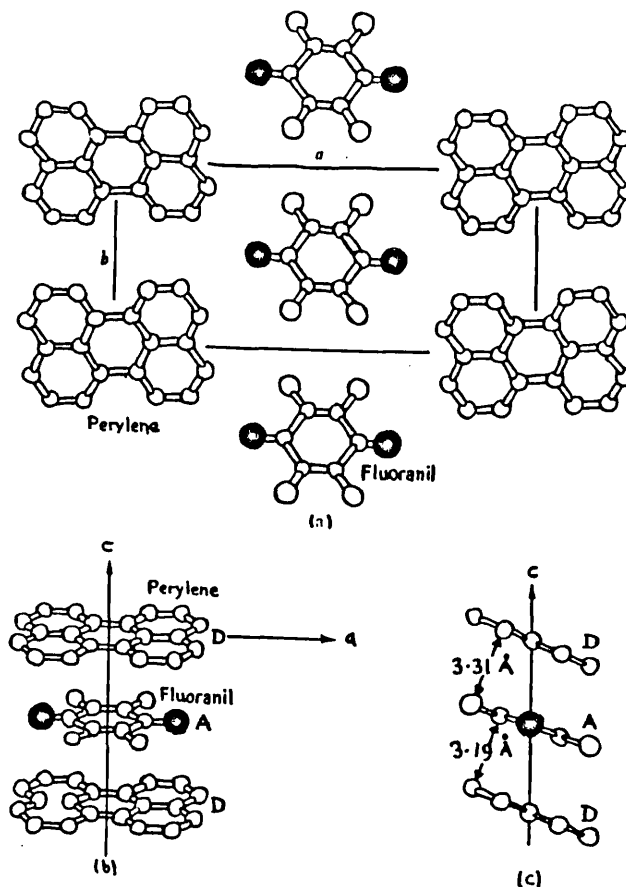


Fig. 5.8

"intercalated" stacks. The intermolecular spacing between the D and A molecules in the same stack is less than the 3.4 - 3.6 Å spacing that is characteristic of van der Waals solids.

The other class of D-A complexes consists of the radical-ion salts, e.g. the alkali metal-TCNQ salts and TTF-TCNQ (tetrathiafulvalene-tetracyanoquinodimethane) type salts⁴⁴⁻⁴⁸, shown in figure 5.9. In many

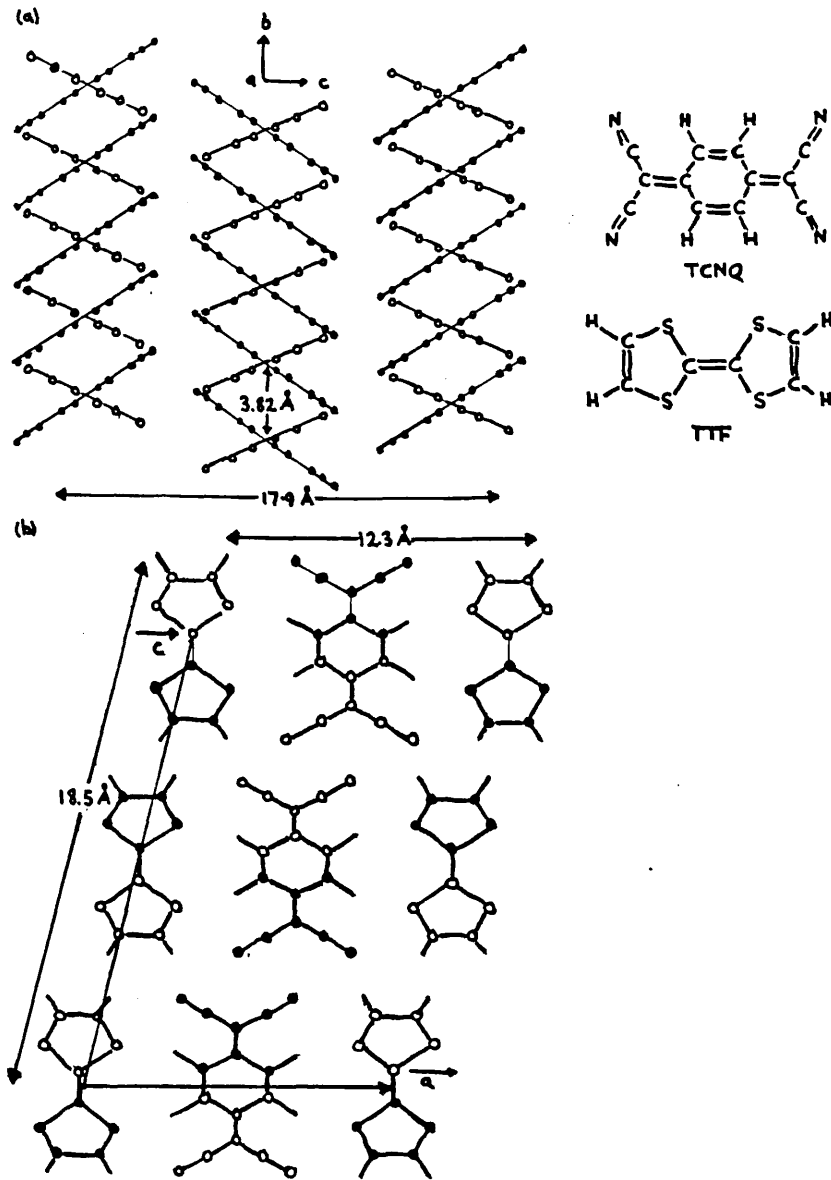


Figure 5.9

of the radical salts, the donors and acceptors are arranged in separate stacks, as shown in Figure 5.10.



Figure 5.10

In crystalline TTF-TCNQ the molecules in each stack are tilted with respect to the axis of the stack, and adjacent columns are arranged to form a herringbone pattern. A common feature of all radical ion salts and complexes is the planarity of the individual molecules. The metallic conductivities referred to in Table 5.1 appear only in those compounds in which D and A are in separate stacks. TTF-TCNQ, for example, has been referred to as an organic metal, and $(\text{TMTSF})_2\text{PF}_6$ (di-($\Delta^{2,2'}$ -bi-4,5-dimethyl-1,3-diselenole)-hexafluorophosphate) is a superconductor³⁹.

Organic radical-ion salts are of practical interest because they have already demonstrated superconductivity, and they are interesting theoretically because they exhibit a quasi-one-dimensional behaviour. As has been mentioned, the D and A molecules in single crystals of the radical-ion salts are often arranged in separate and parallel stacks, and the carrier motion seems to be confined mostly to the particular stack in which the carrier is generated. Occasionally, the carrier will hop out of its stack. If there were no forces of interaction between neighbouring stacks, this system would be truly 1-D and the conductivity would be zero in two directions; since there must be forces of attraction in order to form the crystal in the first place, the radical-ion salts are quasi-1-D systems. Nevertheless, these salts provide a convenient and challenging testing ground for 1-D theories.

In particular, the research in quasi-1-D crystals has been spurred by the hope of finding high-temperature superconductivity or high conductivity produced by some collective mechanism other than the quasi-Bose-Einstein condensation of Cooper-pairs⁴⁹. The idea that superconductivity might be found in conjugated aromatic compounds first appeared in the work of London⁵⁰ who looked upon the motion of the

electrons in the half-filled π -orbitals of the benzene molecule as being non-dissipating: the magnetic field generated by this motion had an appropriately diamagnetic character. Pursuing this concept, he then suggested that superconductivity is a manifestation of quantum behaviour on a macroscopic scale; he viewed the superconductivity as a gigantic molecule over which the charge was delocalised in unsaturated orbitals.

This idea was taken up and given greater relevance by Little⁵¹, who proposed that an attractive potential between conduction electrons could be mediated by an intramolecular polarisability, producing an effect similar to that of lattice phonons in the creation of Cooper-pairs. Little envisaged the constitution of a polymer-like molecule, consisting of a conducting spine and polarisable side groups; an electron travelling along the spine would polarise the side groups, and this polarisation could act as an attractive potential to the next electron coming along the spine. Figure 5.11 illustrates the superconducting backbone of a polymer chain and cyanine dye side groups initially suggested by Little.

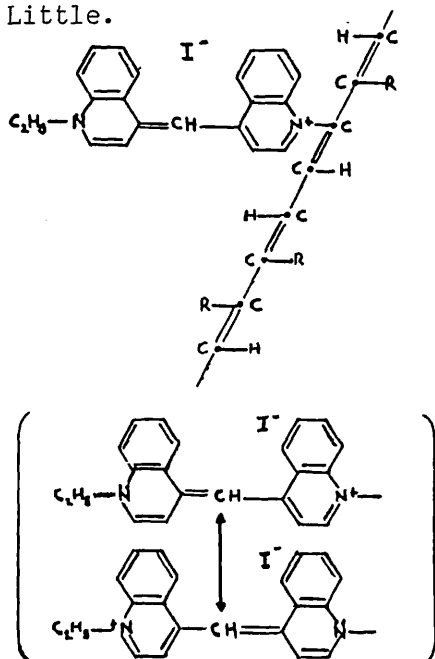


Figure 5.11

Although this material has not been made, several analogs of this polymer have been synthesised⁵², but unfortunately, none displays superconductivity.

The TCNQ salts which have a 1:1 composition ratio of cations to TCNQ (i.e. simple salts) and which have separate (segregated) cations and TCNQ stacks comprise $\approx 25\%$ of the known TCNQ compounds. Figure 5.12

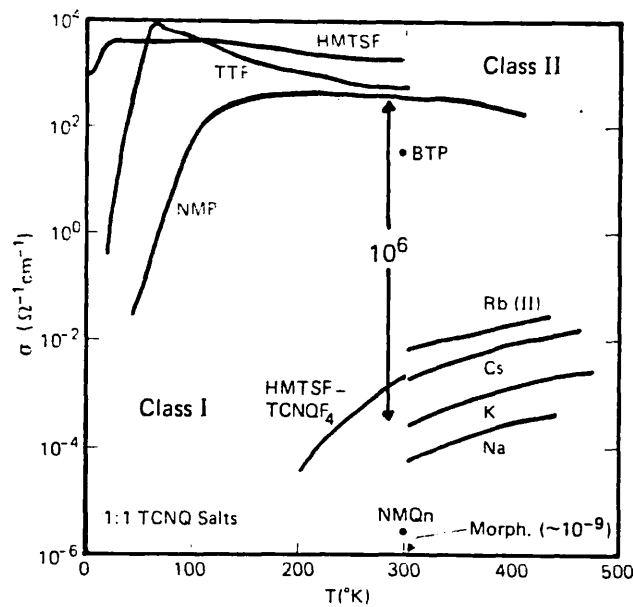
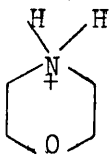
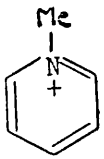
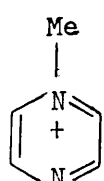
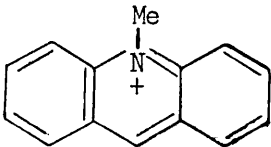


Figure 5.12

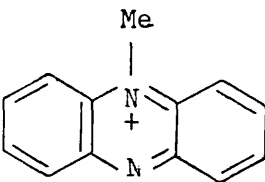
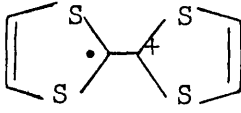
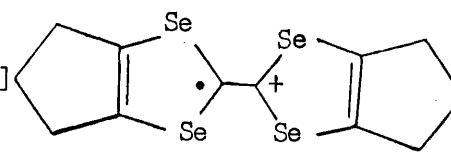
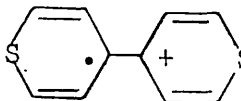
shows the dc conductivity data taken along the stacking axis of single crystals of a number of simple (1:1) TCNQ salts known to form segregated stacks. The cations of these salts are listed in Tables 5.2 and 5.3 along with a number of other examples³⁸.

Table 5.2

		$\sigma(\Omega^{-1}\text{cm}^{-1})$
Na ⁺		3×10^{-5}
(Li ⁺ , K ⁺ , Cs ⁺ , Rb ⁺)		$(10^{-4} - 10^{-6})$
Triethylammonium [TEA]	Et_3NH^+	10^{-9}
Ammonium	NH_4^+	2×10^{-5}
		
Morpholinium [Morph]		10^{-9}
N-methylpyridinium [NMPy]	Me 	10^{-5}
(pyridinium)		(10^{-6})
(4-cyano-NMPy)		(10^{-6})
	Me 	
N-methylpyrazinium [NMPyz]		3×10^{-8}
	Me 	
N-methylacridinium		2×10^{-5}
(NMAc)		

(Cations of Class I TCNQ salts with their 300 K powder conductivities).

Table 5.3

		$\sigma(\Omega^{-1}\text{cm}^{-1})$
N-methylphenazinium [NMP]		2
Tetrathiafulvalinium [TTF] (tetraselenafulvalinium [TSeF])		10 (18)
hexamethylene-TSeF[HMTSF]		25
Δ 4,4' bithiopyranium [BTP]		1

(Cations of Class II TCNQ salts with their 300 K powder conductivities).

On the basis of the magnitude of the conductivity, at say, 300 K, these salts separate into two distinct groups Class I salts are semiconducting and Class II salts have a very high conductivity, which initially increases with decreasing temperature below 300^o K, hence they are called "metallic" (even though they are generally not metallic at low temperatures).

There are many differences between, for example, K⁺ (Class I) and TTF⁺ (Class II) that could be responsible for the large difference in the conductivities of their TCNQ salts. The differences, however, are not so easily found for the N-methylacridinium (NMAd) vs. the N-methylphenazinium (NMP) salts of TCNQ where the cations differ only by one heterocyclic nitrogen.

Salts in both classes contain face-to-face stacks of TCNQ molecules with strong π -molecular overlap along the stacking direction, resulting in a large tight-binding charge-transfer integral, t . Both theoretical and experimental estimates of the electronic bandwidth, $4t$, are about 0.5 eV. One would think that, with one unpaired electron per TCNQ molecule in a simple non-interacting electron (or molecular orbital) theory, the band (or orbital) would be only half-filled and that, with such a large overlap, all of these materials should be potentially highly conducting. For this reason, some workers have approached the problem by asking; why are Class I salts poorer conductors?

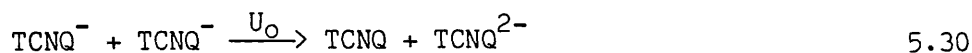
It has been suggested^{53,54} that distortions in the TCNQ stacks play an important role in the conductivity of these salts. Indeed, the X-ray crystal structures of K-, Na-, and Rb (phase I) - TCNQ show⁵⁵ that the spacing between the molecules in the stacks strongly alternates at 300 K while that in NMP- and TTF-TCNQ is uniform⁵⁶. Such a pairing of molecules or dimerisation would be expected for a simple Peierls transition and would be expected to make the distorted salts far less conducting than those with uniform stacks. Furthermore, the alkali-TCNQ salts have a phase transition at T_c , below which they are dimerised, but above which the stacks are uniform⁵⁵. For example, for K, Na and Rb (phase II), $T_c = 395, 345$ and 227 K, respectively, and yet above T_c , where the stacks are uniform, the conductivity is still at least four orders of magnitude lower than that of typical class II salts.

Thus, class I salts are semiconducting even when they have uniform stacks, and hence stack distortions cannot account fully for the large differences in conductivity.

In these materials, Coulomb interactions have important effects. The magnitude of the Coulomb repulsion energy between two electrons separated by a distance r is given by $e^2/r = 14.3 \text{ eV}/r$ (r is in Å). In these salts r is typically about 3 - 4 Å, and therefore the characteristic Coulomb energies are large, i.e., about 3 - 4 eV. If these repulsive interactions are not appreciably reduced in the solid, they will be larger than the bandwidth associated with delocalising the electrons on to adjacent molecules; the bandwidth, $4t$, is about 0.5 eV. The ground state of the $(\text{TCNQ}^-)_2$ dimer, for example, will then have the unpaired electrons localised on each TCNQ^- . The lowest excitation will be a charge-transfer excitation with an energy U given by

$$U = h\nu_{\text{CT}} = U_0 - V_1 \quad 5.29$$

U is thus the difference between the Coulomb repulsion energy (U_0) when two electrons are on the same TCNQ molecule and the repulsion (V_1) when they are on adjacent molecules. U_0 may also be viewed as the disproportionation energy of the reaction



Similarly, the unpaired electrons on a stack of TCNQ^- anions will be localised if the Coulomb interactions are large. The lowest excitation will also be a charge-transfer band, at an energy $h\nu_{\text{CT}} \approx U$ given by equation 5.29. Since the conductivity along the stack is achieved by exciting an electron down the stack, the conductivity will be limited by a large activation energy, $\approx U$. If the energy U is large (compared to $4t$), the material will be an insulator.

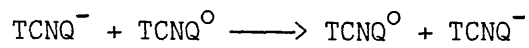
In close analogy with the mechanism for organic superconductivity proposed by Little⁵¹, Le Blanc⁵⁷ proposed that the excitonic polarisability of the cations of class II sufficiently reduces (screens) the repulsion interactions (U) on the TCNQ stacks so the U becomes small compared to the band width $4t$. In this event, the 300 K conductivity would become metallic for class II salts, while those of class I would remain semiconducting with large unreduced Coulomb energies U .

The differences in polarisability between NMA^+ and NMP^+ , however, cannot be large enough to be the most important difference between these salts. Therefore, the cations in Table 5.3 are apparently neither polarisable enough nor close enough to the TCNQ stack⁵⁸ to substantially decrease U .

On the basis of optical experiments, it was suggested⁵⁹ that the difference between classes was caused by a difference in the amount of charge, ρ , transferred from donor to TCNQ, i.e. that in class I salts this charge transfer is complete ($\rho = 1$) and the TCNQ molecules are completely reduced to TCNQ^- . For class II salts, on the other hand, it is suggested that the charge transfer is incomplete ($\rho < 1$), hence the TCNQ molecules are only partially reduced. For class I salts there is $\rho = 1$ unpaired electron on each TCNQ molecule and the lowest excitation corresponds to exciting an electron from TCNQ^- to a neighbouring (occupied) TCNQ^- molecule. This charge-transfer transition requires an energy $h\nu_{\text{CT}} \approx U$, as discussed earlier.

In class II salts, on the other hand, there are only electrons (with $\rho < 1$) transferred from the donor. Hence on a short time scale,

the stack may be viewed as containing both neutral TCNQ° and ionic TCNQ^{-} molecules. In such a mixed-valence stack, it is possible to excite an electron from TCNQ^{-} to a neighbouring neutral TCNQ° molecule, hence not having to overcome the strong Coulombic repulsion energy, U , as



shown schematically in figure 5.13.

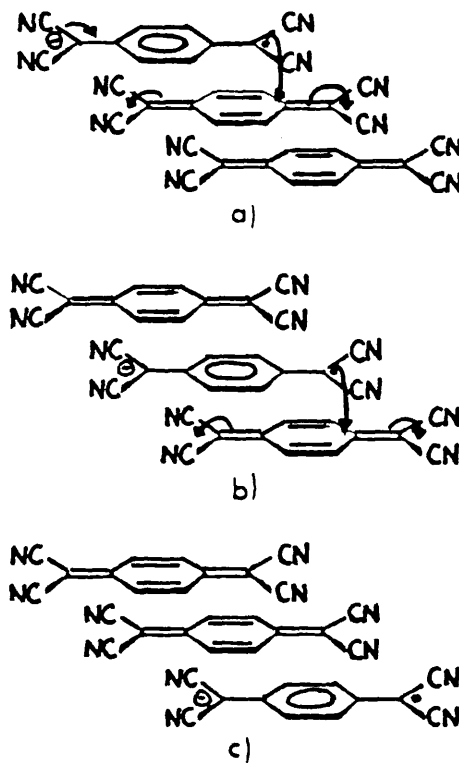


Figure 5.13

5.6. Aims and Objectives (electrically)

The crystal structure of the hydroxypyridone trimethine oxonol MI1579² showed the anions to be planar and ordered one above the other along the b axis with an interplanar separation of 3.67 Å, figure 5.14.

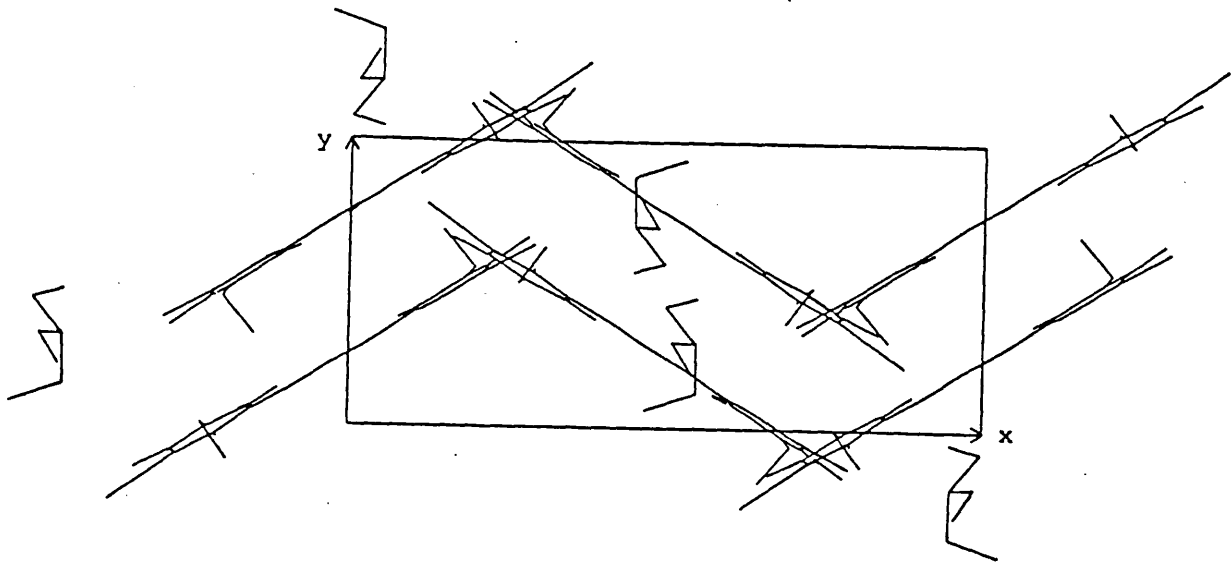


Figure 5.14

MI1579 was found to have a dc conductivity $\sigma = 5.75 \times 10^{-11} \Omega^{-1} \text{cm}^{-1}$ at 373 K (compacted powder). The insulating nature of MI1579, however, was not altogether surprising as in order for efficient electronic migration to occur an interplanar distance of less than or equal to van der Waals spacing (3.4 Å) would be required.

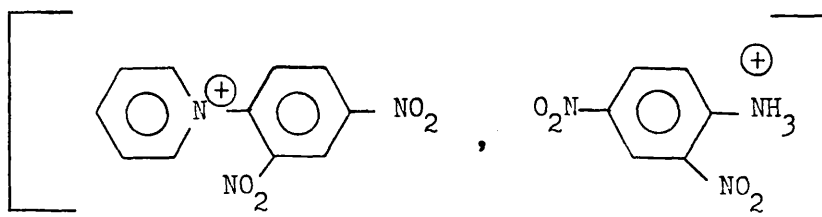
The result did, however, encourage us to look for ways of modifying the dye structure to improve the dc conductivity.

(a) In the short term this might have been achieved by:

i. shortening the N-alkyl substituent. From figure 5.14, the N-ethyl group did appear to hinder closest packing of the anions;

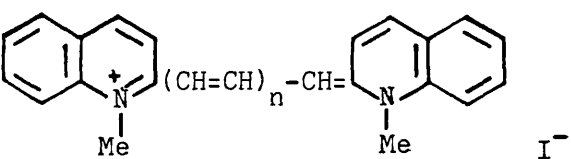
ii. introducing additional potential charge carriers. This would involve enriching the structures with π -electrons either via the cation

e.g.



or via the anion by introducing N-aryl substituents or by increasing the methine chain length. Increasing methine chain lengths had been shown to decrease thermal activation energies and increase dc conductivities in the cyanine dyes^{60,61}, Table 5.4.

Table 5.4



n	N	$\lambda_{\text{max}}/\text{nm}$	$\Delta\epsilon/\text{eV}$	$\sigma/\Omega^{-1}\text{cm}^{-1}$
1	8	605	1.8	2×10^{-13}
2	10	710	1.3	10^{-11}
3	12	817	0.69	1.3×10^{-8}

(N is the number of π electrons, $\Delta\epsilon$ the thermal activation energy and σ the conductivity).

iii. Introducing cations or anions with their own inherent conductivity; this would involve the synthesis of radical cation-oxonol dye salts.

(b) In the longer term we hoped to elucidate a general relationship between packing in the crystal and substituent and counter-ion changes. This would involve X-ray crystal structure determination and solid-state n.m.r. spectroscopy.

(c) It was also our intention to investigate conduction in insulating and semi-insulating materials as well as in the semiconductors using dielectric spectroscopy.

(d) The preparation of a range of solids by cocrystallisation of different anionic (oxonol) and cationic (cyanine) dyes, of similar molecular dimensions, in the hope of forming charge transfer complexes was also planned.

CHAPTER 6

Structural Studies in the Solid State

6.1. X-ray Crystal Structure Analyses

6.1.1. To our knowledge only two other oxonol dye crystal structures are known⁶². This, recent publication concerns co-crystals of cyanine and oxonol dyes. They show multiple morphology and have potentially interesting electrical and magnetic properties.

The most extensively studied photographic dyes, in terms of structure, are the cyanines and their analogues⁶³. The cyanines are spectral sensitizers, that is, their addition sensitizes silver halides to regions of the spectrum other than just the blue and violet. Their general formula is given in Figure 6.1. The molecular packing in

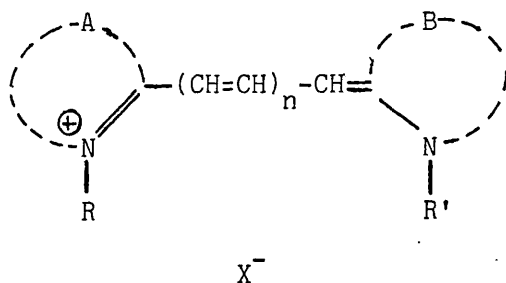


Figure 6.1

(A and B complete heterocyclic nuclei, which may be the same or different)

many of these crystals involves planar dye cations, with angles of less than 15° between planes defined by the two heterocyclic rings, packed plane to plane and end to end in layers. Examples include thiacyanine (I) (bromide⁶⁴ or TCNQ complex⁶⁵), phosphathiacyanine (II) perchlorate⁶⁶, 5,5',6,6'-tetrachlorobenzimidazolocarbo-cyanine (III) iodide⁶⁷ and the acetylenic dye IV 5,6-di-chloro-1,3-diethyl-2[(5,6-dichloro-1,3-diethyl-2-benzimidazolinylidene)-1-propynyl]-benzimidazolium p-toluenesulphonate⁶⁸, Figure 6.2 shows average bond lengths and angles for these four planar dyes and for the nonplanar imidazo[4,5,-b]-quinoxalinocyanine V iodide⁶⁹.

Steric interactions are often relieved by twisting about the central methine carbon. In V, for example, the reported angle of twist is 55° . Nearly equivalent bond lengths in the two heterocyclic rings for almost every symmetrical cyanine, even in the presence of significant distortion of the methine bridge, suggests that the charge on the dye is delocalised over the chromophore. The cation-cation arrangements of most interest have been those for 1,1'-diethyl-2,2'-quinocyanine chloride⁷⁰, 5,5',6,6'-tetrachloro-1,1',3,3'-tetraethylbenzimidazolocarbo-cyanine iodide⁶⁷ and 5,5'-dichloro-3,3',9-tri-ethylthiacarbo-cyanine bromide⁷¹. The heterocyclic rings of these three dyes have plane-to-plane orientations, and interplanar distances of 3.3 to 3.6 Å. The lateral shift of adjacent dye chromophores in the benzimidazole dye is 12 to 13 Å (Figure 6.3A). The atoms in the quinocyanine dye exhibit a more complex relationship, where the highly twisted chromophore introduces an inversion centre relating atoms of adjacent chromophores. In contrast

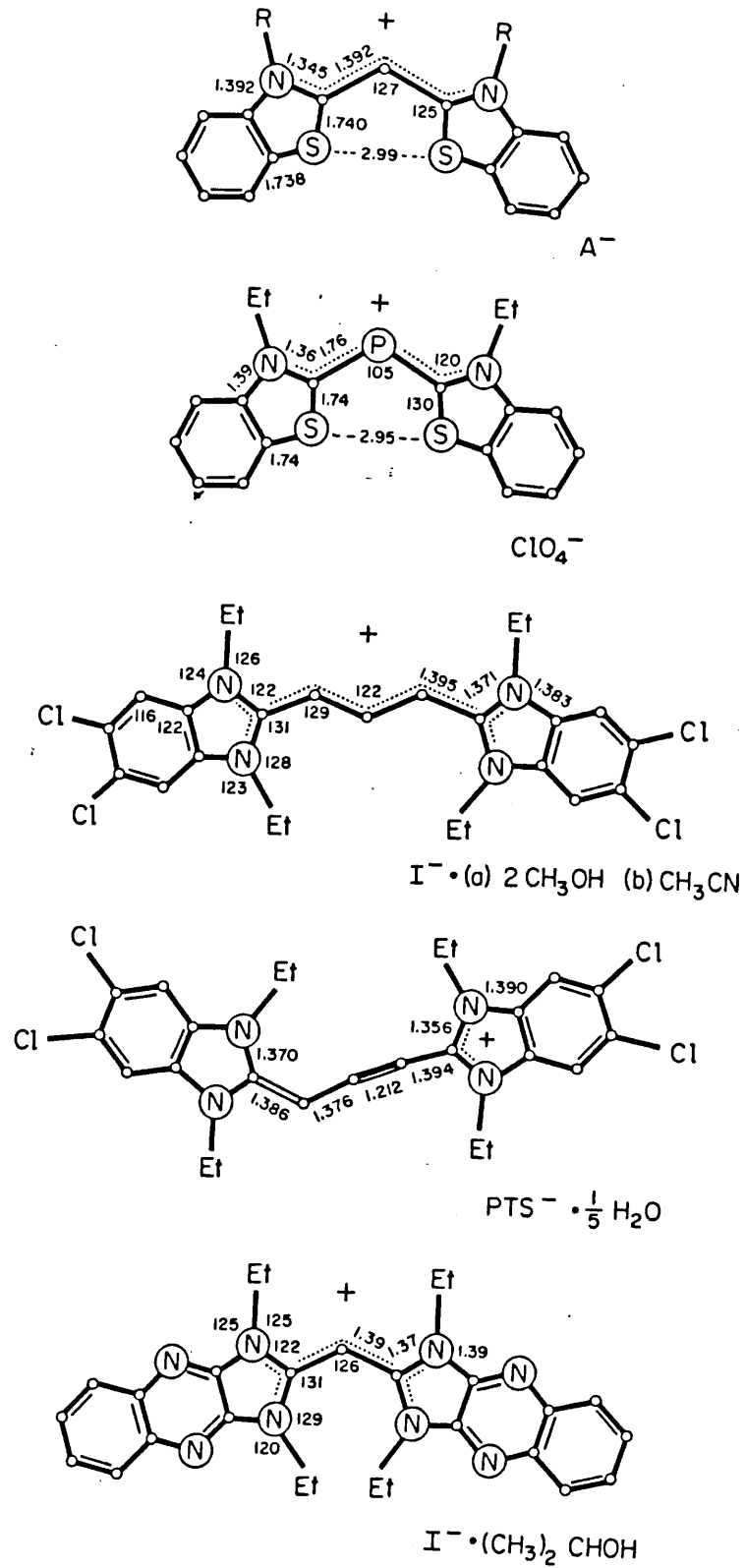


Figure 6.2

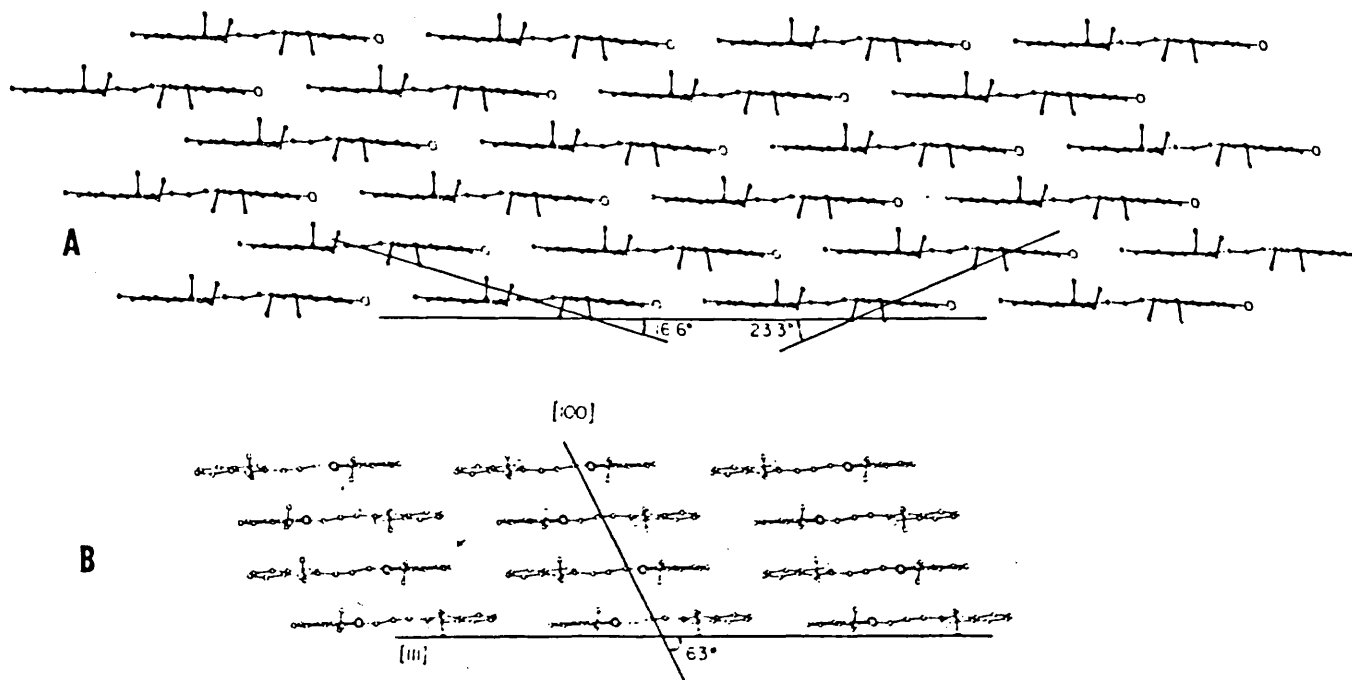


Figure 6.3

to this, 3,3'-diethylthiacarbocyanine^{72,73} (Fig. 6.3B) with similar interplanar distances (≈ 3.6 A) exhibits a lateral shift of adjacent chromophores of only 4.05 A. This lateral displacement of adjacent chromophores is highly influenced by substituents⁶³.

The structure determination of the hydroxypyridone trimethine oxonol (Ia), Fig. 6.4, carried out by Cheetham, Grossel and Johnson (unpublished results) reveals the anion to be highly planar (angle of

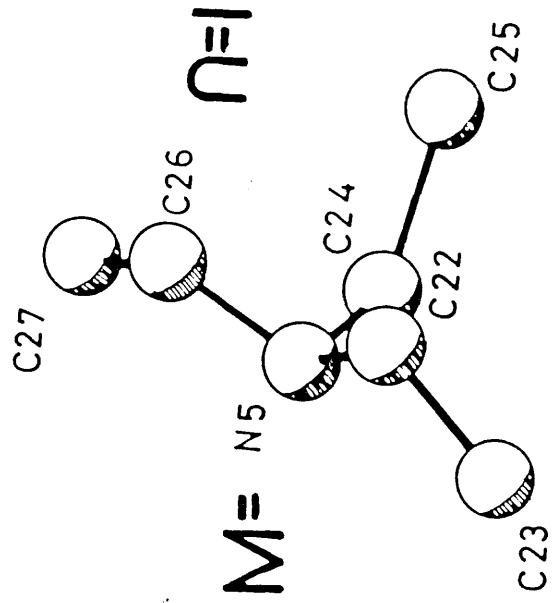
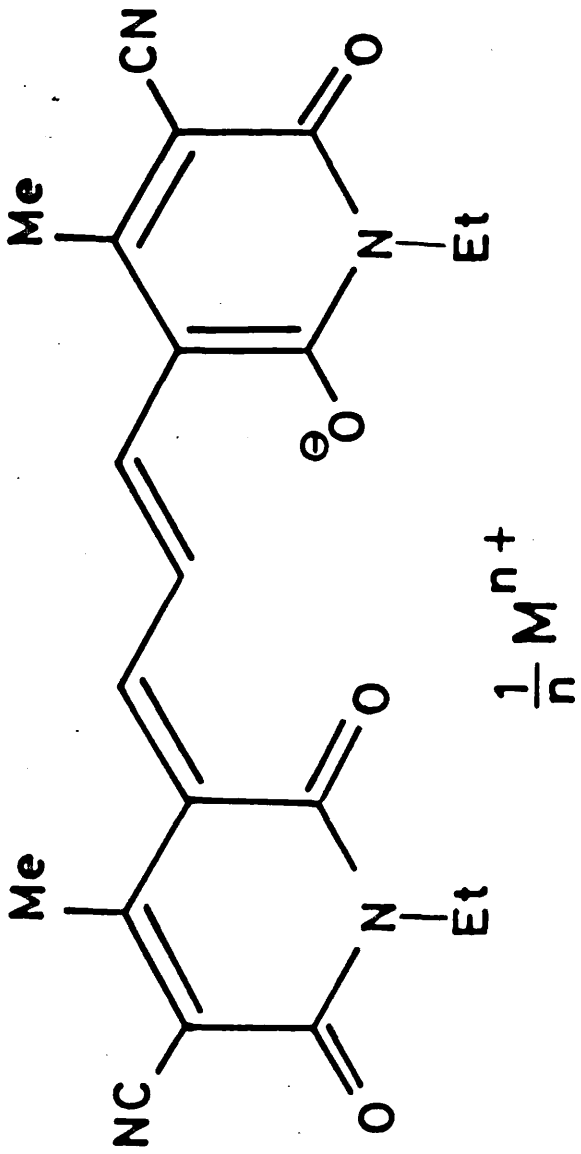


Figure 6.4

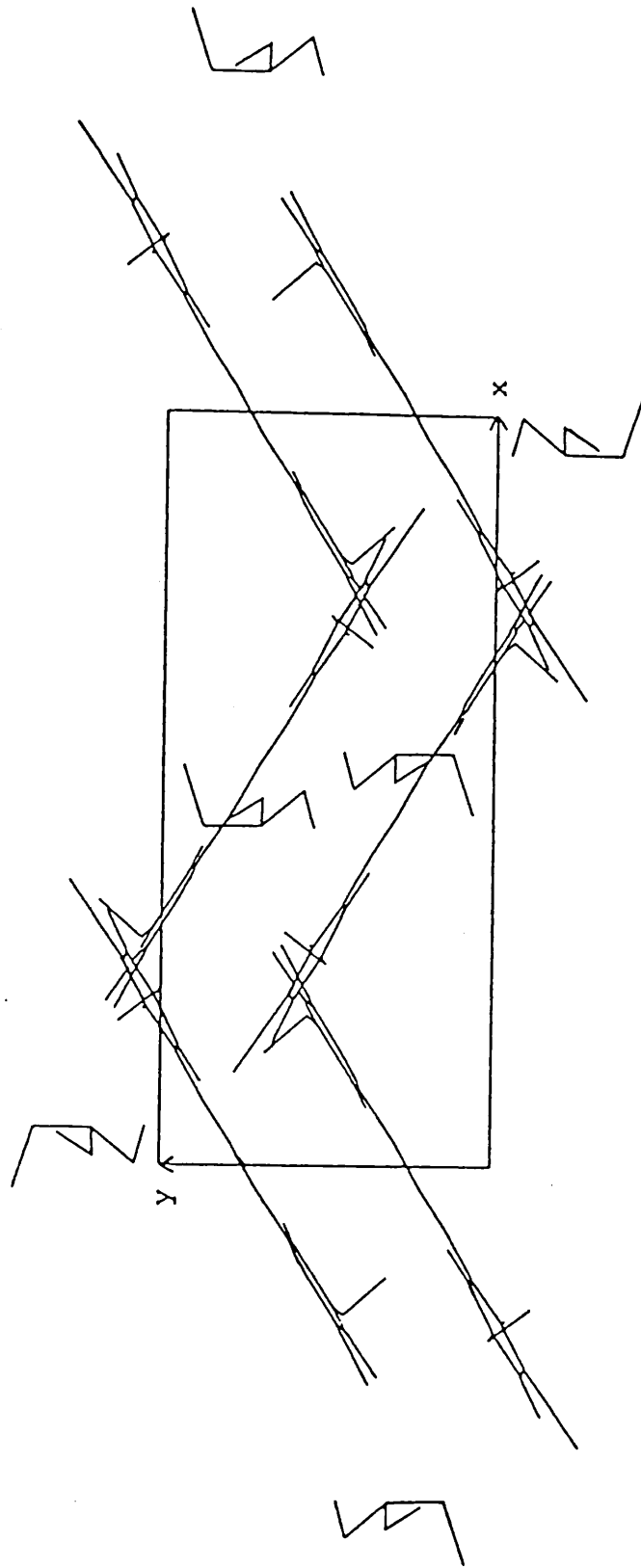


Figure 6.5

twist between planes defined by the two hydroxypyridone rings = 12°), Figure 6.5. This figure also shows the closest approach of the triethylammonium cation to the anion molecule. The interaction of the external hydroxypyridone ring oxygen and the nitrogen of the cation is presumably supplemented by hydrogen bonding, Fig. 6.6. It is also

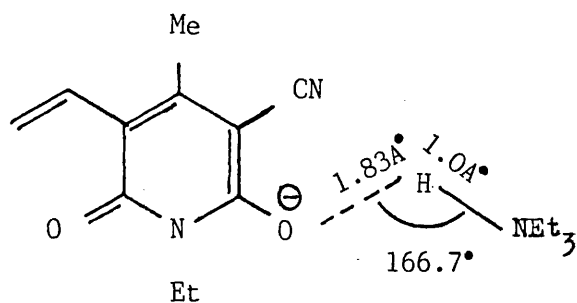


Figure 6.6

apparent that the anions stack in such a way as to minimise electrostatic repulsions between them and this is supported by the positions adopted by the associated cations, Fig. 6.7.

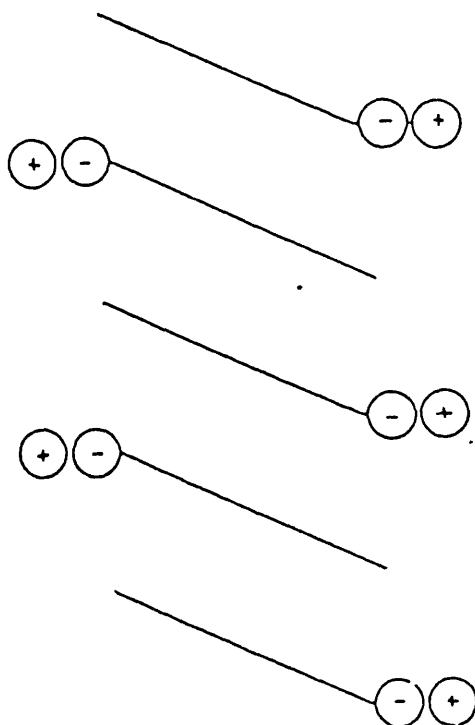


Figure 6.7

The perpendicular distance between the planes of two adjacent anions in the stack is 3.67 Å.

Like many of the cyanine dye structures this planar stacking arrangement lends itself to the possibility of intermolecular electronic charge transfer (van der Waals spacing in solids ≈ 3.4 Å). The semiconductivity of many of the simple cyanine dyes^{60,61} and the almost metallic conductivity of some of their TCNQ complexes⁷⁴ is well known. We therefore set out to investigate how we might modify the mode of packing in the hydroxypyridone oxonols. Our crystallographic studies, due to limited access to diffractometer facilities, were concentrated on the effects of cation variation on anionic stacking.

6.1.2 The structure of tetraphenylphosphonium 1-ethyl-3-cyano-6-hydroxy-4-methyl pyrid-2-one trimethine oxonol (Ib), Fig. 6.8.

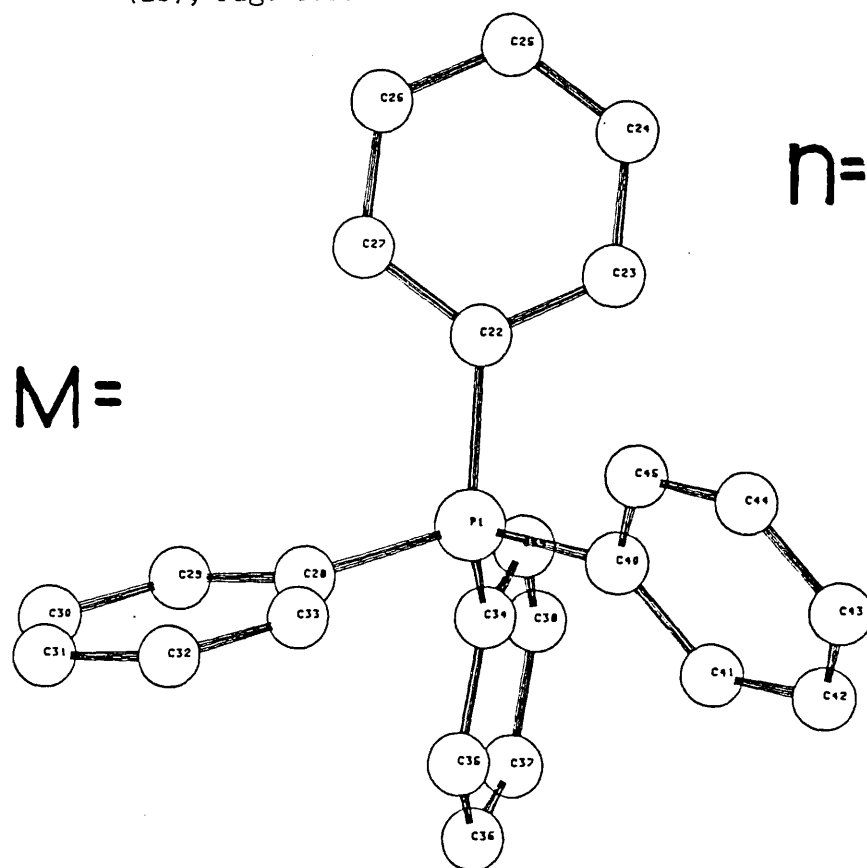


Figure 6.8

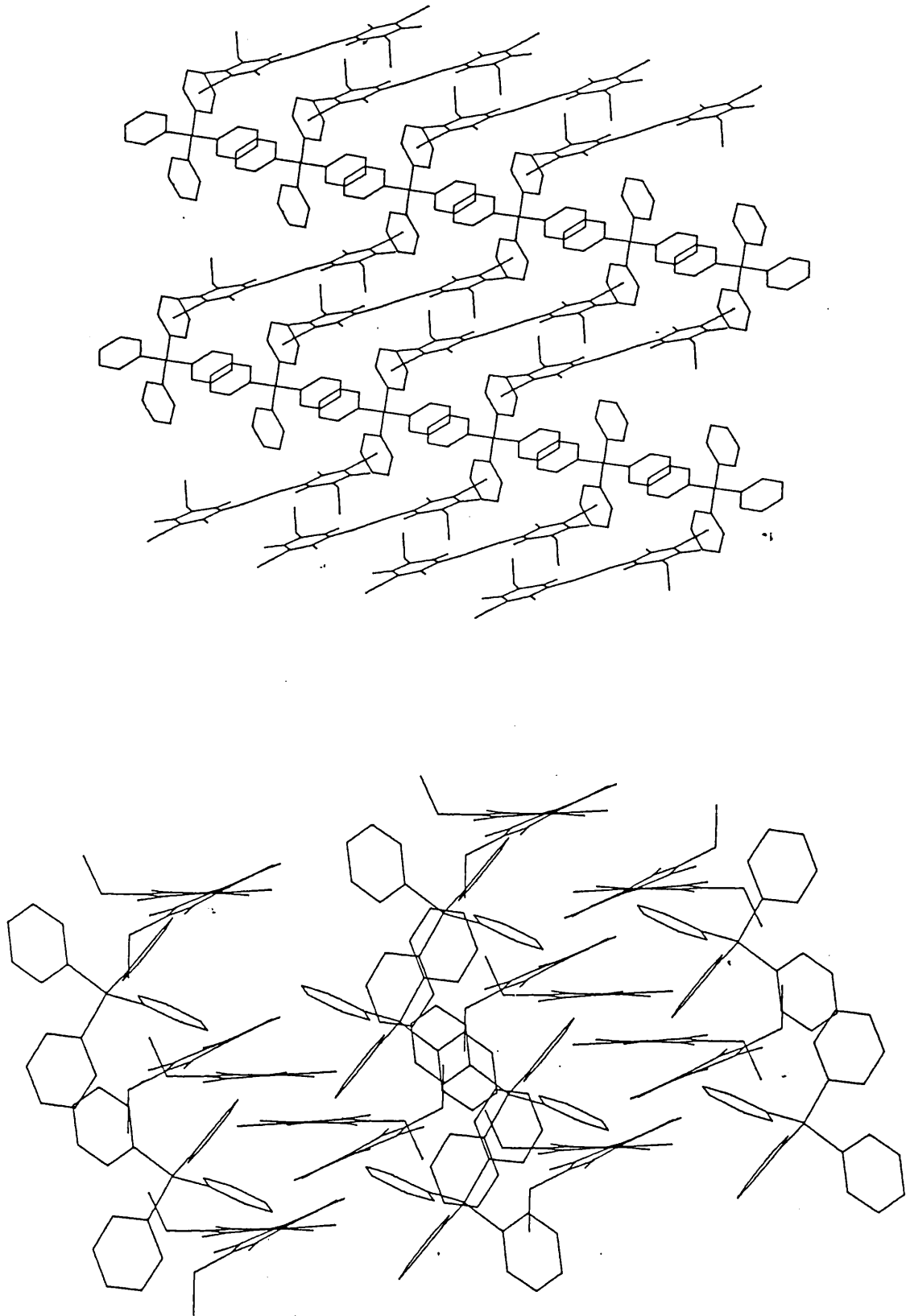


Figure 6.9

The anion is seen to be far less planar (angle of twist about methine bridge = 40.37°), Figure 6.9. Also the molecules of the anionic stack are infinitely parallel in contrast to the herringbone type arrangement in Ia. The interplanar distance has also increased to 4.06 Å.

The fractional atomic coordinates, anisotropic temperature factors, bond lengths and bond angles are listed in Tables 6.1, 6.2, 6.3 and 6.4 respectively.

Table 6.1.

Fractional atom co-ordinates for I(b), with estimated standard deviations in parentheses

Atom	x/a	y/b	z/c
C(1)	0.0091(6)	0.3888(7)	0.1045(6)
C(2)	0.1192(5)	0.3626(5)	0.0838(5)
C(3)	0.1868(4)	0.1726(4)	0.1332(4)
C(4)	0.2000(3)	0.0565(4)	0.1018(3)
C(5)	0.2600(4)	-0.0120(5)	0.1793(4)
C(6)	0.1558(3)	0.0129(4)	0.0062(3)
C(7)	0.1659(5)	-0.1116(5)	-0.0176(5)
C(8)	0.1007(3)	0.0866(4)	-0.0690(3)
C(9)	0.0947(3)	0.2070(4)	-0.0455(3)
C(10)	0.0506(3)	0.0430(4)	-0.1649(3)
C(11)	0.0000(0)	0.1027(6)	-0.2500(0)
C(22)	0.4898(3)	0.2984(4)	0.1337(4)
C(23)	0.5594(4)	0.2093(5)	0.1280(4)
C(24)	0.5539(5)	0.1414(5)	0.0377(5)
C(25)	0.4774(5)	0.1615(5)	-0.0466(5)
C(26)	0.4081(5)	0.2487(6)	-0.0396(4)
C(27)	0.4128(4)	0.3182(5)	0.0489(4)
C(28)	0.6117(4)	0.4798(4)	0.2536(4)
C(29)	0.6901(4)	0.4644(5)	0.1879(4)
C(30)	0.7750(4)	0.5403(5)	0.1972(5)
C(31)	0.7804(5)	0.6269(6)	0.2697(6)
C(32)	0.7009(6)	0.6408(6)	0.3345(6)
C(33)	0.6157(5)	0.5685(5)	0.3259(5)
N(1)	0.1342(3)	0.2428(3)	0.0575(3)
N(2)	0.3103(4)	-0.0656(5)	0.2400(4)
O(1)	0.2182(3)	0.2099(3)	0.2223(3)

Table 6.1 (continued)

O(2)	0.0547(3)	0.2804(3)	-0.1062(2)
P(1)	0.5000(0)	0.3872(1)	0.2500(0)
H(1)	-0.041(5)	0.376(7)	0.043(5)
H(2)	0.004(5)	0.476(6)	0.126(5)
H(3)	-0.017(5)	0.336(6)	0.162(5)
H(4)	0.167(4)	0.379(5)	0.150(4)
H(5)	0.149(4)	0.417(4)	0.029(4)
H(6)	0.208(4)	-0.123(5)	-0.101(4)
H(7)	0.091(5)	-0.154(5)	-0.023(5)
H(8)	0.210(5)	-0.149(6)	0.019(5)
H(9)	0.053(3)	-0.053(4)	-0.177(3)
H(10)	0.000(0)	0.188(5)	-0.250(0)
H(20)	0.611(4)	0.190(5)	0.187(4)
H(21)	0.609(4)	0.074(5)	0.028(4)
H(22)	0.487(4)	0.112(5)	-0.121(5)
H(23)	0.343(5)	0.259(5)	-0.099(5)
H(24)	0.359(4)	0.382(4)	0.053(4)
H(25)	0.691(3)	0.395(4)	0.136(3)
H(26)	0.830(4)	0.525(5)	0.145(4)
H(27)	0.850(4)	0.692(5)	0.269(4)
H(28)	0.691(5)	0.710(6)	0.390(5)
H(29)	0.558(5)	0.585(5)	0.377(4)

Table 6.2

The anisotropic temperature factors for the atoms of I(b),
with estimated standard deviations in parentheses

Atom	u[1,1]	u[2,2]	u[3,3]	u[2,3]	u[1,3]	u[1,2]
C(1)	0.0975(51)	0.0718(46)	0.0698(43)	-0.0126(38)	0.0053(39)	0.0237(40)
C(2)	0.0792(38)	0.0455(31)	0.0528(33)	-0.0105(21)	-0.0199(29)	0.0058(27)
C(3)	0.0459(27)	0.0522(30)	0.0422(25)	0.0021(22)	-0.0096(20)	0.0016(22)
C(4)	0.0381(24)	0.0486(27)	0.0371(24)	0.0071(21)	-0.0087(19)	0.0028(21)
C(5)	0.0568(30)	0.0596(33)	0.0468(28)	0.0040(26)	-0.0142(24)	0.0062(27)
C(6)	0.0361(23)	0.0435(25)	0.0367(23)	0.0055(20)	-0.0018(18)	0.0030(20)
C(7)	0.0600(32)	0.0451(29)	0.0547(31)	0.0018(25)	-0.0086(25)	0.0109(26)
C(8)	0.0351(22)	0.0399(25)	0.0308(22)	0.0031(18)	-0.0038(17)	0.0016(19)
C(9)	0.0408(24)	0.0417(25)	0.0349(22)	-0.0001(20)	-0.0030(18)	-0.0013(20)
C(10)	0.0402(23)	0.00396(26)	0.0360(23)	0.0005(20)	-0.0025(18)	-0.0002(20)
C(11)	0.0404(33)	0.0435(38)	0.0325(31)	0.0000(0)	-0.0045(25)	0.0000(0)
C(22)	0.0420(24)	0.00433(26)	0.0419(26)	-0.0010(21)	-0.0037(20)	0.0003(21)
C(23)	0.0475(29)	0.0515(31)	0.0633(33)	-0.0130(26)	-0.0149(25)	0.0108(24)
C(24)	0.0584(35)	0.0567(35)	0.0789(40)	-0.0233(30)	-0.0067(29)	0.0068(29)
C(25)	0.0734(38)	0.0696(39)	0.0541(34)	-0.0166(30)	-0.0029(28)	-0.0093(31)
C(26)	0.0730(38)	0.0787(42)	0.0455(30)	-0.0017(29)	-0.0173(27)	0.0009(33)
C(27)	0.0501(29)	0.0589(33)	0.0495(29)	0.0033(25)	-0.0084(23)	0.0131(26)
C(28)	0.0401(25)	0.0449(28)	0.0526(30)	0.00030(23)	0.0029(22)	-0.0018(21)
C(29)	0.0459(27)	0.0531(32)	0.0553(31)	0.0121(26)	0.0029(23)	0.0038(24)
C(30)	0.0608(37)	0.0635(40)	0.1003(52)	0.0231(37)	-0.0110(34)	-0.0247(33)
C(32)	0.0834(47)	0.0637(42)	0.1024(53)	-0.0134(40)	0.0190(33)	-0.0206(30)
C(33)	0.0623(38)	0.0583(35)	0.0842(43)	-0.0149(32)	0.0190(33)	-0.0206(30)
N(1)	0.05009(23)	0.0409(22)	0.0359(20)	-0.0030(17)	-0.0142(17)	0.0223(32)
N(2)	0.0964(39)	0.0837(39)	0.0715(34)	0.0105(30)	-0.0363(29)	0.0223(32)
O(1)	0.0840(29)	0.0689(26)	0.0434(20)	-0.0087(19)	-0.0272(19)	0.0068(22)
O(2)	0.0778(25)	0.0405(19)	0.0385(18)	0.0045(16)	-0.0140(17)	0.0022(18)
P(1)	0.0368(8)	0.0385(9)	0.0457(9)	0.0000(0)	0.0005(7)	0.0000(0)

Table 6.3

Bond lengths (A), with estimated standard deviations in parentheses for I(b)

C(1)-C(2)	1.499(9)
C(2)-N(1)	1.469(6)
C(3)-N(1)	1.389(5)
C(3)-O(1)	1.239(5)
C(3)-C(4)	1.441(6)
C(4)-C(5)	1.434(6)
C(4)-C(6)	1.383(6)
C(5)-N(2)	1.144(6)
C(6)-C(7)	1.508(7)
C(6)-C(8)	1.424(5)
C(8)-C(9)	1.456(6)
C(8)-C(10)	1.412(6)
C(9)-O(2)	1.236(5)
C(9)-N(1)	1.414(5)
C(10)-C(11)	1.393(5)
P(1)-C(22)	1.814(5)
C(1)-C(28)	1.773(5)
C(22)-C(23)	1.388(6)
C(22)-C(27)	1.406(6)
C(23)-C(24)	1.391(7)
C(24)-C(25)	1.397(7)
C(25)-C(26)	1.371(8)
C(26)-C(27)	1.383(7)
C(28)-C(29)	1.381(6)
C(29)-C(30)	1.409(7)
C(30)-C(31)	1.370(9)
C(31)-C(32)	1.382(9)
C(32)-C(33)	1.386(8)

TABLE 6.4

Bond Angles ($^{\circ}$) for I(b)

C(1)-C(2)-N(1)	112.7(5)	C(22)-C(23)-C(24)	119.9(5)
C(2)-N(1)-C(3)	119.0(4)	C(22)-C(27)-C(26)	119.2(5)
C(2)-N(1)-C(9)	116.9(4)	C(23)-C(24)-C(25)	120.2(5)
C(3)-N(1)-C(9)	124.1(4)	C(23)-C(22)-C(27)	119.8(5)
N(1)-C(3)-C(4)	116.2(4)	C(24)-C(25)-C(26)	119.5(5)
N(1)-C(3)-O(1)	120.4(5)	C(25)-C(26)-C(27)	121.4(5)
C(4)-C(3)-O(1)	123.5(4)	C(28)-C(29)-C(30)	118.3(5)
C(3)-C(4)-C(6)	122.9(4)	C(28)-C(33)-C(32)	119.6(6)
C(3)-C(4)-C(5)	114.7(4)	C(29)-C(30)-C(31)	121.2(6)
C(5)-C(4)-C(6)	122.3(5)	C(29)-C(28)-C(33)	120.9(5)
C(4)-C(5)-N(2)	178.2(6)	C(30)-C(31)-C(32)	119.6(6)
C(4)-C(6)-C(8)	119.4(4)	C(31)-C(32)-C(33)	120.5(6)
C(4)-C(6)-C(7)	120.0(4)		
C(7)-C(6)-C(8)	120.6(4)		
C(6)-C(8)-C(9)	119.5(4)		
C(6)-C(8)-C(10)	120.3(4)		
C(9)-C(8)-C(10)	120.2(4)		
C(8)-C(9)-N(1)	117.3(4)		
C(8)-C(9)-O(2)	125.8(4)		
N(1)-C(9)-O(2)	116.9(4)		
C(8)-C(10)-C(11)	128.1(5)		
C(10)-C(11)-C(12)	119.2(6)		
C(22)-P(1)-C(28)	111.6(4)		
C(22)-P(1)-C(40)	104.2(4)		
C(28)-P(1)-C(34)	109.9(4)		
P(1)-C(22)-C(23)	119.5(4)		
P(1)-C(22)-C(27)	122.7(4)		
P(1)-C(28)-C(29)	121.9(5)		
P(1)-C(28)-C(33)	117.7(5)		

TABLE 6.4

Bond Angles ($^{\circ}$) for I(b)

C(1)-C(2)-N(1)	112.7(5)
C(2)-N(1)-C(3)	119.0(4)
C(2)-N(1)-C(9)	116.9(4)
C(3)-N(1)-C(9)	124.1(4)
N(1)-C(3)-C(4)	116.2(4)
N(1)-C(3)-O(1)	120.4(5)
C(4)-C(3)-O(1)	123.5(4)
C(3)-C(4)-C(6)	122.9(4)
C(3)-C(4)-C(5)	114.7(4)
C(5)-C(4)-C(6)	122.3(5)
C(4)-C(5)-N(2)	178.2(6)
C(4)-C(6)-C(8)	119.4(4)
C(4)-C(6)-C(7)	120.0(4)
C(7)-C(6)-C(8)	120.6(4)
C(6)-C(8)-C(9)	119.5(4)
C(6)-C(8)-C(10)	120.3(4)
C(9)-C(8)-C(10)	120.2(4)
C(8)-C(9)-N(1)	117.3(4)
C(8)-C(9)-O(2)	125.8(4)
N(1)-C(9)-O(2)	116.9(4)
C(8)-C(10)-C(11)	128.1(5)
C(10)-C(11)-C(12)	119.2(6)
C(22)-P(1)-C(28)	111.6(4)
C(22)-P(1)-C(40)	104.2(4)
C(28)-P(1)-C(34)	109.9(4)
P(1)-C(22)-C(23)	119.5(4)
P(1)-C(22)-C(27)	122.7(4)
P(1)-C(28)-C(29)	121.9(5)
P(1)-C(28)-C(33)	117.7(5)
C(22)-C(23)-C(24)	119.9(5)
C(22)-C(27)-C(26)	119.2(5)
C(23)-C(24)-C(25)	120.2(5)
C(23)-C(22)-C(27)	119.8(5)
C(24)-C(25)-C(26)	119.5(5)
C(25)-C(26)-C(27)	121.4(5)
C(28)-C(29)-C(30)	118.3(5)
C(28)-C(33)-C(32)	119.6(6)
C(29)-C(30)-C(31)	121.2(6)
C(29)-C(28)-C(33)	120.9(5)
C(30)-C(31)-C(32)	119.6(6)
C(31)-C(32)-C(33)	120.5(6)

6.1.3 The structure of tetrabutylammonium 1-ethyl-3-cyano-6-hydroxy-4-methyl pyrid-2-one trimethine oxonol (Ic), Figure 6.10.

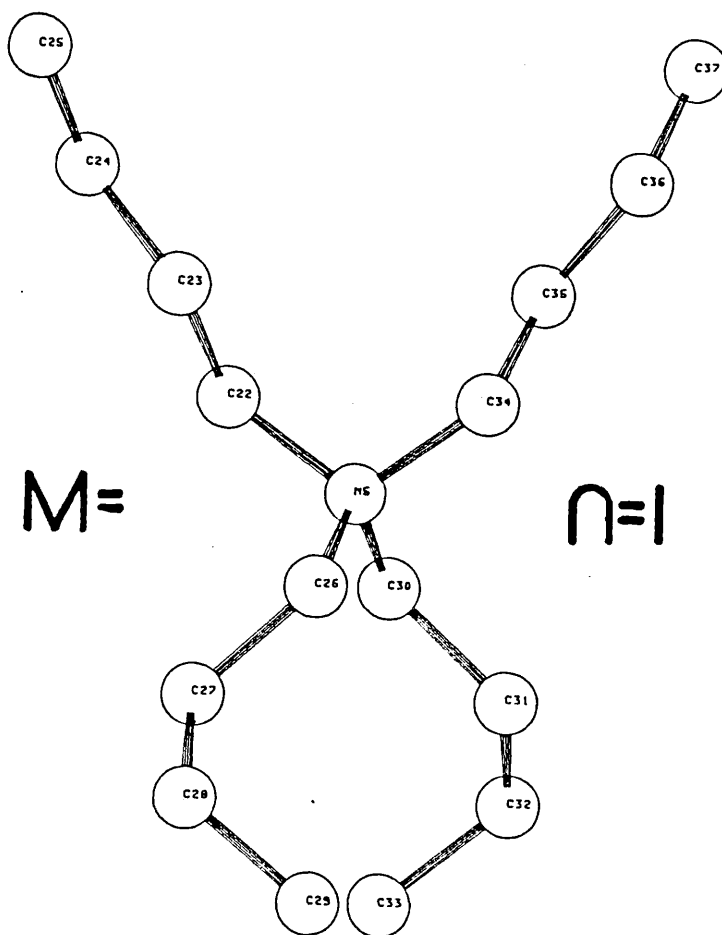


Figure 6.10

Here the anion is intermediate in planarity between Ia and Ib with an angle of twist about the trimethine bridge of 25.62° . The arrangement of the individual molecules within the stack is again different. We observe a dimerisation of molecules within the stack reminiscent of the class I type TCNQ radical anion salts. Two distinctly different interplanar distances of 3.57 and 5.54 Å are seen, Figure 6.11.

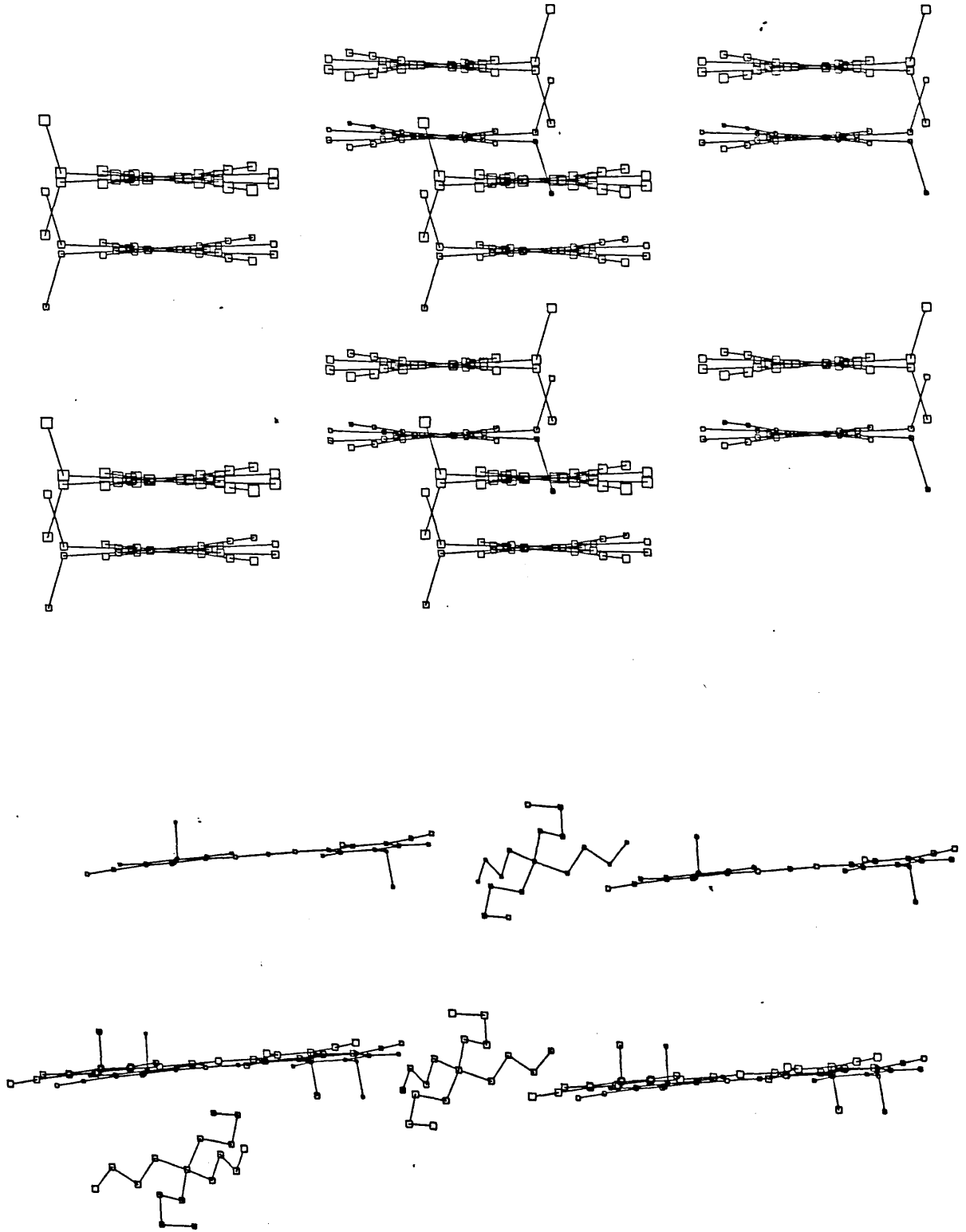


Figure 6.11

The fractional atomic coordinates, anisotropic temperature factors, bond lengths and bond angles are listed in Tables 6.5, 6.6, 6.7 and 6.8 respectively.

TABLE 6.5
Fractional atom co-ordinates for I(c), with estimated
standard deviations in parentheses

Atom	x/a	y/b	z/c
C(1)	0.6109(9)	0.6684(6)	0.9669(3)
C(2)	0.7800(7)	0.6259(5)	0.9486(3)
C(3)	0.8084(6)	0.4078(5)	0.9896(2)
C(4)	0.8161(6)	0.2722(5)	0.9763(2)
C(5)	0.8440(6)	0.1928(5)	1.0299(3)
C(6)	0.8806(6)	0.2208(5)	0.9182(2)
C(7)	0.8068(8)	0.0775(5)	0.9104(3)
C(8)	0.7790(6)	0.3032(5)	0.8667(2)
C(9)	0.7699(6)	0.4413(5)	0.8771(2)
C(10)	0.7663(6)	0.2549(5)	0.8057(2)
C(11)	0.7500(0)	0.3190(7)	0.7500(0)
C(22)	0.7002(6)	0.5510(5)	0.3081(2)
C(23)	0.8248(8)	0.6484(6)	0.3250(3)
C(24)	0.7482(8)	0.7488(6)	0.3693(3)
C(25)	0.8536(10)	0.8502(7)	0.3864(4)
C(26)	0.8970(6)	0.3876(5)	0.2591(2)
C(27)	0.8731(8)	0.2897(6)	0.3118(3)
C(28)	1.0142(9)	0.1981(6)	0.3076(3)
C(29)	1.0192(9)	0.1082(7)	0.2531(4)
N(1)	0.7868(5)	0.4872(4)	0.9384(2)
N(2)	0.8683(8)	0.1341(5)	1.0728(2)
N(5)	0.7500(0)	0.4796(5)	0.2500(0)
O(1)	0.8178(5)	0.4541(4)	1.0419(2)
O(2)	0.7489(5)	0.5212(3)	0.8372(2)
H(1)	0.584(1)	0.635(1)	1.006(0)
H(2)	0.607(1)	0.763(1)	0.968(0)
H(3)	0.538(1)	0.636(1)	0.937(0)
H(4)	0.846(1)	0.647(1)	0.983(0)

H(5)	0.825(1)	0.669(1)	0.909(0)
H(6)	0.716(1)	0.049(1)	0.892(0)
H(7)	0.809(1)	0.038(1)	0.952(0)
H(8)	0.905(1)	0.053(1)	0.882(0)
H(9)	0.768(1)	0.160(1)	0.802(0)
H(10)	0.750(0)	0.414(1)	0.750(0)
H(20)	0.679(1)	0.493(1)	0.345(0)
H(21)	0.601(1)	0.598(1)	0.302(0)
H(22)	0.908(1)	0.605(1)	0.346(0)
H(23)	0.875(1)	0.688(1)	0.385(0)
H(24)	0.697(1)	0.707(1)	0.408(0)
H(25)	0.665(1)	0.792(1)	0.347(0)
H(26)	0.791(1)	0.912(1)	0.415(0)
H(27)	0.938(1)	0.811(1)	0.409(0)
H(28)	0.904(1)	0.896(1)	0.348(0)
H(29)	0.986(1)	0.445(1)	0.268(0)
H(30)	0.928(1)	0.341(1)	0.219(0)
H(31)	0.860(1)	0.335(1)	0.353(0)
H(32)	0.775(1)	0.240(1)	0.307(0)
H(33)	1.115(1)	0.248(1)	0.304(0)
H(34)	1.005(1)	0.147(1)	0.347(0)
H(35)	1.113(1)	0.050(1)	0.252(0)
H(36)	1.022(1)	0.154(1)	0.212(0)
H(37)	0.919(1)	0.058(1)	0.261(0)

Table 6.6

The anisotropic temperature factors for the atoms of I(c),
with estimated standard deviations in parentheses.

Atom	u[1,1]	u[2,2]	u[3,3]	u[2,3]	u[1,3]	u[1,2]
C(1)	0.1179(60)	0.0767(45)	0.0947(49)	-0.0066(37)	-0.0366(42)	0.0093(40)
C(2)	0.0791(40)	0.0632(35)	0.0586(32)	-0.0036(26)	-0.0126(27)	0.0036(30)
C(3)	0.0538(32)	0.0655(33)	0.0511(29)	0.0054(25)	-0.0042(23)	0.0055(26)
C(4)	0.0540(32)	0.0566(32)	0.0536(30)	0.0087(23)	-0.0047(23)	0.0070(24)
C(5)	0.0700(41)	0.0808(32)	0.0605(30)	0.0140(31)	-0.0034(25)	0.0062(28)
C(6)	0.0511(32)	0.0525(30)	0.0598(32)	0.0070(24)	-0.0022(23)	0.0051(23)
C(7)	0.1005(48)	0.0634(36)	0.0681(36)	0.0084(28)	-0.0106(32)	0.0038(33)
C(8)	0.0505(30)	0.0514(28)	0.0471(27)	0.0025(22)	-0.0026(21)	0.0032(22)
C(9)	0.0629(34)	0.00558(31)	0.0461(26)	0.0055(24)	-0.0045(23)	0.0017(25)
C(10)	0.0538(30)	0.0515(28)	0.0575(29)	0.0027(25)	-0.0014(22)	0.0016(24)
C(11)	0.0576(46)	0.0527(41)	0.0530(40)	0.0000(0)	-0.0010(32)	0.0000(0)
C(22)	0.0630(32)	0.0522(32)	0.0603(28)	-0.0086(24)	0.0008(23)	0.0056(27)
C(23)	0.0774(42)	0.0810(41)	0.733(38)	-0.0197(31)	-0.0013(30)	-0.0111(33)
C(24)	0.1043(55)	0.0788(43)	0.0836(45)	-0.0193(36)	-0.0112(37)	-0.0019(38)
C(25)	0.1389(79)	0.0960(57)	0.1418(73)	-0.0272(53)	0.0122(58)	0.0039(53)
C(26)	0.0526(31)	0.0581(31)	0.0624(32)	-0.0023(24)	-0.0096(23)	0.0071(25)
C(27)	0.0868(45)	0.0749(38)	0.0618(34)	-0.0002(29)	-0.0176(29)	0.0154(33)
C(28)	0.0879(51)	0.0825(44)	0.1055(52)	-0.0008(40)	-0.0259(38)	0.0199(37)

Table 6.6. (continued)

C(29)	0.1221(64)	0.0916(54)	0.1268(64)	-0.0133(48)	-0.0267(49)	0.0375(48)
N(1)	0.0660(28)	0.0543(26)	0.0498(24)	0.0003(19)	-0.0065(20)	0.0047(21)
N(2)	0.1352(52)	0.0828(37)	0.0714(33)	0.0211(28)	-0.0144(31)	0.0185(35)
N(5)	0.0488(34)	0.0562(33)	0.0463(30)	0.0000(0)	-0.0034(24)	0.0000(0)
O(1)	0.0948(30)	0.0789(27)	0.0495(21)	-0.0050(19)	-0.0140(18)	0.0056(22)
O(2)	0.1262(36)	0.0514(22)	0.0548(22)	0.0022(18)	-0.0148(21)	0.0113(22)

TABLE 6.7

Bond lengths (Å), with estimated standard deviations
in parentheses for I(c)

C(1)-C(2)	1.493(8)
C(2)-C(1)	1.466(6)
C(3)-N(1)	1.398(6)
C(3)-O(1)	1.224(6)
C(3)-C(4)	1.444(7)
C(4)-C(5)	1.432(5)
C(4)-C(6)	1.368(7)
C(5)-N(2)	1.155(5)
C(6)-C(7)	1.507(7)
C(6)-C(8)	1.423(6)
C(8)-C(9)	1.460(7)
C(8)-C(10)	1.405(6)
C(9)-O(2)	1.219(5)
C(9)-N(1)	1.408(6)
C(10)-C(11)	1.382(6)
C(22)-N(5)	1.518(5)
C(26)-N(5)	1.533(6)
C(22)-C(23)	1.531(8)
C(23)-C(24)	1.504(8)
C(24)-C(25)	1.454(9)
C(26)-C(27)	1.514(7)
C(27)-C(28)	1.517(8)
C(28)-C(29)	1.489(9)

TABLE 6.8
Bond Angles ($^{\circ}$) for I(c)

C(1)-C(2)-N(1)	110.7(5)
C(2)-N(1)-C(3)	118.5(4)
C(2)-N(1)-C(9)	117.9(4)
C(3)-N(1)-C(9)	123.6(4)
N(1)-C(3)-C(4)	115.9(4)
N(1)-C(3)-O(1)	120.1(5)
C(4)-C(3)-O(1)	123.9(5)
C(3)-C(4)-C(6)	123.7(4)
C(3)-C(4)-C(5)	114.3(4)
C(5)-C(4)-C(6)	122.1(4)
C(4)-C(5)-N(2)	178.3(4)
C(4)-C(6)-C(8)	119.6(5)
C(4)-C(6)-C(7)	119.3(5)
C(7)-C(6)-C(8)	121.1(5)
C(6)-C(8)-C(9)	119.2(4)
C(6)-C(8)-C(10)	121.5(5)
C(9)-C(8)-C(10)	119.3(4)
C(8)-C(9)-N(1)	118.0(4)
C(8)-C(9)-O(2)	125.3(5)
N(1)-C(9)-O(2)	116.7(4)
C(8)-C(10)-C(11)	129.9(5)
C(10)-C(11)-C(12)	121.9(7)
C(22)-N(5)-C(26)	111.1(3)
C(22)-N(5)-C(34)	105.4(3)
N(5)-C(22)-C(23)	115.5(4)
N(5)-C(26)-C(27)	115.5(4)
C(22)-C(23)-C(24)	110.8(5)
C(23)-C(24)-C(25)	115.9(6)
C(26)-C(27)-C(28)	110.3(5)
C(27)-C(28)-C(29)	113.3(6)

- 6.1.4 The structure of dimethylammonium ethyl methacrylate
 1-Ethyl-3-cyano-6-hydroxy-4-methyl pyrid-2-one trimethine
 oxonol
 (Id), Figure 6.12

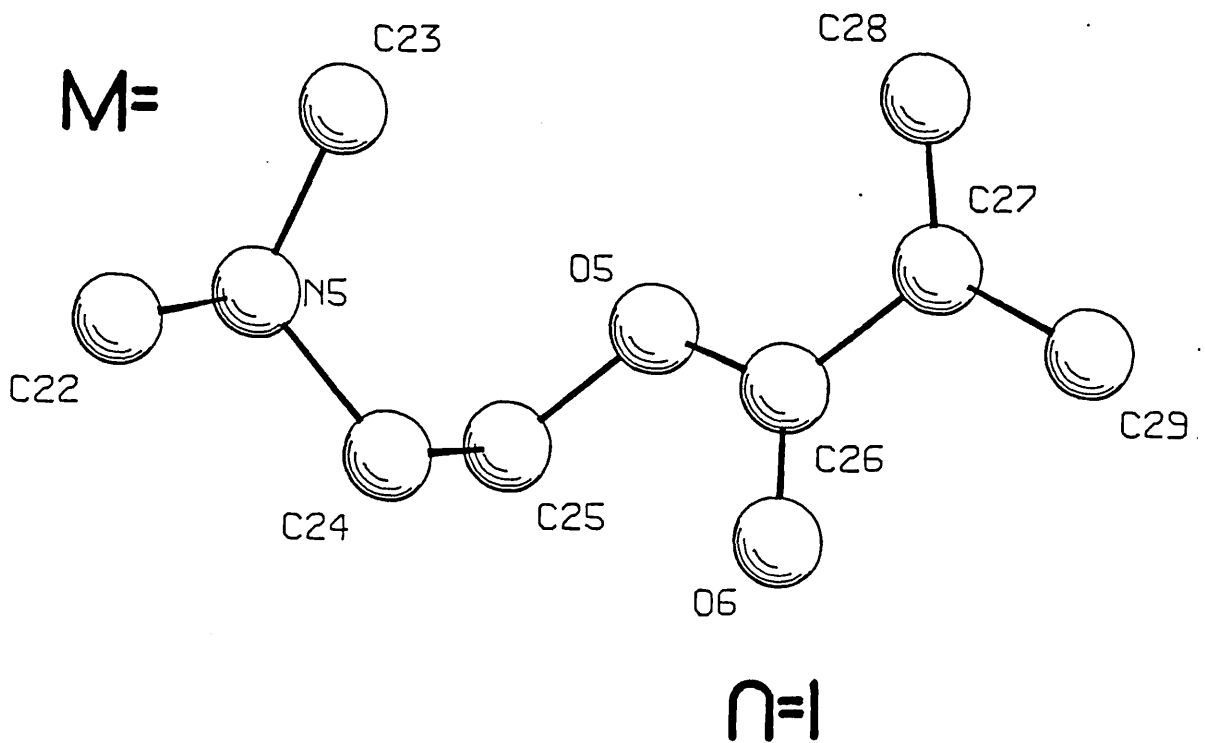


Figure 6.12

This structure is very similar to that of Ia. The anions are very nearly planar (angle of twist about the methine bridge = 14°) and stack in a herringbone type fashion, Figure 6.13. It also seems likely

that the ionic interaction between anion and cation is supplemented by hydrogen bonding between the external hydroxypyridone ring oxygen atom and the nitrogen of the cation ($N5-O1 = 2.74 \text{ \AA}$; $O1-H35 = 1.91 \text{ \AA}$; $N5-H35 = 0.99 \text{ \AA}$).

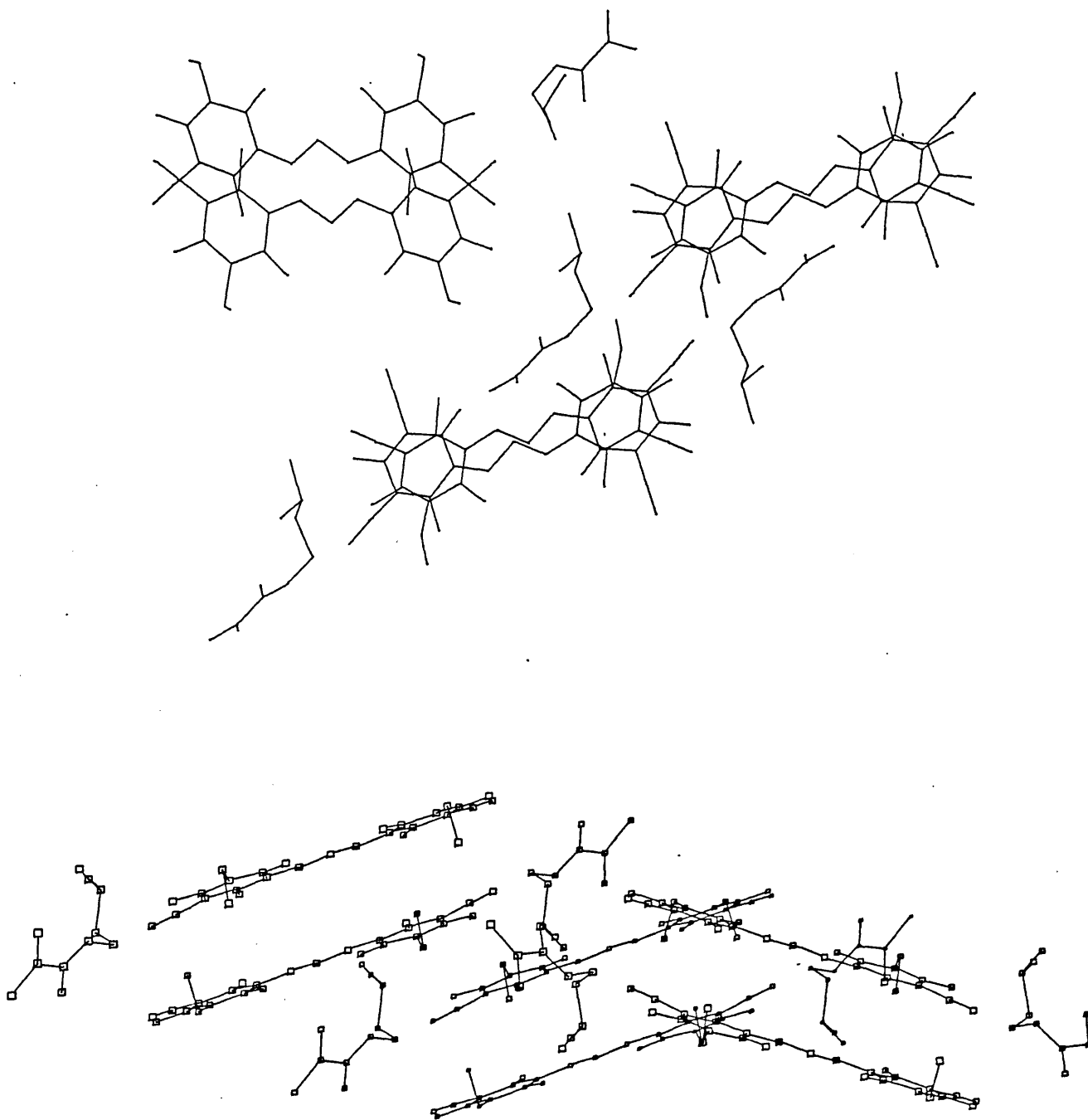


Figure 6.13

The interplanar distance, however, has increased to 4.53 Å. The closest approach of the vinyl groups of the cation is 12.83 Å.

One unique feature of this structure is that the terminal carbon atoms of the two N-ethyl substituents of the hydroxypyridone rings both point in the same direction.

The fractional atomic coordinates, anisotropic temperature factors, bond lengths and bond angles are listed in Tables 6.9, 6.10, 6.11 and 6.12 respectively.

TABLE 6.9
Fractional atom coordinates for 1(d), with estimated
standard deviations in parentheses

Atom	x/a	y/b	z/c
C(1)	0.6909(5)	0.0387(21)	0.4699(6)
C(2)	0.6818(4)	0.1980(20)	0.4939(5)
C(3)	0.6615(3)	0.0872(14)	0.5791(5)
C(4)	0.6297(3)	0.0627(12)	0.6107(4)
C(5)	0.6455(4)	0.0120(14)	0.6629(5)
C(6)	0.5865(3)	0.1035(12)	0.5929(4)
C(7)	0.5556(3)	-0.0795(14)	0.6311(4)
C(8)	0.5724(3)	0.1652(11)	0.5398(4)
C(9)	0.6033(3)	0.1860(13)	0.5057(5)
C(10)	0.5276(3)	0.2068(12)	0.5215(5)
C(11)	0.5078(3)	0.2675(12)	0.4715(5)
C(12)	0.4622(3)	0.3050(13)	0.4668(5)
C(13)	0.4342(3)	0.3668(12)	0.4211(4)
C(14)	0.3893(3)	0.3931(12)	0.4243(5)
C(15)	0.3718(3)	0.3556(13)	0.4735(4)
C(16)	0.3617(3)	0.4549(13)	0.3786(5)
C(17)	0.3160(3)	0.4902(13)	0.3775(5)
C(18)	0.3754(3)	0.4913(13)	0.3293(5)
C(19)	0.4342(4)	0.4932(15)	0.2774(5)
C(20)	0.4371(4)	0.3188(17)	0.2479(5)
C(21)	0.4490(4)	0.4024(14)	0.3720(5)
C(22)	0.7561(3)	0.1676(14)	0.7217(4)
C(23)	0.8112(3)	0.2169(14)	0.6670(5)
C(24)	0.7792(3)	-0.0884(14)	0.6737(4)
C(25)	0.7900(3)	-0.1550(15)	0.6218(5)
C(26)	0.8624(3)	-0.2684(15)	0.6426(5)
C(27)	0.9089(4)	-0.2446(20)	0.6394(6)
H(21)	0.9276(4)	-0.5105(18)	0.6431(7)

H(22)	0.7085(4)	0.2419(20)	0.5174(5)
H(23)	0.6710(4)	0.2908(20)	0.4669(5)
H(24)	0.4635(4)	0.5477(15)	0.2857(5)
H(25)	0.4142(4)	0.5759(15)	0.2543(5)
H(26)	0.8046(3)	-0.1165(14)	0.7018(4)
H(27)	0.7532(3)	-0.1506(14)	0.6819(4)
H(28)	0.7810(3)	-0.2819(15)	0.6153(5)
H(29)	0.7728(3)	-0.0777(15)	0.5941(5)
H(30)	0.9532(4)	-0.0788(18)	0.6201(5)
H(31)	0.9004(4)	-0.0069(18)	0.6050(5)
H(32)	0.5079(3)	0.1959(12)	0.5476(5)
H(33)	0.5232(3)	0.2820(12)	0.4412(5)
H(34)	0.4502(3)	0.2859(13)	0.4997(5)
H(35)	0.7510(2)	0.1463(10)	0.6399(4)

Table 6.10

The anisotropic temperature factors for the atoms of I(d),
with estimated standard deviations in parentheses

Atom	u[1,1]	u[2,2]	u[3,3]	u[2,3]	u[1,3]	u[1,2]
C(1)	0.1176(146)	0.1381(168)	0.1438(189)	0.0166(139)	0.0309(140)	-0.0368(119)
C(2)	0.0970(114)	0.1532(160)	0.0835(140)	-0.0282(117)	-0.0009(72)	-0.0000(118)
C(3)	0.0500(72)	0.0514(77)	0.0415(96)	-0.0013(68)	-0.0009(72)	-0.0118(61)
C(4)	0.0446(62)	0.0310(66)	0.0425(80)	0.0085(58)	0.0162(60)	0.0018(50)
C(5)	0.0565(72)	0.0476(77)	0.0439(80)	-0.0063(65)	-0.0092(64)	0.0114(64)
C(6)	0.0386(58)	0.0251(62)	0.0526(82)	0.0009(55)	0.0031(61)	0.0068(49)
C(7)	0.0554(67)	0.0528(76)	0.0503(90)	0.0066(66)	-0.0076(68)	0.0081(59)
C(8)	0.0477(63)	0.0248(65)	0.0378(85)	0.0021(57)	-0.0057(61)	-0.0028(51)
C(9)	0.0520(69)	0.0366(69)	0.0533(106)	0.0058(64)	-0.0034(69)	-0.0105(55)
C(10)	0.0423(65)	0.0307(66)	0.0615(94)	-0.0160(60)	-0.0138(63)	-0.0036(54)
C(11)	0.0482(72)	0.0318(69)	0.0687(101)	0.0055(60)	-0.0071(66)	-0.0043(54)
C(12)	0.0541(73)	0.0308(70)	0.0609(102)	-0.0035(63)	-0.0126(73)	0.0032(58)
C(13)	0.0453(68)	0.0246(66)	0.0488(88)	-0.0042(59)	-0.0107(62)	-0.0046(49)
C(14)	0.0507(66)	0.0240(63)	0.0534(103)	-0.0009(61)	-0.0114(65)	0.0026(53)
C(15)	0.0526(66)	0.0444(80)	0.0665(108)	-0.0051(69)	0.0040(73)	0.0147(60)
C(16)	0.0424(65)	0.0351(73)	0.0625(102)	-0.0107(67)	-0.0221(67)	-0.0096(55)
C(17)	0.0524(69)	0.0342(70)	0.0794(101)	-0.0040(67)	-0.0171(71)	-0.0018(57)

Table 6.10 continued

C(18)	0.0482(70)	0.0368(70)	0.0588(89)	0.0049(63)	-0.0046(72)	-0.0074(55)
C(19)	0.0804(96)	0.0734(94)	0.0576(92)	0.0203(80)	0.0100(84)	-0.0011(78)
C(20)	0.0909(107)	0.1047(120)	0.0845(127)	-0.0051(97)	0.0184(98)	-0.0064(91)
C(21)	0.0567(78)	0.0452(77)	0.0704(101)	0.0122(70)	-0.0052(82)	-0.0056(66)
C(22)	0.0670(74)	0.0491(80)	0.0562(107)	-0.0066(70)	-0.0052(71)	0.0078(61)
C(23)	0.0496(0)	0.0438(0)	0.1196(0)	0.0092(0)	-0.0010(0)	-0.0240(0)
C(24)	0.0464(63)	0.0551(83)	0.0502(66)	-0.0059(66)	-0.0003(65)	-0.0019(61)
C(25)	0.0405(67)	0.0638(87)	0.0874(109)	-0.0139(75)	0.0018(69)	-0.0031(57)
C(26)	0.0553(76)	0.0477(77)	0.0838(114)	-0.0121(73)	0.0122(77)	-0.0085(59)
C(27)	0.0403(0)	0.1191(0)	0.0980(0)	-0.0191(0)	-0.0017(0)	0.0020(0)
C(28)	0.1017(0)	0.1146(0)	0.0804(0)	0.00142(0)	0.0266(0)	-0.0598(0)
C(29)	0.0827(0)	0.1026(0)	0.2066(0)	0.0414(0)	0.0045(0)	0.0341(0)
N(1)	0.0479(61)	0.0719(75)	0.0445(82)	0.0009(58)	0.0092(68)	0.0075(51)
N(2)	0.0698(68)	0.0654(74)	0.0710(82)	0.0132(66)	-0.0140(63)	0.0029(56)
N(3)	0.0526(62)	0.0689(73)	0.1292(123)	0.0022(72)	-0.0045(72)	-0.0005(56)
N(4)	0.0607(64)	0.0459(64)	0.0641(80)	0.0114(56)	-0.0062(63)	-0.0123(49)
N(5)	0.0515(55)	0.0414(59)	0.0545(77)	-0.0020(51)	-0.0123(55)	0.0113(45)
O(1)	0.0399(43)	0.0591(53)	0.0836(71)	-0.0045(48)	-0.0147(49)	0.0085(38)
O(2)	0.0614(57)	0.0994(70)	0.0508(69)	0.0257(54)	-0.0052(57)	-0.0087(50)
O(3)	0.0397(47)	0.1159(73)	0.0903(83)	0.0375(63)	-0.0062(54)	-0.0030(48)
O(4)	0.0660(50)	0.0605(56)	0.0769(73)	0.0101(48)	-0.0440(52)	0.0088(41)
O(5)	0.0521(48)	0.0526(55)	0.1033(83)	0.0002(51)	0.0184(52)	0.0018(40)
O(6)	0.0834(0)	0.0684(0)	0.1798(0)	0.0251(0)	0.0363(0)	0.0037(0)

Table 6.11

Bond lengths (Å), with estimated standard deviations
in parentheses, for 1(d)

C(1) - C(2)	1.387(17)
C(2) - N(1)	1.532(14)
C(3) - N(1)	1.389(12)
C(3) - O(1)	1.268(11)
C(3) - C(4)	1.403(13)
C(4) - C(5)	1.443(13)
C(4) - C(6)	1.378(12)
C(5) - N(2)	1.148(13)
C(6) - C(7)	1.505(12)
C(6) - C(8)	1.420(12)
C(8) - C(9)	1.427(13)
C(8) - C(10)	1.426(12)
C(9) - O(2)	1.235(12)
C(9) - N(1)	1.421(11)
C(10) - C(11)	1.387(13)
C(11) - C(12)	1.435(13)
C(12) - C(13)	1.401(12)
C(13) - C(14)	1.438(13)
C(13) - C(21)	1.436(13)
C(14) - C(15)	1.484(12)
C(14) - C(16)	1.393(12)
C(16) - C(17)	1.452(13)
C(16) - C(18)	1.428(13)
C(17) - N(3)	1.147(12)
C(18) - O(4)	1.256(11)
C(18) - N(4)	1.377(12)
C(19) - N(4)	1.465(12)
C(19) - C(20)	1.510(15)
C(21) - N(4)	1.418(12)
C(21) - O(3)	1.222(12)
C(22) - N(5)	1.495(11)
C(23) - N(5)	1.478(11)

Table 6.11 continued

C(23) - N(5)	1.478(11)
C(24) - N(5)	1.510(12)
C(24) - C(25)	1.509(13)
C(25) - O(5)	1.451(10)
C(26) - O(5)	1.357(12)
C(26) - O(6)	1.227(12)
C(26) - C(27)	1.484(14)
C(27) - C(28)	1.287(16)
C(27) - C(29)	1.489(16)

Table 6.12

Bond Angles ($^{\circ}$) for 1(d), with estimated
standard deviations in parentheses

C(1) - C(2) - N(1)	
C(2) - N(1) - C(3)	118.6(9)
C(2) - N(1) - C(9)	118.0(1.0)
C(3) - N(1) - C(9)	123.1(9)
N(1) - C(3) - C(4)	117.2(9)
N(1) - C(3) - O(1)	117.8(1.0)
C(4) - C(3) - O(1)	125.0(1.1)
C(3) - C(4) - C(6)	122.7(1.0)
C(3) - C(4) - C(5)	114.9(9)
C(5) - C(4) - C(6)	122.5(1.0)
C(4) - C(5) - N(2)	177.9(1.3)
C(4) - C(6) - C(8)	120.0(9)
C(4) - C(6) - C(7)	118.1(1.0)
C(7) - C(6) - C(8)	122.0(8)
C(6) - C(8) - C(9)	119.3(9)
C(6) - C(8) - C(10)	119.8(1.0)
C(9) - C(8) - C(10)	120.9(1.0)
C(8) - C(9) - N(1)	117.7(1.0)
N(1) - C(9) - O(2)	116.2(1.0)
C(8) - C(9) - O(2)	126.0(1.0)
C(8) - C(10) - C(11)	128.1(1.1)
C(10) - C(11) - C(12)	114.2(1.1)
C(11) - C(12) - C(13)	126.3(1.1)
C(12) - C(13) - C(14)	117.8(1.1)
C(12) - C(13) - C(21)	122.1(1.0)
C(14) - C(13) - C(21)	120.1(1.1)
C(13) - C(14) - C(15)	122.6(1.1)
C(13) - C(14) - C(16)	117.3(1.1)
C(15) - C(14) - C(16)	120.0(9)
C(14) - C(16) - C(17)	122.1(1.1)
C(14) - C(16) - C(18)	124.0(9)

Table 6.12 continued

C(17) - C(16) - C(18)	113.8(1.1)
C(16) - C(17) - N(3)	179.0(1.2)
C(16) - C(18) - O(4)	122.5(1.0)
C(16) - C(18) - N(4)	117.3(1.0)
N(4) - C(18) - O(4)	120.3(1.1)
C(18) - N(4) - C(21)	122.6(1.0)
C(18) - N(4) - C(19)	119.8(1.1)
C(19) - N(4) - C(21)	117.6(1.0)
N(4) - C(19) - C(20)	111.8(9)
C(13) - C(21) - N(4)	118.8(1.0)
C(13) - C(21) - O(3)	125.4(1.2)
N(4) - C(21) - O(3)	115.8(1.1)
C(22) - N(5) - C(23)	110.1(9)
C(22) - N(5) - C(24)	108.8(8)
C(23) - N(5) - C(24)	113.6(8)
N(5) - C(24) - C(25)	111.1(9)
C(24) - C(25) - O(5)	114.1(9)
C(25) - O(5) - C(26)	116.3(8)
O(5) - C(26) - O(6)	121.4(1.0)
O(5) - C(26) - C(27)	115.0(1.1)
O(6) - C(26) - C(27)	123.6(1.2)
C(26) - C(27) - C(28)	120.3(1.3)
C(26) - C(27) - C(29)	114.6 (1.3)
C(28) - C(27) - C(29)	125.1(1.2)

6.1.5 Other Investigations

Attempts were made to investigate the structures of two other dyes. Crystals of HPT297 (I(e), M = Ph₃MeP⁺) proved to be too small for satisfactory data collection, and our efforts to obtain better specimens of this key material were unsuccessful (10.4.1.6). The N-methyl morpholinium salt (HPT308) produced two crystal habits (dark blue needles and metallic green cubes). Preliminary photographs of the cuboid form revealed that the structure was disordered at room temperature. Time did not permit a low temperature data collection to be carried out. The needles were of much poorer quality, many being twinned and have not yet been further investigated.

6.1.6 The three solid-state structures fully determined provided an example of each of the cyanine dye structural classes and a second example of the herringbone structure first observed for MI1579 (Ia).

75,76,77

6.2 Solid State NMR Spectroscopic Studies

6.2.1 Our aim was to investigate how structural features observed from the X-ray crystal structure might influence the materials solid state ¹³C n.m.r. spectrum. In the longer term, we hoped to use solid state n.m.r. as a routine analytical tool to predict potentially interesting structures. These investigations were primarily concerned with how the ¹³C solid state n.m.r. spectrum of the anion was influenced by the changing structural features induced by variation of the cation.

6.2.2 The Spectra

Figure 6.14 shows the ^{13}C solid state spectra of 1(a), (b), (c) and (d) compared to the solution ($\text{d}^6\text{-DMSO}$) ^{13}C spectrum of 1(a). The assignment of the solution spectrum is listed in Table 6.13, the carbon atom numbering being consistent with Figure 6.4.

Table 6.13

$\delta(\text{d}^6\text{-DMSO, ppm})$	Assignment
8.52	C(23), C(25), C(27)
13.01	C(1), C(20)
18.47	C(7), C(15)
33.82	C(2), C(19)
45.91	C(22), C(24), C(26)
92.15	C(6), C(14)
110.42	C(8), C(13)
117.64	C(5), C(17)
120.89	C(11)
157.05	C(10), C(12)
158.03	C(4), C(16)
161.41	C(3), C(9)
161.86	C(18), C(21)

Common to all of the solid state spectra is the broadening/splitting of any peak when the corresponding carbon atom bears a nitrogen atom. Nitrogen being a quadrupolar nucleus, one would expect to observe doublets for these carbon atom peaks, presumably as a result of the poorer resolution of the 200 MHz machine we only see a broadening.

The spectrum of most interest in figure 6.14 is clearly that of 1(a) where splitting of the peaks corresponding to C(1), C(20); C(6), C(14) and C(8), C(13) is seen. A number of possible explanations might enable us to account for this apparent disymmetry about the two halves of the anion molecule.

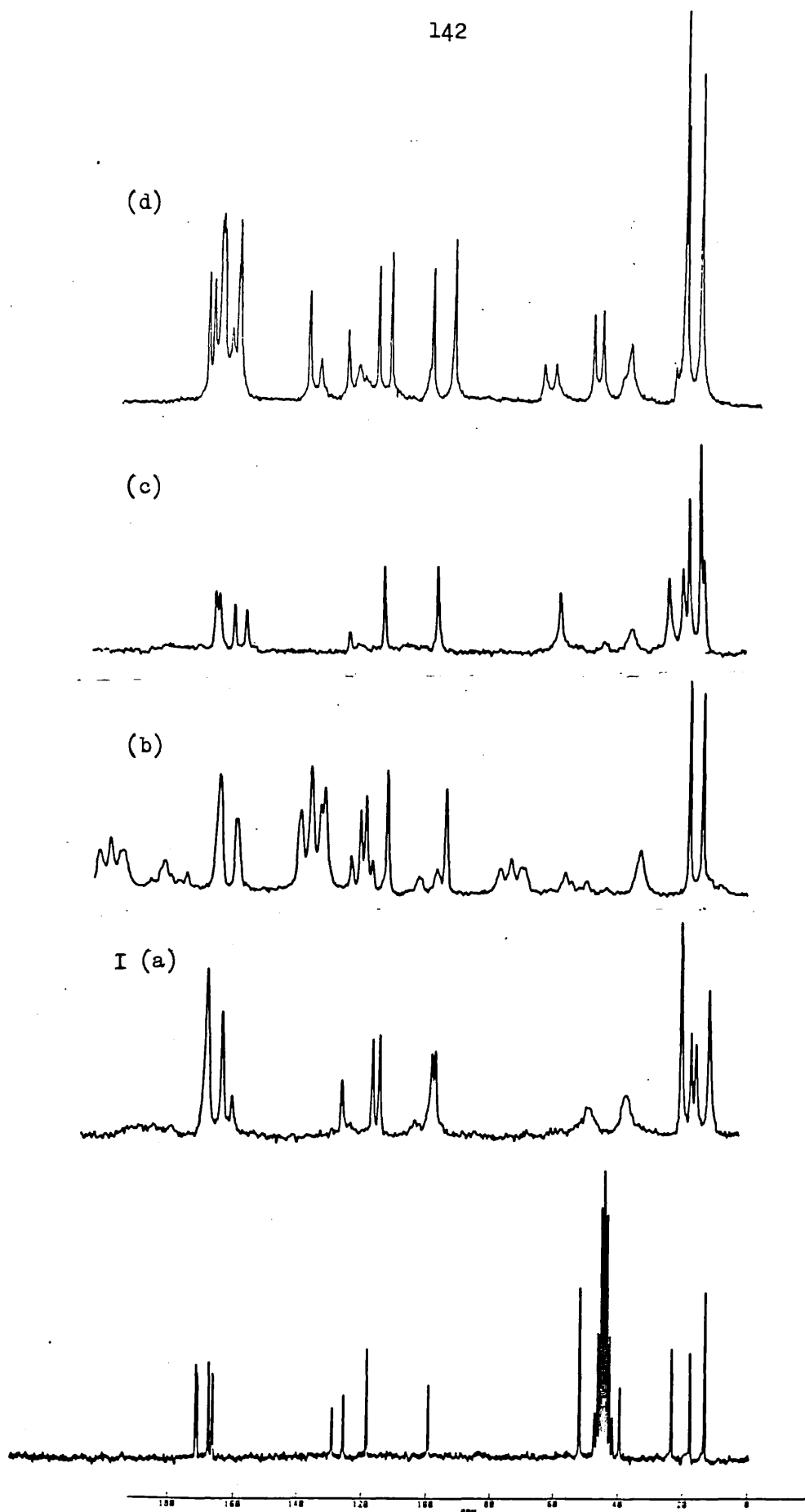


Figure 6.14

For example, it might be:

- (i) the distortion about the methine bridge,
- (ii) the hydrogen bonded cation on one side, or even
- (iii) an intermolecular interaction between adjacent molecules within the stack.

But however:

(1) The material with the largest angle of twist about the methine bridge, 1(b), shows no splitting,

(2) Similar splitting is observed for (HPT 297, I(e)), figure 6.15, where a hydrogen bond between anion and cation is not a possibility.

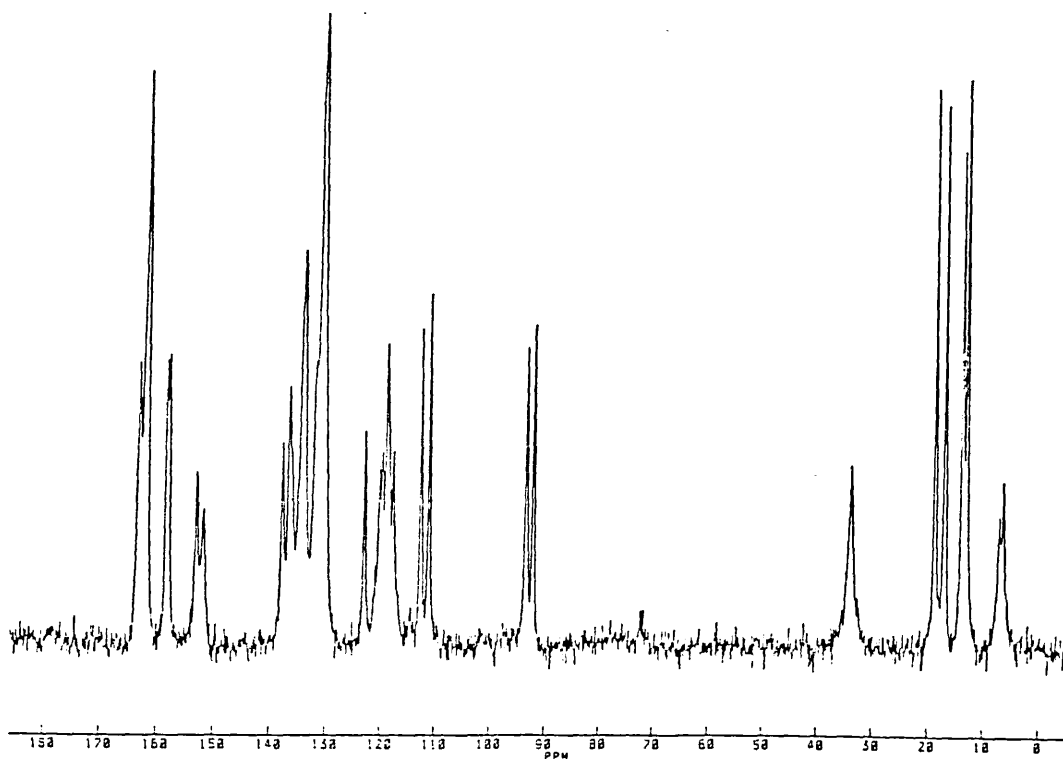


Figure 6.15

HPT 297 is of particular interest as not only does the replacement of a phenyl ring (Ib) for a methyl group in this phosphonium cation introduce this characteristic splitting but also a 3-4 order of magnitude increase in d.c. conductivity.

(3) Materials I(a) - I(d) have the interplanar distances significantly larger than van der Waals spacing (3.4 \AA). Were the interplanar distance $< 3.4 \text{ \AA}$ one might realistically expect the possibility of shielding/deshielding effects between adjacent molecules within a stack.

Why the ^{13}C solid state n.m.r. spectra of I(a) and I(e) show this characteristic splitting is not clear. Obviously a more extensive range of materials has to be investigated. The crystal structure of I(e) alone would be highly enlightening.

CHAPTER 7

Electrochemical Investigations : The Design of a
Radical Cation-Dye Complex

7.1⁷⁸ It is well known that radical-ion salts may be prepared electrochemically by inducing either the reduction or oxidation of the parent species. The method involves the electrolysis of a solution of the donor or acceptor in the presence of a source of the adductant, resulting in the electrocrystallisation of the desired adduct on one of the electrodes. Usually either the current or the potential is kept constant during electrolysis; these are termed galvanostatic and potentiostatic electrolyses, respectively. The electrocrystallisation may be anodic (donors) or cathodic (acceptors). For the anodic method, the donor may be an organic compound, such as a thio donor, for example, tetra-thiafulvalene, TTF, or its selenium analogue. The donor may be a metal from a sacrificial metal anode, on which the adduct grows, as in the case of TTF (AgNO_3)_{0.67}. Examples of the adductant in the anodic method are anions of tetracyanoquinodimethane, (TCNQ), thiocyanate, (SCN^-), azide (N_3^-), acetate (AcO^-), and halides (Cl^- , Br^- or I^-); their sources being the corresponding salts or acids. For the cathodic method, the acceptor may be, for example, TCNQ. Adductant cations, include copper (Cu^{2+}), silver (Ag^+), or chromium (Cr^{3+}), their sources again being salts.

This method is known to yield products reported to be unobtainable by chemical means such as TTF(N_3)_{0.74} and is preferably performed under an oxygen-free atmosphere. The electrocrystallisation potential can initially be determined voltammetrically. That giving the highest current is selected for the start of the galvanostatic preparation and the current is maintained at its highest value by an adjacent galvanostat.

Our intention, was then, to carry out an anodic electrocrystallisation using TTF as a donor with an oxonol dye salt adductant. Before this could be achieved the electrochemistry of both TTF and a range of oxonol dye salts had to be investigated by cyclic voltammetry^{79,80,81}.

7.2. The Electrochemistry of Tetrathiafulvalene, TTF.

Figure 7.1(b) shows the cyclic voltammogram of TTF in acetonitrile as solvent in the presence of a tetrabutylammonium perchlorate supporting electrolyte using Pt electrodes. Figure 7.1(a) is the voltammogram of the supporting electrolyte in acetonitrile demonstrating that neither solvent nor supporting electrolyte have any electrochemistry of their own in this region. As can be seen, TTF undergoes two oxidation reactions, the first

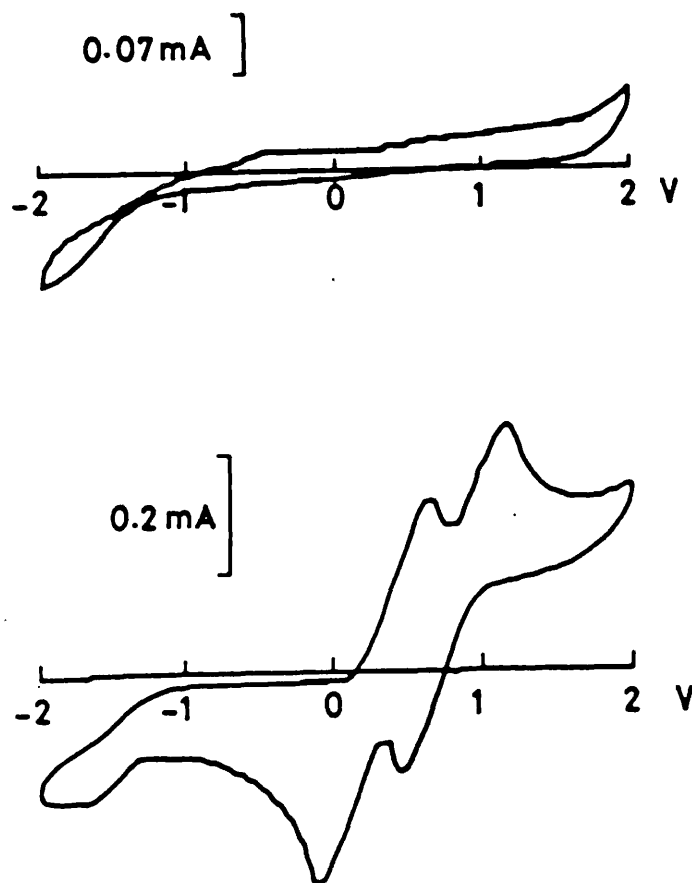
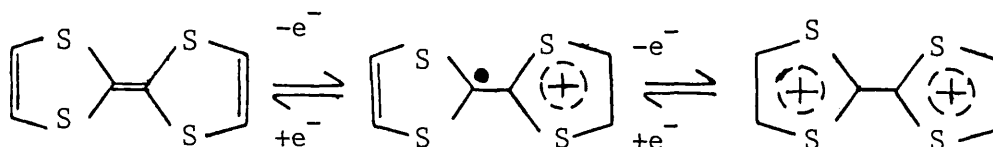


Figure 7.1

leads to the formation of the TTF radical monovalent cation the second to the divalent cation, both being reversible processes, Scheme 7.1.



Scheme 7.1.

It is the unpaired electron of the radical cation which is the potential charge carrier and which makes the most significant contribution to electronic conduction in TTF complexes. Hence we need to stop the reaction at the first oxidation stage, and thus an electrocrystallisation potential of about 0.7 V v's S.C.E. is required.

7.3. The Electrochemistry of a Selection of Oxonol Dye Salts

Figures 7.2. and 7.3. show the voltammograms of a range of oxonol dyes in acetonitrile in the presence of a tetrabutylammonium supporting electrolyte with Pt electrodes, Figure 7.2. demonstrates the effect on the electrochemistry of varying the N-alkyl substituent on the pyridone rings and Figure 7.3. the effect of increasing the methine chain length. It can be seen that the electrochemistry remains largely unaffected by variation of cation, N-alkyl substituent or methine chain length. The

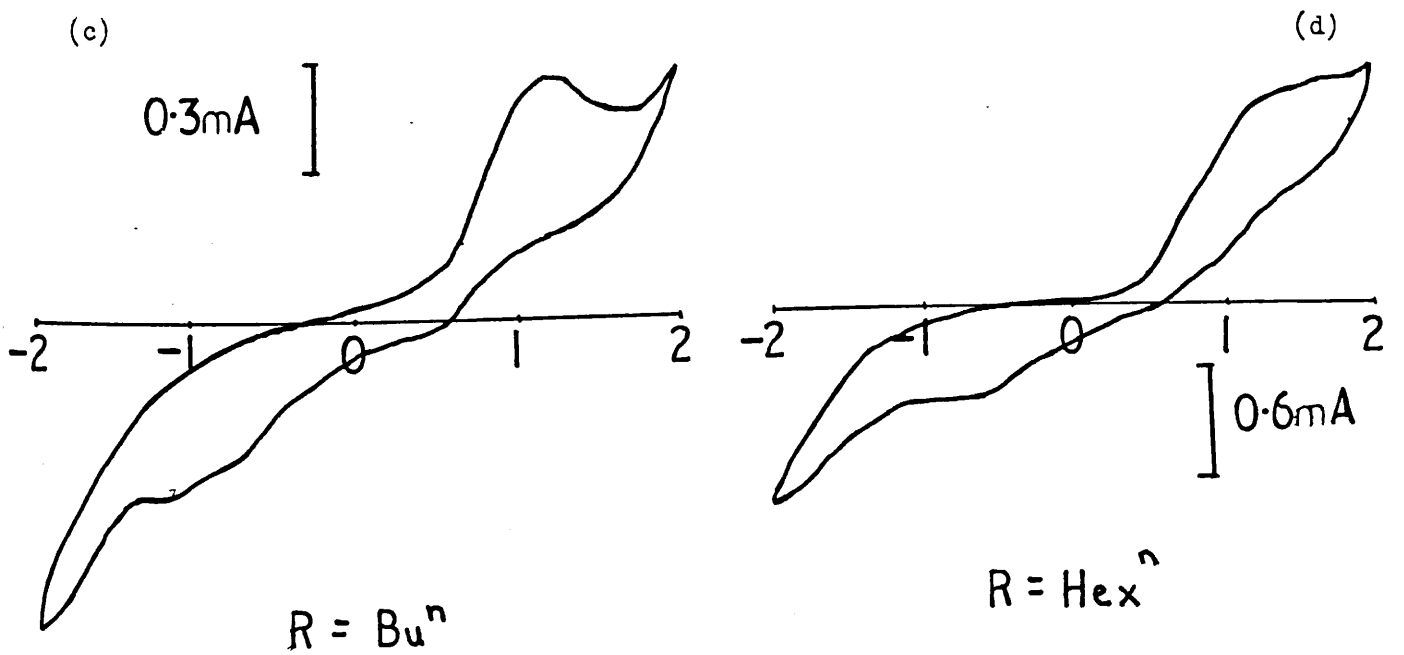
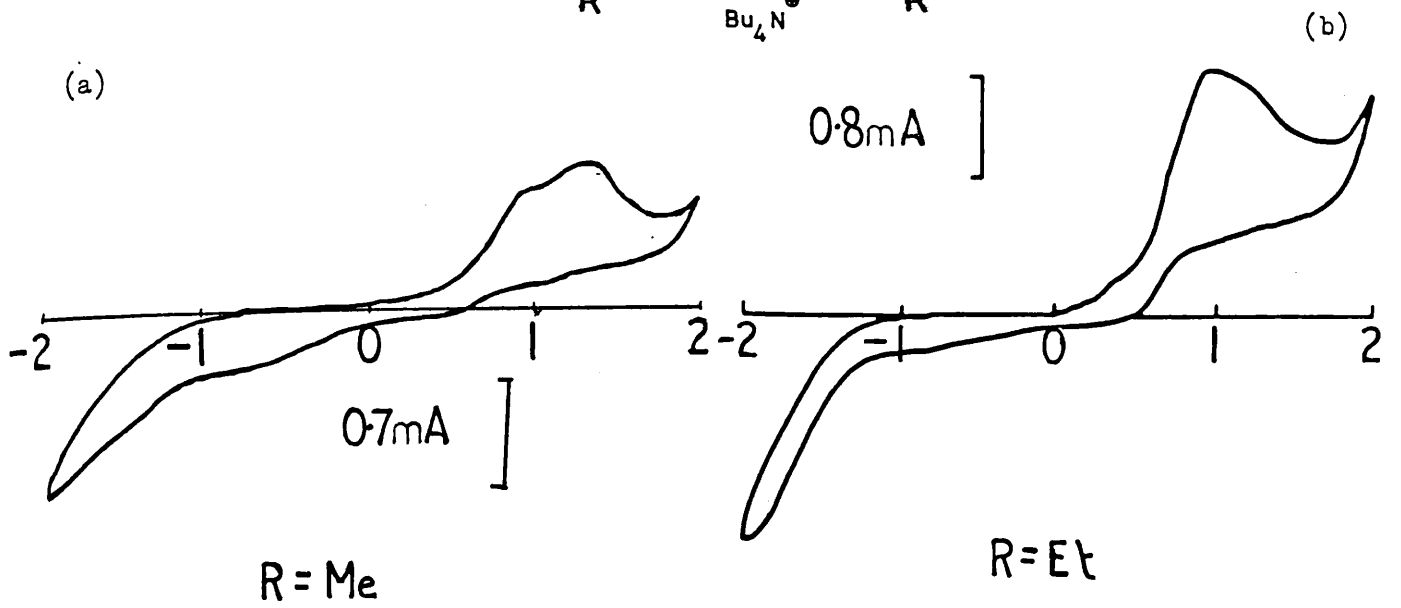
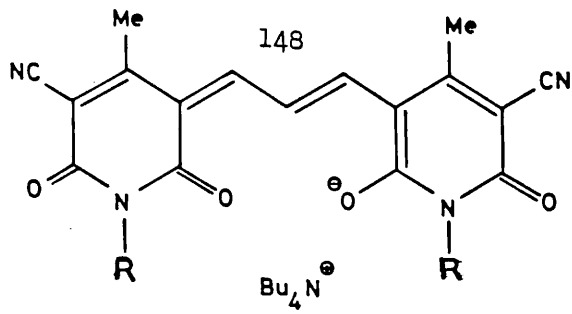


Figure 7.2

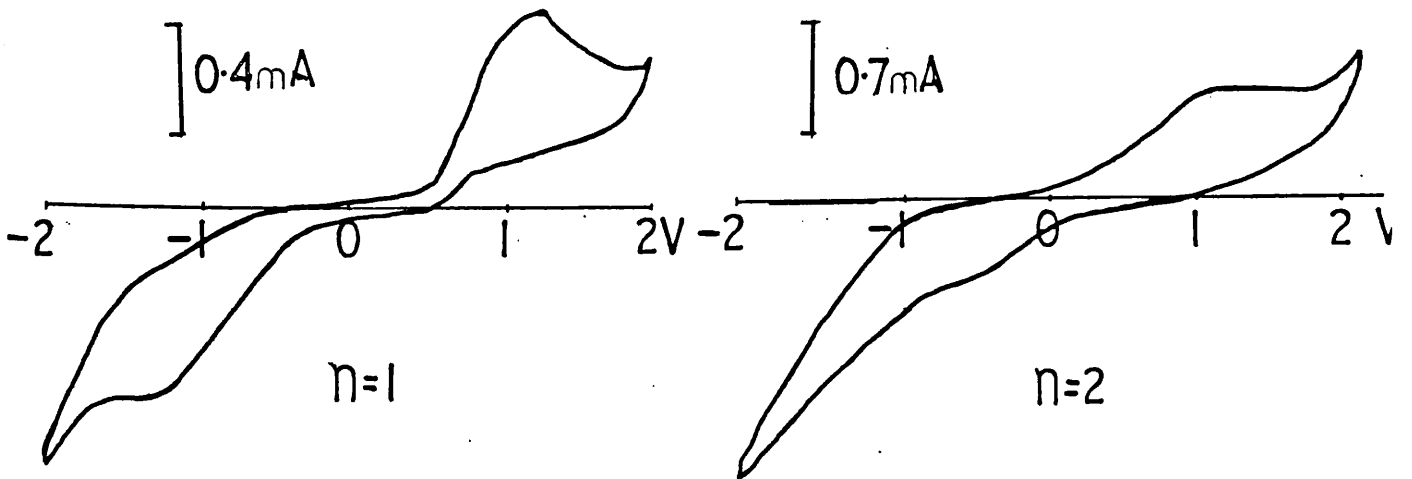
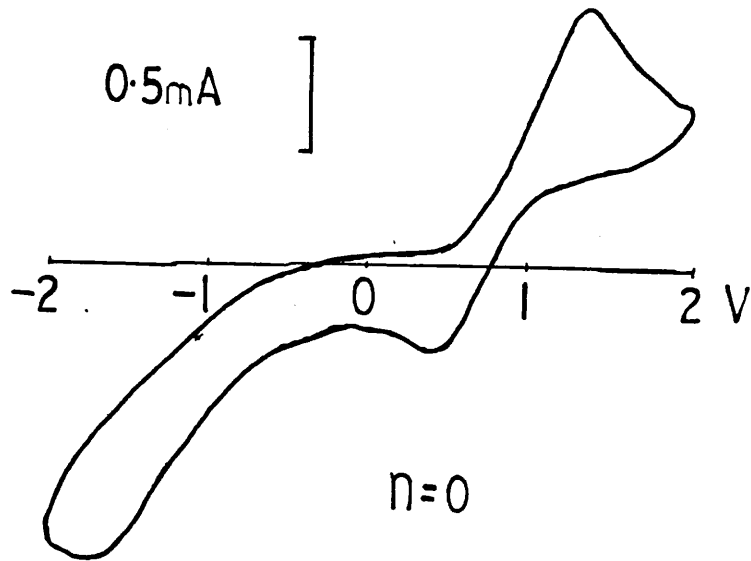
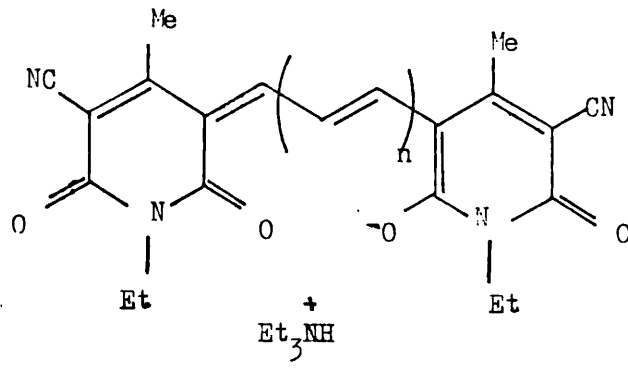
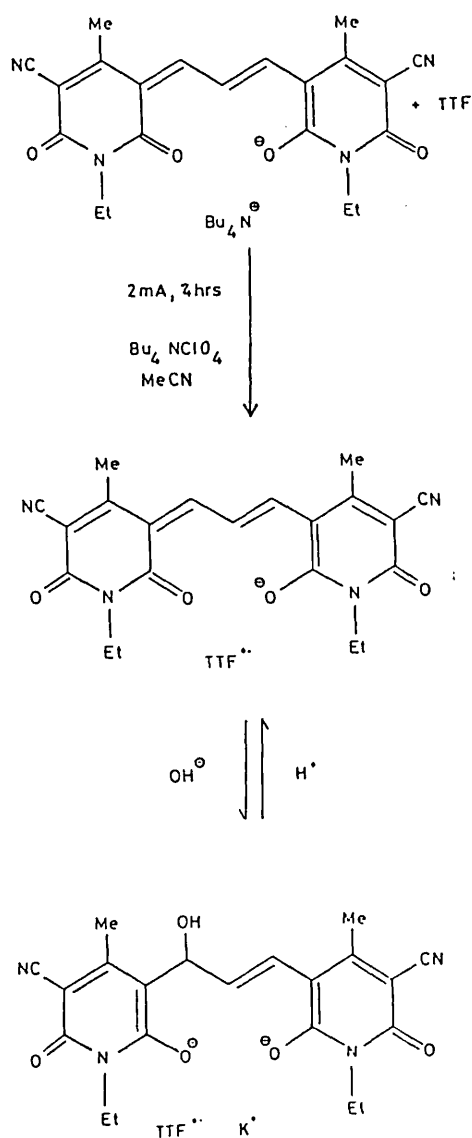


Figure 7.3

dyes undergo oxidation, in some cases, irreversibly. The "bleaching" of the solutions during the cycle suggests this oxidation to be of the methine bridge.

7.4. The Preparation of a TTF-Oxonol Dye Complex

We chose dye I, Scheme 7.2. mainly as a result of its high solubility in acetonitrile; Figure 7.2.(b) shows its cyclic voltammogram. It shows one irreversible oxidation at 1.0 V v's S.C.E. With an



Scheme 7.2

electrocrystallisation potential of 0.7 V v's S.C.E. (generating TTF radical cations at the anodes surface) the adductant dye should undergo no electrochemistry of its own. The dye anion simply co-crystallises with the TTF radical cations forming the complex on the anode. Scheme 7.2 shows the eventual reaction conditions (2mA, 4 hrs, Pt electrodes). II forms as a black crystalline solid on the anode. Its solution (50:50, H₂O: MeCN) and solid state e.s.r. spectra are shown in Figure 7.4.

As well as having a room temperature d.c. conductivity of $\approx 10^{-3} \Omega^{-1} \text{cm}^{-1}$, II maintains a number of its photographic dye properties. Notably it can be "bleached" (the α, β -unsaturated carbonyl centre provides a soft electrophilic centre susceptible to nucleophilic attack by a range of nucleophiles thereby destroying the chromophore and bleaching the semiconductor, Scheme 7.2). In the case of hydroxide ion this process is reversible.

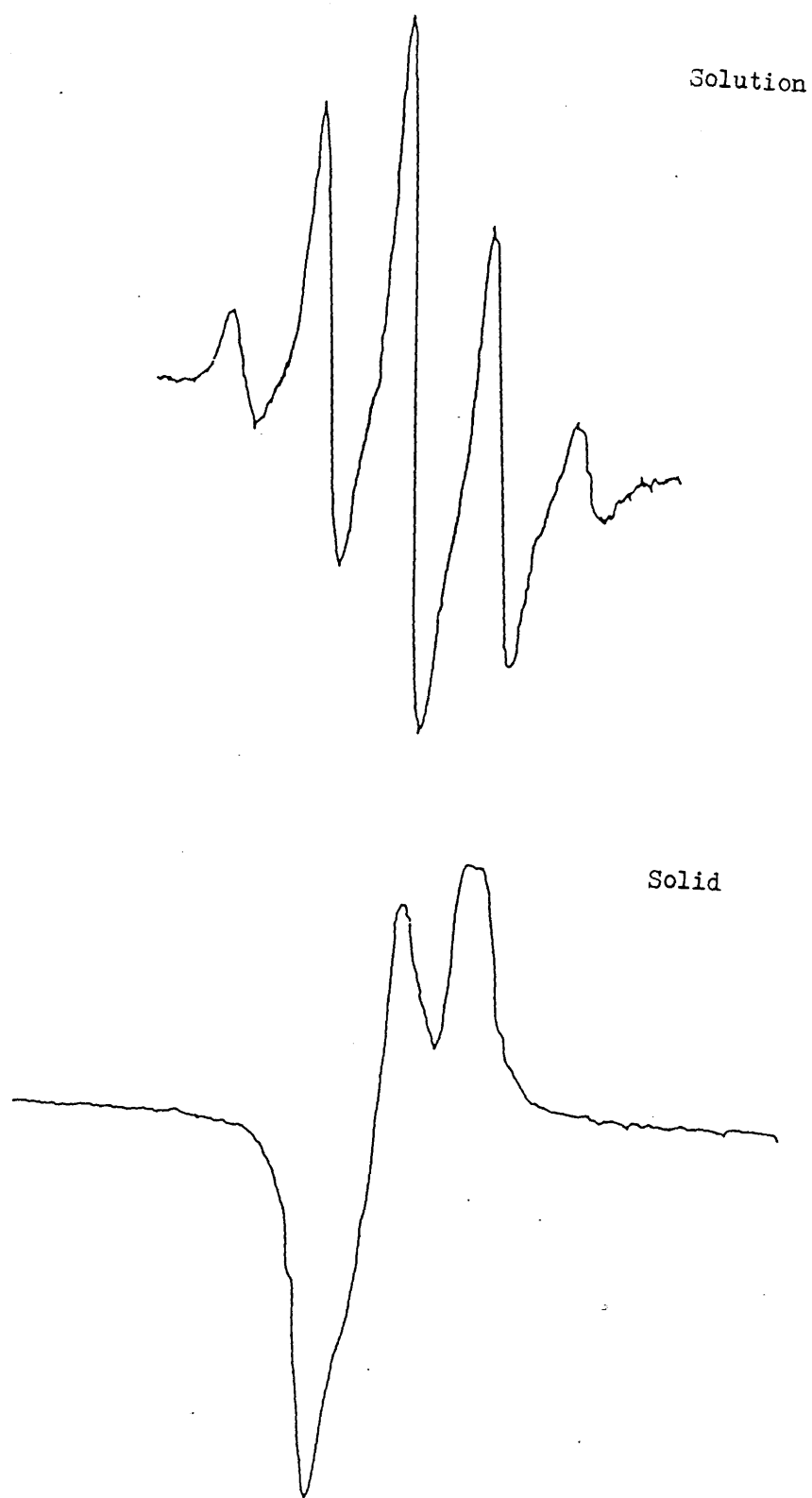


Figure 7.4

7.5. The preparation of these TTF-dye complexes by direct chemical means, that is the co-crystallisation of either neutral TTF or of a TTF salt with oxonol dye salts proved unsuccessful. Therefore electrocrystallisation appears to be the synthetic method of choice, although the possibility of co-sublimation has not yet been explored.

The electrochemistry of the oxonol dyes, as illustrated by Figures 7.2. and 7.3. appears to be remarkably non-versatile, that is structural changes induce little variation in oxidation potentials. In the case of the formation of complex II, above, we were fortunate that the dye's inherent electrochemistry could not interfere. However, when attempting to prepare the dibenzotetrathiafulvalene complex we obtained highly impure material. The cyclic voltammogram of dibenzo TTF, (Figure 7.5) suggests

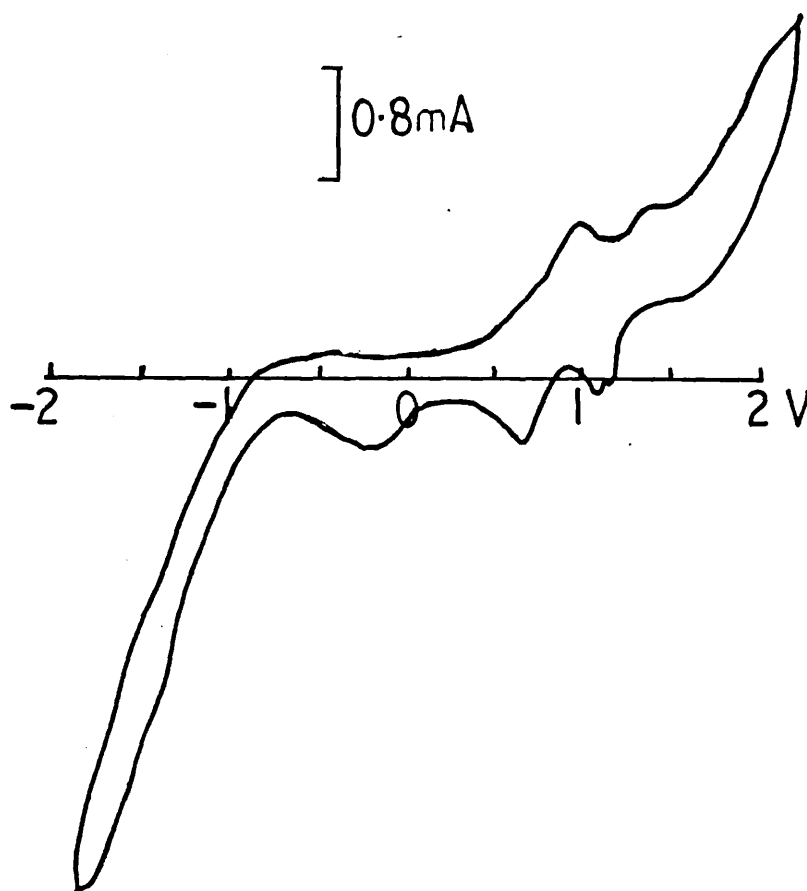
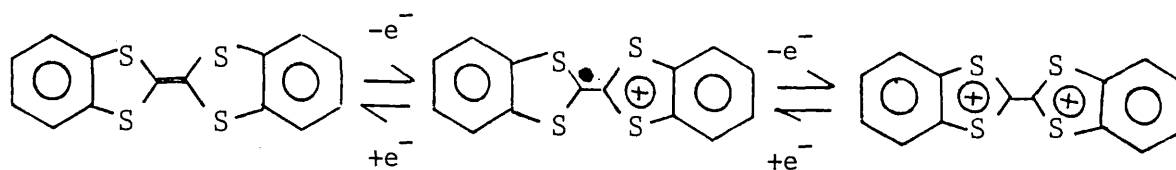


Figure 7.5

why. Its first oxidation potential, Scheme 7.3., coincides with that of the initial dye I. We therefore have to be careful in our selection of



donors. Their electrocrystallisation potentials have to lie within a limited range of potentials (< 0.9 V v's S.C.E., Pt electrodes, MeCN).

These radical cation-dye complexes have a wide range of potential applications commercially, e.g., as antistatic agents in film assemblies, gas detectors, infrared radiation detectors, and indeed complex II is undergoing evaluation at present.

CHAPTER 8

D.C. Conductivity and Dielectric Spectroscopic Measurements

8.1 D.C. Conductivity

The current (I) vs. voltage (V) characteristics at varying temperatures revealed Ohmic behaviour for all of our samples where silver dag contacts were employed. Thus from Ohms Law (8.1)

$$\frac{V}{I} = R \quad 8.1$$

the resistance (R) and hence from (8.2)

$$\sigma_0 = \frac{L}{A} \frac{1}{R} \quad 8.2$$

(where L is the thickness and A the cross-sectional area of the sample), the d.c. conductivity (σ_0), at varying temperatures could be obtained.

If the material is assumed to be intrinsic (refer to Chapter 5) then

$$\sigma_0 = A \exp -\Delta\epsilon/2kT \quad 8.3$$

and from $\ln \sigma$ vs. $\frac{1}{T}$ plots, thermal activation energies or band gap energies, can be obtained, for each of the samples.

8.2 Dielectric Spectroscopy

Refer to Appendix 2

It was our intention not only to investigate the bulk properties of our materials but also to look more deeply into the contact effects; dielectric spectroscopy enabled us to do both. In general four different types of dielectric response were seen for our samples, each of which is shown theoretically mimiced by conventional R.C. (Resistance-Capacitance) circuits in Figure 8.1.

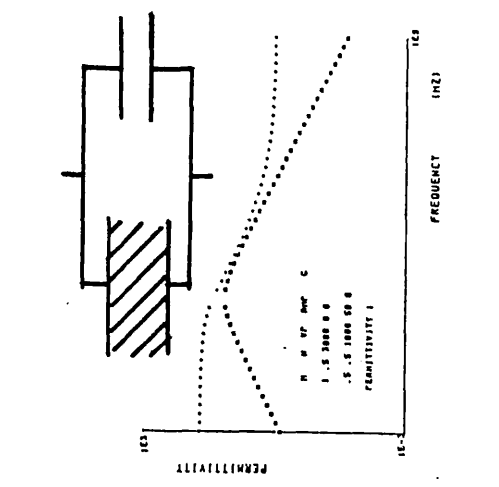
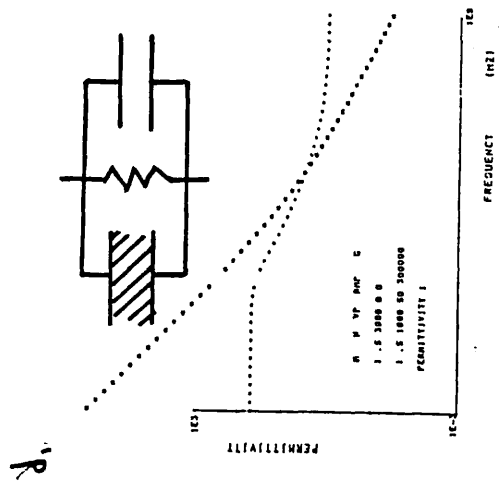
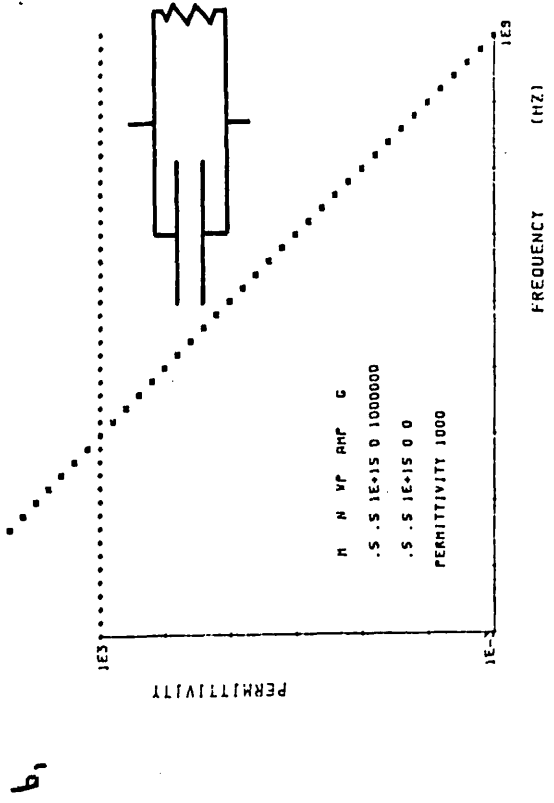
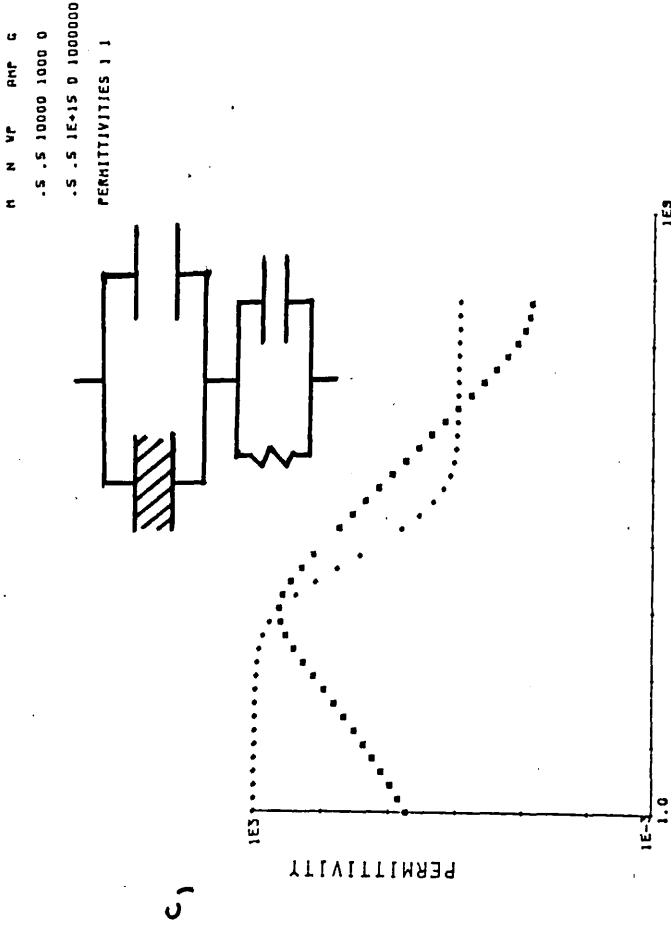
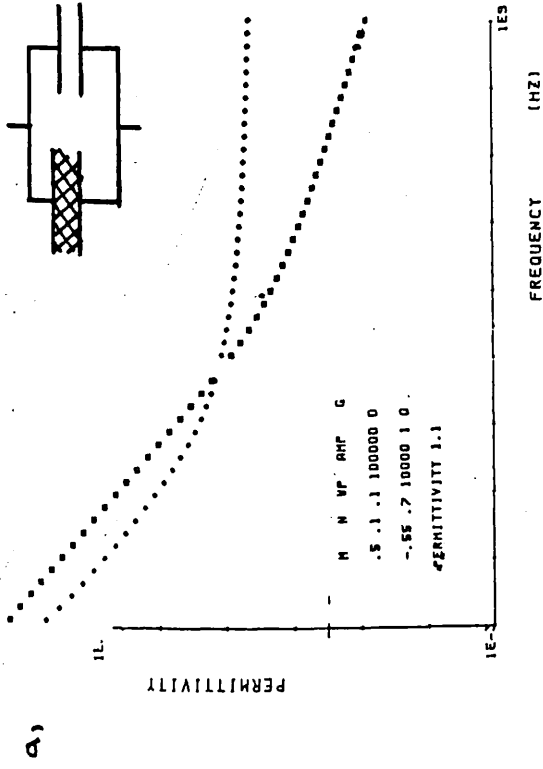


Figure 8.1

(a), which is discussed in detail in Appendix 2, shows the so-called low frequency dispersion (L.F.D.) or quasi d.c. conductivity and is shown represented by a parallel combination of two capacitances, one dispersive the other non-dispersive in nature;

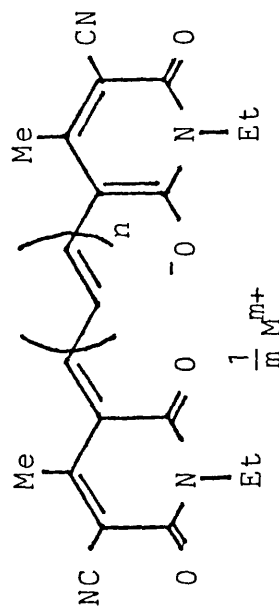
(b) like (a) is a carrier dominated response, however, in contrast, here we are seeing charges moving from one electrode to the other, the real susceptibility $\chi'(\omega)$ remains constant and the imaginary susceptibility $\chi''(\omega)$ has the frequency dependence of ω^{-1} . This is a d.c. conductivity dominated response, which is represented by a parallel combination of a non-dispersive capacitance and a resistance (conductance);

(c) illustrates the Maxwell-Wagner effect. It is an interfacial phenomenon caused, in general, by blocking contacts. It is simply represented as a series combination of a bulk resistance and a capacitance arising from the interfacial contact barrier. The responses seen in (d) (i) and (ii) are the result of diffusion. Whether it be on a microscopic scale as in the diffusion of ions or, as in our case, on a macroscopic scale in the diffusion of the silver paint of our electrodes into the bulk material.

(d)(i) and (ii) shows this diffusion with and without additional d.c. conductivity present, respectively and their corresponding circuit representations.

8.3 The measurements

The dielectric response curves to follow are shown with LOG(C)/LOG(G/ω) vs. LOG(F) axes as a consequence of equations (2.31(A)) and (2.32(A)), Appendix 2; where $\chi'(\omega) \propto C'(\omega)$ and $\chi''(\omega) \propto G(\omega)/\omega$; also refer to the experimental section, 10.6.5.



HPT N^o

288

299

261

324

289

338

(MI1579)

335

336

314

297

(HPP337)

332

n

1

1

1

1

1

0

1

1

1

1

2

2

1

1

1

1

1

1

1

1

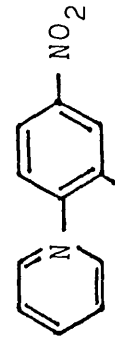
1

M

Bu₄N

(Ph₃PCH₂)₂

Ca



Ph₄P

Et₃NH

Et₃NH

Ni

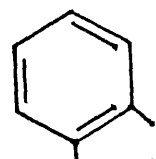
Co

H₂C=C(Me)CO₂CH₂CH₂NH(Me)₂

Ph₃MeP

Et₃NH

TTF



Me

CN

O

N

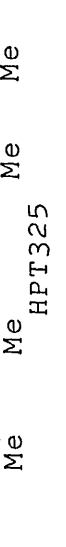
Et

S

N

Et

HPT320



(CH₂)₃

(CH₂)₃

(CH₂)₃

(CH₂)₃

(CH₂)₃

(CH₂)₃

2I⁻

3

3

(CH₂)₃

(CH₂)₃

(CH₂)₃

(CH₂)₃

(CH₂)₃

(CH₂)₃

S

N

Et

HPT320

HPT325

HPT325

All of the theoretical curve fits for the dielectric responses below are either one or a combination of two or more of those shown in Figure 8.1 with slightly modified parameters (m , n , ω_p , amp , and G). Where m and n are exponents of the power laws, equation (2.43(A)) and equation (2.44(A)), described in Appendix 2, ω_p is the loss peak frequency, amp is the loss peak amplitude and G is the conductance of the sample.

8.4. Class I Type Material

These materials are semi-insulating. D.c. conductivity is only apparent at the higher temperature. All have d.c. conductivities lower than $1 \times 10^{-8} \Omega^{-1} \text{m}^{-1}$ at 373 K and have thermal activation energies (assuming materials to be intrinsic) greater than 1.45 eV. The dielectric response is therefore dominated by the polarisation of bound charges, essentially ionic polarisation.

8.4.1. HPT 288

The dielectric measurements suggest the existence of a small amount of d.c. conductivity at the highest temperature of 373 K, Figure 8.3. However, conformation of this by theoretical curve fitting is not possible as we have very little information at the low frequency end of the spectrum where the conductance dominates. We, however, have a measured d.c. conductivity of $6.92 \times 10^{-9} \Omega^{-1} \text{m}^{-1}$ at 373 K, Figure 8.2.

8.4.2. HPT 299

Essentially identical to HPT 288, Figure 8.5 differing however in its measured d.c. conductivity of $1.92 \times 10^{-9} \Omega^{-1} \text{m}^{-1}$ at 373 K, Figure 8.4.

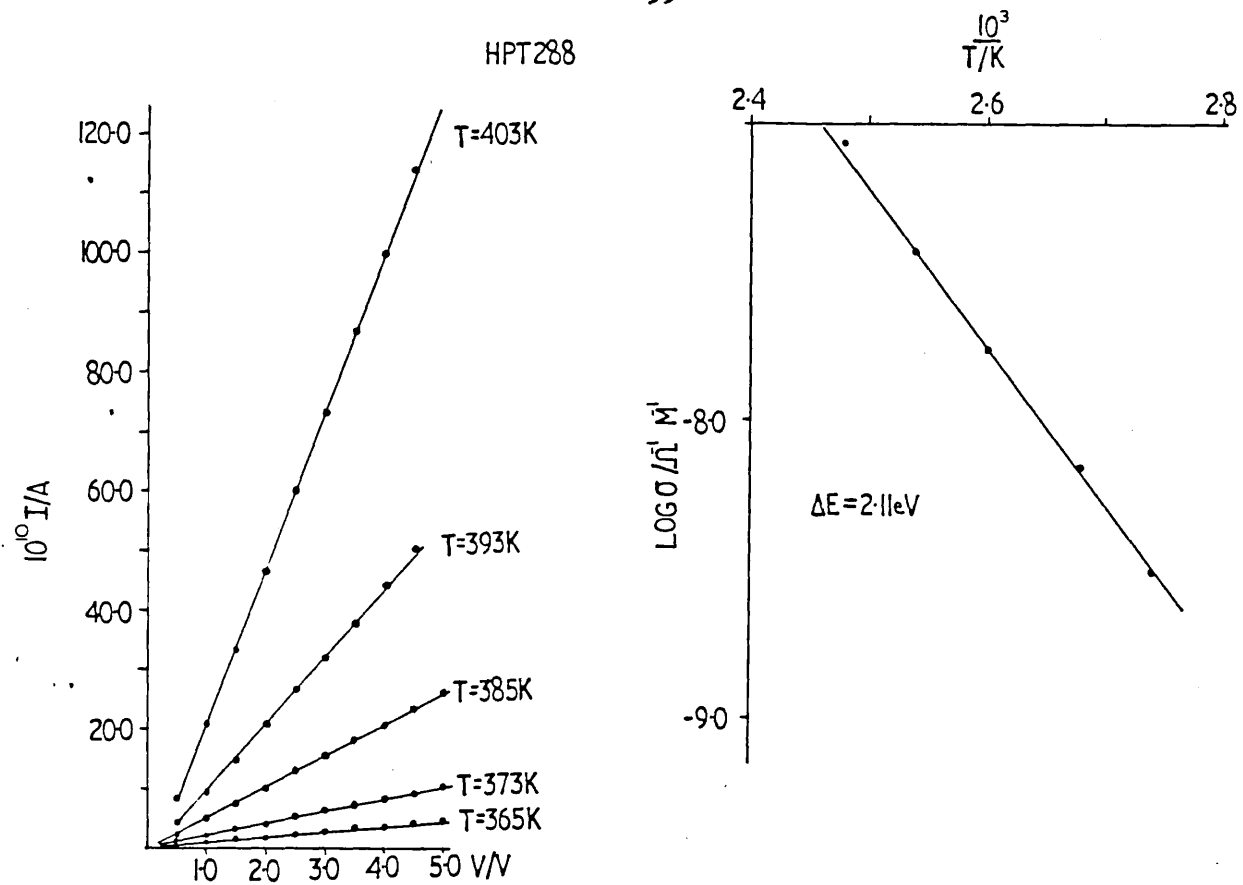


Figure 8.2

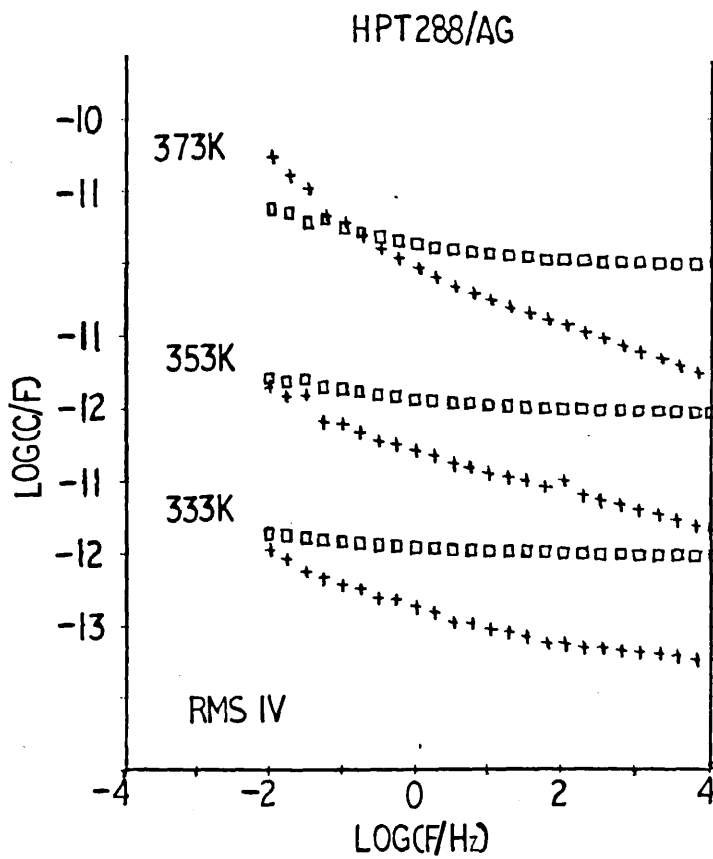


Figure 8.3

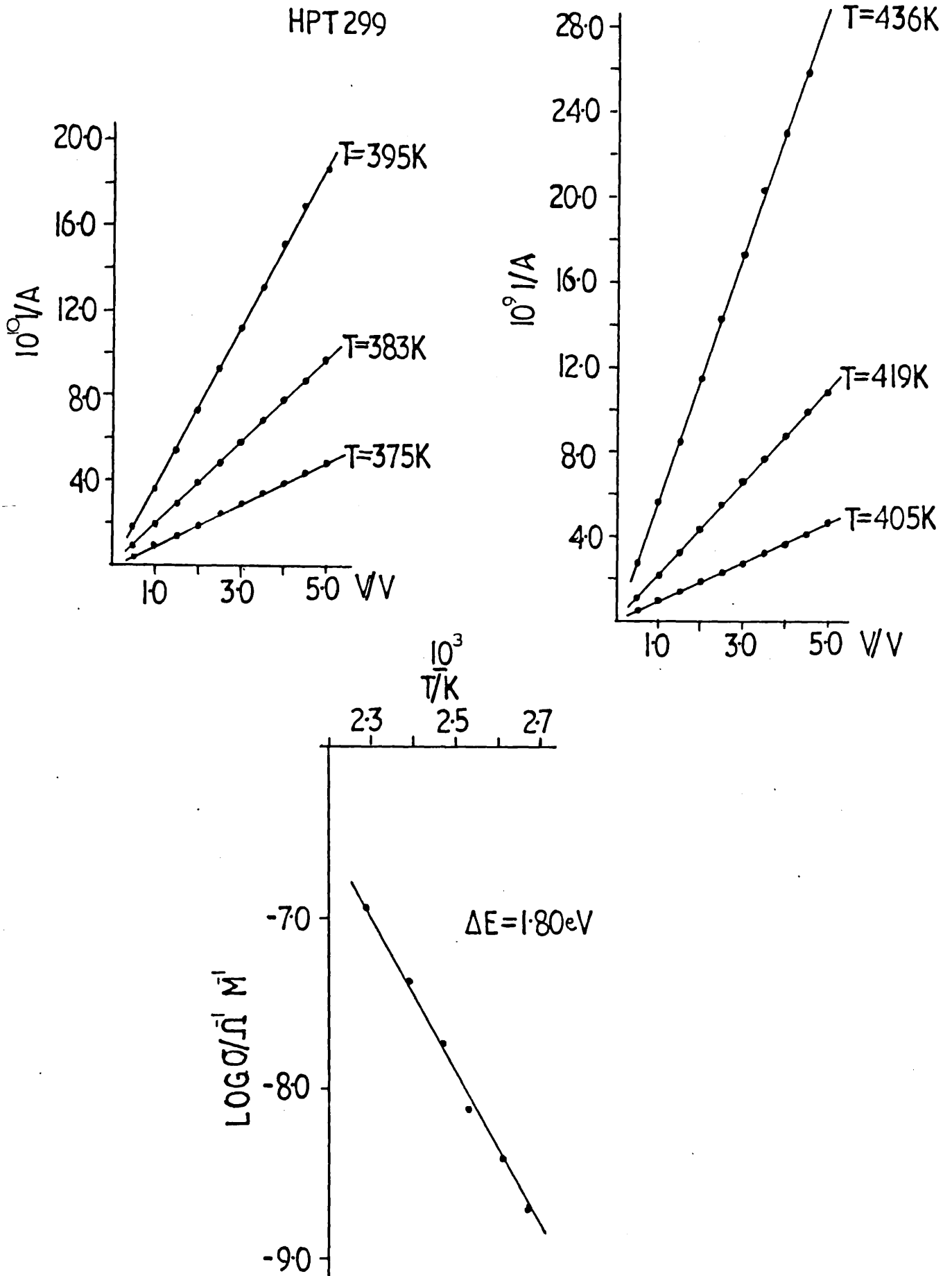


Figure 8.4

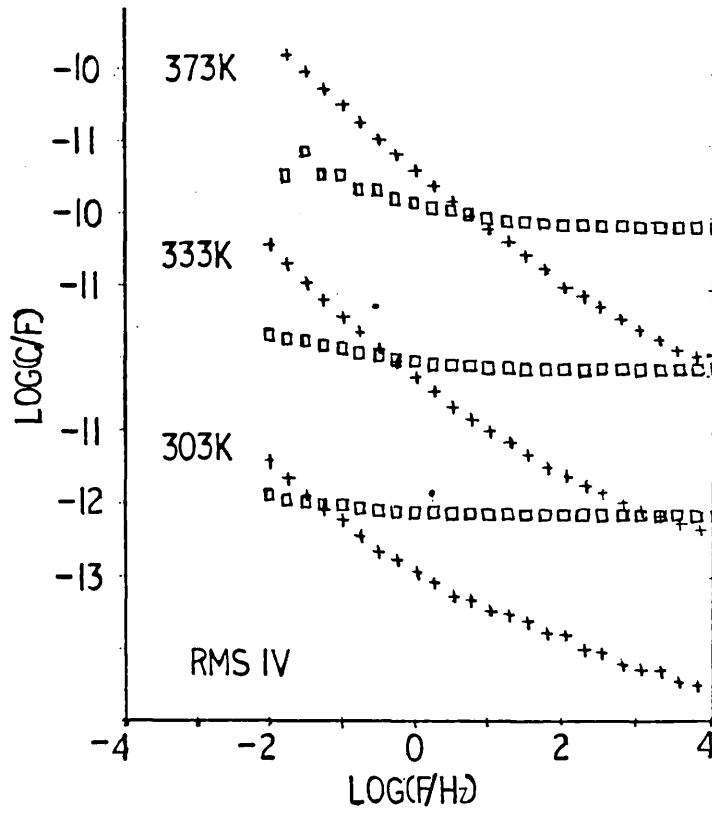


Figure 8.5

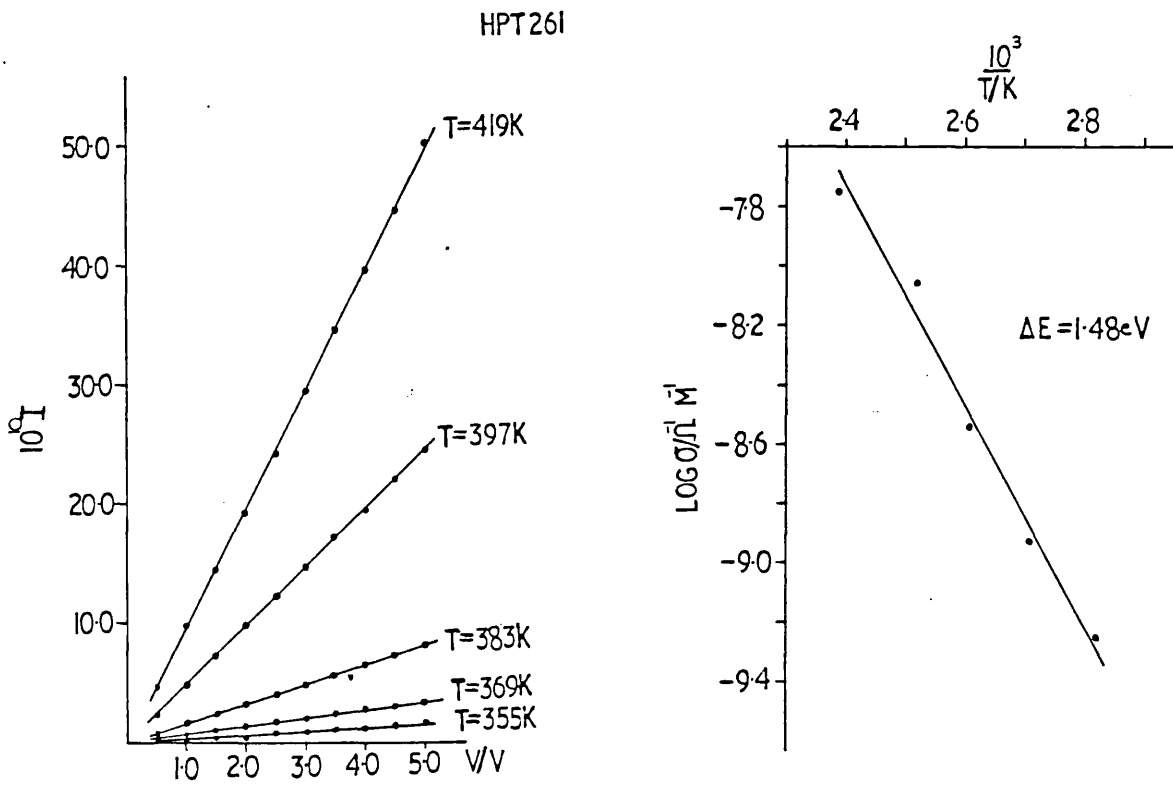


Figure 8.6

8.4.3. HPT 261 and HPT 324

Dielectric spectra were not measured for these two materials as from examination of their d.c. characteristics, Figures 8.6 and 8.7, similar responses to those seen for HPT 288 and HPT 299 were expected.

8.4.4. HPT 289

Two different contacts were tried for this sample (Ag, Al) each gave essentially the same dielectric response. The dominant spectral feature for both contacts is that of LFD or quasi d.c. conduction which is confirmed by curve fitting, Figures 8.9, 8.10. The slight dispersion in complex capacitance at the lower frequency end of the higher temperature spectra for the silver contacted sample suggests, also the existence of a diffusive process (Ag diffusion; see Class II type material). Figure 8.8 shows the d.c. characteristics.

8.4.5. HPT 338

The spectra show a number of interesting features. At the lower temperatures a loss peak is clearly visible, caused by the polarisation and subsequent relaxation of bound charges (in our case ions). At the higher temperatures there is evidence for an interfacial contact barrier limiting the d.c. transport in the system; this is reflected in the saturation of both χ' and χ'' at low frequency, Figure 8.12. Figure 8.11 shows the d.c. characteristics.

HPT324

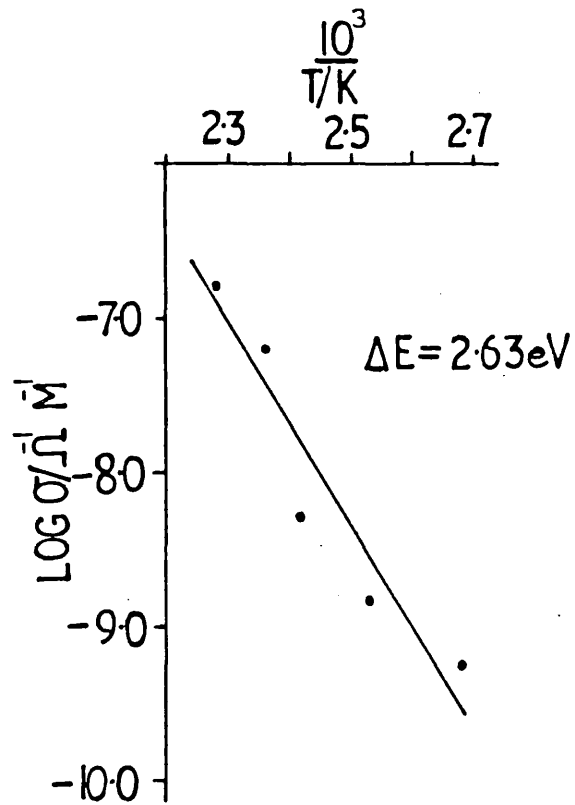
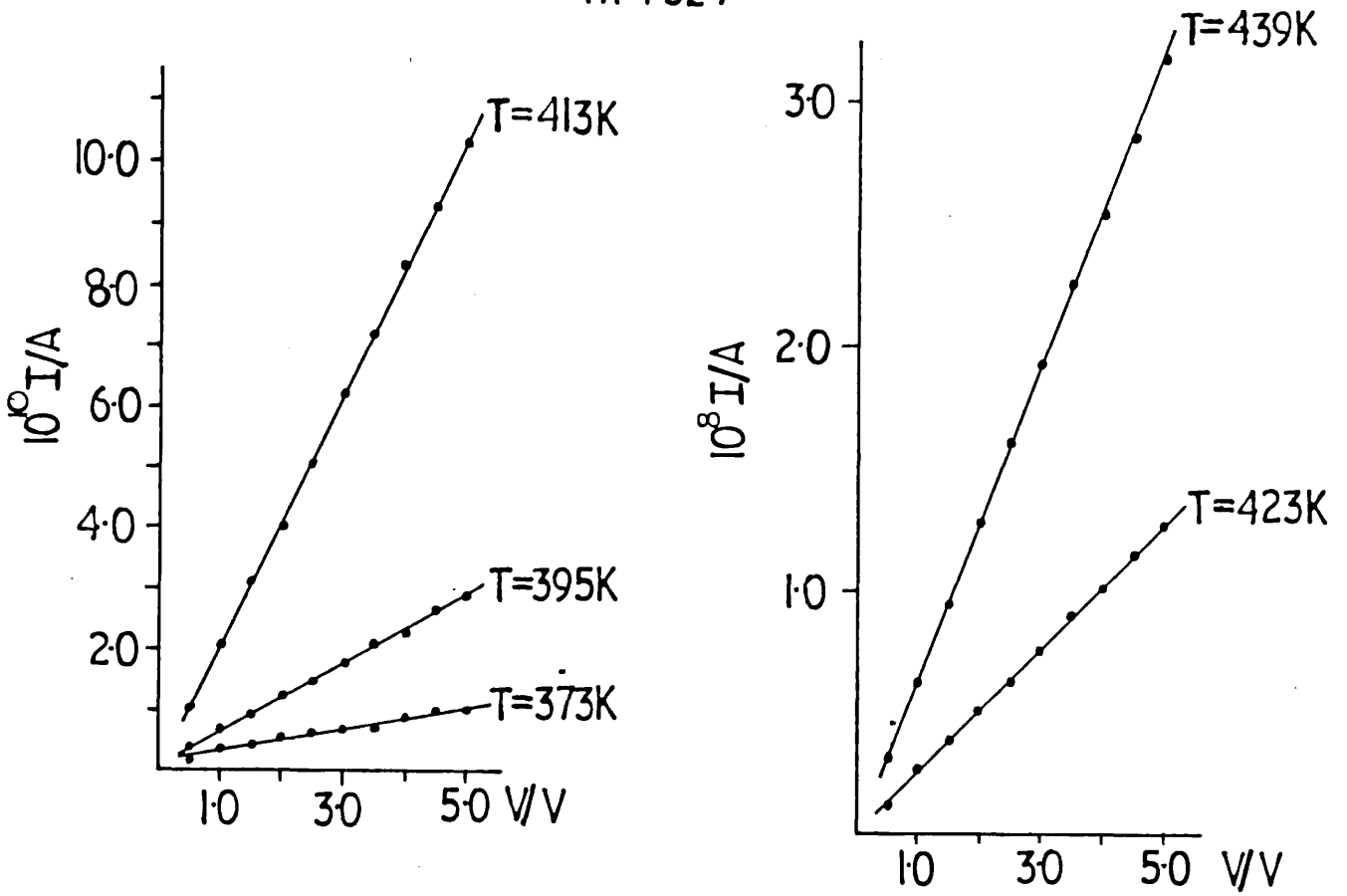


Figure 8.7

HPT 289

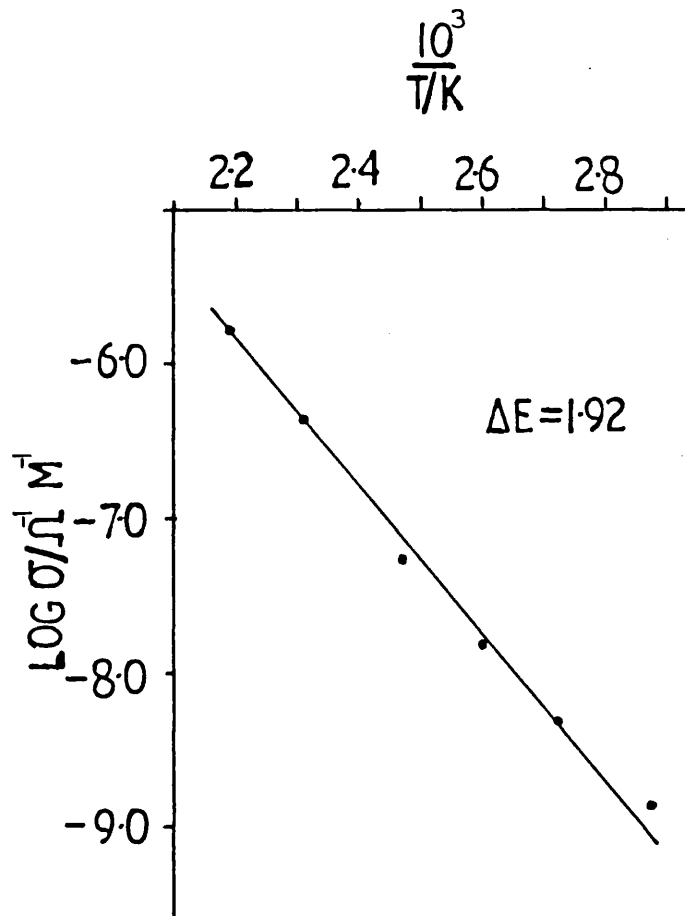
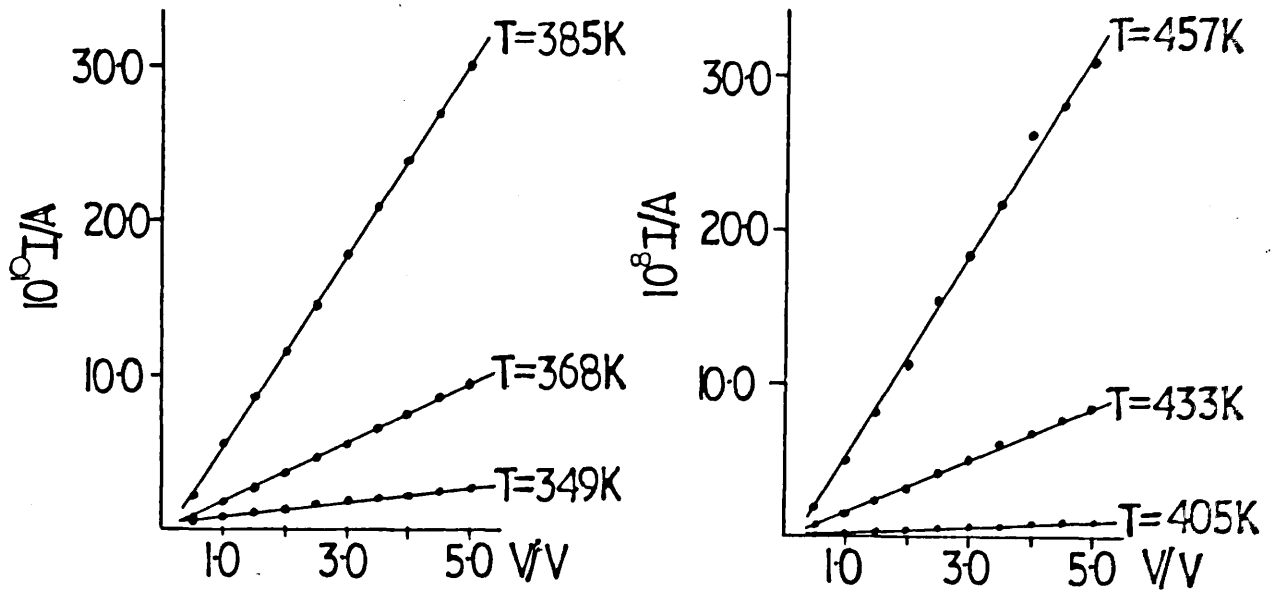


Figure 8.8

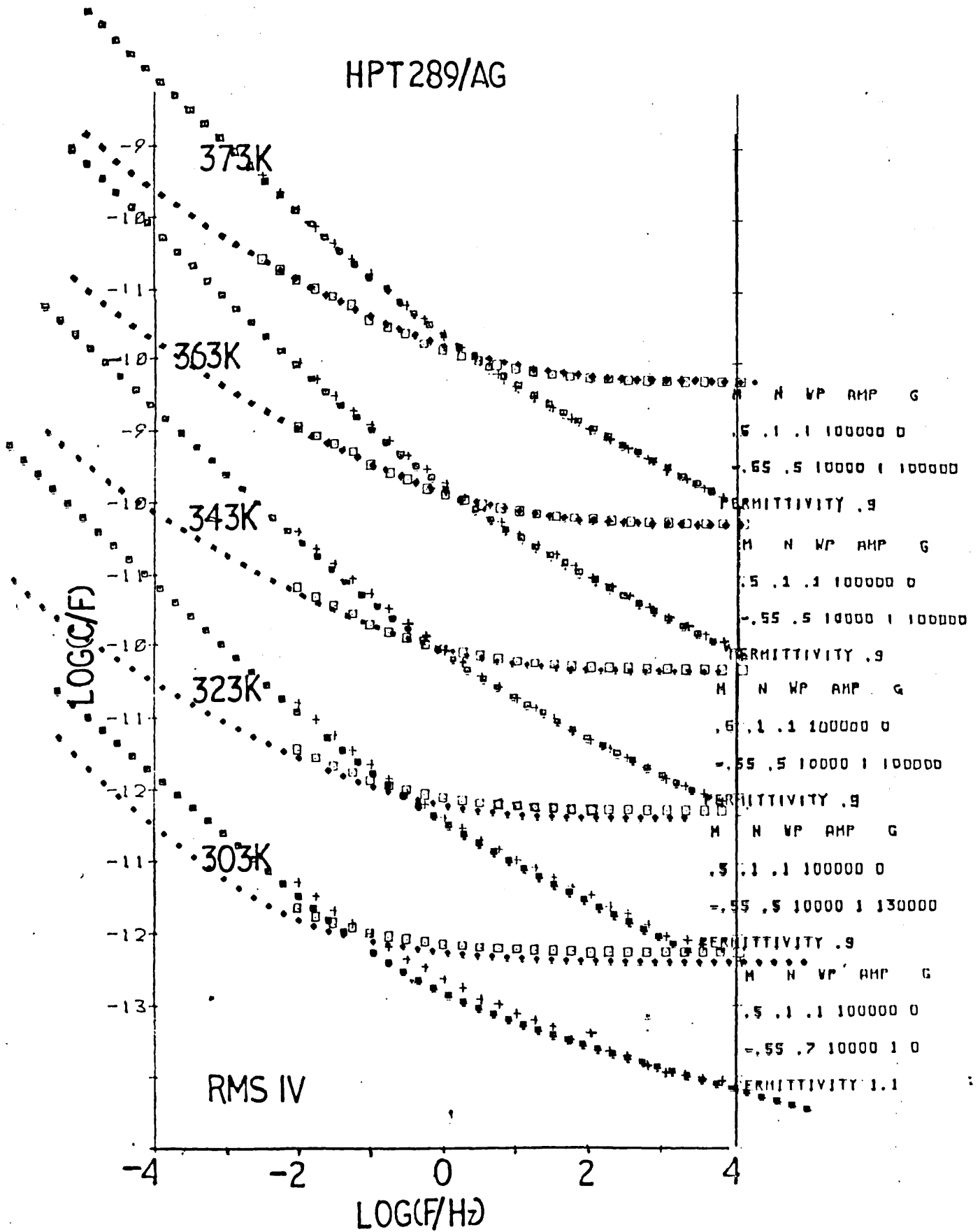


Figure 8.9

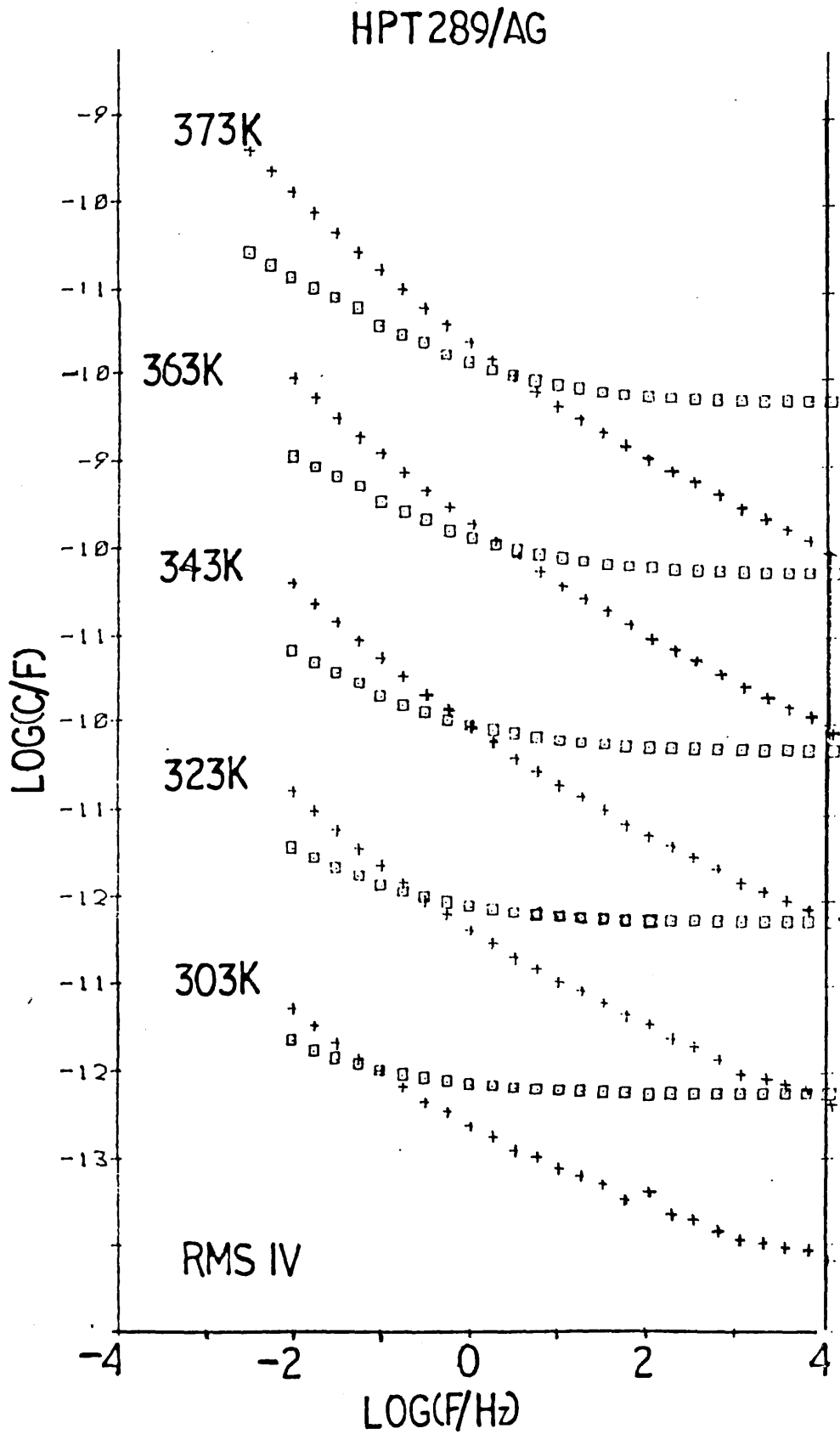


Figure 8.9

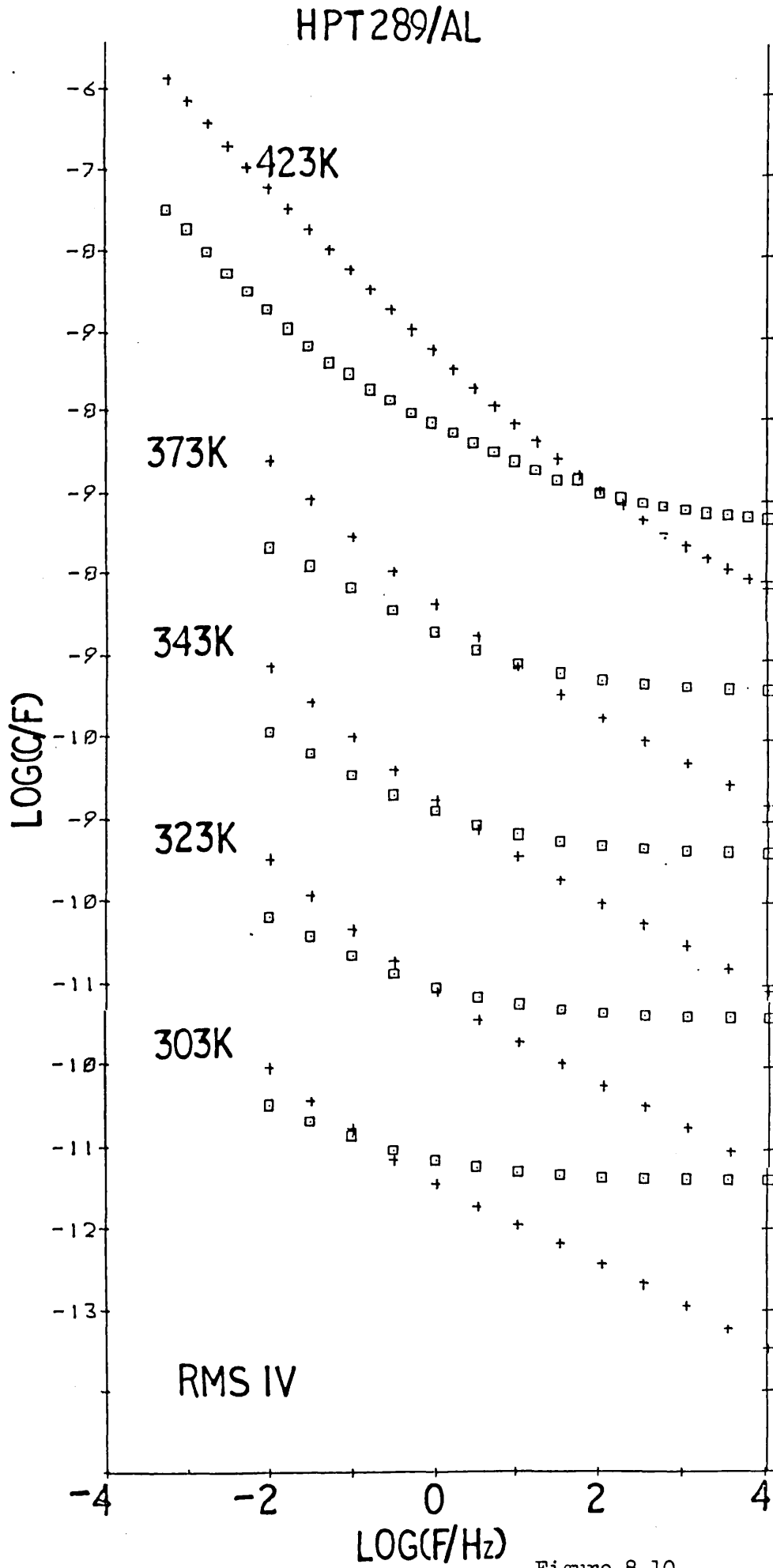


Figure 8.10

HPM(CHPT 338)

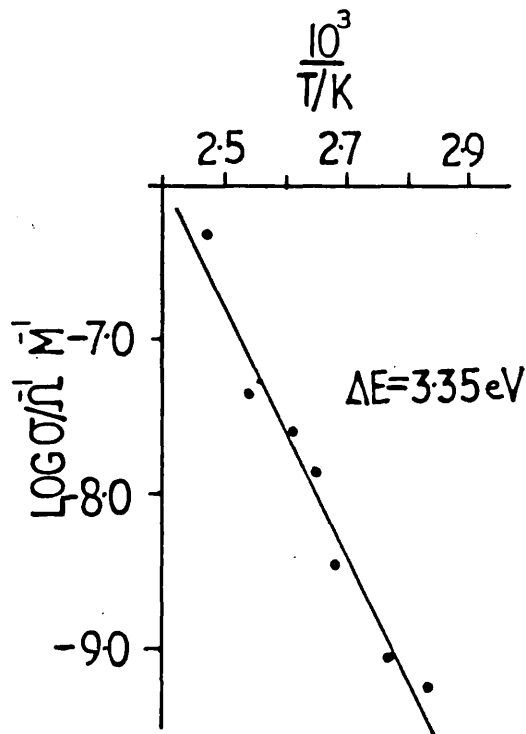
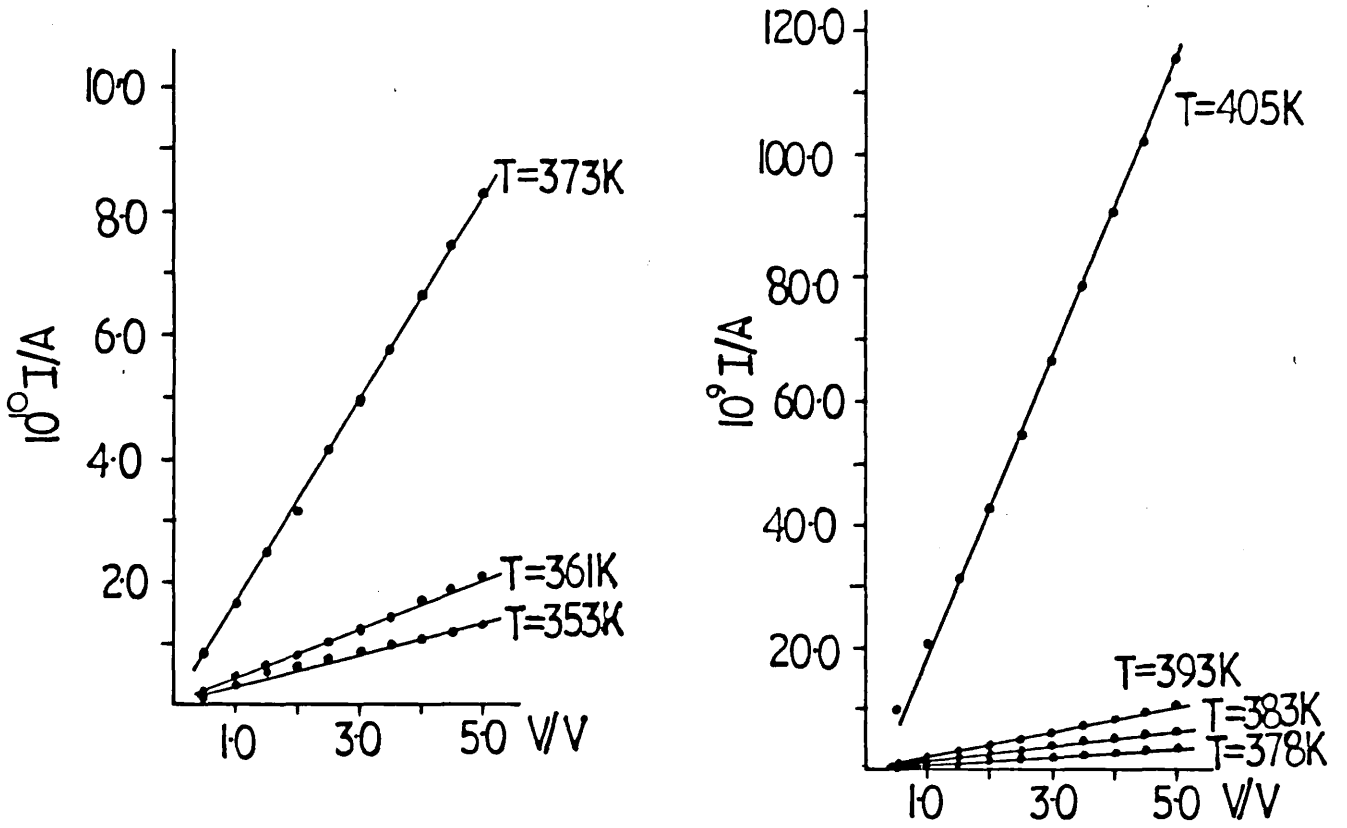


Figure 8.11

HPM I/HPT338

AG

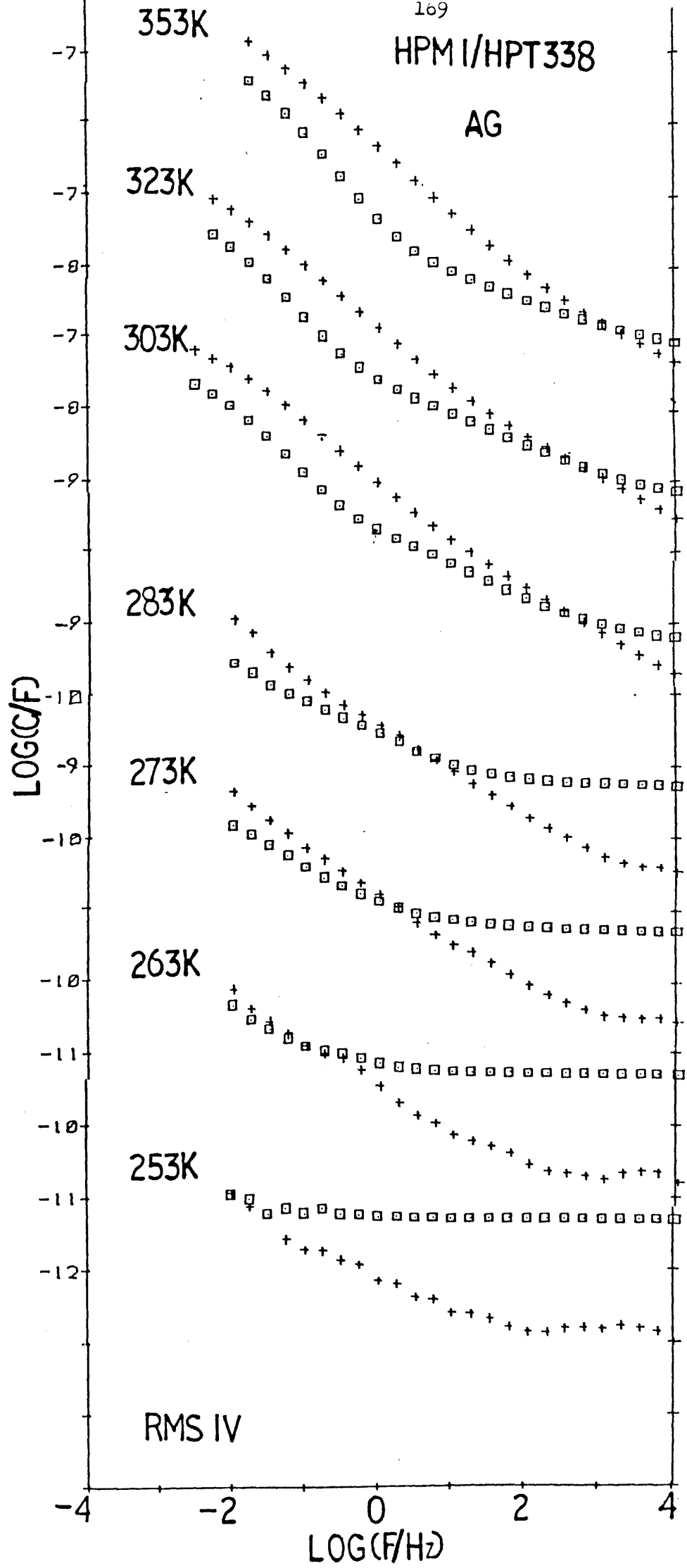


Figure 8.12

8.4.6. MI 1579

Again two contacts were investigated (Ag, Al). For the Ag contacted material the lower temperature spectral signatures are similar to those of HPT 338 in that a loss peak is present, it is however in this case, far more clearly defined. The complex capacitance in the higher temperature responses appears to be saturating and resembles very closely Figure 8.1(d)(i) where we have a diffusive process with parallel d.c. conductivity, Figure 8.14. The Al contacted material at these elevated temperatures exhibits a classic example of LFD, Figure 8.15. All features being clearly confirmed by theoretical curve fitting. The samples d.c. characteristics are shown in Figure 8.13.

MI1579

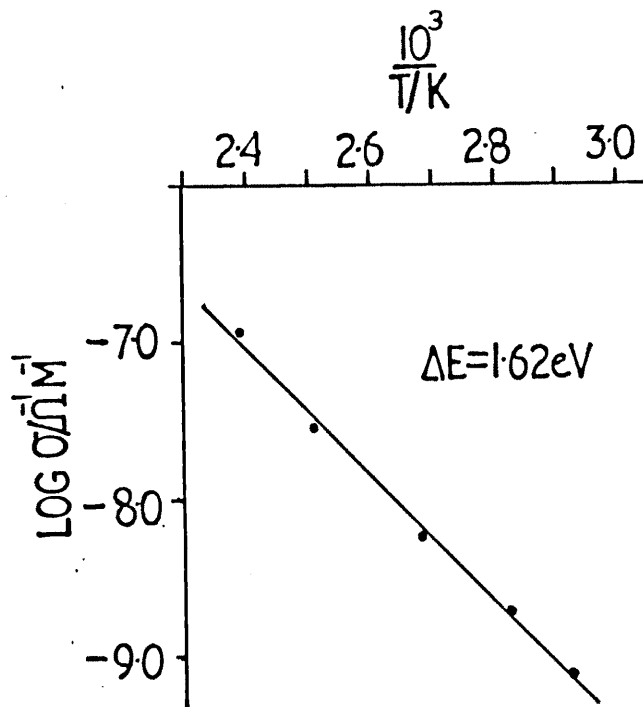
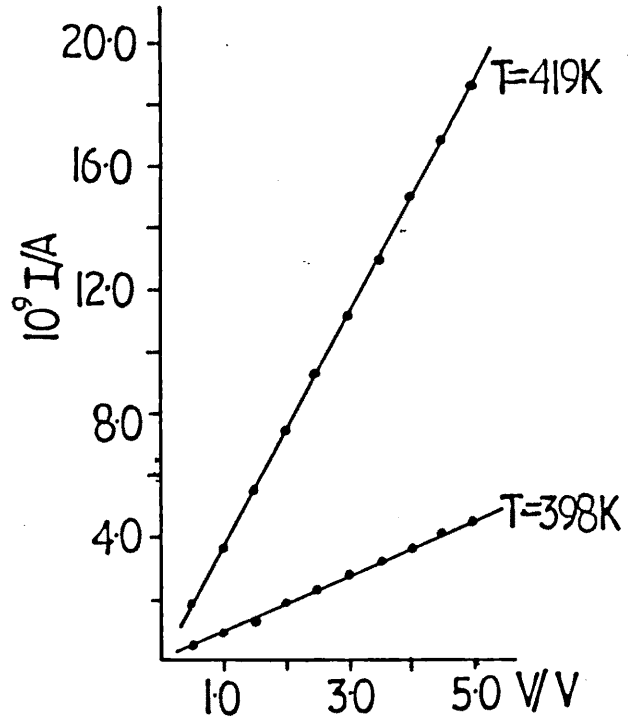
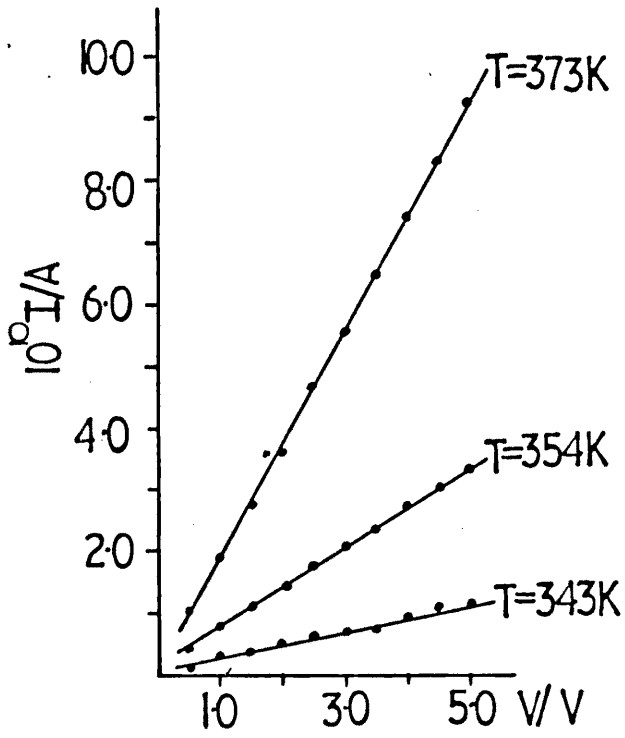


Figure 8.13

MI1579/AG

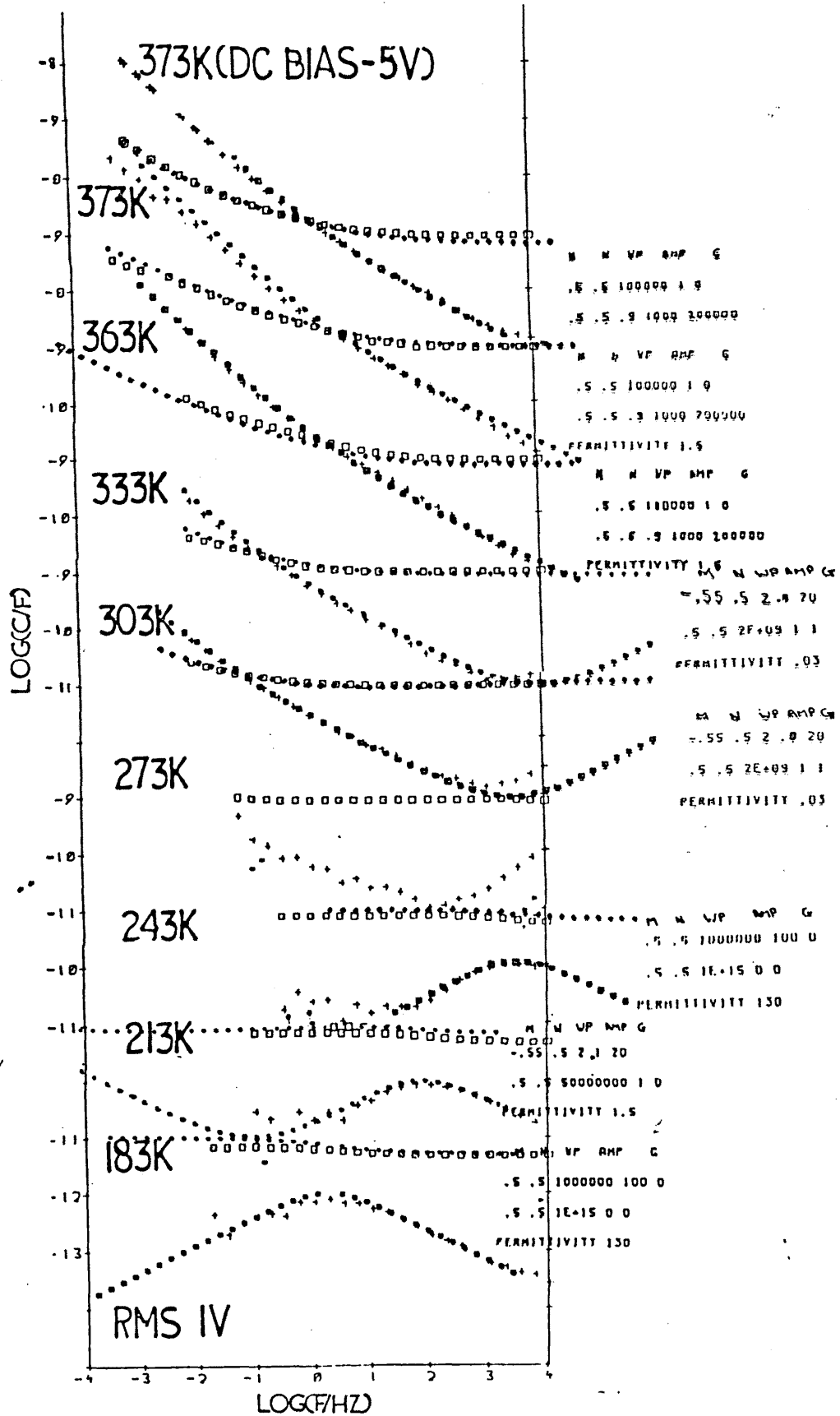


Figure 8.14

MI1579/AG

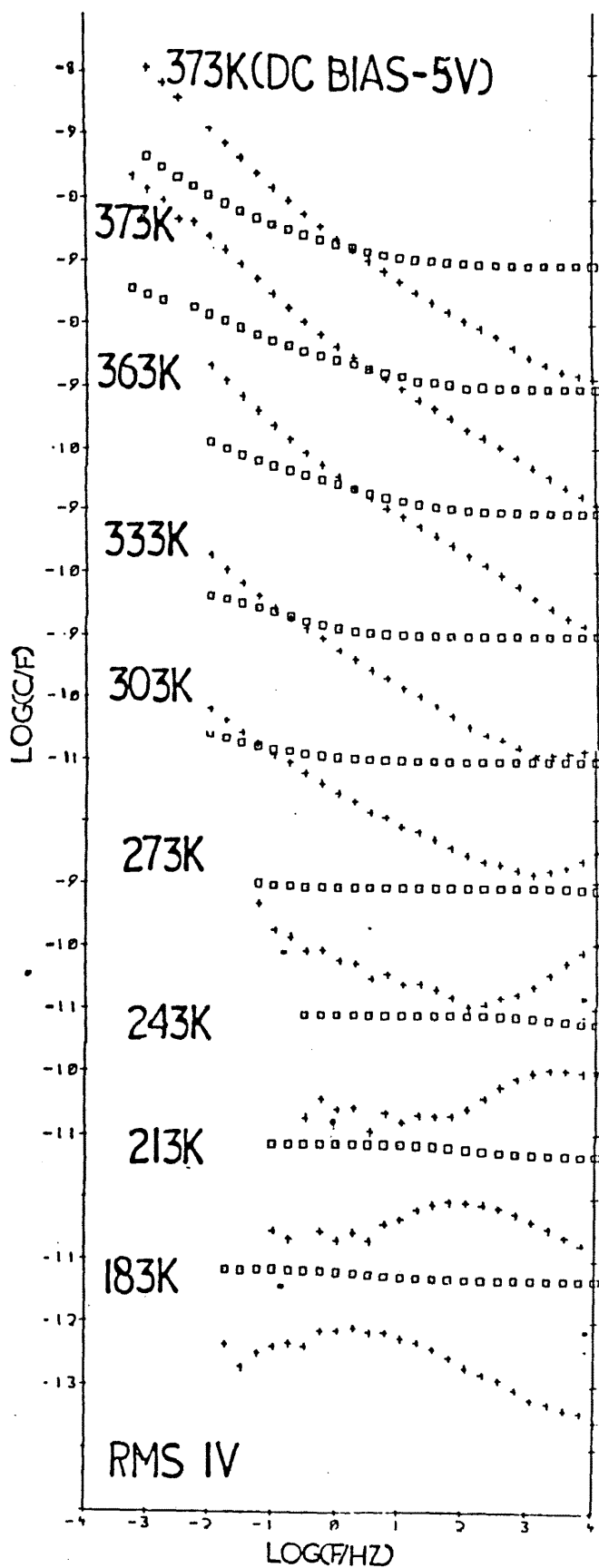


Figure 8.14

MI1579/AL

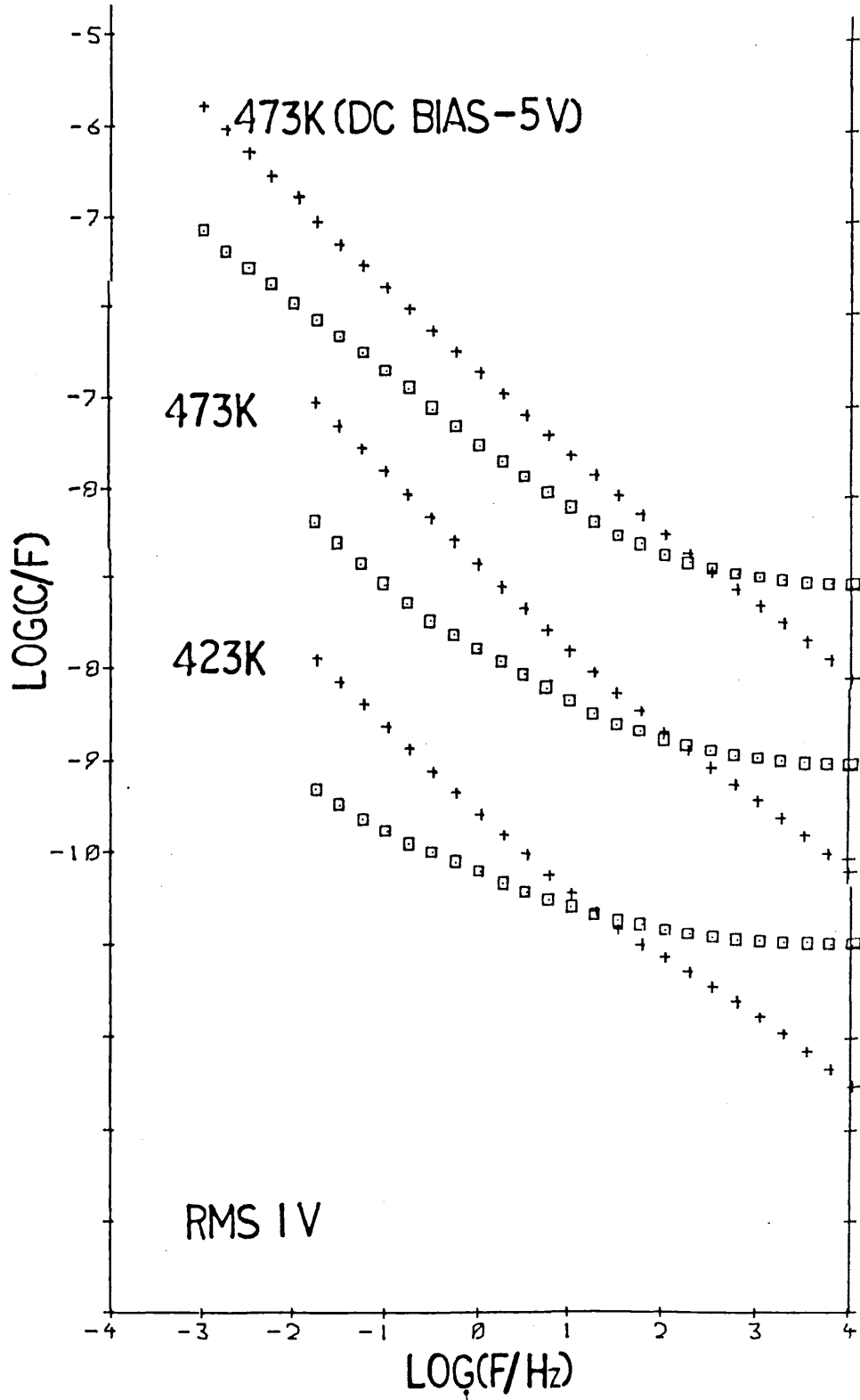


Figure 8.15

8.5. Class II Type Material

These materials HPT 335, HPT 336 and HPT 314, although still generally classed as semi-insulating, have d.c. conductivities of two orders of magnitude higher and significantly lower thermal activation energies than those materials of the Class I type.

The dielectric spectra of both HPT 336, Figure 8.17 and HPT 314, Figure 8.19, are dominated by a diffusive process with parallel d.c. conductivity very similar to that seen for Ag contacted MI 1579 at its higher temperatures. These responses are supported by theoretical curve fitting. It was expected that the dielectric response for HPT 335 would be similar. Figure 8.16, 8.18 and 8.20 show the d.c. characteristics of HPT 336, HPT 314 and HPT 335 respectively. Samples of HPT 335 and HPT 336 were left overnight and a repeat measurement of their d.c. characteristics was attempted. However, on doing so, both sample assemblies produced a shorting-out ($R = 0$) of the circuit.

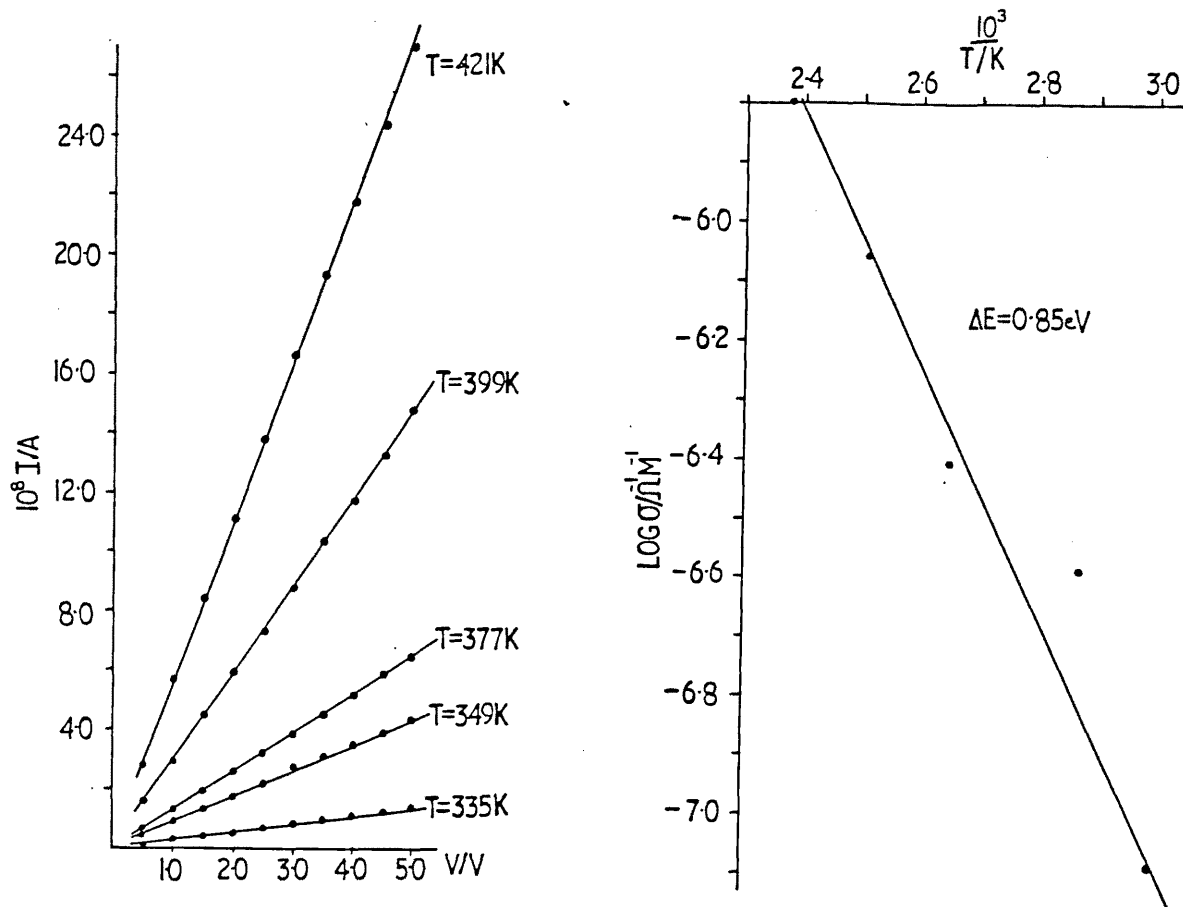


Figure 8.16

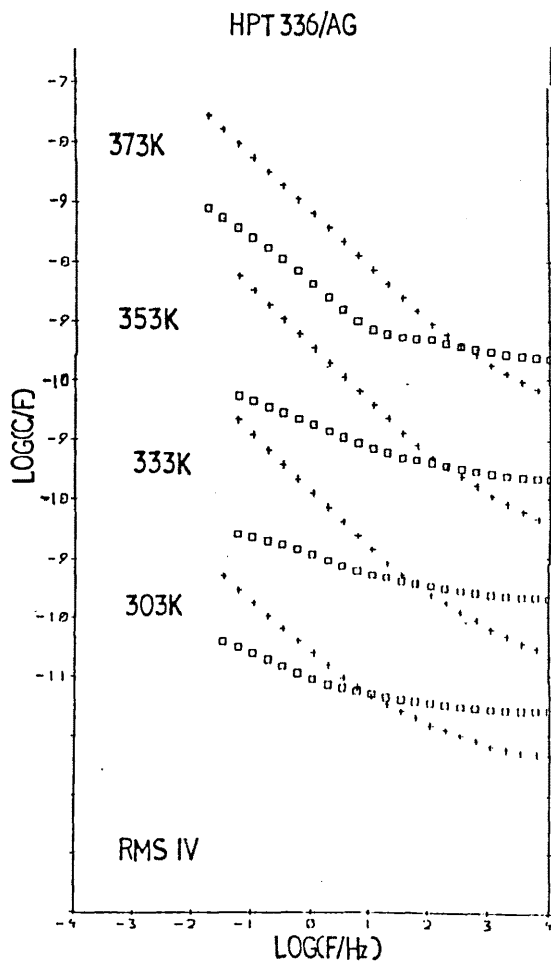


Figure 8.17

HPT 314

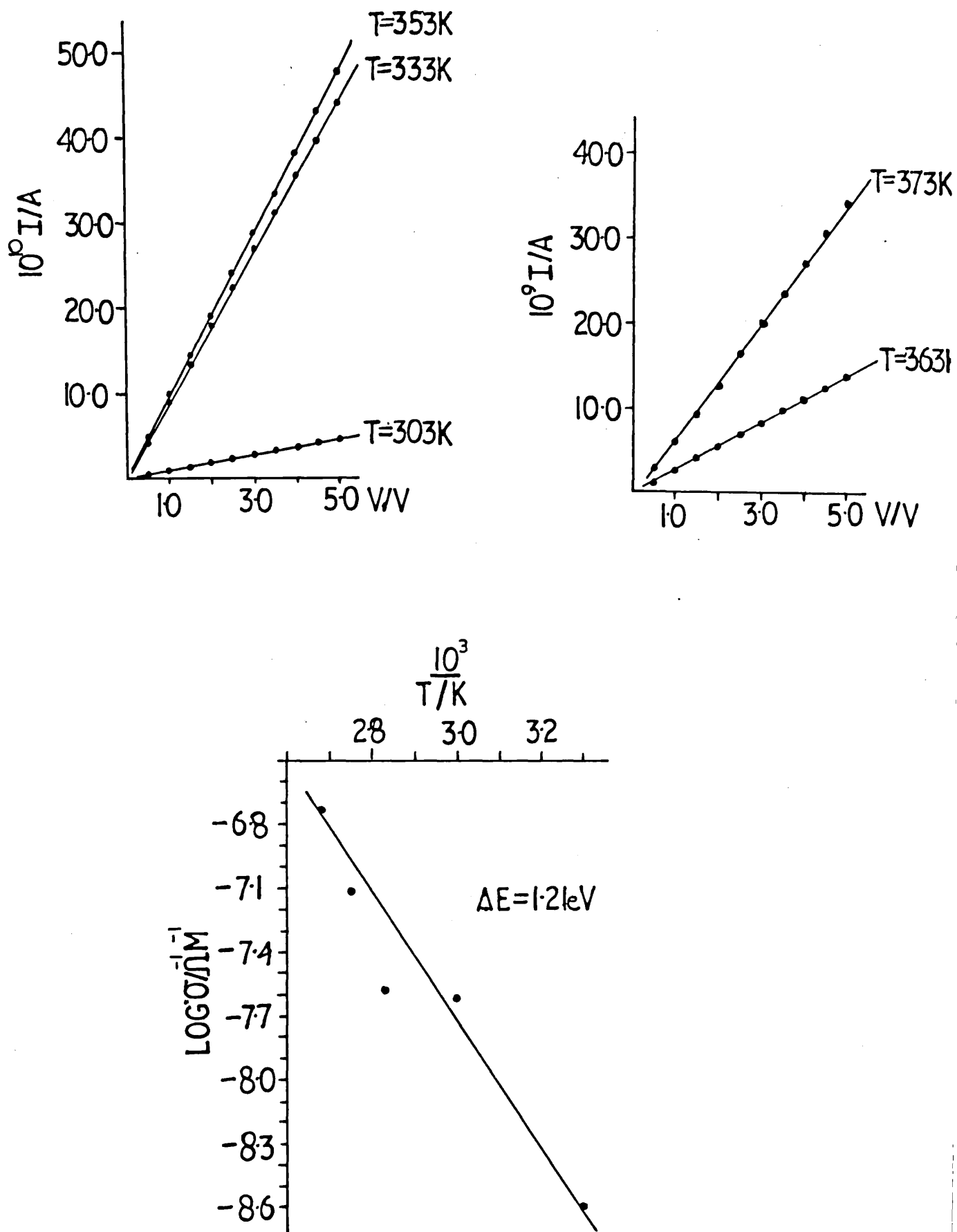


Figure 8.18

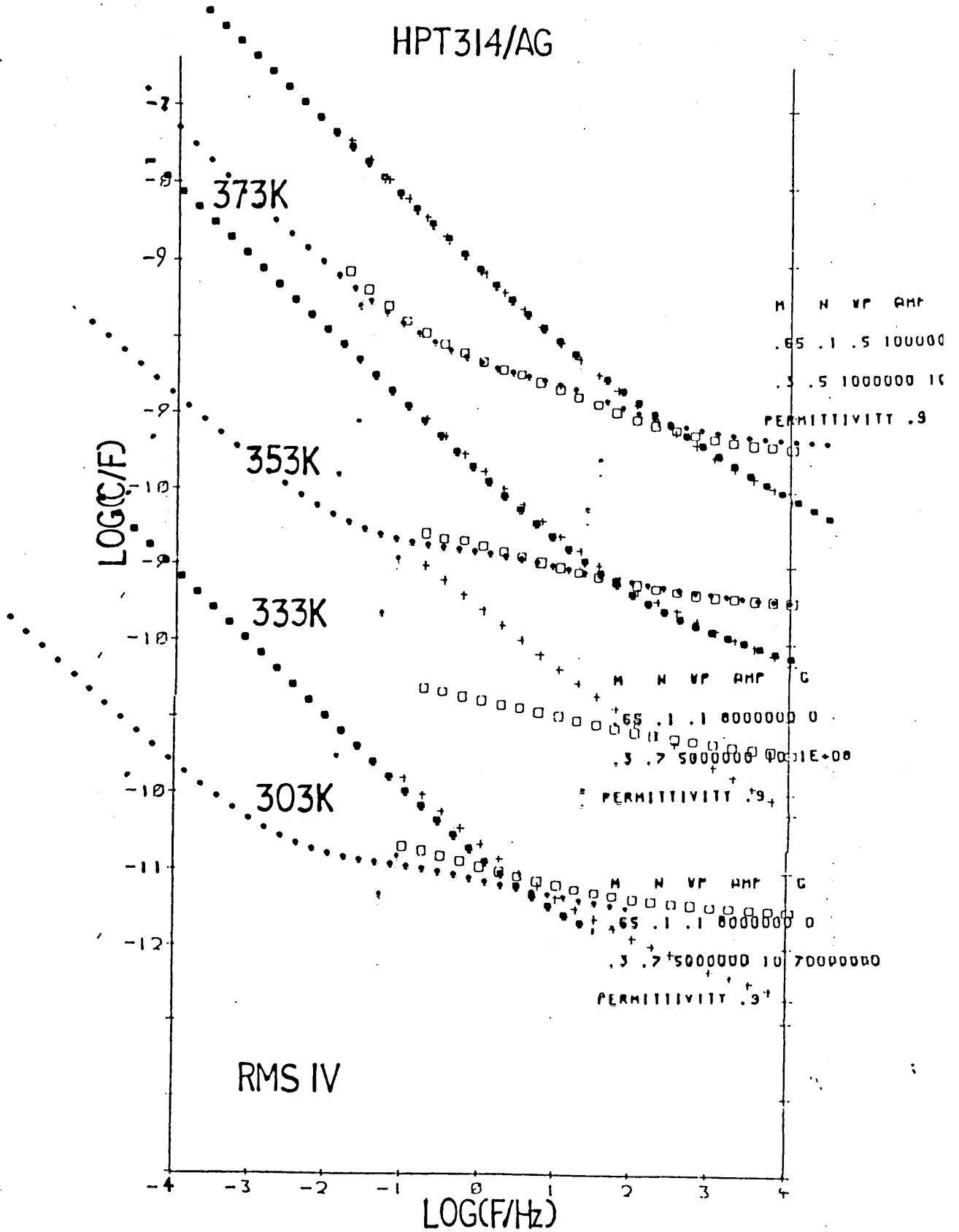


Figure 8.19

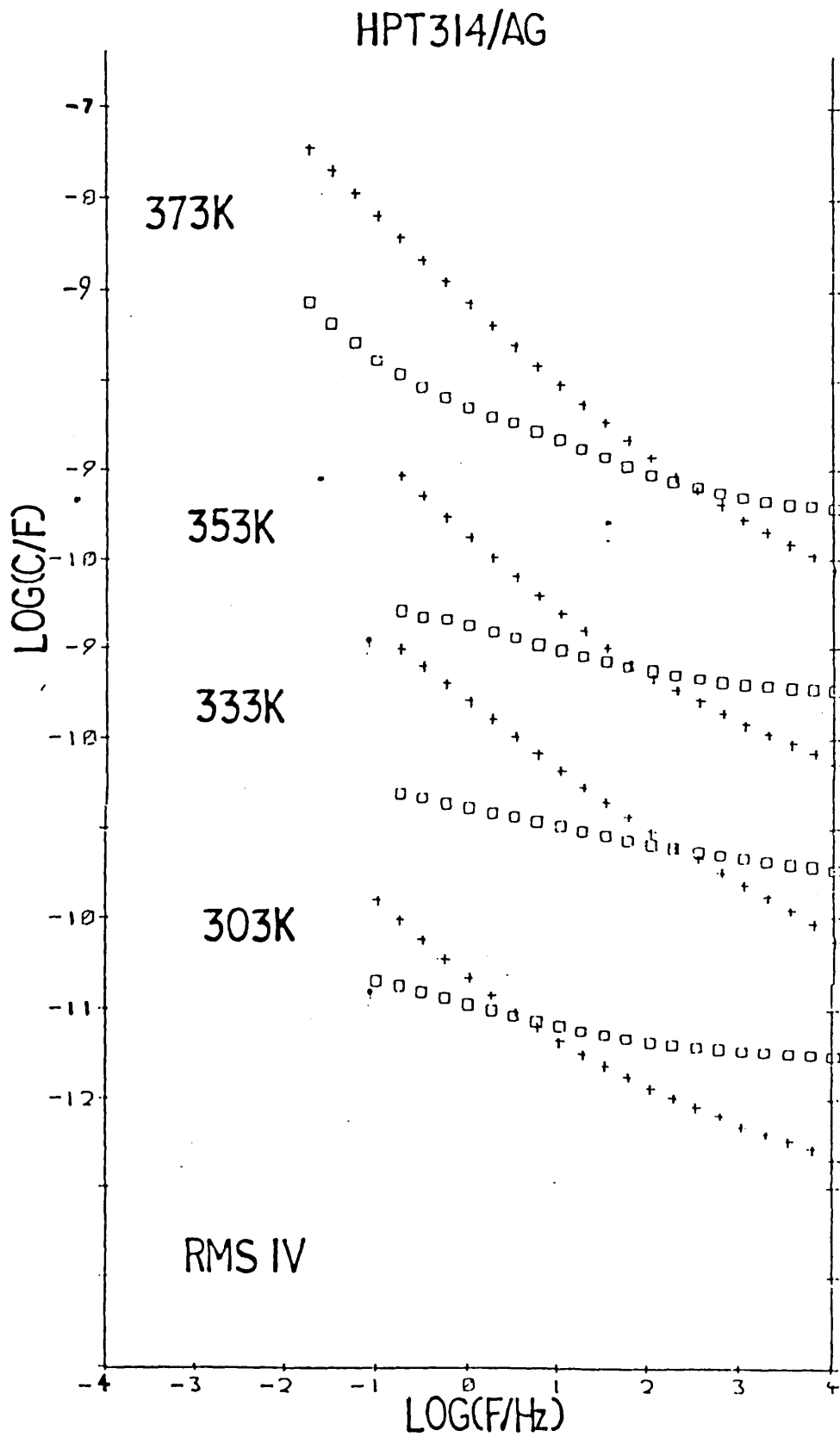
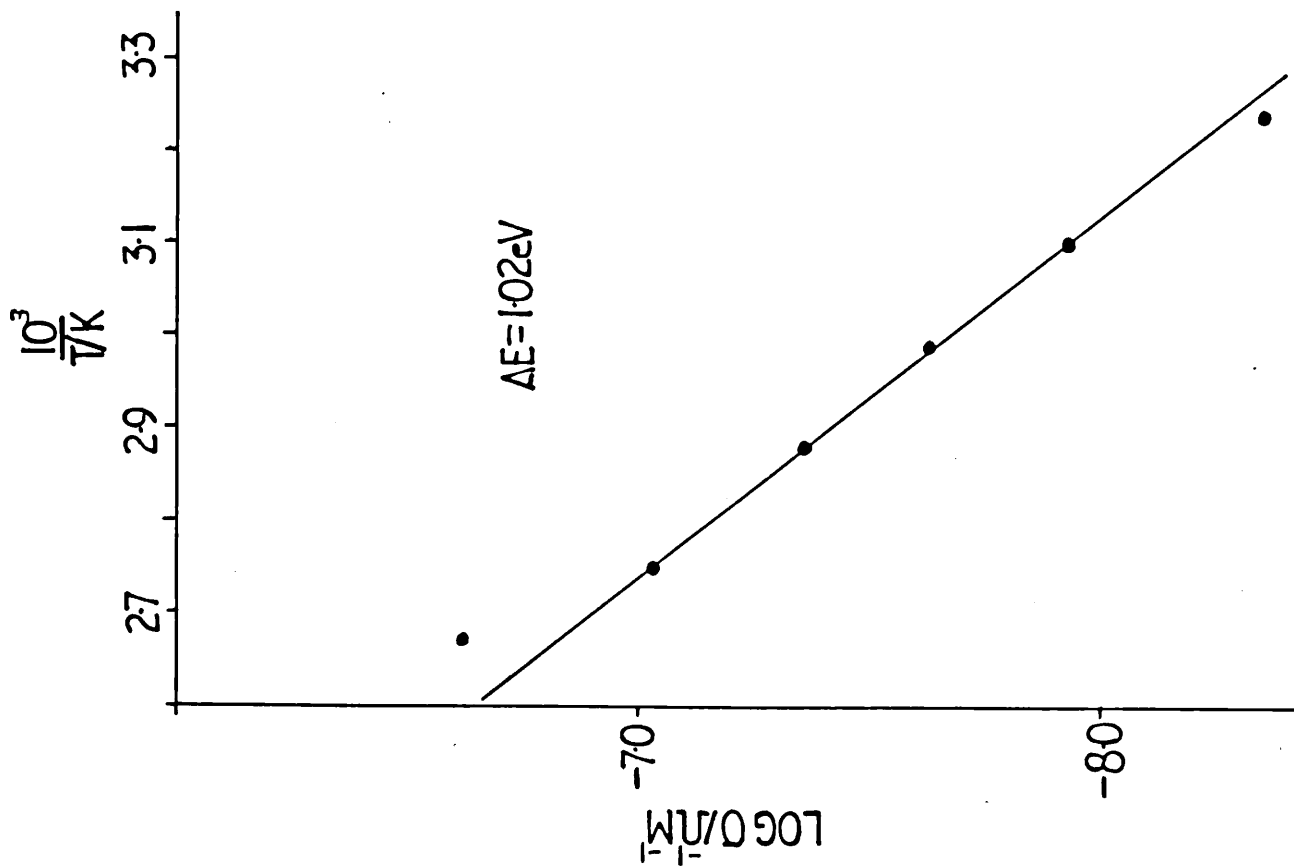


Figure 8.19

HPT335/AG



$T = 375K$

$T = 363K$

$T = 347K$

$T = 335K$

$T = 323K$

$T = 309K$

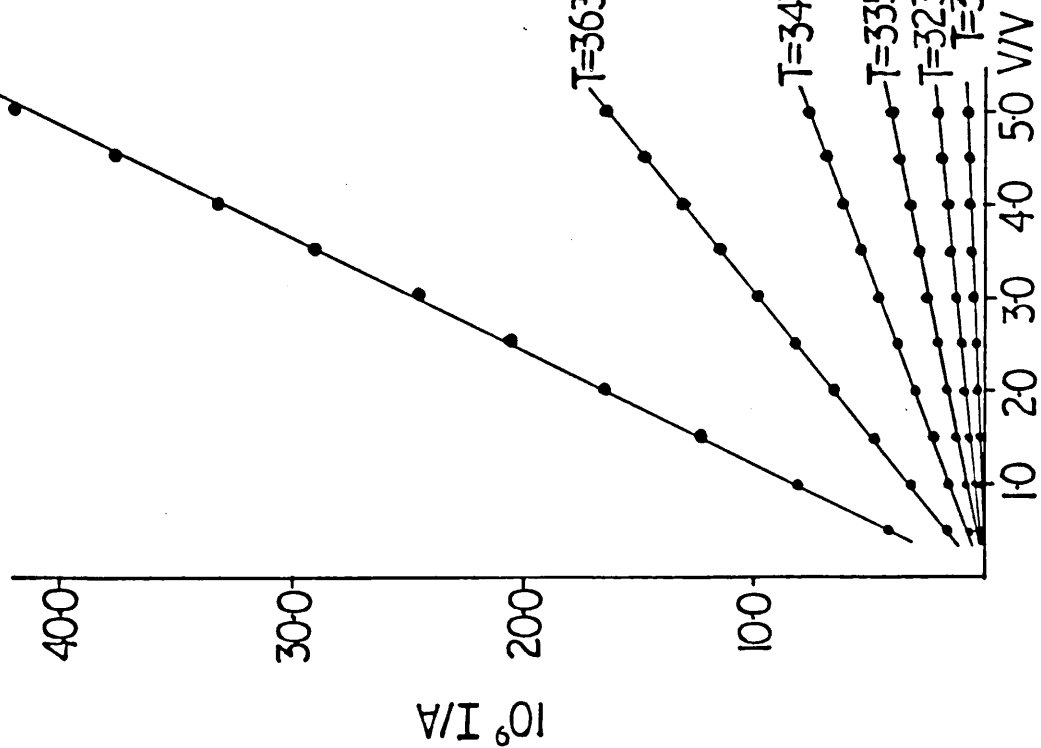


Figure 8.20

8.6 Class III Type Material

This material (HPT 297) is semi-conducting with a d.c. conductivity of $4.82 \times 10^{-6} \Omega^{-1} \text{m}^{-1}$ at 373 K and a thermal activation energy of 0.66 eV (assuming the material to be intrinsic), Figure 8.21. It has been placed in a class of its own for two reasons: (i) its three order of magnitude increases in d.c. conductivity over HPT 289 has been brought about simply by the replacement of one of the phenyl rings of the Ph_4P^+ cation by a methyl group, and (ii) its Ag contacted dielectric response classically illustrates a diffusive process.

Three different contacts were investigated. The silver paint contacted material shows two distinct dispersions in the complex capacitance, and the ω^{-1} frequency dependence of the loss component shows clear evidence for d.c. conductivity even at the lower temperatures, Figure 8.22. The In contacted material shows a distinctive saturation of the complex capacitance at low frequencies, however the diffusive process is still evident. The pressure contact, however, which involves sandwiching the sample between two copper disc electrodes, shows LFD, Figure 8.23(b).

Both the Ag paint and In contacted materials involve the application of Ag paint to the sample; the former directly and the latter to attach the vacuum deposited In layer via copper wire to the external measuring circuit. Thus it is possible in both cases for silver paint to diffuse into the bulk material itself. This appears to be borne out, in that, contact effects (silver paint diffusion), are seen in the dielectric spectra of both samples. Whereas, in the absence of Ag paint, as in the pressure contacted material, no contact effects are visible. It appears then, that the diffusive processes observed in many of our samples

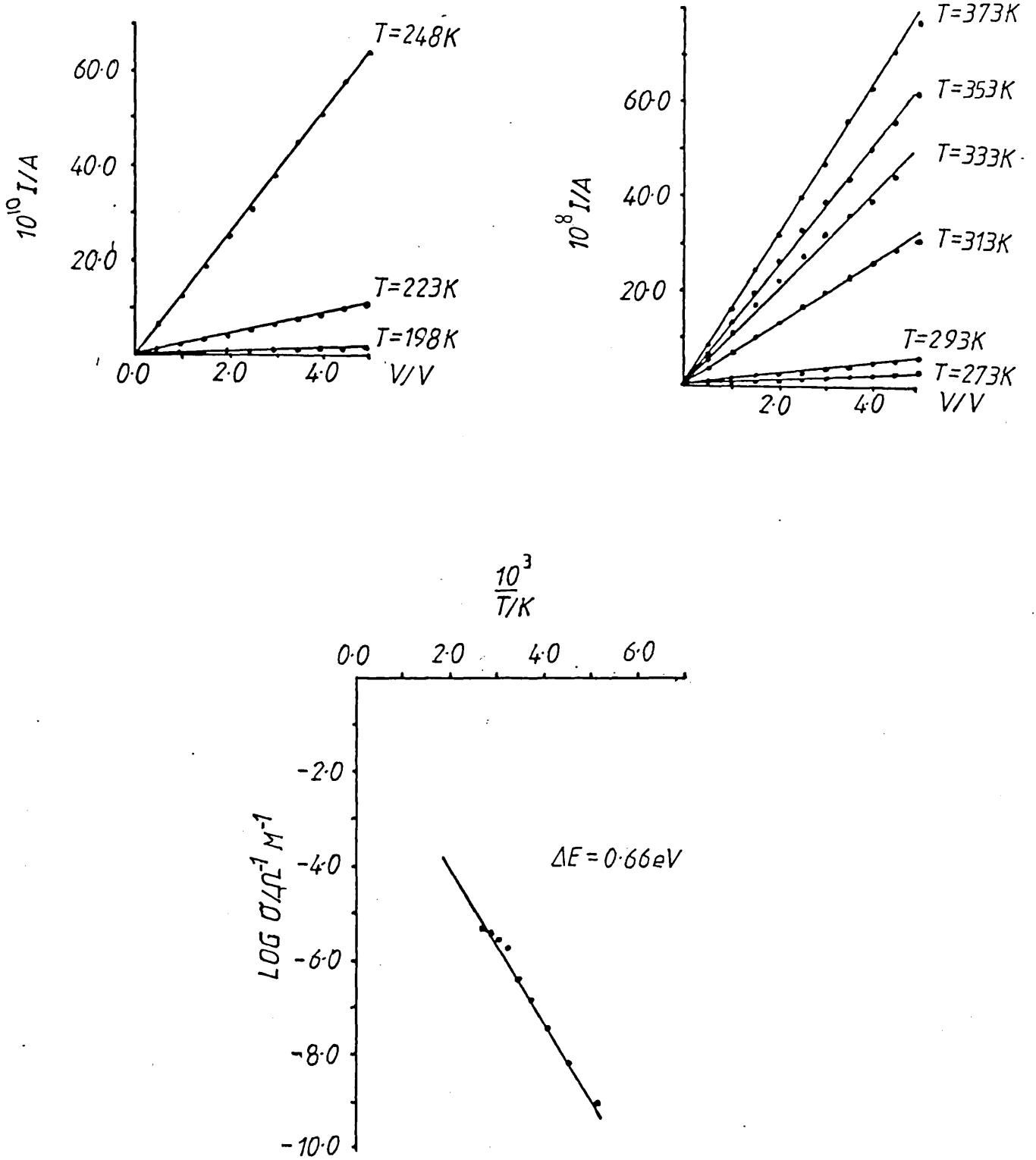


Figure 8.21

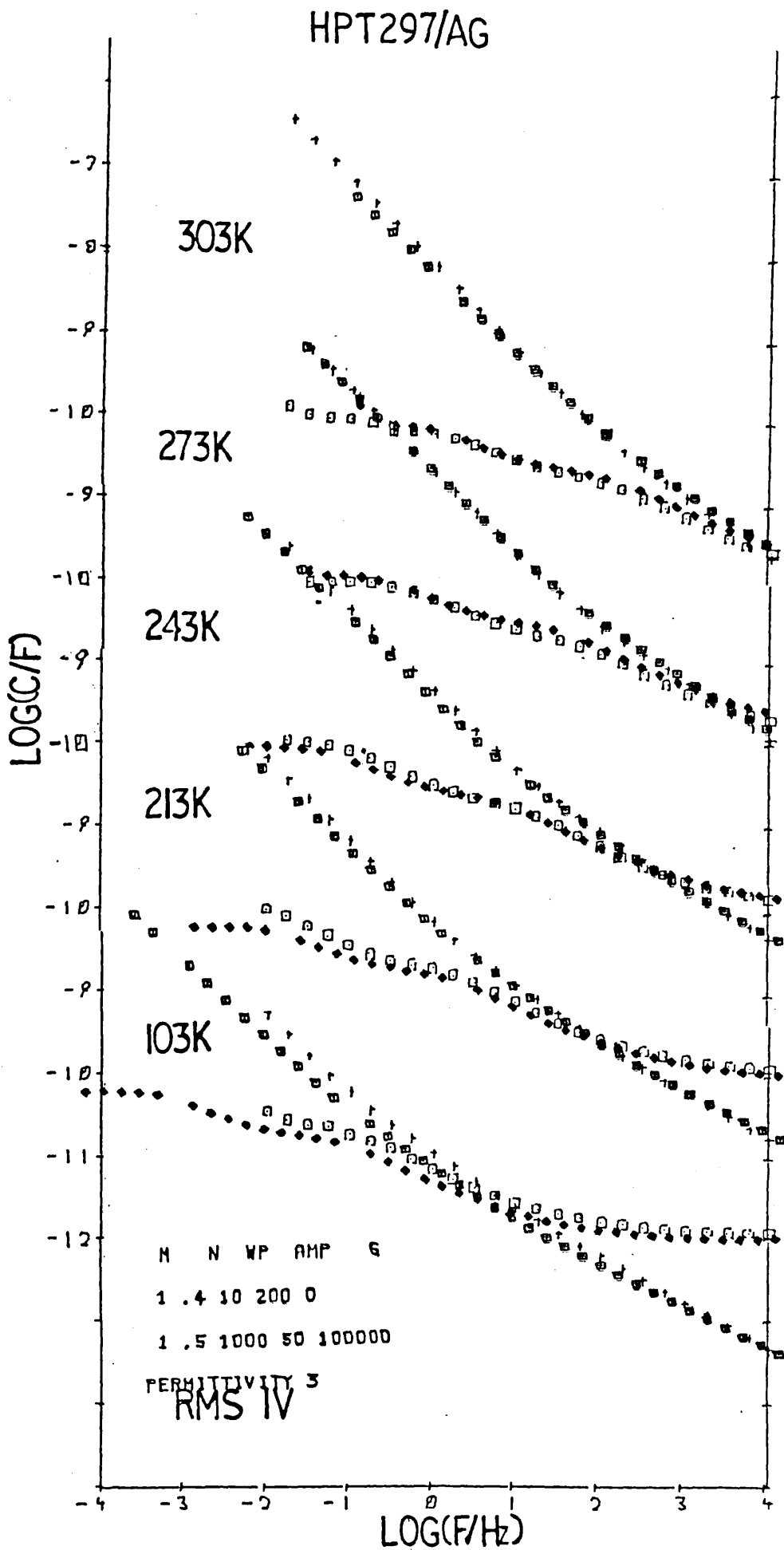


Figure 8.22

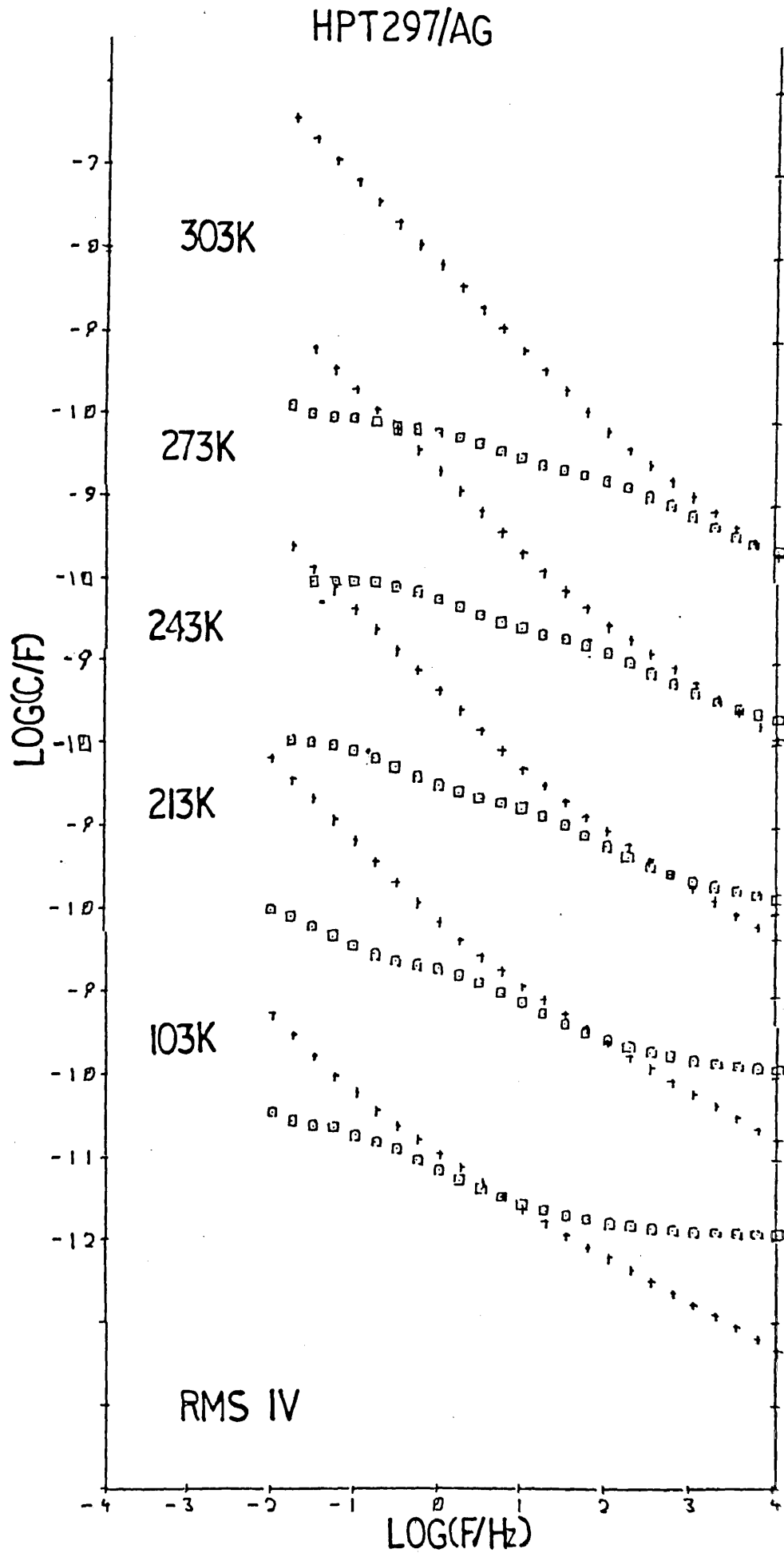
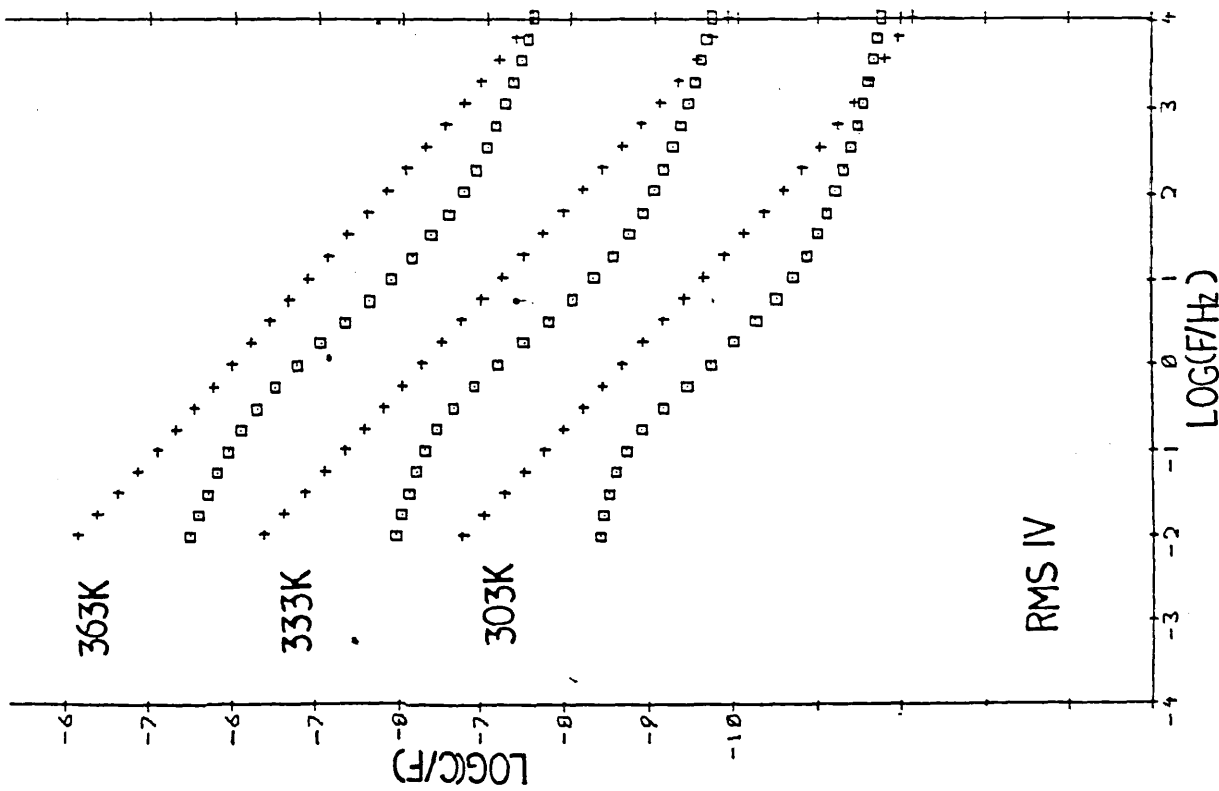


Figure 8.22

HPT 297/IN



HPT 297/PRESSURE

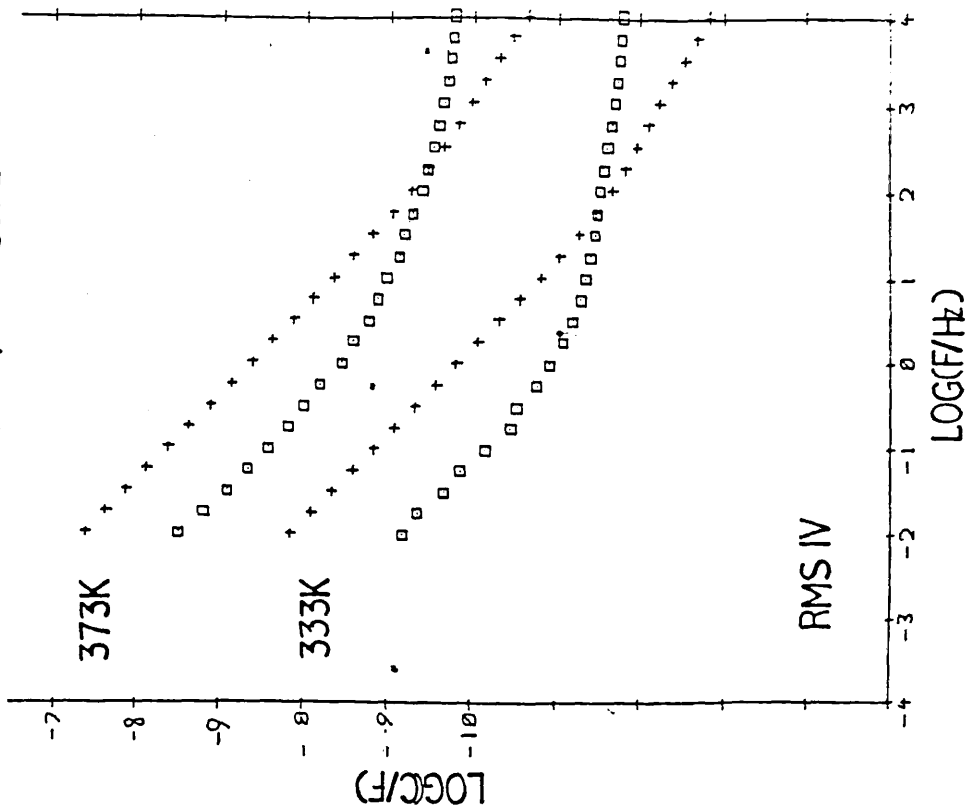


Figure 8.23

dielectric responses are most likely the result of Ag paint diffusion.

8.7. Class IV Type Material

These materials like HPT 297 are semi-conducting with d.c. conductivities of the order of $10^{-5} \Omega^{-1} m^{-1}$ at 373 K, Figures 8.24, 8.26 and 8.28. There is evidence to suggest the existence of two different types of charge carrier being present in these materials (electronic as well as ionic). This is supported by the theoretical curve fits.

The dielectric responses of HPP 337, HPT 320 and HPT 325, Figures 8.25, 8.27 and 8.29, respectively, are virtually identical showing at higher temperatures a small, followed by a very large, dispersion in complex capacitance.

HPP337/AG

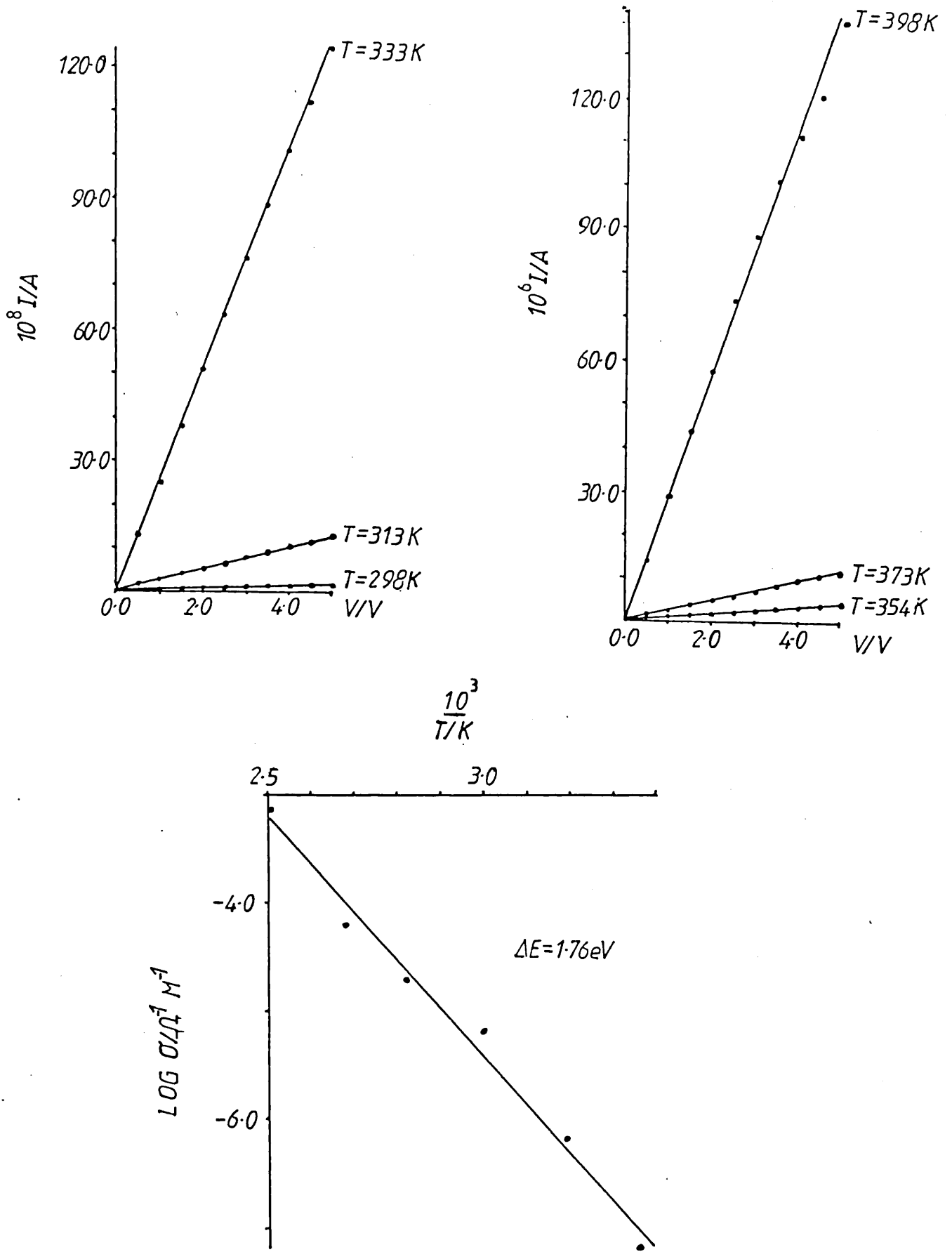
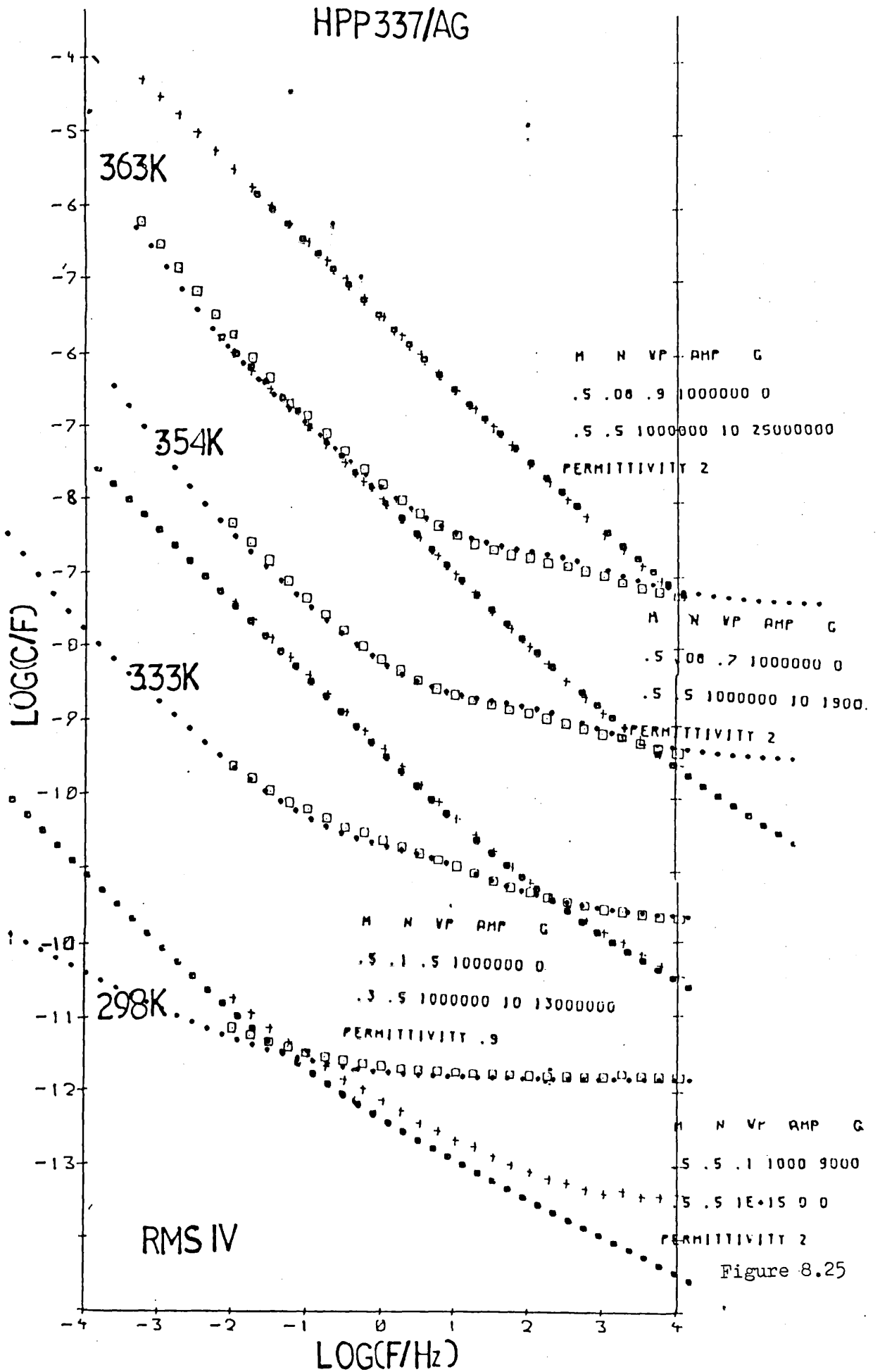


Figure 8.24



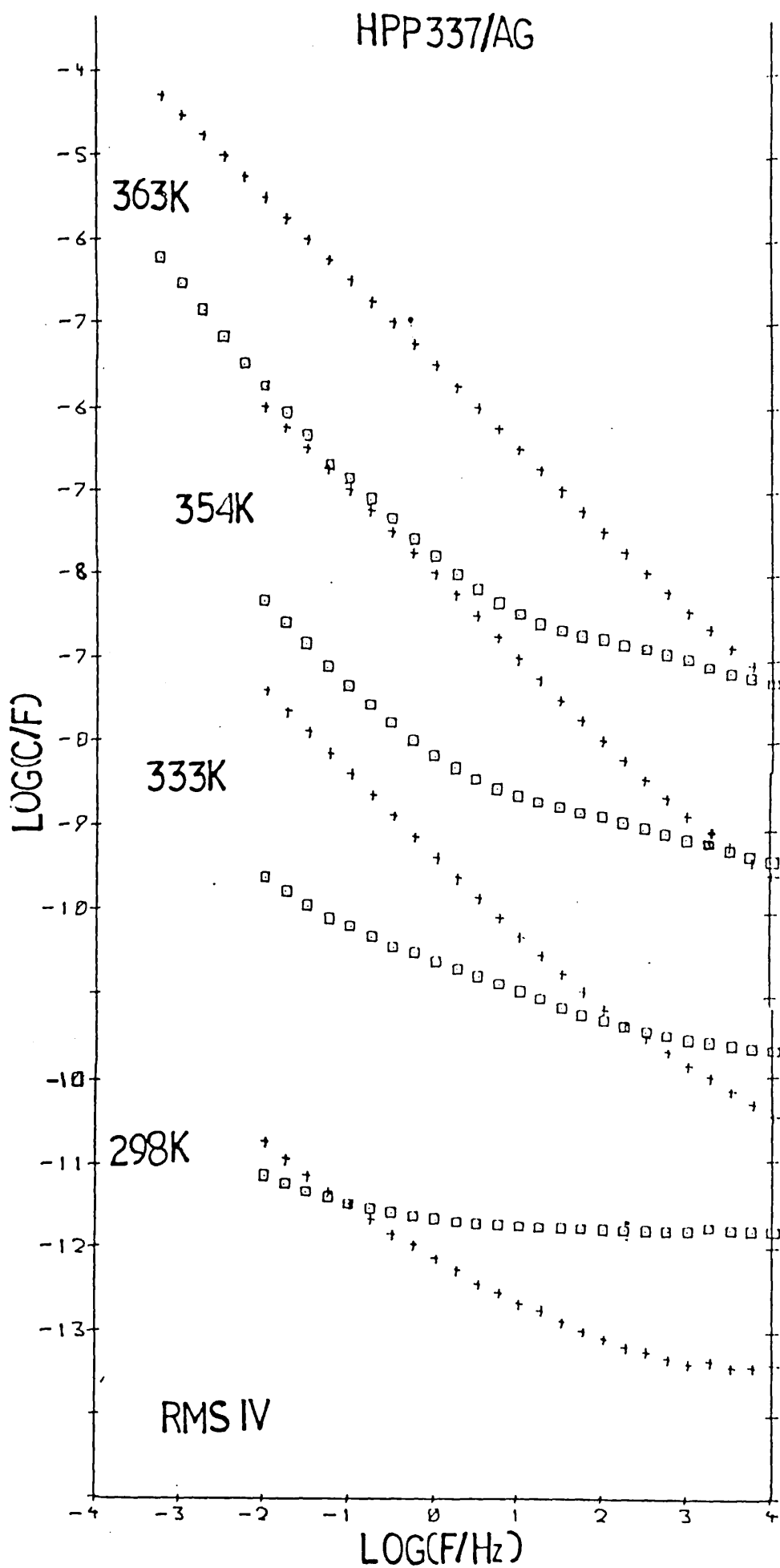


Figure 8.25

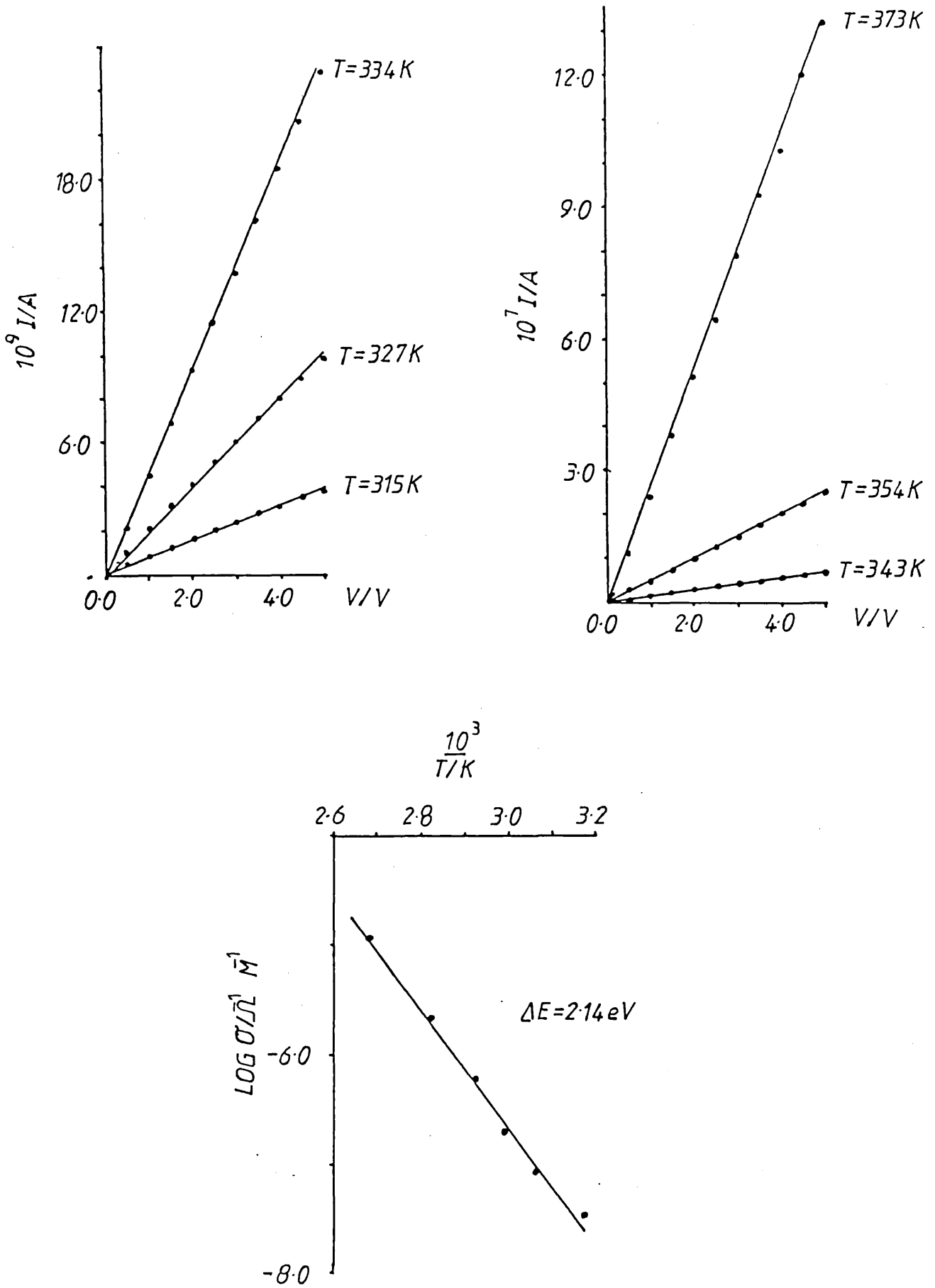


Figure 8.26

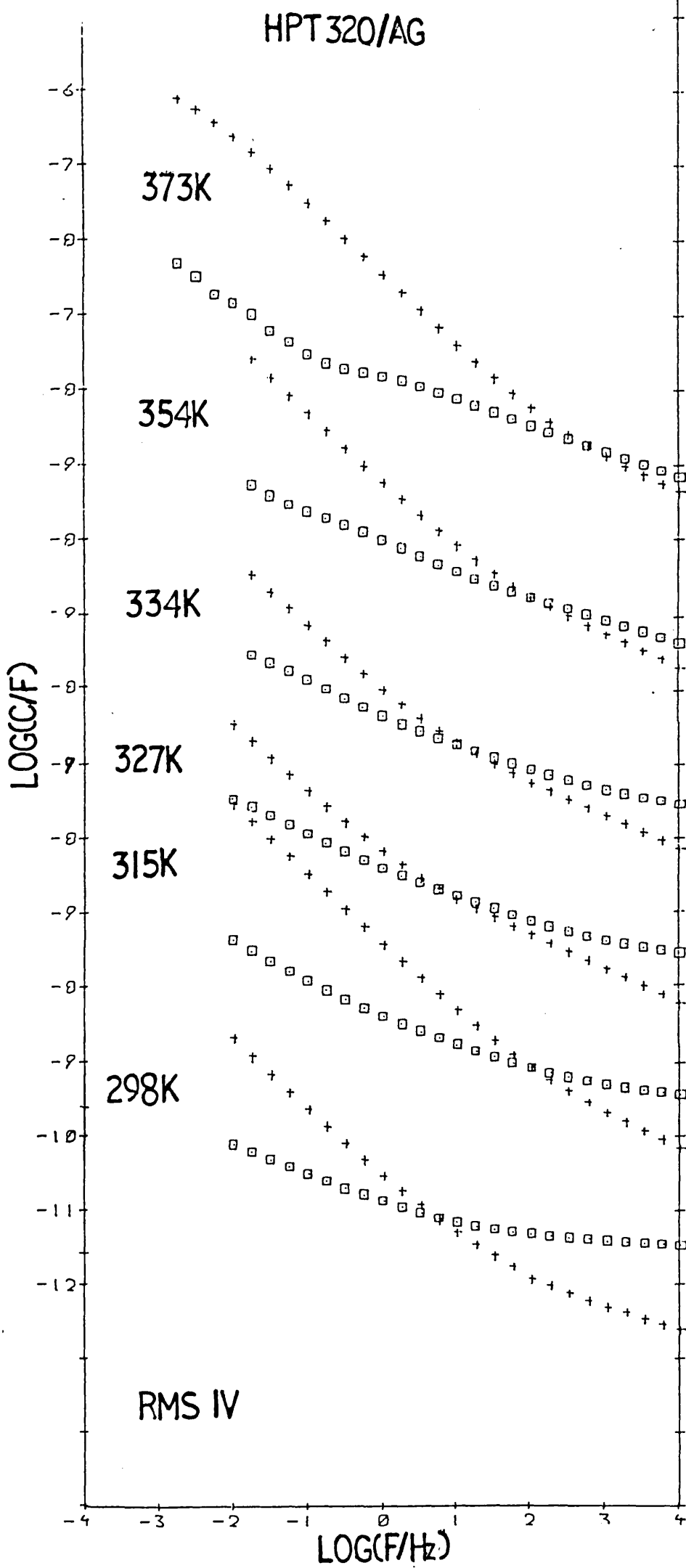


Figure 8.27

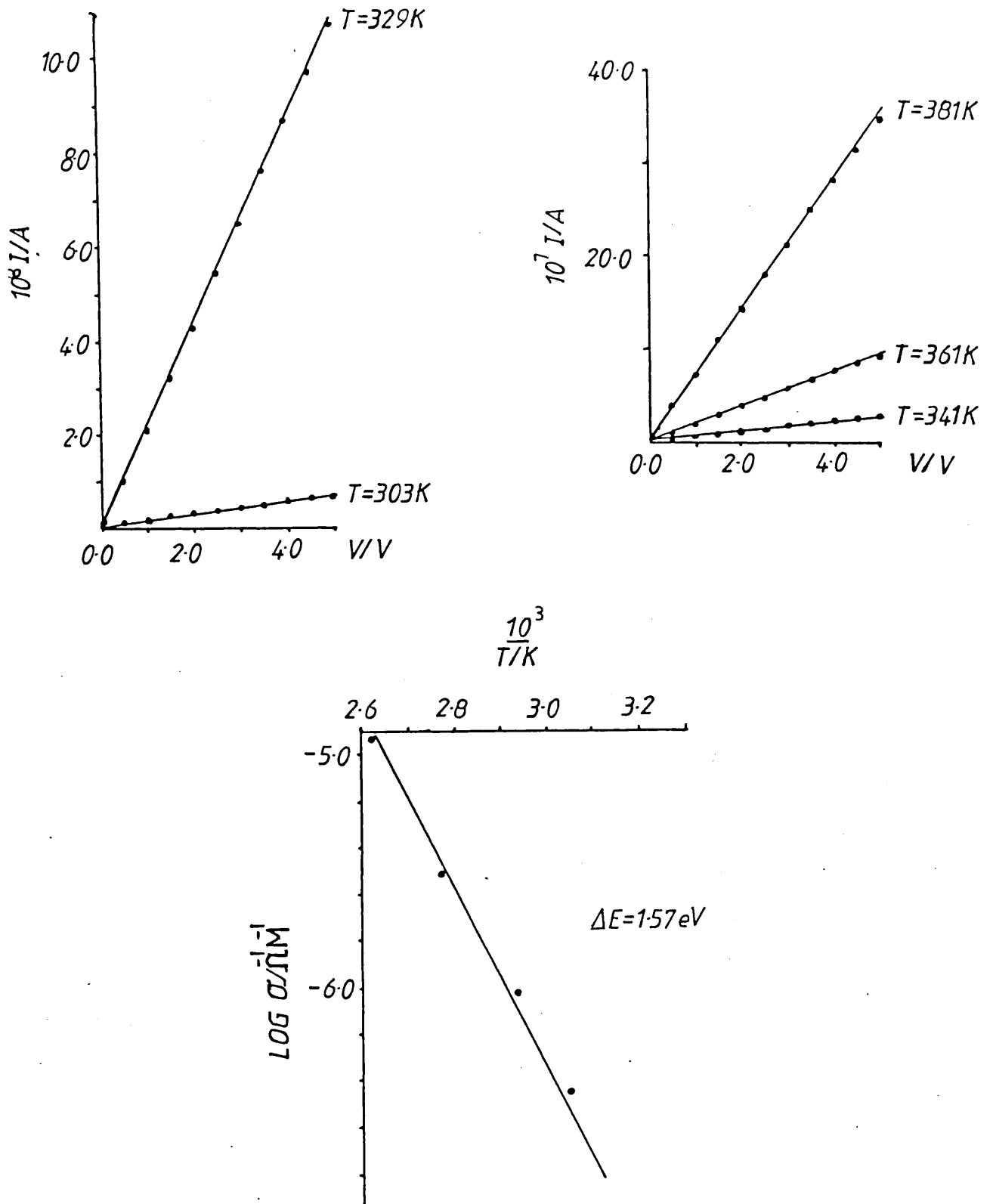


Figure 8.28

HPT 325/AG

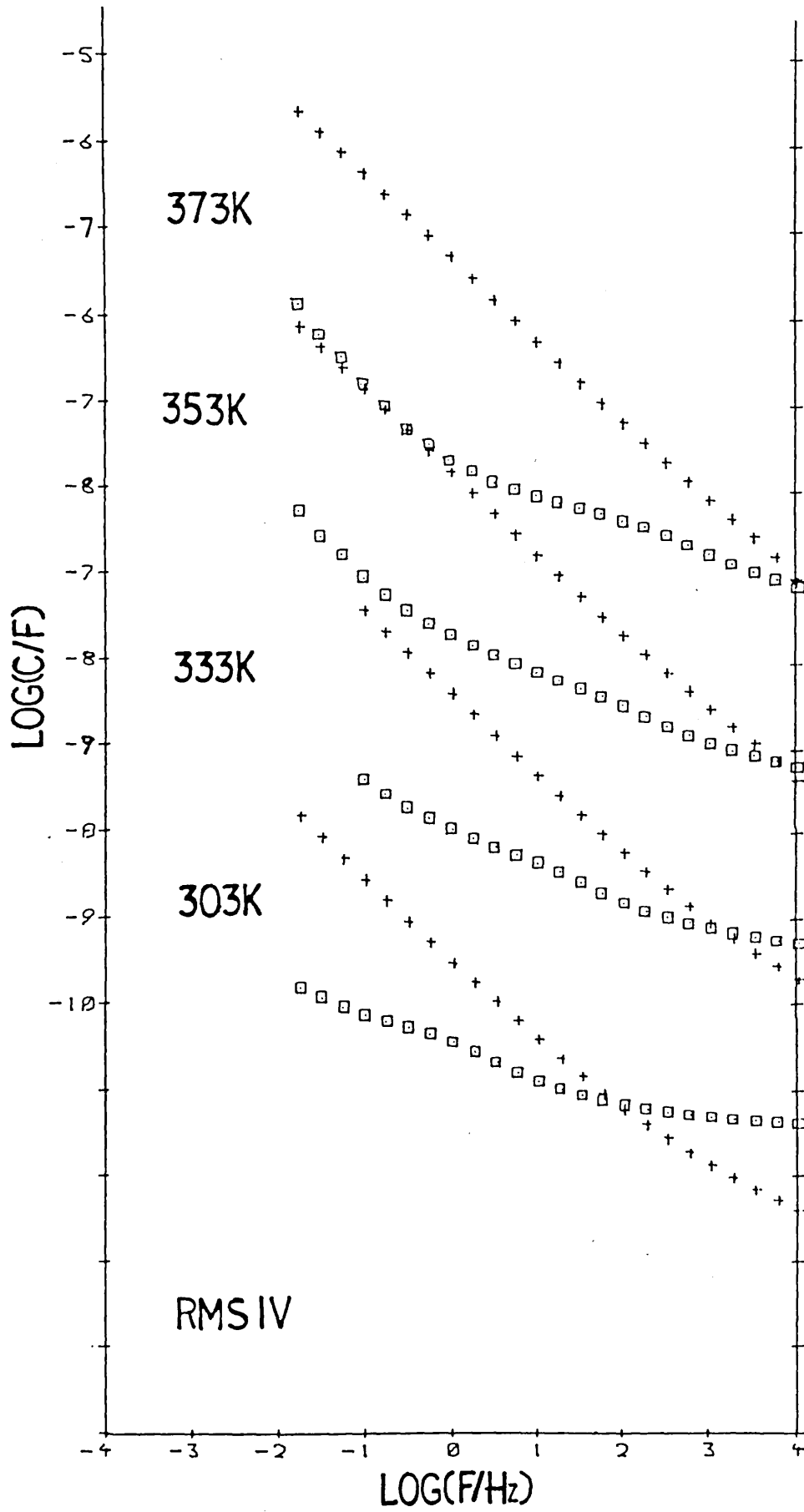


Figure 8.29

8.8. Class V Type Material

Both the d.c. conductivity and dielectric response measurements were carried out on a sample of this tetrathiafulvalene dye complex HPT 332 sandwiched between two copper disc electrodes to overcome the considerable problems of silver paint diffusion encountered. Possibly as a result we observed non-linear current-voltage characteristics (non-Ohmic), Figure 8.30. The dielectric spectra reveal a d.c. conductivity, carrier dominated response, Figure 8.31. This infers that charges are moving from one electrode to the other and that contact barrier effects are absent, which seemingly contradicts the d.c. measurements. One has to bear in mind, however, that for the dielectric measurements we are dealing with voltages of the order 0.1 V. It is not clear from our d.c. measurements whether the non-Ohmic behaviour extends to these lower voltage values. Time did not permit further detailed investigation of this sample, however, we were able to obtain an estimate of the d.c. conductivity (at room temperature) by measuring the current passing through our sample at 0.1 V and hence from equations 8.1 and 8.2 deduce a value ($\sigma_0 = 8.0 \times 10^{-4} \Omega^{-1} \text{ cm}^{-1}$).

8.9. This work has given us a great deal of information about contact (or electrode) effects and has stressed their importance in influencing electrical behaviour. This is an area that many of our co-workers in the field have totally neglected.

Consider for example, the question of the Ohmic nature of contacts. Equation (8.2) provides the route

$$\sigma_0 = G \frac{L}{A} \quad \text{where} \quad G = \frac{1}{R} \quad 8.2$$

HPT 332/PRESSURE

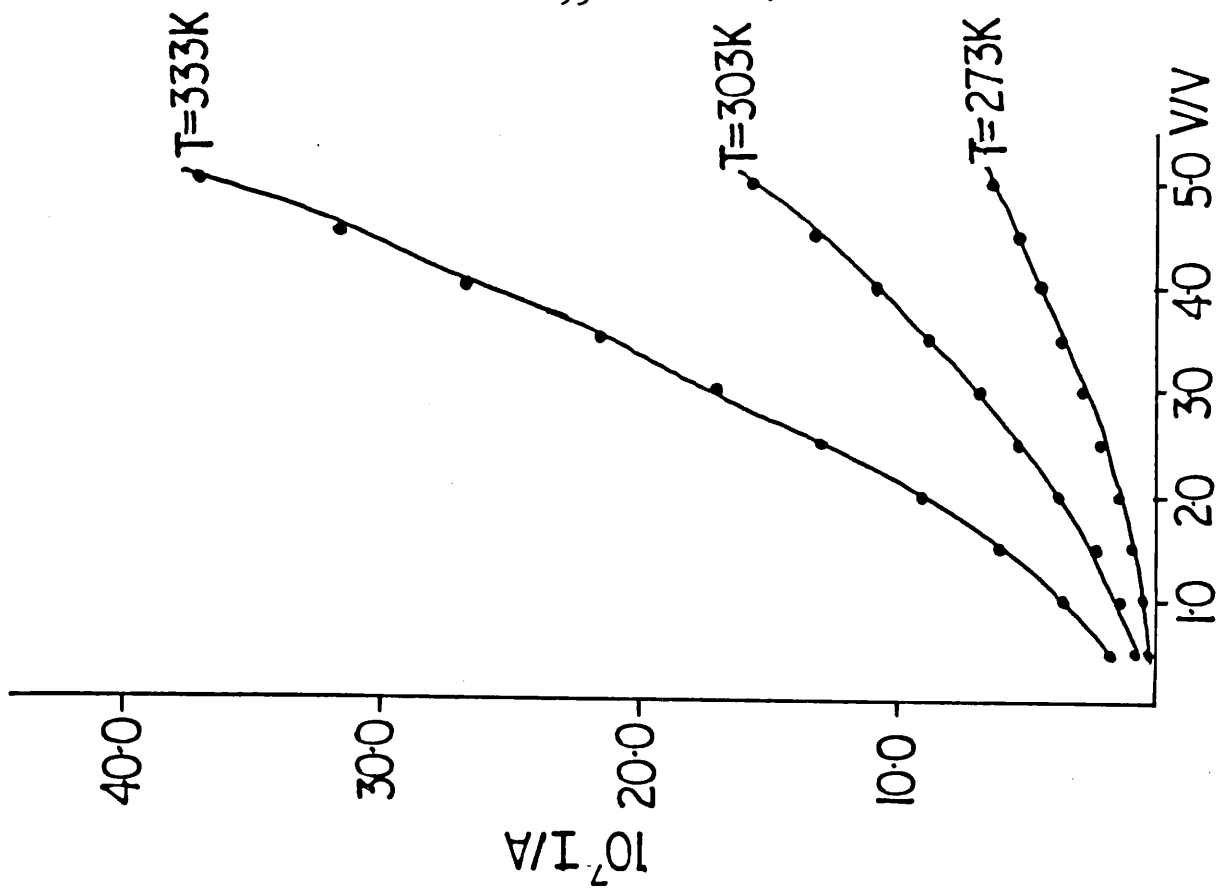
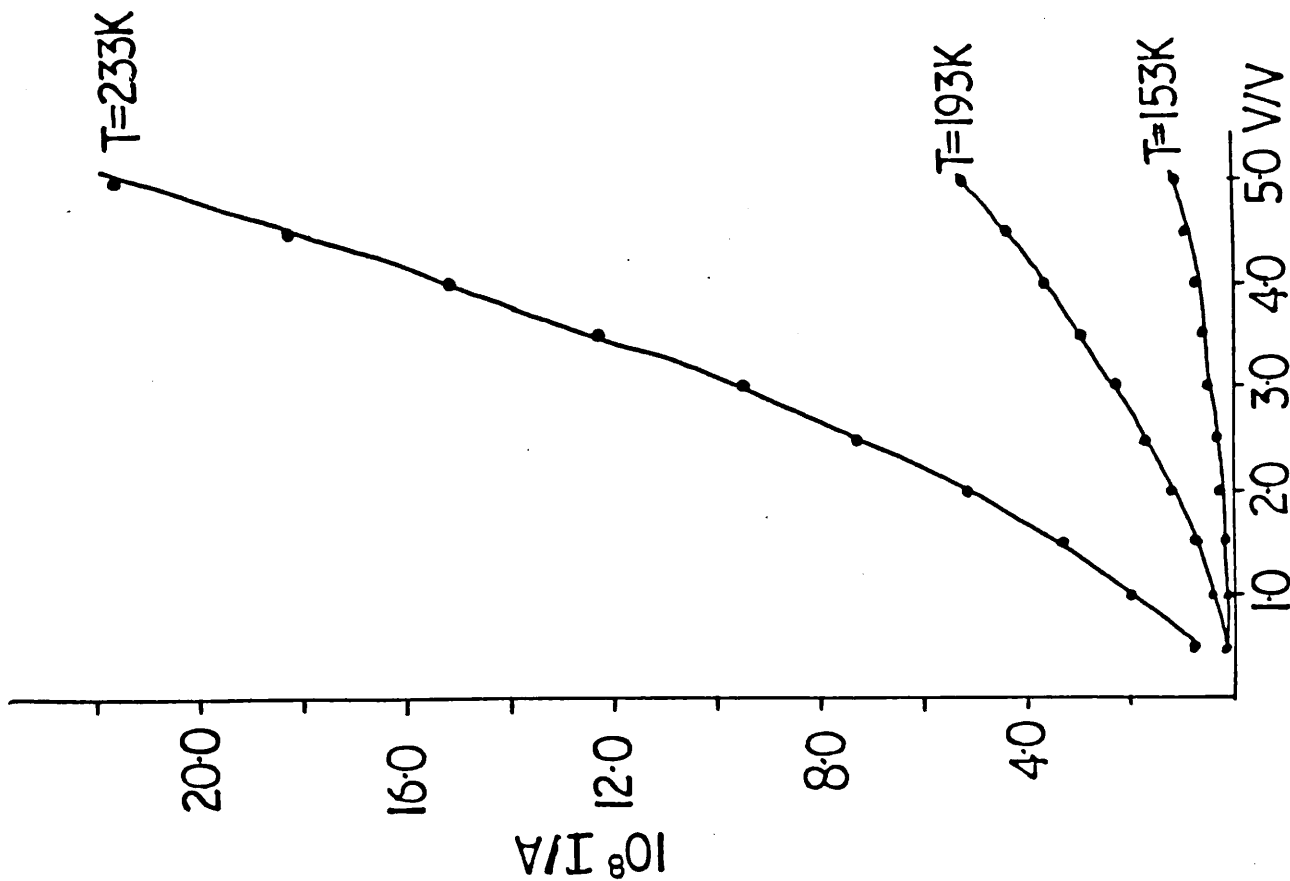


Figure 8.30

HPT 332/PRESSURE

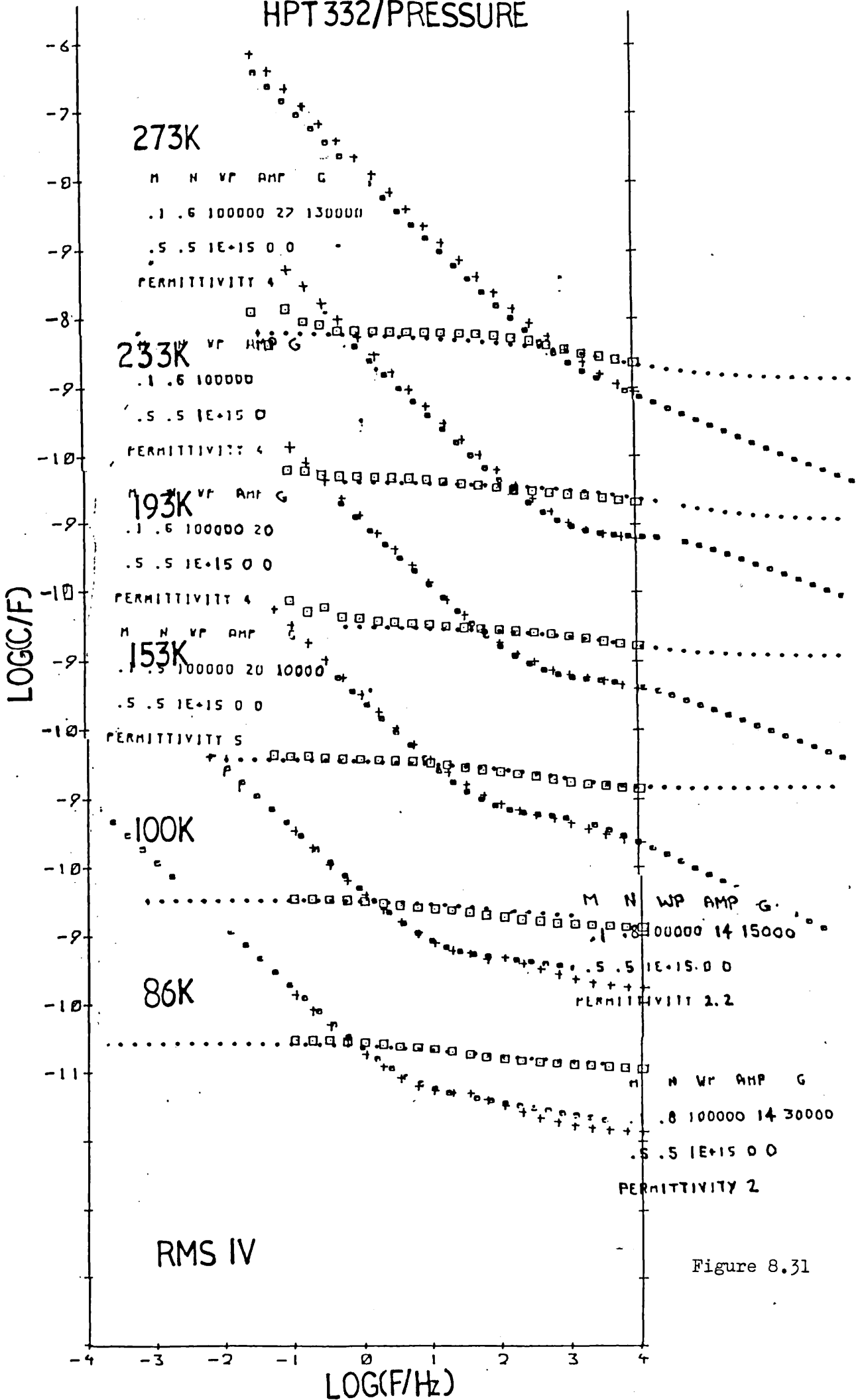


Figure 8.31

HPT 332/PRESSURE

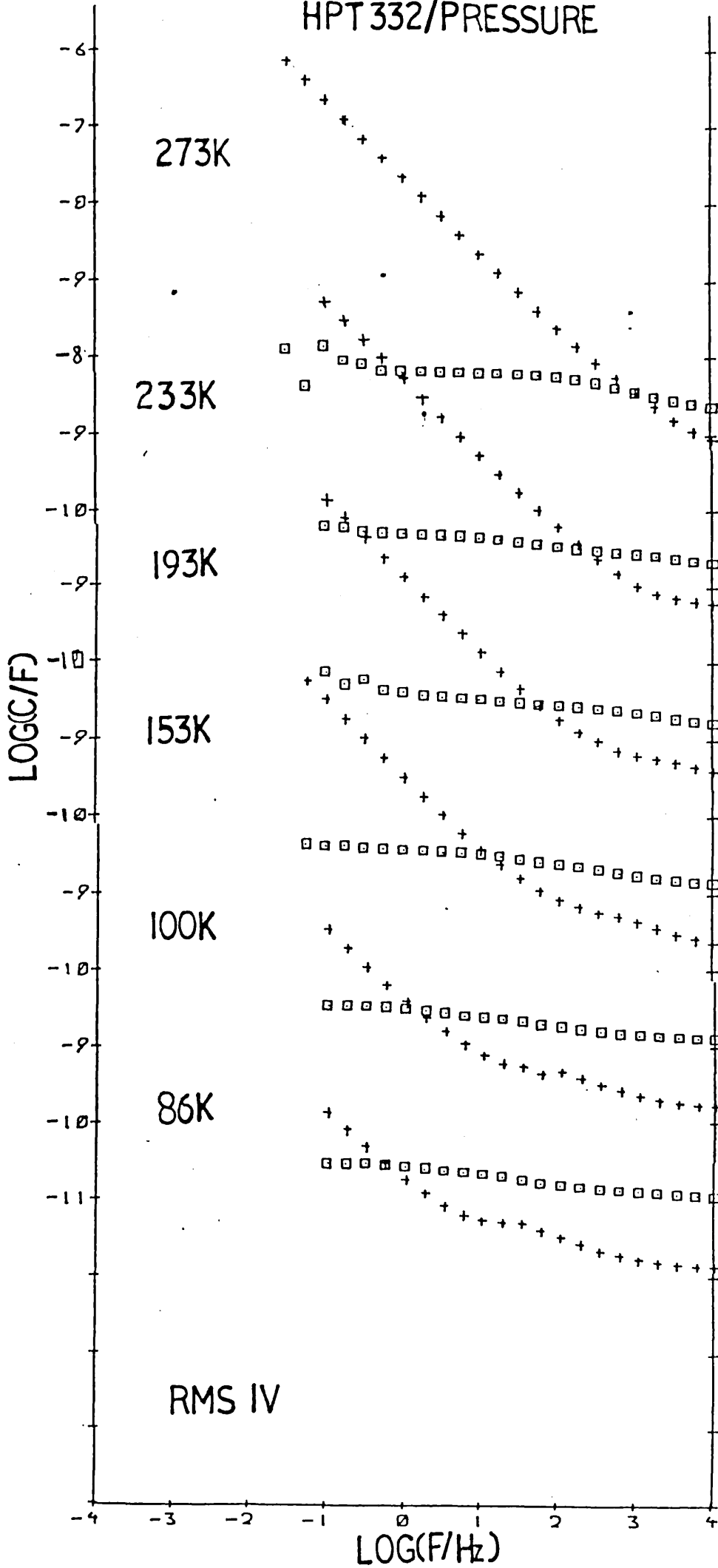


Figure 8.31

to obtaining d.c. conductivities, σ_0 . If there is not a linear relationship between current and voltage, as seen in Figure 8.30 then the resistance, R , is not a constant (voltage independent) at a particular temperature and hence neither is the conductance, G , nor conductivity, σ_0 . The literature is full of d.c. conductivity values calculated on the strength of one isolated conductance measurement, neglecting the nature of the contact.^{37,48} These numbers mean nothing on their own.

Silver paint is the most commonly used material for contacts. We have seen its diffusive properties, section 8.4. This has a number of effects on d.c. conduction. Firstly, if the silver paint is diffusing into the sample then we cannot accurately define either L or A from equation (8.2). Secondly, the non-uniformity of the electrodes will give rise to a non-uniform field across the sample, Figure 8.32. If one takes an isolated point at which silver has diffused, then at that point there will be a high field intensity (b). This then results in the drift of ions, where present, towards their oppositely charged electrodes where they are oxidised or reduced. This process, then, continues until, as in the case of the metal ion, M^+ ((c) to (d)), it produces a thin metal filament through the sample eventually short-circuiting the system. The rate at which this process occurs is obviously dependent on a number of factors, e.g. charge and size of the drifting ion, etc. This process (electrophoresis) is not confined to charged species, formally neutral entities behave in exactly the same way (dielectrophoresis).⁸²

Blocking contacts (section 8.1.2) and electron injection (section 5.4.5) from electrodes are two other significant effects that are very often overlooked. One might have a highly conducting material, yet if

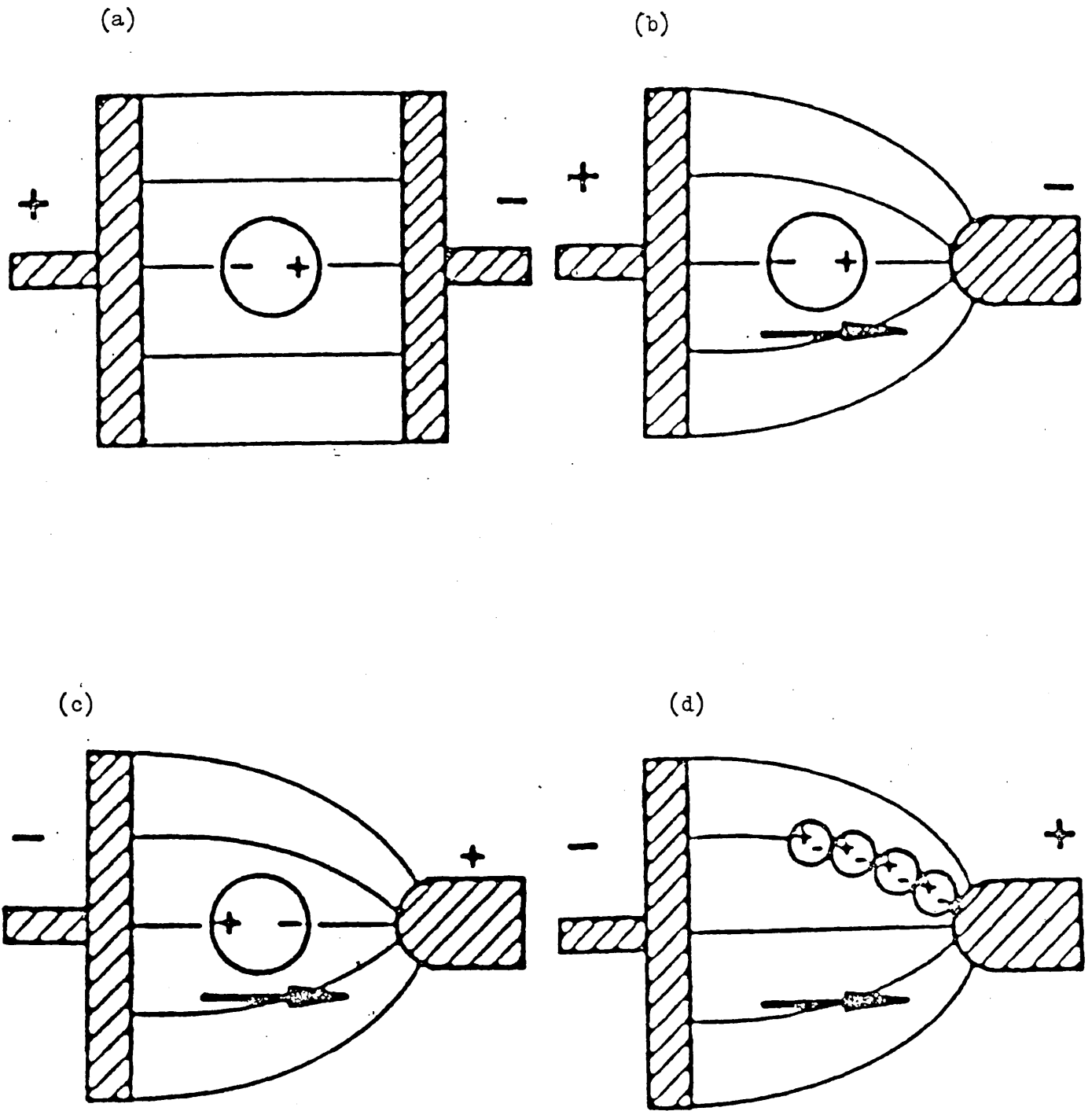


Figure 8.32

blocking contacts are in effect, and the charge carriers are being prevented from entering the external circuit, then there is no current and, of course, no way of measuring conductivity. Similarly one might have an insulating material and electrons are being injected into its conduction band from the electrode which then gives rise to a significant amount of conductivity.

Sample purity is a major problem. In order to present d.c. conductivity data we have to assume our materials to be intrinsic (pure), therefore enabling us to use equation (8.3). The solid-state physicists refer

$$\sigma_0 = A \exp(-\Delta\varepsilon/2kT) \quad 8.3$$

to impurity levels in parts per billion, and their effects at such levels are significant. Germanium, for example, containing a few p.p.b. of arsenic, Figure 5.2, becomes an n-type extrinsic semi-conductor. The majority of the literature on organic materials quotes d.c. conductivities and activation energies as being for intrinsic material.³⁷⁻⁴⁸ It is highly unlikely that any of these materials are truly intrinsic; their conductivity is extrinsic resulting from the promotion of charge-carriers to and from impurity levels within the forbidden gap. The development of ultra-purification techniques is a must.

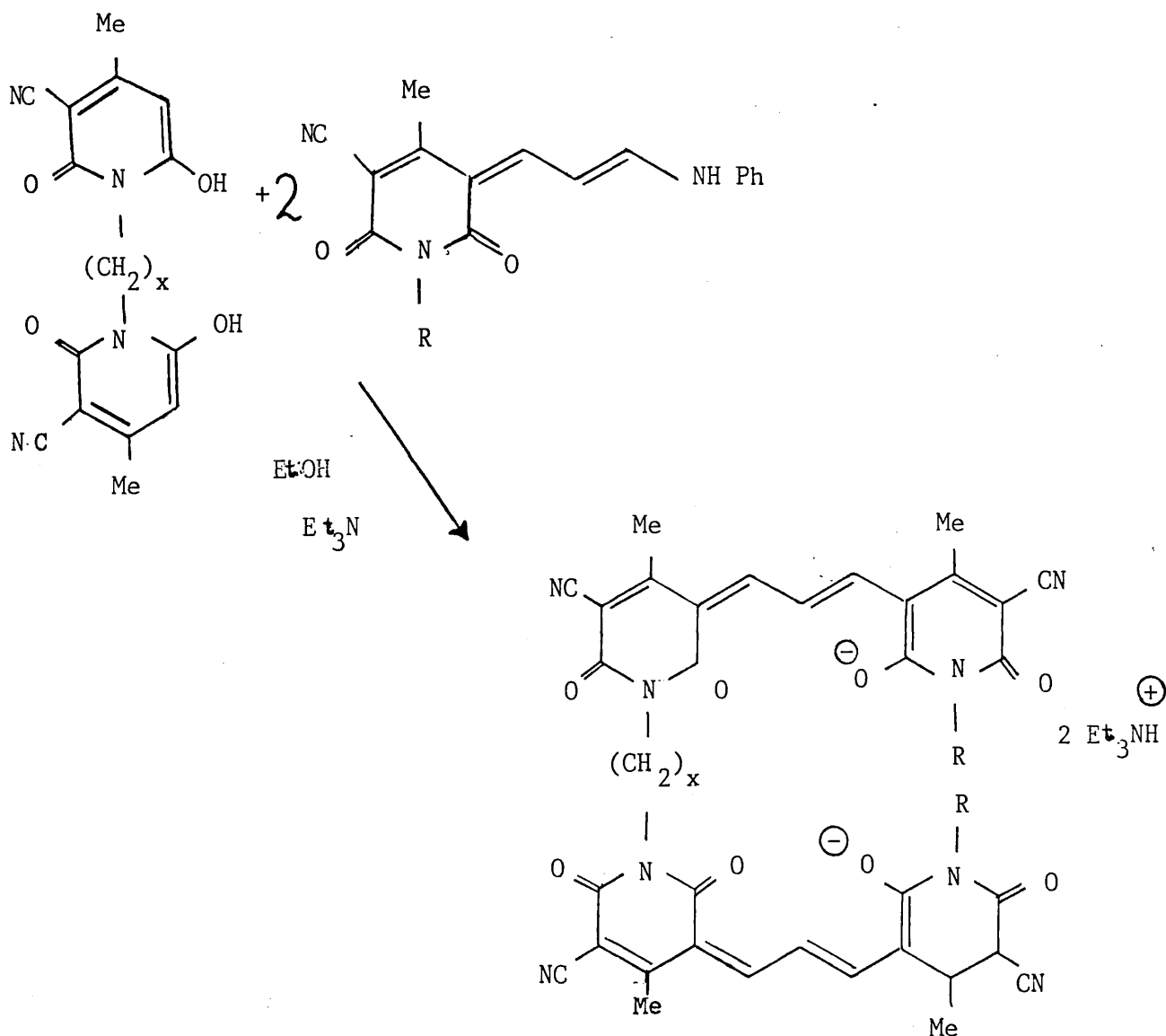
So, although our d.c. measurements do provide a general qualitative guide, we have to be aware of their limitations and try wherever possible to support them with data acquired from other techniques. Dielectric spectroscopy allows us to study both the contact and bulk properties of our materials and quite obviously has enormous potential as an analytical tool for studying solid-state conduction.

CHAPTER 9

Conclusions

As far as the photographic side of our work was concerned the initial objectives were, in the main, achieved.

The step-wise condensation oligomer prepared in Chapter 3 has been patented⁸³ as a new anti-halation underlayer system. Further work is now in progress to synthesise dimeric material, Scheme 9.1, which is easily isolable and more readily characterised.



Scheme 9.1

The bleaching reaction studies for the sulphite ion case pointed to the major process being Michael-type conjugate attack of the methine bridge. Further investigation is necessary to elucidate fully the mechanistic details, in particular, for nucleophiles other than the sulphite ion.

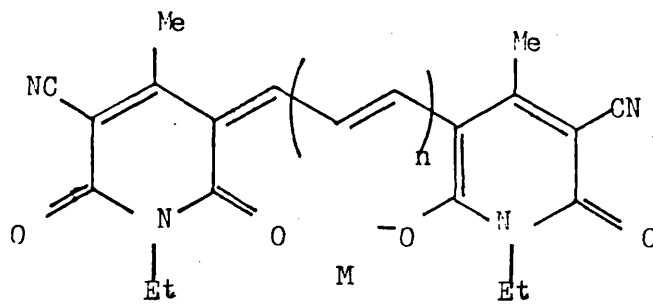
Our more extensive solid-state studies revealed a number of interesting features.

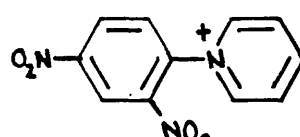
We observed a second example of anionic stacking in a herringbone arrangement first seen in MI 1579. We encountered selective peak splitting in the solid state ^{13}C n.m.r. spectra of MI 1579 and HPT 297. The reason for this is not clear.

The electrical properties of the oxonol dyes were varied. We found materials ranged from insulators to semi-conductors and their conductivities from being ionic to electronic in nature. More importantly, however, these measurements gave us an appreciation of the importance of contact effects and sample purity and as a result the limitations associated with d.c. conductivity data.

The effects on structure of cation variation is striking, however, these structural differences appear to have little effect on conductivity, Table 9.1. This is not surprising as all of those materials whose structure is known are insulating with large interplanar distances providing little hope of a pathway for intermolecular electronic charge transfer.

Table 9.1



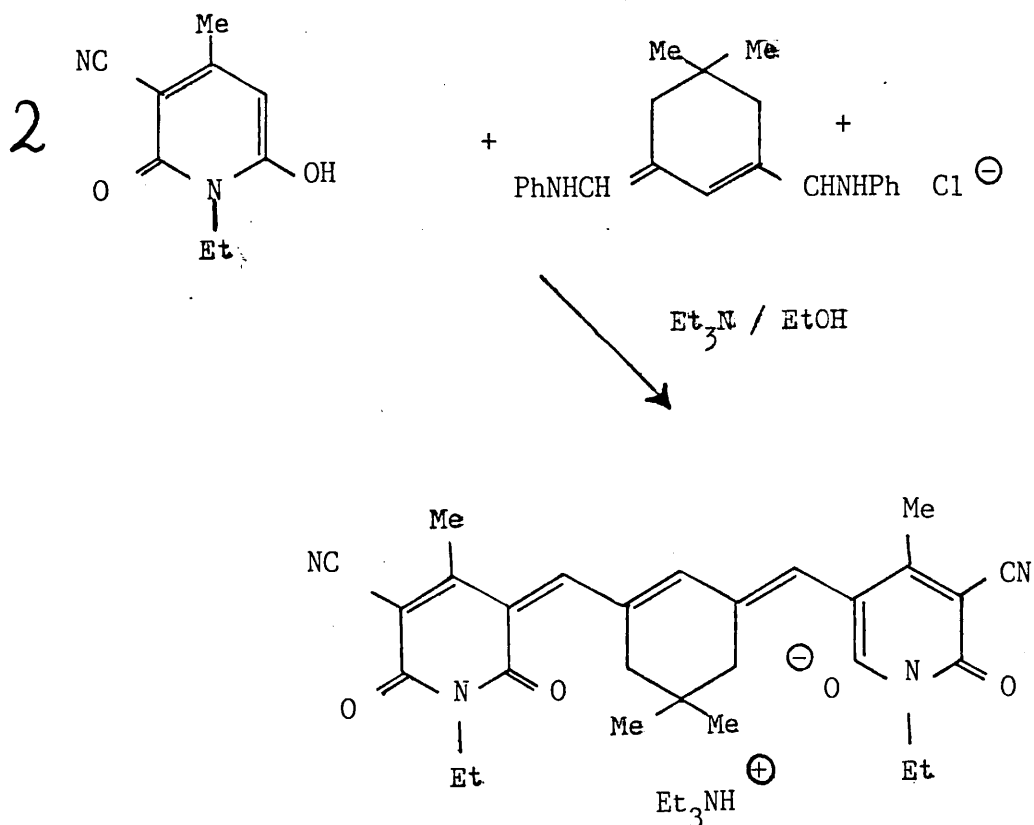
M	n	Interplanar Distance/Å	(a) Angle of twist/°	(b) Conductivity at 373 K/ $\Omega^{-1}\text{cm}^{-1}$
$\text{Et}_3\text{NH}^{\oplus}$	1	3.76	12.2	5.75×10^{-11}
$\text{Ph}_4\text{P}^{\oplus}$	"	4.06	40.4	7.24×10^{-11}
$\text{Bu}_4\text{N}^{\oplus}$	"	3.57, 5.56	25.6	6.92×10^{-11}
$\text{H}_2\text{CC}(\text{Me})\text{-CO}_2(\text{CH}_2)_2\text{NHMe}_2^{\oplus}$	"	4.54	14.1	9.98×10^{-10}
	"			5.47×10^{-12}
$\text{Ph}_3\text{PMe}^{\oplus}$	"			4.82×10^{-8}
TTF ⁺	"			$\approx 10^{-3}$ (c)
$\text{Et}_3\text{NH}^{\oplus}$	2			6.12×10^{-7}

(a) angle between the two planes defined by the two hydroxypyridone rings

(b) compacted powders

(c) room temperature (estimated by measurement of resistance at 0.1 V, see section 8.8, Chapter 8)

Enriching the dye structures with potential charge carrying π -electrons via both the anion and cation had little effect. It seems likely that the incorporation of these bulky aryl groups was counter-productive pushing the molecules within the anionic stacks even further apart. Introducing additional π -electrons by increasing the methine chain length, however, produced three to four order of magnitude increases in conductivity. Increasing the chain length above five carbon atoms becomes difficult as these larger straight chained dyes are very unstable. It is, however, possible to stabilise the bridge by rigidising it, e.g. with a cyclohexene ring, Scheme 9.2. There is a vast amount of literature



Scheme 9.2

covering the cyanine dye sensitisers with rigidised chains.⁸⁴⁻⁸⁸ Oxonol dyes of this type are now being synthesised.

The incorporation of cations with their own inherent conductivity led us to prepare a TTF (tetrathiafulvalene)-oxonol dye salt which not only appeared to be relatively highly conducting but was also reversibly bleached. This material has a number of potential commercial applications and has been patented⁸⁹. The preparation of TTF-straight-chained penta- and rigidised-penta- and heptamethine oxonol dyes are now being investigated, as are other radical cation dye salts.

The reason for the three-order of magnitude difference in conductivity between HPT 289 ($M = Ph_4P^+$) and HPT 297 ($M = Ph_3PMe$), Table 9.1, has remained unsolved. Attempts are under way to grow good quality crystals of HPT 297 for X-ray crystal structure determination. We would then, hopefully, be in a better position to offer a possible explanation.

CHAPTER 10

Experimental

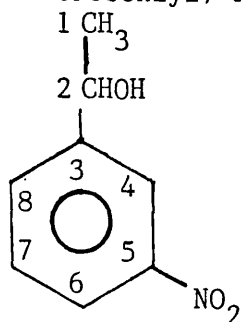
10.1. Syntheses

10.1.1. Instrumentation

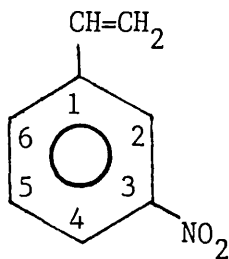
Routine ^1H and ^{13}C n.m.r analyses were carried out on the Perkin Elmer R24-B and the Jeol FX-90Q instruments. Infra-red analyses of nujol and/or hexachlorobutadiene mulls were carried out on the Perkin-Elmer 197 machine. Elemental analyses of novel compounds were carried out on the Perkin Elmer 240 Elemental Analyzer.

10.1.2 Aluminium Isopropoxide, $\text{Al}(\text{iOPr})_3$.¹²

Isopropanol was dried by refluxing it over freshly calcined calcium oxide for 4 hrs. Aluminium turnings (55.0 g, 2.0 mol) were placed in a 2 litre flask with 1 litre of dry isopropanol. Mercuric chloride (0.2 g, 0.7 mmol) was added and the mixture heated to reflux with good cooling of the reflux condenser (two double surface condensers were used). The hydrogen evolution soon became very violent and the flask was placed into an ice/water bath. At the end of the stormy evolution of the hydrogen the flask was heated on a water bath until the metal had vanished (12 hours). On standing the mixture at room temperature overnight a grey sludge was formed and this was covered by a nearly colourless solution. This was diluted with isopropanol to 2 litres, to yield an approximately 1.0 M solution.

10.1.3 α -Methyl-(*m*-nitrobenzyl) alcohol¹²

m-Nitroacetophenone (99.0 g, 0.6 mol) was reduced by 300 ml of the 1M-aluminium isopropoxide solution to yield 54.3 g (54%) of the alcohol (recryst. toluene, m.p. = 61.0-62.5°, lit. m.p. = 62.0°; ¹H n.m.r. δ (CDCl₃, ppm.) 1.66 (d) C¹H₃, 2.86 (s) OH, 5.04 (q) C²H, 7.92 (m) C₆H₄; ¹³C nmr. δ (CDCl₃, ppm) 25.68 (C¹), 69.57 (C²), 120.69, 122.57, 129.79, 132.20 (C⁴, C⁶, C⁷, C⁸), 148.45 (C⁵); infra-red 3300-3220 (O-H), 2985 (C¹-H), 1535 (N-O), 1345 (N-O) cm⁻¹.

10.1.4 *m*-Nitrostyrene¹³ 7 8

Used α -methyl-(*m*-nitrobenzyl) alcohol (50.0 g, 0.3 mol) tert-butylcatechol (0.05g, 0.3 mmol) and A.R. orthophosphoric acid (400 ml, 3.5 mol). The solution was maintained at 75-80° for 10 min and then diluted with an equal quantity of water and steam distilled for 5 hrs. The *m*-nitrostyrene was then obtained from the distillate by extraction with A.R. benzene, the benzene solution being dried over potassium carbonate and the benzene removed by distillation. Pure *m*-nitrostyrene was obtained by vacuum distillation under nitrogen yielding

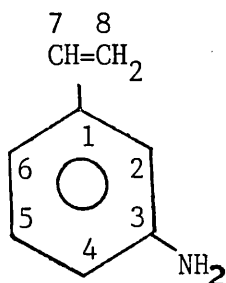
18.6 g (42%), b.p. = 81-82°/1.0 mm Hg, lit. m.p. 81-82°C/1.0 mm Hg;

^1H nmr δ (CDCl_3 , ppm) 6.58 - 8.25 (m) (C^7H , C^8H_2 , C_6H_4);

^{13}C nmr δ (CDCl_3 , ppm) 112.83, 113.54, 114.84, 117.06 ($\text{C}^2, \text{C}^4, \text{C}^5, \text{C}^6$), 129.41 (C^8), 137.09 (C^7), 138.78 (C^1), 146.45 (C^3); i.r.

3085 ($\text{C}^7\text{-H}$), 3010 ($\text{C}^2\text{-H}$), 1632 ($\text{C}^7\text{=C}$), 1530 (N-O), 1355 (N-O), 925 ($\text{C}^7\text{-H}$) cm^{-1} .

10.1.5 m-Aminostyrene¹⁴

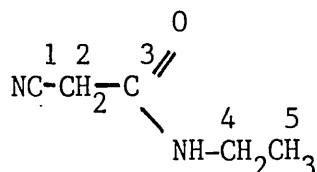


m-Nitrostyrene (15.3 g, 0.1. mol), stannous chloride (92.0 g, 0.4 mol) and concentrated hydrochloric acid (92 ml, 1.0 mol) in ethanol (50 ml) were refluxed for 30 mins cooled, and then poured into aqueous sodium hydroxide (136.0 g in 460.0 ml). The oil which separated from the steam distillate (steam distillation time of 4 hrs) was extracted with benzene. The extract was dried over potassium carbonate, and the benzene distilled off after the addition of a little quinol. Distillation of the product under nitrogen gave 4.52 g (38%), b.p. = 68°C/0.8 mmHg, lit. b.p. = 68°C/0.8 mmHg; ^1H nmr δ (CDCl_3 , ppm) 3.53 (s) NH_2 , 6.44 - 7.26 (m)/ $\text{C}^7\text{H}_1\text{C}^8\text{H}_2, \text{C}_6\text{H}_4$); ^{13}C nmr δ (CDCl_3 , ppm) 112.70, 113.48, 114.71, 116.80 ($\text{C}^2, \text{C}^4, \text{C}^5, \text{C}^6$), 129.35 (C^8), 137.02 (C^7), 138.58 (C^1), 146.65 (C^3); i.r. 3440-3360 (N-H), 3025 (C-H), 2975 (C-H), 1620 ($\text{C}^7\text{=C}$), 1492 (C=C), 1300 (C-N) cm^{-1} .

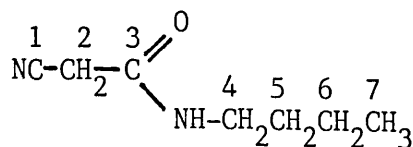
10.1.6 Cyanoacetamide¹⁰ $\text{NCCH}_2\text{CONH}_2$

Ethyl cyanoacetate (75.3 ml, 0.7 mol) and concentrated aqueous ammonia solution (60 ml, 0.9 mol) were used. After drying the crude white amide weighed 50.3 g. An additional 6.3 g of amide was obtained by evaporating the original mother liquor to dryness under reduced pressure. This gave a total yield of 56.6 g (75%) (recryst. methylated spirit, m.p. = 118-119°, lit. m.p. = 119-120°; ¹H nmr δ(d⁶-DMSO, ppm) 3.65 (s) C²H₂, 7.46 (d, broad) NH₂; ¹³C nmr δ(d⁶-DMSO, ppm) 25.48 (C²), 116.27 (C¹), 164.58 (C³); i.r. 3400-3200 (N-H) 2955 (C-H), 2925 (C-H), 2255 (C≡N), 1680 (C=O), 1408 (C-N), 1375 (C-N) cm⁻¹.

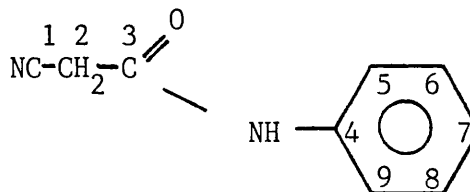
10.1.7 N-Ethyl cyanoacetamide



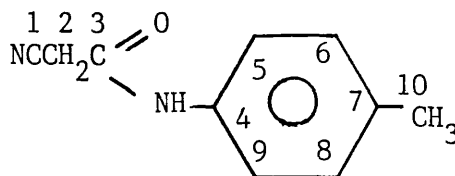
Used methyl cyanoacetate (308.5 ml, 3.5 mol) and ethylamine (253.1 ml, 4.5 mol). The total yield of amide was 211.1 g (54%) (recryst. methylated spirit, m.p. = 71.5-72.5°C, lit. m.p. = 72.0 °C; ¹H nmr δ(d⁶-DMSO, ppm) 1.07 (t) C⁵H₃, 3.16 (q) C⁴H₂, 3.58 (s) C²H₂, 8.17 (s) NH; ¹³C nmr δ(d⁶-DMSO, ppm) 14.44 (C⁵), 25.95 (C²), 35.38 (C⁴), 114.97 (C¹), 161.15 (C³), i.r. 3250 (N-H), 2250 (C≡N), 1680 (C=O), 1250 (C-N) cm⁻¹.

10.1.8 N-Butyl cyanoacetamide¹⁷.

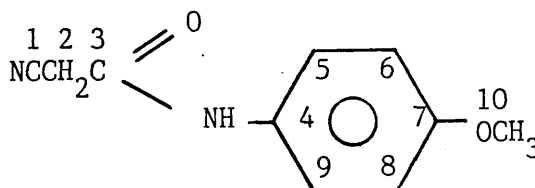
Ethyl cyanoacetate (49.0 g, 0.43 mol) was dripped into N-butylamine (31.6 g, 0.43 mol) over a 40 min period, the temperature rose to 45°. The mixture was then heated to 80° for 1 hr. The product crystallised out on cooling and on filtering weighed 60.0 g (98%) (recryst. toluene; m.p. = 68.5°, lit. m.p. = 69.0°; ¹H nmr δ(d⁶-DMSO, ppm) 0.81-0.87(m) C⁷H₃, 1.30(m) (C⁶H₂, C⁵H₂), 3.02(m) C⁴H₂, 3.48(s) C²H₂, 8.10(s) NH; ¹³C nmr δ(d⁶-DMSO, ppm) 12.36 (C⁷), 18.47 (C⁶), 24.26 (C⁵), 29.85 (C⁴), 37.85 (C²), 114.91 (C¹), 160.89 (C³).

10.1.9 N-Phenyl cyanoacetamide¹⁷

A mixture of aniline (40.91 ml, 0.45 mol) and methyl cyanoacetate (308.5 ml, 0.35 mol) in toluene (50 ml) was refluxed for 20 hrs. The crude amide filtered off after cooling weighed 18.2 g (32%) (recryst. methylated spirit, m.p. = 199-201°, lit. m.p. = 199-200°; ¹H nmr δ(d⁶-DMSO, ppm) 3.90 (s) C²H₂, 7.33 (m) C₆H₅, 10.44 (s) OH; ¹³C nmr (poor signal to noise); i.r. 3270-3210 (N-H). 3140 (C⁵-H); 2250 (C≡N), 1665 (C=O), 1560 (C⁵=C), 760 (C⁵-H) cm⁻¹.

10.1.10 N-(p-Tolyl)cianoacetamide

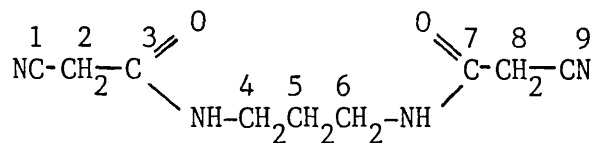
A mixture of p-toluidine (10 g, 0.1 mol) and methyl cyanoacetate (10.6 ml, 0.12 mol) in toluene (30 ml) was refluxed for 48 hrs. The reaction mixture was allowed to cool, the light brown residue was filtered off, 5.15 g (33%) (recryst. methylated spirit, m.p. = 186.0-187.0°; ^1H nmr δ (d^6 -DMSO, ppm) 2.29 (s) CH_3 , 3.88 (s) CH_2 , 7.33 (m) C_6H_4 , 10.18 (s) OH; ^{13}C nmr δ (d^6 -DMSO, ppm) 20.35 (C^{10}), 26.52 (C^2), 115.81 (C^1), 119.32, 129.14 ($\text{C}^5, \text{C}^6, \text{C}^8, \text{C}^9$), 132.98 (C^7), 135.78 (C^4), 160.55 (C^3); i.r. 3270-3210 (N-H), 3140, 3090 (C^5 -H), 2955, 2925 (C^2 -H), 2255 ($\text{C} \equiv \text{N}$), 1665 ($\text{C}=\text{O}$) cm^{-1} ; Calcd for $\text{C}_{10}\text{H}_{10}\text{N}_2\text{O}$: C, 68.94; H, 5.80; N, 16.08; Found: C, 68.92; H, 5.79; N, 15.97.

10.1.11 N-(p-Anisyl)cianoacetamide)

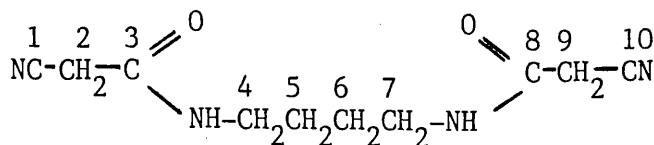
A mixture of p-anisidine (10 g, 0.08 mol) and methyl cyanoacetate (9.2 ml, 0.09 mol) in toluene (30 ml) was refluxed for 48 hrs. The reaction mixture was allowed to cool, the greyish residue was filtered off 4.64 g (31%) (recryst. methylated spirit, m.p. = 131-133°; ^1H nmr

δ (d⁶-DMSO, ppm) 3.78 (s) OCH₃, 3.89 (s) CH₂, 7.27 (m) C₆H₄, 10.36 (s) OH; ¹³C nmr δ (d⁶DMSO, ppm) 26.59 (C²), 55.07 (C¹⁰), 113.86 (C⁶,C⁸), 115.81 (C¹), 120.88 (C⁵,C⁹), 131.29 (C⁷), 155.61 (C⁴), 160.29 (C³); i.r. 3310-3215 (N-H), 3150-3100 (C⁵-H), 2950-2930 (C²-H), 2250 (C \equiv N), 1658 (C=O), 1032 (C-O); Calcd for C₁₀H₁₀N₂O₂: C, 63.14; H, 5.31; N, 14.73; Found: C, 62.93; H, 5.27; N, 14.64.

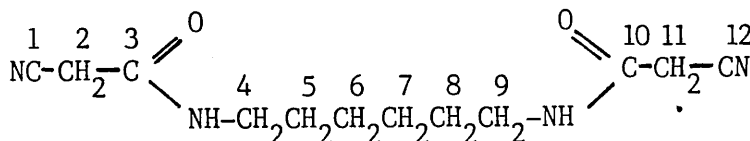
10.1.12 N,N'-Dicyanoacetyl-1,3-diaminopropane



A mixture of ethyl cyanoacetate (30.51 g, 0.27 mol) and 1,3-diaminopropane (10 g, 0.14 mol) in ethanol (20 ml) was refluxed with stirring for 4 hrs. The reaction was allowed to cool and the solid residue was filtered off and dried over P₂O₅. The yellow solid weighed 7.46 g (27%) (recryst. ethanol m.p. = 158-159⁰; ¹H nmr δ (d⁶-DMSO, ppm) 1.64 (m) C⁵H₂, 3.16 (m) C⁴H₂, 3.64 (s) C²H₂, 8.17 (t) OH; ¹³C nmr δ (d⁶-DMSO, ppm) 27.83 (C⁵) 31.09 (C²), 39.54 (C⁴), 118.52 (C¹), 164.59 (C³), i.r. 3284 (N-H), 2956 (C-H), 2260 (C \equiv N), 1651 (C=O) cm⁻¹; Calcd. for C₉H₁₂N₄O₂: C, 51.91; H, 5.82; N, 26.91; Found: C, 51.60; H, 5.85; N, 26.59.

10.1.13 N,N'-Dicyanoacetyl-1,4-diaminobutane

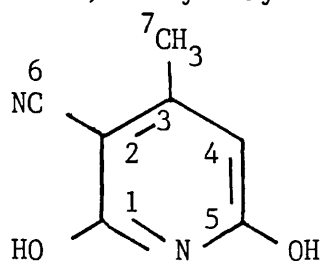
A mixture of 1,4-diaminobutane (20 g, 0.23 mol) and ethylcyanoacetate (51.3 g, 0.46 mol) in ethanol (50 ml) was refluxed for 4 hrs. to yield 42.7 g (85%) of a yellow solid (recryst. ethanol m.p. = 147.0-148.0°C; ^1H nmr δ (d^6 -DMSO, ppm) 1.78 (m) C^5H_2 , 3.40 (m) C^4H_2 , 3.88 (s) C^2H_2 , 8.36 (t) OH; ^{13}C nmr δ (d^6 -DMSO, ppm) 25.23 (C^5), 26.14 (C^2), 38.76 (C^4), 115.96 (C^1), 161.86 (C^3); i.r. 3279 (N-H), 2950 (C-H), 2256 ($\text{C} \equiv \text{N}$), 1660 ($\text{C}=\text{O}$) cm^{-1} ; Calcd. for $\text{C}_{10}\text{H}_{14}\text{N}_4\text{O}_2$: C, 54.04; H, 6.36; N, 25.21; Found: C, 54.61; H, 6.18; N, 24.82.

10.1.14 N,N'-Dicyanoacetyl-1,6-diaminohexane

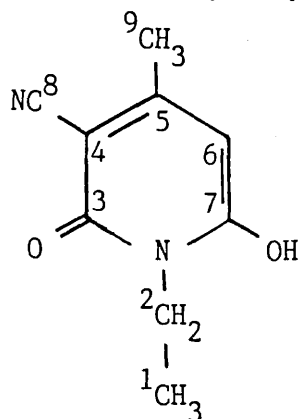
A mixture of 1,6-diaminohexane (58.0 g, 0.5 mol) and ethylcyanoacetate (113.0 g, 1.0 mol) in ethanol (100 ml) was refluxed for 4 hrs to yield 98.7 g (79%) of a buff precipitate (recryst. ethanol m.p. = 149.0-151.0°C; ^1H nmr δ (d^6 -DMSO, ppm) 1.33 (s, broad), 3.12 (m) $\text{C}^{4,5,6}\text{H}_2$, 3.60 (s) C^2H_2 , 8.18 (m) OH; ^{13}C nmr δ (d^6 -DMSO, ppm)

25.30 (C⁶), 25.95 (C⁵), 28.68 (C²), 39.21 (C⁴), 115.82 (C¹),
 161.80 (C³), i.r. 3289 (N-H), 3096 (C-H), 2960 (C-H), 2255 (C \equiv N), 1665
 (C=O) cm⁻¹; Calcd. for C₁₂H₁₈N₄O₂: C, 57.57; H, 7.26; N, 22.39:
 Found C, 57.51; H, 7.24; N, 22.24.

10.1.15 3-Cyano-2,6-dihydroxy-4-methyl pyridine¹¹.

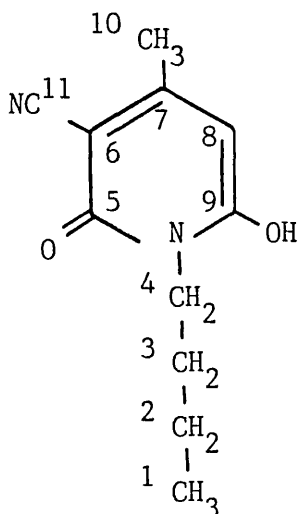


A mixture of cyanoacetamide (16.8 g, 0.2 mol), ethyl acetoacetate (25.4 ml, 0.2 mol) in methanol (45 ml) was warmed to obtain solution and a paste of potassium hydroxide in methanol (13.8 g, 0.25 mol) was added. After acidification, filtration and drying the crude white hydroxypyridone weighed 19.0 g (63%) (recryst. aqueous ethanol, m.p. = 313.0-315.0^o, lit. m.p. = 316-319^o, ¹H n.m.r. δ (d⁶-DMSO, ppm) 2.28 (s) CH₃, 5.67 (s) CH, 10.56 (s) OH; ¹³C nmr. δ (d⁶-DMSO, ppm) 20.82 (C⁷), 89.02 (C⁴), 92.73 (C³), 116.92 (C⁶), 160.16 (C²), 160.88, 161.72 (C¹, C⁵), i.r. 3350-2300 (O-H), 2215 (C \equiv N), 1610 (C=C), 1300 (C-O) cm⁻¹.

10.1.16 1-Ethyl-3-cyano-6-hydroxy-4-methyl pyrid-2-one¹¹

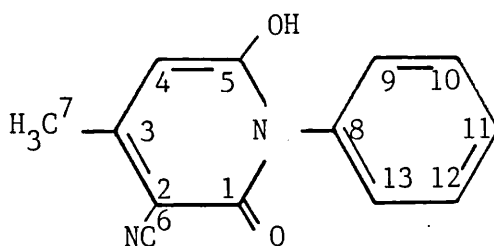
To a solution of N-ethyl cyanoacetamide (35.8 g, 0.32 mol) and ethyl acetoacetate (41.6 ml, 0.32 mol) in methanol (70 ml) was added potassium hydroxide in methanol (22.0 g, 0.4 mol). The crude white hydroxypyridone weighed 21.3 g (38%) (recryst. ethanol; m.p. = 245.0 - 246.0°, lit. m.p. = 246.0-248.0°; ¹H nmr δ(d⁶-DMSO, ppm) 1.14 (t) C¹H₃, 2.24 (s) C⁹H₃, 3.97 (q) CH₂, 5.71 (s) CH, 10.68 (s) OH; ¹³C nmr. δ(d⁶-DMSO, ppm) 12.944 (C¹), 20.48 (C⁹), 35.83 (C²), 88.64 (C⁶), 92.02 (C⁵), 117.38 (C⁸), 158.03 (C⁴), 160.17 (C³, C⁷); i.r. 3080-2300 (O-H, C-H), 2220 (C ≡ N), 1640 (C=O), 1610 (C=C), 1290 (C-N) cm⁻¹.

10.1.17 1-Butyl-3-cyano-6-hydroxy-4-methyl pyrid-2-one



N-Butyl cyanoacetamide (28.0 g, 0.2 mol) and ethyl acetoacetate (26.0 g, 0.2 mol) were added to a solution of sodium (4.6 g, 0.2 mol) in 200 ml methanol and the mixture refluxed for 7 hrs. On cooling the solid deposited was filtered off. The filtrate was then diluted with its own volume of water and the hydroxypyridone precipitated out with 25.0 ml concentrated hydrochloric acid. On drying the white solid weighed 21.1 g (51%) (recryst. ethanol; m.p. = 212.5 - 214.0°; lit. m.p. 212.0°; ¹H nmr δ(d⁶-DMSO, ppm) 1.24 (m) C₄H₉, 2.30 (s) C¹⁰H₃, 3.98 (m) C₄H₉, 5.72 (s) CH, 13.40 (s) OH; ¹³C nmr δ(d⁶-DMSO, ppm) 12.62 (C¹), 18.67 (C²), 19.58 (C¹⁰), 28.62 (C³), 39.54 (C⁴), 88.12 (C⁸), 90.98 (C⁷), 116.41 (C¹¹), 157.18 (C⁶), 159.33 (C⁵, C⁹); i.r. 3094 - 2961 (O-H), 2936-2877 (C-H), 2219 (C≡N), 1662 (C = O), 1611 (C=C) cm⁻¹.

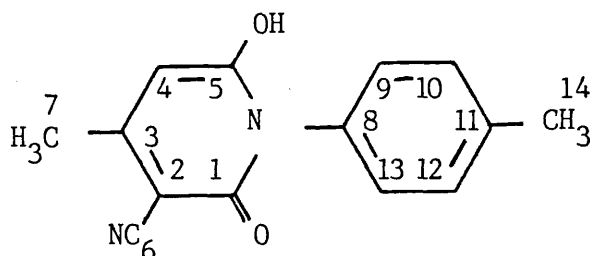
10.1.18 1-Phenyl-3-cyano-6-hydroxy-4-methyl pyrid-2-one



Sodium (0.6 g, 25 mmol) was dissolved in methanol (25 ml) while stirring. After cooling the paste, N-phenyl cyanoacetamide (4.0 g, 25 mmol) and ethyl acetoacetate (3.3 g, 25 mmol) were added. The reaction mixture was refluxed with stirring for 7 hrs. The solution was then allowed to cool and was diluted with its own volume of water. On adding

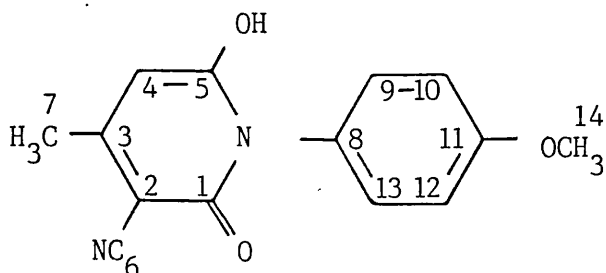
1.0 ml of concentrated hydrochloric acid the phenyl hydroxypyridone precipitated out and a further 2 ml of acid was added. The buff coloured filter cake was then washed with several portions of cold water, followed by ether, and dried by suction to yield 3.1 g (54%) (recryst. toluene m.p. = 316.0- 318.0°; ^1H nmr. δ (d^6 -DMSO, ppm) 2.31 (s) CH_3 , 5.70 (s) C-H, 7.42 (m) C_6H_5 ; ^{13}C nmr (poor signal to noise); i.r. 3080 (O-H), 2220 ($\text{C}\equiv\text{N}$), 1660 ($\text{C}=\text{O}$), 760 (C-H) cm^{-1} ; Calcd. for $\text{C}_{13}\text{H}_{10}\text{N}_2\text{O}_2$: C, 69.01; H, 4.46; N, 12.38; Found: C, 69.29; H, 4.55; N, 12.52.

10.1.19 1-(p-Tolyl)-3-cyano-6-hydroxy-4-methyl pyrid-2-one



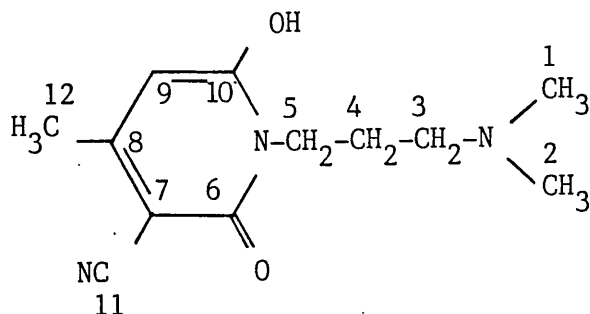
Procedure as for 10.1.18 above, dissolving sodium (0.3 g, 0.01 mol) in methanol (12 ml) and adding p-tolyl cyanoacetamide (2.0 g, 0.01 mol) and ethyl acetoacetate (1.5 g, 0.01 mol). On acidification 1.4 g (57%) of an olive green precipitate was obtained (recryst. toluene m.p. > 350°; ^1H nmr δ (d^6 -DMSO, ppm) 2.29 (s) C^7H_3 , 2.37 (s) C^{14}H_3 , 5.89 (s) CH, 7.23 (m) C_6H_4 ; ^{13}C nmr δ (d^6 -DMSO, ppm) 20.28, 20.54 ($\text{C}^7, \text{C}^{14}$), 87.91 (C^4), 92.40 (C^3), 117.50 (C^6), 122.96 (C^{11}), 127.91, 129.21 ($\text{C}^{10}, \text{C}^{12}$), 129.86 (C^8), 132.65, 137.47 ($\text{C}^9, \text{C}^{13}$), 158.67 (C^2), 160.81 (C^1, C^5); i.r. 3070 (O-H), 2200 ($\text{C}\equiv\text{N}$), 1658 ($\text{C}=\text{O}$), 1612 ($\text{C}=\text{C}$) cm^{-1} ; Calcd for $\text{C}_{14}\text{H}_{12}\text{N}_2\text{O}_2$: C, 69.98; H, 5.04; N, 11.66; Found: C, 69.72; H, 4.92; N, 11.59.

10.1.20 1-(p-Anisyl)-3-cyano-6-hydroxy-4-methyl pyrid-2-one



Procedure as for 10.1.18 dissolving sodium (0.2 g, 8.0 mmol) in methanol (10 ml) and adding p-anisyl cyanoacetamide (1.5 g, 8.0 mmol) and ethyl acetoacetate (1.0 ml, 8.0 mmol). On acidification 1.4 g (67%) of a buff precipitate was obtained (recryst. toluene, m.p. = 265.0-267.0°;

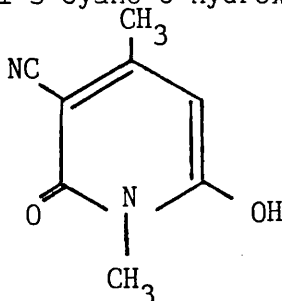
^1H nmr δ (d^6 -DMSO, ppm) 2.28 (s) C^7H_3 , 3.80 (s) C^{14}H_3 , 5.80 (s) C^4H , 7.08 (m) C_6H_4 ; ^{13}C nmr δ (d^6 DMSO, ppm) 20.67 (C^7), 55.27 (C^{14}), 88.30 (C^4), 92.40 (C^3), 113.86 (C^{11}), 114.06 ($\text{C}^{10}, \text{C}^{12}$), 117.50 (C^6), 127.71 (C^8); 129.21 ($\text{C}^9, \text{C}^{13}$), 158.86 (C^2), 160.94, 161.07 (C^1, C^5); i.r. 3070 (O-H), 2200 ($\text{C}\equiv\text{N}$), 1660 ($\text{C}=\text{O}$), 1610 ($\text{C}=\text{C}$); Calcd. for $\text{C}_{14}\text{H}_{12}\text{N}_2\text{O}_3$: C, 65.61; H, 4.73; N, 10.93; Found: C, 65.31; H, 4.68; N, 10.66.

10.1.21 1-(Dimethylaminopropyl)-3-cyano-6-hydroxy-4-methyl-pyrid-2-one¹⁷

3-Dimethylaminopropylamine (125.0 ml, 1.0 mol) was added to ethyl cyanoacetate (106.0 ml, 1.0 mol) over a 15 min period; temperature rose

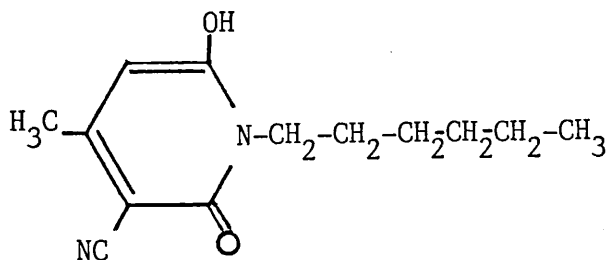
to 65°. The solution was then heated to a gentle reflux and ethyl acetoacetate (127.0 ml, 1.0 mol) was added. The mixture was then refluxed for a further 15 hrs. On cooling the product crystallised out, was filtered and dried to yield 95.3 g (41%) of a white powder (m.p. = 208.0 - 209.0°, lit. m.p. = 209°, ¹H n.m.r. δ(d⁶-DMSO, ppm) 1.65 (m) C⁴H₂, 1.77 (s) C¹²H₃, 2.55 (s) C¹H₃, 2.73 (t) C³H₂, 3.62 (t) C⁵H₂, 4.91 (s) C⁹H, i.r. 3430 - 3027 (O-H), 2957 (C-H), 2188 (C≡N), 1613 (C=C) cm⁻¹.

10.1.22 1-Methyl-3-cyano-6-hydroxy-4-methyl pyrid-2-one



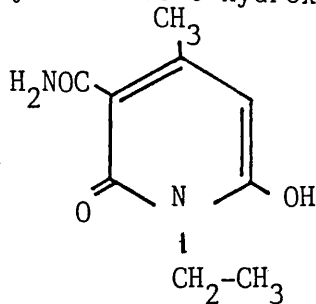
Supplied by Ilford Ltd. (m.p. = 276.0 - 277.0°; lit. m.p.¹⁷ = 275.0°).

10.1.23 1-Hexyl-3-cyano-6-hydroxy-4-methylpyrid-2-one

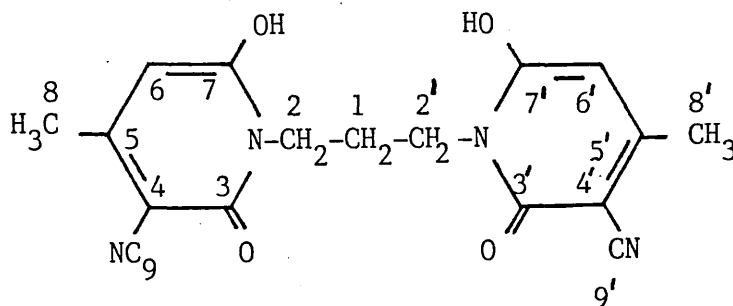


Supplied by Ilford Ltd (m.p. = 187.0 - 188.0°, lit. m.p.¹⁷ = 187.0 - 188.0°).

10.1.24 1-Ethyl-3-amido-6-hydroxy-4-methyl pyrid-2-one

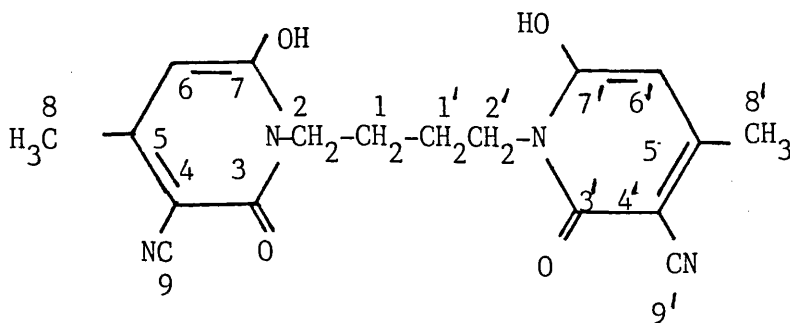


Supplied by Ilford Ltd. (m.p. = 158.5 - 159.5° lit. m.p.¹⁷ = 159.0 - 160.0°).

10.1.25 N,N'-Trimethylene-bis-(3-cyano-6-hydroxy-4-methyl pyrid-2-one)

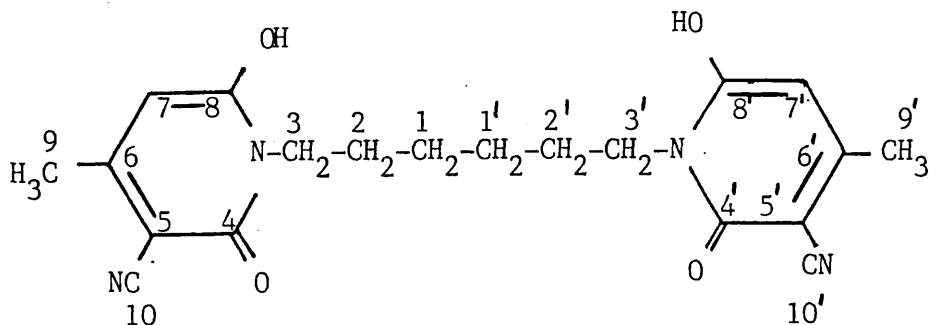
To a solution of sodium (1.1 g, 0.048 mol) in methanol (50 ml) was added N,N'-dicyanoacetyl-1,3-diaminopropane (5.0 g, 0.048 mol) and ethyl acetoacetate (6.3 g, 0.048 mol); the reaction mixture was then refluxed for 18 hrs. After cooling any solid deposited was filtered off. To the filtrate was added 80 ml water which was then acidified with 5 ml concentrated hydrochloric acid. The resulting precipitate was filtered off and dried over P₂O₅. The pale yellow solid weighed 5.45 g (67%) (recryst. ethanol, m.p. = 251.0 - 253.0° (decomp); ¹H nmr δ(d⁶-DMSO, ppm) 1.88 (m) C¹H₂, 2.25 (s) CH₃, 4.00 (m) C²H₂, 5.65 (s) CH, 7.84 (s) OH; Calcd. for C₁₇H₁₆N₄O₄: C, 59.99; H, 4.75; N, 16.47; Found C, 59.45; H, 4.77; N, 16.56.

10.1.26 N,N'-Tetramethylene-bis-(3-cyano-6-hydroxy-4-methyl
pyrid-2-one)



To a solution of sodium (2.1 g, 0.09 mol) in 100 cm³ methanol was added N,N'-dicyanoacetyl-1,4-diaminobutane (10.0 g, 0.045 mol) and ethyl acetoacetate (11.7 g, 0.09 mol). The mixture was refluxed for 18 hrs to yield 9.6 g (60%) of the yellow product after acidification (recryst. ethanol m.p. = 272.0-275.0° (decomp); ¹H nmr δ(d⁶-DMSO, ppm) 1.50 (m) C¹H₂, 2.16 (s) CH₃, 3.89 (m) C²H₂, 5.58 (s) CH, 7.52 (s) OH; ¹³C nmr δ(d⁶-DMSO, ppm) 20.55 (C⁸), 25.04 (C¹), 40.26 (C²), 88.18 (C⁶), 92.48 (C⁵), 117.64 (C⁹), 157.90 (C⁴), 160.56 (C³, C⁷); Calcd. for C₁₈H₁₈N₄O₄: C, 61.01; H, 5.13; N, 15.81: Found C, 59.83; H, 5.41; N, 16.09.

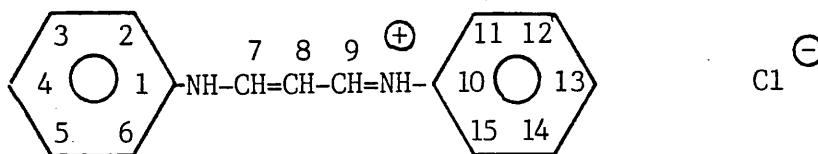
10.1.27 N,N'-Hexamethylene-bis-(3-cyano-6-hydroxy-4-methyl
pyrid-2-one)



N,N'-Dicyanoacetyl-1,6-diaminohexane (125.0 g, 0.05 mol) and ethyl acetoacetate (130.0 g, 1.0 mol) were added to a solution of sodium

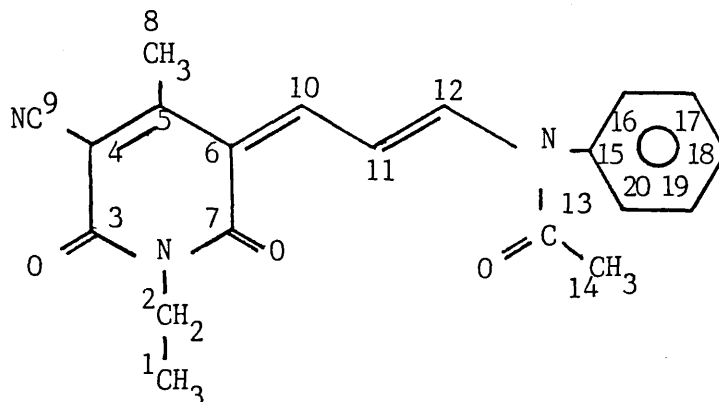
(23.0 g, 1.0 mol) in 500 cm³ methanol and the mixture refluxed for 18 hrs. On cooling and after acidification 138.2 g (72%) of this yellow product was obtained (recryst. ethanol m.p. = 236.0 - 238.0° (decomp); ¹H nmr δ(d⁶-DMSO, ppm) 1.42 (m) C¹,²H₂, 2.26 (s) CH₃, 3.94 (m) C³H₂, 5.75 (s) CH, 8.54 (s) OH; ¹³C nmr δ(d⁶-DMSO, ppm) 20.68 (C⁹), 26.14, 27.57 (C¹,C²), 40.91 (C³), 88.51 (C⁷), 93.13 (C⁶), 117.84 (C¹⁰), 158.29 (C⁵), 160.95 (C⁴,C⁸); i.r. 3791 (O-H), 2937 (C-H), 2217 (C≡N) 1634 (C=C) cm⁻¹; Calcd. for C₂₀H₂₂N₄O₄: C, 62.81; H, 5.81; N, 14.65: Found: C, 62.84; H, 6.09, N, 15.06.

10.1.28 β-Anilinoacrolein anil hydrochloride ¹⁵.



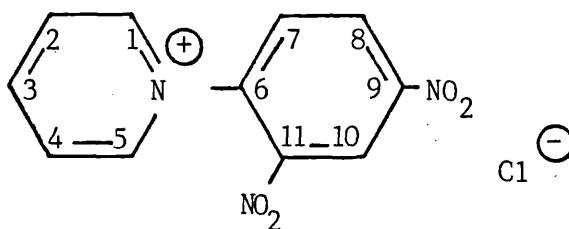
Aniline (31.3 ml, 0.33 mol) and tetramethoxypropane (26.8 ml, 0.16 mol) in 100 ml ethanol were stirred together at room temperature. The mixture was cooled to 0° and concentrated hydrochloric acid (38.0 ml, 0.4 mol) was added dropwise so as not to allow the temperature to rise above 10°C. The reaction mixture was left to stand overnight and was then refluxed for 2 hrs. After cooling the product was collected by filtration, washed with 40 ml cold ethanol and dried over P₂O₅ to yield 26.7 g (65%) (m.p. = 227.0-228.0°; lit. m.p. = 229.0-230.0°, ¹H nmr δ(d⁶-DMSO, ppm) 3.57 (s) NH, 6.64 (t) C⁸H, 7.37 (m) C₆H₅, 9.19 (m) C⁷H; i.r. 3108 (C²-H), 3060 (C⁷-H), 1632 (C⁷=C⁸), 1567 (C² = C³) cm⁻¹.

10.1.29 3-(3'-Acetanilidoallyldiene)-1-ethyl-4-methyl-5-cyano
pyrid-2,6-dione¹⁶.



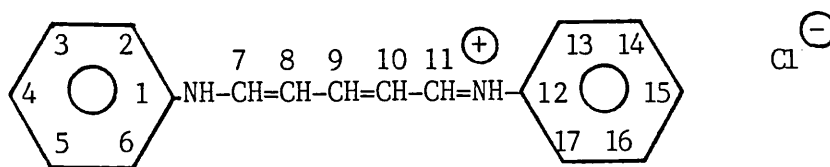
A mixture of 1-ethyl-3-cyano-6-hydroxy-4-methyl pyrid-2-one (4.5 g, 0.03 mol) and β -anilinoacrolein anil hydrochloride (6.5 g, 0.03 mol) suspended in 30 ml acetic anhydride was stirred at 75° for 1 hr. After filtering, the black solid was washed with acetic acid and dried, yielding 8.1 g (93%) (m.p. = 208.0-210.0°; lit. m.p. = 208.0-210.0°; ¹H nmr δ (d⁶-DMSO, ppm) 1.14 (t) C¹H₃, 2.21 (s) C⁸H₃, 2.46 (s) C¹⁴H₃, 3.90 (q) CH₂, 6.53 (m) C¹⁰H, 7.43 (s) C₆H₅, 9.01 (t) C¹¹H, 12.66 (d) C¹²H; ¹³C nmr δ (d⁶-DMSO, ppm) 12.88 (C¹), 18.41 (C⁸), 20.29 (C¹⁴), 35.57 (C²), 98.52 (C⁵), 110.36 (C⁶), 117.32 (Ar), 117.90 (C⁹), 120.83 (C¹¹), 125.64, 129.54, 138.52 (Ar), 157.05 (C¹⁰, 10¹²), 157.77 (C⁴), 158.35 (C¹³), 160.04, 161.86 (C³, C⁷); i.r. 3190 (C¹⁶-H), 2941 (C¹-H), 2206 (C \equiv N), 1633 (C=O) 1567 (C \equiv C) cm⁻¹.

10.1.30 N-(2,4-Dinitrophenyl)pyridinium chloride¹⁷.

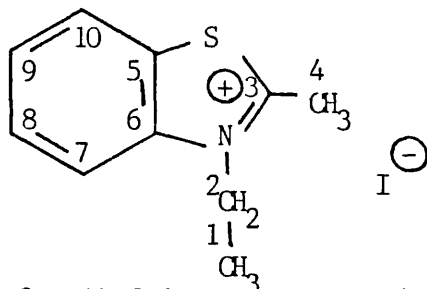


A mixture of pyridine (36.2 ml, 0.45 mol) and 1-chloro-2,4-dinitrobenzene (91.5 g, 0.45 mol) in 400 ml toluene was refluxed for 3 hrs. After cooling and filtering the buff precipitate was washed with three 50 ml portions of cold acetone and allowed to dry. The product weighed 56.8 g (45 %) m.p. = 203.0 - 203.5° (subl.) lit. m.p. = 204.0°. ^1H nmr $\delta(\text{D}_2\text{O}$; ppm) 8.49 (m) $\text{C}^{7,8,10}\text{H}$, 9.02-9.48 (m) C^{1-5}H ; ^{13}C nmr $\delta(\text{D}_2\text{O}$, ppm) 125.05, 131.10, 133.25, 133.83 (CH), 141.12, 145.34 ($\text{C}^9, \text{C}^{11}$) 147.88, 151.85 (CH), 152.11 (C^6); i.r. 3118, 3072, 3058 (C-H), 1610, 1563 (C = C), 1544, 1343 (N-O) cm^{-1} .

10.1.31 Glutaconic dialdehyde dianil hydrochloride¹⁷.

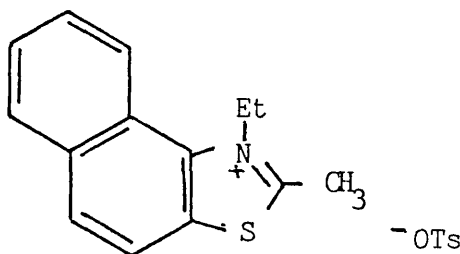


N-(2,4-Dinitrophenyl)pyridinium chloride (42.3 g, 0.15 mol) was suspended in 200 ml ethanol and cooled in an ice bath. Aniline (41.1 ml, 0.45 mol) was then added dropwise over a 30 min period. The reaction mixture was then refluxed for 1 hr, cooled and the red precipitate filtered off and washed with 3 x 25 ml portions acetone and dried to yield 40.8 g (96%) (recryst. ethanol m.p. = 148.0 - 149.0°, lit. m.p. = 148.0-150.0°; ^1H nmr $\delta(\text{d}^6\text{-DMSO}$, ppm) 3.52 (s) NH, 6.67-9.36 (m) C_6H_5 , CH; ^{13}C nmr $\delta(\text{d}^6\text{DMSO}$, ppm) 119.85 (Ar), 123.17 (Ar), 128.83 (C^8 or C^9), 129.02 (Ar), 135.39 (C^8 or C^9), 149.89 (C^7); i.r. 3450 (N-H), 3106 ($\text{C}^2\text{-H}$), 3072 ($\text{C}^7\text{-H}$), 1631 ($\text{C}^7 = \text{C}^8$), 1566 ($\text{C}^1 = \text{C}^2$) cm^{-1} .

10.1.32 2-Methyl-3-ethyl benzothiazolium iodide¹⁷.

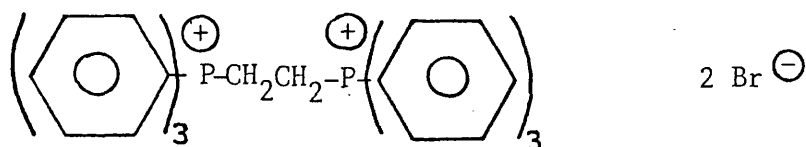
A mixture of 2-methyl benzothiazole (10.0 ml, 0.08 mol) and ethyl iodide (10.0 ml, 0.13 mol) was refluxed for 6 hrs on a water bath. The product was then filtered off, washed with ether and allowed to air dry, yielding 3.2 g (13%) of a pale green solid (m.p. = 194.0-196.0°; lit. m.p. = 196.0°; ¹H nmr δ(d⁶-DMSO, ppm) 1.58 (t) C¹H₃, 3.32 (s) C⁴H₃; 4.84 (q) CH₂, 8.16 (m) C₆H₄; ¹³C nmr δ(d⁶-DMSO, ppm) 13.06 (C¹), 16.97 (C⁴), 44.67 (C²), 116.46, 124.46, 127.71, 128.82 (C⁷, C⁸, C⁹, C¹⁰), 129.08 (C⁵), 140.20 (C⁶), 176.42 (C³); i.r. 3070 (C⁷-H), 2975, 2925 (C¹H), 1615 (C = C) cm⁻¹.

10.1.33 1-Ethyl-2-methyl-β-naphthothiazolium tosylate



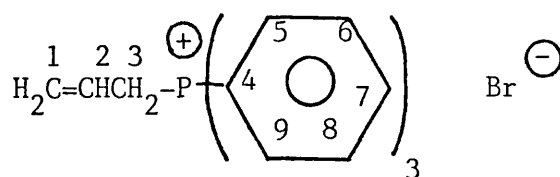
Supplied by Ilford Ltd. (m.p. = 151.0-154.0°)

10.1.34 Ethylene bis-(triphenylphosphonium) bromide



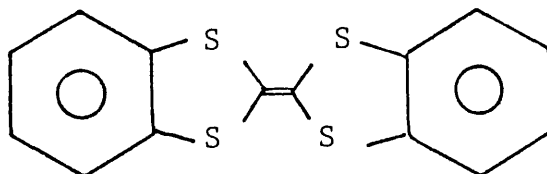
A mixture of triphenylphosphine (20.0 g, 0.076 mol) and 1,2-dibromoethane (60.0 g, 0.32 mol) was heated at 140° for 30 mins. The white product was then filtered off and dried and weighed 26.0 g (48%) (m.p. = 305.0 - 306.0°, lit. m.p.⁹⁰ = 308.0 - 315.0°); ¹H nmr δ(D₂O, ppm) 3.82 (s, broad) CH₂, 7.69 (m) Ph₃.

10.1.35 Allyl triphenylphosphonium bromide



A mixture of triphenylphosphine (20.0 g, 0.076 mol) and allyl bromide (13.2 ml, 0.15 mol) (redist. 25° at 162 mmHg) in 100 ml benzene was refluxed for 2 hrs. The white crystalline product was filtered off and washed with several portions of benzene and after drying weighed 27.6 g (95%) m.p. = 213.0 - 214.0°; lit. m.p.⁹¹ = 209.0°; ¹H nmr δ(d⁶-DMSO, ppm) 4.48 (m), 4.74 (m), 5.31 (m), C¹H₂, CH², C³H₂, 7.56 (m) Ph₃.

10.1.36. Dibenzotetrathiafulvalene^{18,92,93}.



A solution of anthranilic acid (42.5 g, 0.3 mol) in dioxane (100 ml) was added dropwise over a period of 1.5 hrs to a stirred and gently refluxing solution of isoamyl nitrite (43.3 g, 0.4 mol), isoamyl alcohol

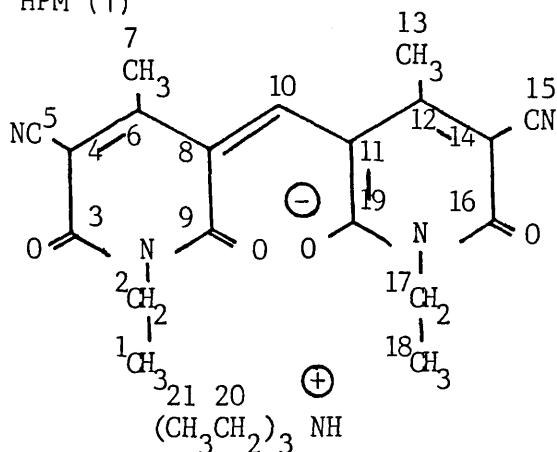
(54.6, 0.6 mol) and carbon disulphide (150 ml) in 1,2-dichloroethane (800 ml). After the addition was completed, the mixture was refluxed for $\frac{1}{2}$ hr. The resultant red reaction mixture was washed successively with water, aqueous sodium carbonate, and water and dried over anhydrous magnesium sulphate. Solvent and excess reagents were removed under reduced pressure and the red viscous oily residue was purified by distillation in vacuo yield; 32.0 g (44%) pale yellow oil, b.p. = 121° 0.1 mmHg. The black crystalline distillation residue was washed with benzene to give 4.7 g dibenzotetrathiafulvalene.

A further 1.5 g pure dibenzotetrathiafulvalene was obtained from the thermal decomposition of the 2-alkoxy-1,3-benzodithiole (yellow oil) at 200° for 1 hr, after recrystallisation from benzene, total yield = 6.2 g (14%); m.p. = $233.0 - 235.0^{\circ}$, lit. m.p. = 234° , Calcd. for $C_{14}H_8S_4$: C, 55.25, H, 2.63. Found: C, 55.27, H, 2.74.

Oxonols

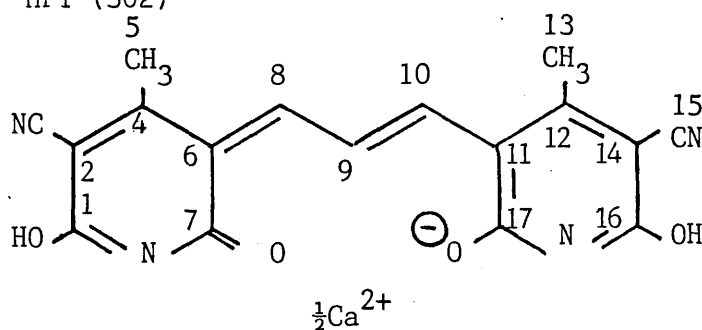
Many of the dyes in this section have identical anions. As a result, only very small differences in the anion peaks chemical shifts in the 1H and ^{13}C n.m.r. spectra and absorption band frequencies, in the i.r. spectra, are observed, as the cation varies. Therefore the n.m.r. and i.r. spectral characterisations of the first member of each anion class are reported in full, subsequent members show only assignments of the peaks and bands which are in addition to those of the anion.

10.1.37 HPM (1)



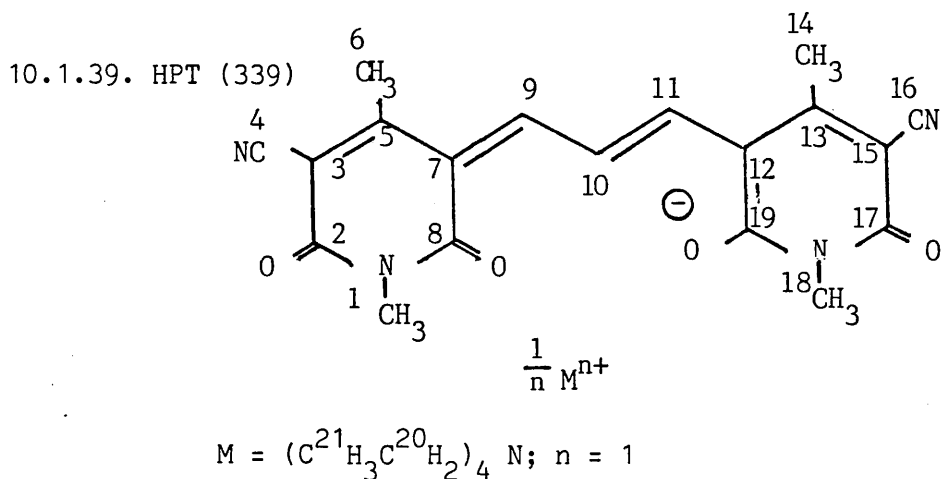
A mixture of 1-ethyl-3-cyano-6-hydroxy-4-methyl pyrid-2-one (5.0 g, 0.028 mol), triethyl orthoformate (2.1 g, 0.014 mol) and triethylamine (1.42 g, 0.014) in 50 ml ethanol was refluxed for 3 hrs. The reaction mixture was allowed to cool, the product filtered off and dried to yield 3.5 g (53%) (recryst. ethanol (purple needles)); m.p. = 185.0 - 186.0° (decomp); ^1H nmr δ (d^6 -DMSO, ppm) 1.21 (m) C^{21}H_3 , C^1H_3 , 2.33 (s), C^7H_3 , 3.15 (m) C^{20}H_2 , 3.82 (q) C^2H_2 , 8.00 (s), C^{10}H ; uv/visible; λ_{max} (EtOH) 549 nm (ϵ_{max} , $8.90 \times 10^3 \text{ mol}^{-1} \text{ dm}^3 \text{ cm}^{-1}$) Calcd. for $\text{C}_{25}\text{H}_{33}\text{N}_5\text{O}_4$: C, 64.21, H, 7.13, N, 14.98. Found C, 63.92; H, 6.85, N, 14.70.

10.1.38. HPT (302)



A mixture of 3-cyano-2,6-dihydroxy-4-methyl pyridine (5.0 g, 0.03 mol), tetramethoxypropane (TMP) (2.3 ml, 0.015 mol) and calcium hydroxide (0.52, 0.007 mol) in 40 ml 9:1 ethanol:acetic acid was refluxed for 1 hr.

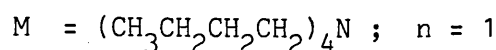
After cooling, filtering and drying the blue precipitate weighed 5.0 g (94%) (m.p. $> 360.0^{\circ}$; ^1H nmr $\delta(\text{d}^6\text{-DMSO, ppm})$ 2.18 (s) CH_3 , 5.45 (s) NH, 7.75 (d) C^8H , 8.93 (t) C^9H ; ^{13}C nmr $\delta(\text{d}^6\text{-DMSO, ppm})$ 18.92, 20.67 ($\text{C}^5, \text{C}^{13}$), 92.34, 94.74 ($\text{C}^4, \text{C}^{12}$), 110.93 ($\text{C}^6, \text{C}^{11}$), 117.76, 118.15 ($\text{C}^3, \text{C}^{15}$), 120.95 (C^9), 156.91, 158.80 ($\text{C}^8, \text{C}^{10}$), 160.29 ($\text{C}^2, \text{C}^{14}$), 162.24, 162.50, 162.83, 163.22 ($\text{C}^1, \text{C}^7, \text{C}^{16}, \text{C}^{17}$); i.r. 3600-3000 (O-H, N-H), 2210 ($\text{C}\equiv\text{N}$), 1625 (C=O), 1608 ($\text{C}=\text{C}$), 1460 ($\text{C}^5\text{-H}$), 1360 (C-N), 1308 (C-O), u.v./visible λ_{max} (H_2O) 588 ($\epsilon_{\text{max}} 4.26 \times 10^4$), 545 nm (sh, $1.91 \times 10^3 \text{ mol}^{-1} \text{ dm}^3 \text{ cm}^{-1}$).



A mixture of 1-methyl-3-cyano-6-hydroxy-4-methyl pyrid-2-one (1.0 g, 0.006 mol), 1,1',3,3'-tetramethoxypropane (TMP) (0.5 g, 0.003 mol) and tetraethylammonium iodide (0.8 g, 0.003 mol) in 20 ml ethanol was refluxed for 12 hrs. The reaction mixture was allowed to cool and the blue crystalline material filtered off and dried, yielding 1.1 g (79%) (recryst. methanol (blue needles)) m.p. = $270.0\text{-}271.0^{\circ}\text{C}$; ^1H nmr $\delta(\text{d}^6\text{-DMSO, ppm})$ 0.44 (m) C^{21}H_3 , 1.71 (s) C^6H_3 , 2.43 (s) C^1H_3 , 2.52 (m) C^{20}H_2 ; 7.10 (d) C^9H , 8.36 (t) C^{10}H ; ^{13}C nmr $\delta(\text{d}^6\text{-DMSO, ppm})$ 7.02 (C^{21}), 18.59 ($\text{C}^6, \text{C}^{14}$), 25.94 ($\text{C}^1, \text{C}^{18}$), 51.43 (C^{20}), 92.08 ($\text{C}^5, \text{C}^{13}$), 110.35 ($\text{C}^7, \text{C}^{12}$), 117.70

(C⁴,C¹⁶), 120.88 (C¹⁰), 157.43 (C⁹,C¹¹), 158.02 (C³,C¹⁵),
 161.79 162.44 (C²,C⁸,C¹⁷,C¹⁹); Calcd. for C₂₇H₃₅N₅O₄: C,
 65.69; H, 7.16; N, 14.19: Found; C, 65.92; H, 7.08; N, 14.18.

10.1.40. HPT (326)



Procedure as for 10.1.39 using 1-methyl-3-cyano-6-hydroxy-4-methyl
 pyrid-2-one (4.6 g, 0.029 mol), TMP (2.3 g, 0.014 mol) and tetrabutyl-
 ammonium bromide (4.5 g, 0.014 mol) in 50 ml ethanol. Reflux time = 4
 hrs. Yield = 6.43 g (77%), (recryst. methanol (dark green cubes); m.p. =
 249.0 - 250.0°; ¹H nmr δ(d⁶-DMSO, ppm) 1.00 (m), C²³H₃, 1.49 (m)
 C^{21,22}H₂, 3.22 (m) C²⁰H₂; ¹³C n.m.r. δ(d⁶-DMSO, ppm) 19.12
 (C²³), 23.02 (C²¹, C²²), 57.55 (C²⁰); u.v/visible λ_{max} (EtOH)
 599 (ε_{max} 1.29 x 10⁵), 555 nm (sh, 3.37 x 10⁴ mol⁻¹ dm³cm⁻¹);
 Calcd. for C₃₅H₅₁N₅O₄: C, 69.38; H, 8.50; N, 11.56: Found: C,
 68.90; H, 8.53; N, 12.09..

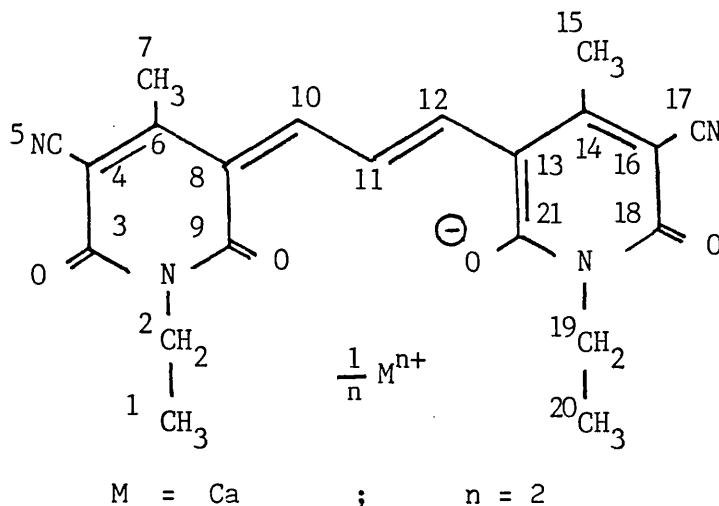
10.1.41. HPT (340)



Procedure as for 10.1.39 using 1-methyl-3-cyano-6-hydroxy-4-methyl
 pyrid-2-one (5.0 g, 0.03 mol), methyltriphenylphosphonium bromide (5.5 g,
 0.015 mol) and TMP (2.5 g, 0.015 mol) in 50 ml ethanol. Reflux time = 2
 hrs. Yield = 5.8 g (60%), (recryst. ethanol (green cubes)); m.p. 205.5 -
 207.0°, ¹³C nmr δ(d⁶-DMSO, ppm) 6.84, 7.97 (C²⁰), 118.99, 120.95,

129.93, 130.21, 133.32, 134.75 (Ph_3); Calcd. for $\text{C}_{38}\text{H}_{33}\text{N}_4\text{O}_4\text{P}$: C, 71.23; H, 5.20; N, 8.75: Found C, 70.82; H, 5.45; N, 8.80.

10.1.42. HPT (261).



A mixture of 1-ethyl-3-cyano-6-hydroxy-4-methyl pyrid-2-one (5.0 g, 0.028 mol), 1,1',3,3'-tetramethoxypropane (2.4 ml, 0.014 mol) and calcium hydroxide (0.52 g, 0.007 mol) in 50 ml of 9:1 ethanol:acetic acid was refluxed for 2 hrs. The reaction mixture was allowed to cool and the green precipitate filtered off and dried, yielding 4.7 g (82%) (m.p. > 360.0°; lit. m.p.¹⁷ > 360.0°; ¹H nmr δ (d⁶-DMSO, ppm) 1.09 (t) C¹H₃, 2.44 (s) C⁷H₃, 3.90 (q) CH₂, 7.71 (d) C¹⁰H, 9.0 (t) C¹¹H; ¹³C n.m.r. δ (d⁶-DMSO, ppm) 13.08 (C¹, C²⁰), 18.55 (C⁷, C¹⁵), 33.82 (C², C¹⁹), 92.21 (C⁶, C¹⁴), 110.40 (C⁸, C¹³), 117.72 (C⁵, C¹⁷), 120.93 (C¹¹), 157.36 (C¹⁰, C¹²), 158.13 (C⁴, C¹⁶) 161.39, 161.97 (C³, C⁹, C¹⁸, C²¹); i.r. 2975-2930 (C-H, ali), 2200 (C≡N), 1660 (C=O), 1615 (C=C, ar), 1265 (C-N) cm⁻¹.

10.1.43. HPT (336)

M = Co ; n = 2

Procedure as for 10.1.42 using 3-cyano-6-hydroxy-4-methyl pyrid-2-one (2.5 g, 0.014 mol), TMP (1.2 ml, 0.007 mol) and cobaltous acetate tetrahydrate (0.9 g, 0.004 mol) in 20 ml ethanol. Reflux time = 1 hr. Yield = 2.0 g (68%) (dark blue powder; m.p. = 344.0-345.5°, lit. m.p.¹⁷ = 346.0° u.v./visible $\lambda_{\max}(\text{H}_2\text{O})$ 589 (ϵ_{\max} , 8.32×10^4), 548 (sh, $3.53 \times 10^4 \text{ mol}^{-1} \text{ dm}^3 \text{ cm}^{-1}$).

10.1.44. HPT (335)



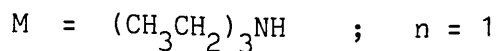
Procedure as for 10.1.42 using 1-ethyl-3-cyano-6-hydroxy-4-methyl pyrid-2-one, (2.5 g, 0.014 mol), TMP (1.2 ml, 0.007 mol) and nickel acetate tetrahydrate (0.9 g, 0.004 mol) in 20 ml ethanol. Reflux time = 1 hr. Yield = 1.64 g (56 %) (dark blue powder; m.p. > 350.0°, lit. m.p.¹⁷ > 360°; u.v./visible $\lambda_{\max}(\text{H}_2\text{O})$ 589 (ϵ_{\max} , 1.13×10^5), 545 nm (sh, $5.29 \times 10^4 \text{ mol}^{-1} \text{ dm}^3 \text{ cm}^{-1}$).

10.1.45. HPT (334)



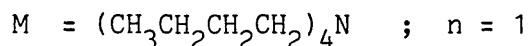
Procedure as for 10.1.42 using 1-ethyl-3-cyano-6-hydroxy-4-methyl pyrid-2-one (2.5 g, 0.014 mol), TMP (1.2 ml, 0.007 mol) and aluminium acetate tetrahydrate (0.44 g, 0.0012 mol) in 20 ml ethanol. Reflux time = 1 hr. Yield = 2.2 g (77%), (dark blue powder; m.p. > 350.0°, lit. m.p.¹⁷ > 360°; u.v./visible $\lambda_{\max}(\text{H}_2\text{O})$ 589 (ϵ_{\max} , 6.44×10^4), 548 nm (sh, $2.44 \times 10^4 \text{ mol}^{-1} \text{ dm}^3 \text{ cm}^{-1}$).

10.1.46. MI1579



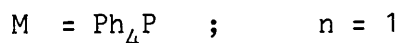
Procedure as for 10.1.42 using 1-ethyl-3-cyano-6-hydroxy-4-methyl pyrid-2-one (35.6 g, 0.20 mol), TMP (16.7 ml, 0.10 mol) and triethylamine (13.9ml, 0.10 mol) in 100 ml ethanol. Reflux time = 6 hrs. Yield = 33.4 (68%), (recryst. methanol (black needles) m.p. = 259.0-260.0°; lit. m.p.¹⁷ = 259.0-260.0°; ¹H nmr δ(d⁶-DMSO, ppm) 1.21 (m) C²³H₃, 3.12 (m) C²²H₂; ¹³C nmr δ(d⁶-DMSO, ppm) 8.52 (C²³), 45.91 (C²²).

10.1.47. HPT (288)



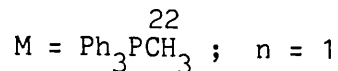
Procedure as for 10.1.42 using 1-ethyl-3-cyano-6-hydroxy-4-methyl pyrid-2-one (6.6 g, 0.037 mol), TMP (3.0 ml, 0.019 mol) and tetrabutylammonium iodide (6.9 g, 0.019 mol) in 150 ml ethanol. Reflux time = 6 hrs. Yield = 5.9 g (50%), (recryst. methanol (metallic green needles); m.p. = 186.0-187.0°, lit. m.p.¹⁷ = 187.0°; ¹H nmr (d⁶-DMSO, ppm) 1.09 (m) C²⁵H₃, 1.50 (m) C^{23,24}H₂, 3.31 (m) C²²H₂; ¹³C nmr δ(d⁶-DMSO, ppm) 18.98 (C²⁵), 22.95 (C²³, C²⁴), 57.61 (C²²).

10.1.48. HPT (289)



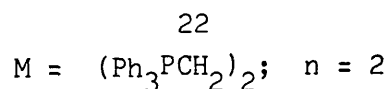
Procedure as for 10.1.42 using 1-ethyl-3-cyano-6-hydroxy-4-methyl pyrid-2-one (4.5 g, 0.025 mol), TMP (2.1 ml, 0.0125 mol) and tetraphenylphosphonium bromide (5.3 g, 0.0125 mol) in 20 ml ethanol. Reflux time = 6 hrs. Yield = 8.5 g (92%), (recryst. methanol (gold octahedra) m.p. = 254.0-255.0°, lit. m.p.¹⁷ = 254.0-255.0°.

10.1.49. HPT (297)



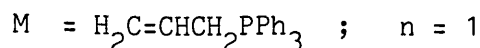
Procedure as for 10.1.42 using 1-ethyl-3-cyano-6-hydroxy-4-methyl pyrid-2-one (5.0 g, 0.028 mol), TMP (2.3 g, 0.014 mol) and methyl-triphenylphosphonium bromide (5.0 g, 0.014 mol) in 100 ml ethanol. Reflux time = 8 hrs. Yield = 8.31 g (89%), (recryst. methanol (dark blue needles) m.p. = 220.0 - 221.0° (decomp), lit. m.p.¹⁷ = 221.0°, ¹H nmr $\delta(\text{d}^6\text{-DMSO, ppm})$ 3.16 (d) C²²H₃, 7.84 (m) Ph₃, ¹³C nmr $\delta(\text{d}^6\text{-DMSO, ppm})$ 9.70 (d) (C²²), 119.79, 129.74, 130.26, 132.86, 133.31, 134.94 (Ph₃).

10.1.50. HPT (299)



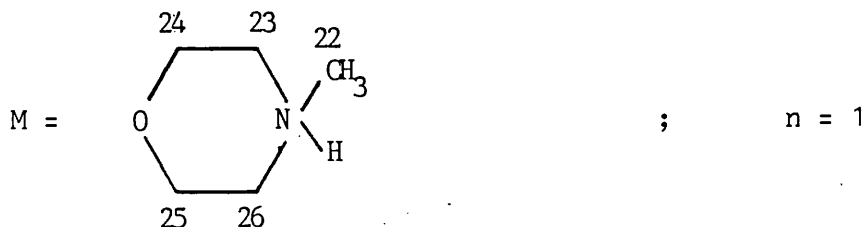
Procedure as for 10.1.42 using 1-ethyl-3-cyano-6-hydroxy-4-methyl pyrid-2-one, (5.0 g, 0.028 mol), TMP (2.3 g, 0.014 mol) and ethylene bis(triphenylphosphonium) dibromide (5.0 g, 0.007 mol) in 50 ml ethanol. Reflux time = 22 hrs. Yield = 7.2 g (77%), (recryst. ethanol (silver needles) m.p. = 270.5-271.5° (decomp); ¹H nmr $\delta(\text{d}^6\text{-DMSO, ppm})$ 3.55 (s) C²²H₂, 7.84 (s, broad) Ph₃; u.v./visible $\lambda_{\text{max}}(\text{H}_2\text{O})$ 589 (ϵ_{max} , 9.40×10^4), 546 nm (sh, $4.33 \times 10^4 \text{ mol}^{-1} \text{ dm}^3 \text{ cm}^{-1}$); Calcd. for C₄₀H₃₆N₄O₄P: C, 71.95; H, 5.45; N, 8.39; Found C, 71.92; H, 5.46; N, 8.43.

10.1.51. HPT (327)



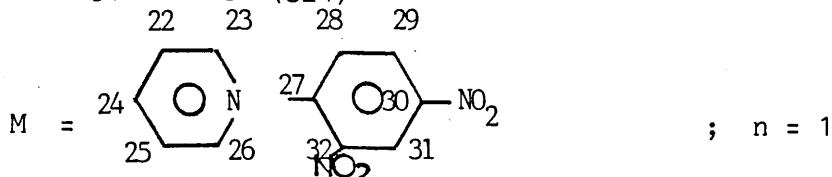
Procedure as for 10.1.42 using 1-ethyl-3-cyano-6-hydroxy-4-methyl pyrid-2-one (5.0 g, 0.028 mol), TMP (2.3 g, 0.014 mol) and allyl triphenylphosphonium bromide (5.4 g, 0.014 mol) in 75 ml ethanol. Reflux time = 5 hrs. Yield = 6.1 g (63%), (recryst. ethanol (green needles); m.p. = 206.5-207.5°; ¹H nmr δ(d⁶-DMSO, ppm) 3.81 (m), 3.89 (m), 5.47 (m), CH₂, CH, C H₂, 7.85 (m) Ph₃; u.v./visible λ_{max} (EtOH) 601 nm (ε_{max}, 1.13 x 10⁵ mol⁻¹ dm³ cm⁻¹); Calcd. for C₄₂H₃₉N₄O₄P: C, 72.60; H, 5.67; N, 8.07: Found C, 72.67; H, 5.64; N, 8.00.

10.1.52. HPT 328)



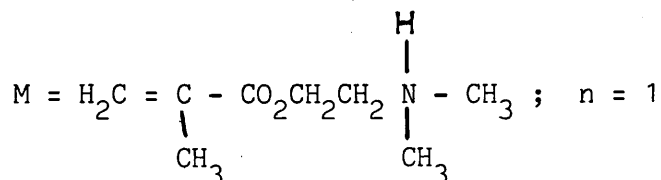
Procedure as for 10.1.42 using 1-ethyl-3-cyano-6-hydroxy-4-methyl pyrid-2-one (5.0 g, 0.028 mol), TMP (2.3 g, 0.014 mol) and n-methyl morpholine (1.43 g, 0.014 mol) in 50 ml ethanol. Reflux time = 17 hrs. Yield = 5.0 g (72%), (recryst. methanol (purple needles); m.p. = 271.0-272.0° (decomp); ¹H nmr δ(d⁶-DMSO, ppm) 2.83 (s) C²²H₃, 3.47 (m), 3.91 (m), C^{23,24,25,26}H₂, u.v./visible λ_{max} (H₂O) 589 (ε_{max}, 1.15 x 10⁵), 545 nm (sh, 3.4 x 10⁴ mol⁻¹ dm³ cm⁻¹); Calcd. for C₂₆H₃₁N₅O₅: C, 63.27; H, 6.33; N, 14.19: Found C, 63.29; H, 6.13; N, 14.03.

10.1.53 HPT (324)

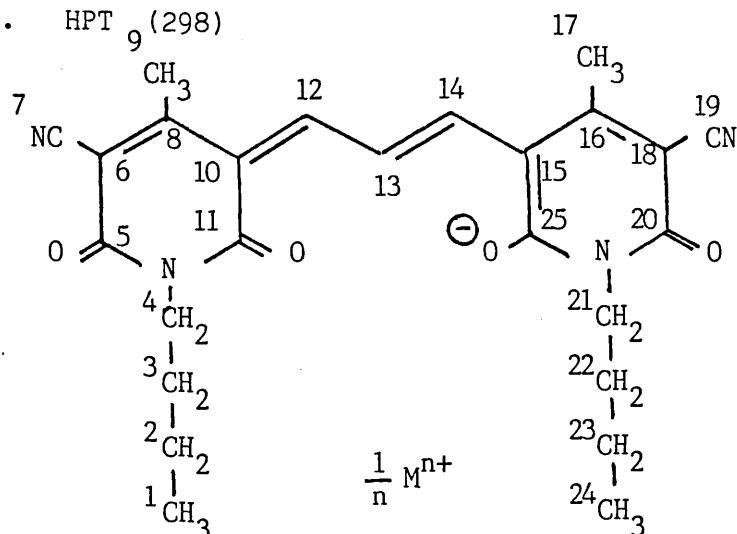


Procedure as for 10.1.42 using 1-ethyl-3-cyano-6-hydroxy-4-methyl pyrid-2-one (2.5 g, 0.014 mol), TMP (1.15 g, 0.007 mol) and N-(2,4-dinitrophenyl)-pyridinium chloride in 50 ml ethanol. Reflux time = 4½ hrs. Yield = 3.4 g (76%), (recryst. ethanol (green cubes); m.p. = 261.5° (decomp); ¹H nmr δ(d⁶-DMSO, ppm) 8.95 (m) C²²⁻²⁶H, C^{28,29,31}H; u.v./visible λ_{max} (H₂O) 589 (ε_{max} 9.49 x 10⁴ 547 nm (sh, 4.65 x 10⁴ mol⁻¹ dm³ cm⁻¹); Calcd. for C₃₂H₂₇N₇O₈; C, 60.28; H, 4.27; N, 15.38: Found C, 60.37; H, 4.54; N, 15.21.

10.1.54. HPT (314)



Procedure as for 10.142 using 1-ethyl-3-cyano-6-hydroxy-4-methyl pyrid-2-one (10.0g, 0.056 mol), TMP (4.6 g, 0.028 mol) and dimethyl-aminoethyl methacrylate (4.4 g, 0.028 mol) in 80 ml ethanol. Reaction time = kept at 60°C for 24 hrs. Yield = 5.8 g (38%), (recryst. ethanol (blue needles); m.p. = 216.0-217.0°; ¹H n.m.r.δ(d⁶-DMSO, ppm) 1.91 (s) C²⁷H₃; 2.90 (s) C²²H₃, 3.49 (m) C²⁵H₂, 4.42 (m) C²⁴H₂, 5.36 (s) NH, 5.75 (m) C²⁹H₂, 6.15 (m) C²⁹H₂; Calcd. for C₂₉H₃₅N₅O₆: C, 63.37; H, 6.42; N, 12.74: Found C, 62.97; H, 6.43; N, 12.54.

10.1.55. HPT₉ (298)

M = Na ; n = 1

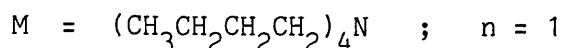
A mixture of 1-butyl-3-cyano-6-hydroxy-4-methyl pyrid-2-one (10.0 g, 0.049 mol), 1,1',3,3'-tetramethoxypropane (4.0 ml, 0.024 mol) and sodium acetate (2.0 g, 0.024 mol) was refluxed for 20 hrs in 50 ml ethanol. On cooling an olive green precipitate was obtained which after filtering off and drying weighed 9.24 g (82%) (recryst. EtOH (green cubes) (m.p. = 349.0-350.0°C; lit. m.p.¹⁷ = 349.0-350.0°C; ¹H nmr δ(d⁶-DMSO, ppm) 1.13 (m) C¹H₃, 1.62 (m) C^{2,3}H₂, 2.66 (s) C⁹H₃, 4.08 (m), C⁴H₂, 8.04 (d) C¹²H, 9.38 (t) C¹³H; ¹³C nmr δ(d⁶-DMSO, ppm). 13.58 (C¹,C²⁴), 18.40 (C⁹,C¹⁷), 19.76 (C²,C²³), 29.52 (C³,C²²), 38.49 (C⁴,C²¹), 92.08 (C⁸,C¹⁶), 110.22 (C¹⁰,C¹⁵), 117.63 (C⁷,C¹⁹), 120.82 (C¹³), 157.24 (C¹²,C¹⁴), 157.95 (C⁶,C¹⁸), 161.46, 161.92 (C⁵,C¹¹,C²⁰,C²⁵).

10.1.56. HPT (309)

M = Li ; n = 1

Procedure as for 10.1.55 using 1-butyl-3-cyano-6-hydroxy-4-methyl pyrid-2-one (10.0 g, 0.049 mol), TMP (4.0 ml, 0.024 mol) and lithium carbonate (0.90g, 0.012 mol) in 50 ml ethanol. Reflux time = 20 hrs. Yield 9.7 g (89%). (recryst. ethanol (green cubes); m.p.¹⁷ > 360°. lit. m.p. > 360° .

10.1.57. HPT (182)



Procedure as for 10.1.55 using 1-butyl-3-cyano-6-hydroxy-4-methyl pyrid-2-one (5.0 g, 0.024 mol), TMP (22.0 ml, 0.012 mol) and tetrabutylammonium bromide (3.9 g, 0.012 mol) in 50 ml ethanol. Reflux time = 7 hrs. Yield = 0.6 (7%) (recryst. ethanol (mauve powder); m.p. 178.0 - 180.0°; ¹H nmr δ(d⁶-DMSO, ppm) 1.00 (m) C²⁹H₃, 1.45 (m) C^{27,28}H₂, 3.43 (m) C²⁶H₂; Calcd. for C₄₁H₆₃N₅O₄: C, 71.36; H, 9.22; N, 10.15; Found C, 71.77; H, 8.89; N, 9.91.

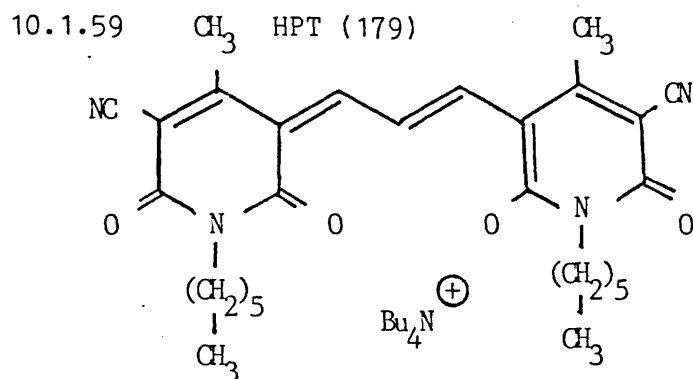
10.1.58 HPT (308)



Procedure as for 10.1.55 using 1-butyl-3-cyano-6-hydroxy-4-methyl pyrid-2-one (2.5 g, 0.012 mol), TMP (1.0 ml, 0.006 mol) and n-methyl morpholine (0.64 g, 0.006 mol) in 20 ml ethanol. Reflux time = 4 hrs. Yield = 0.6 g (19%). (recryst. ethanol (two crystal habits; dark blue needles (m.p. = 218.5-219.5°), green cubes (m.p. = 218.5-219.5°); ¹³C nmr δ(d⁶-DMSO, ppm) 42.52 (C²⁶), 52.60 (C²⁸, C²⁹), 63.33

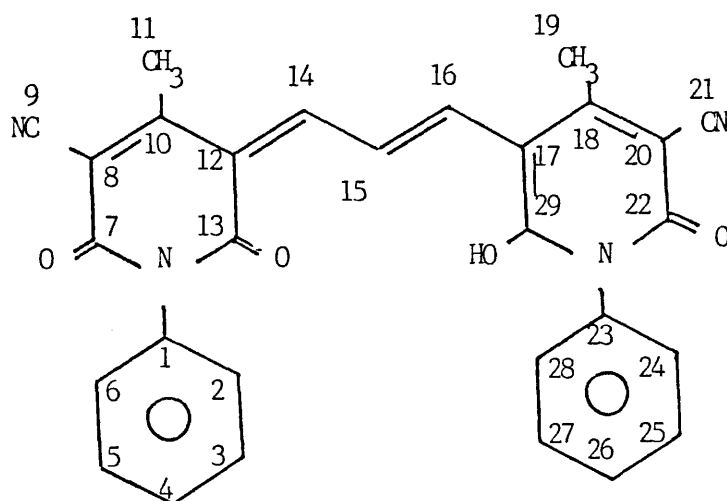
(C²⁷, C³⁰); u.v./visible λ_{\max} (EtOH) 602 (ϵ_{\max} , 1.68×10^5) 555 nm (sh, $4.07 \times 10^4 \text{ mol}^{-1} \text{ dm}^3 \text{ cm}^{-1}$). Calcd. for C₃₀H₃₆N₅O₅:

C, 65.55; H, 7.1; N, 12.74: Found C, 65.91; H, 7.20; N, 12.80.



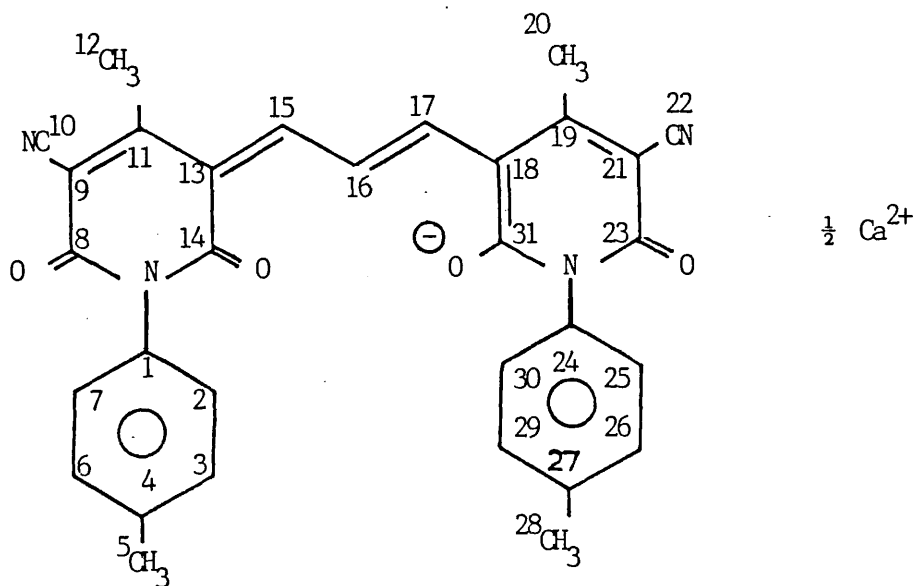
Supplied by Ilford Ltd. (λ_{\max} (H₂O) 596 nm (ϵ_{\max} , $1.74 \times 10^5 \text{ mol}^{-1} \text{ dm}^3 \text{ cm}^{-1}$)).

10.1.60 HPT (282)



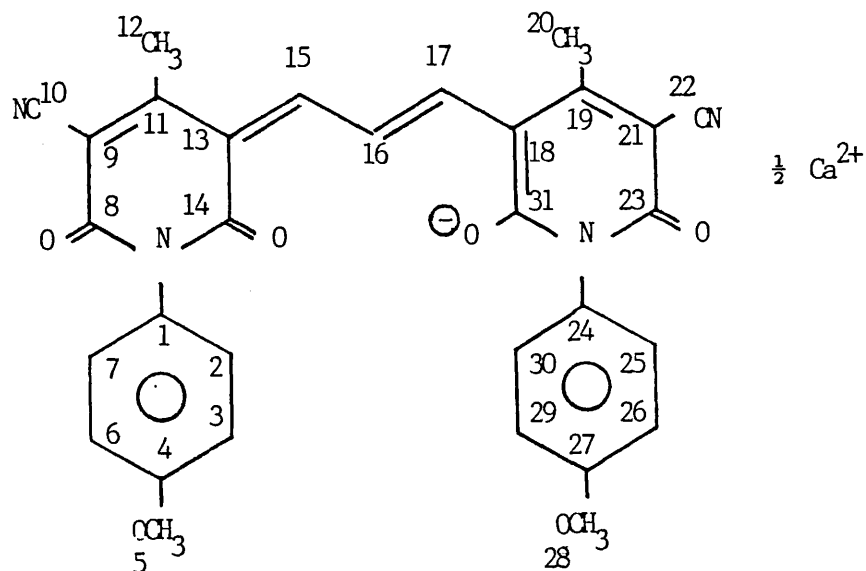
A mixture of 1-phenyl-3-cyano-6-hydroxy-4-methyl pyrid-2-one (2.5 g, 0.01 mol) and 1,1',3,3'- tetramethoxypropane (0.09 ml, 0.005 mol) in 20 ml acetic acid was refluxed for 1 hr. The product was precipitated out with ether, filtered and dried, yielding 0.6g (26%) (recryst. methanol, (dark purple powder). m.p. 261.0-263.0°; ^1H nmr $\delta(\text{d}^6\text{-DMSO})$ 1.92 (s) C^{11}H_3 , 7.39 (m) C^{14}H , Ph, 8.88 (t) C^{15}H ; ^{13}C nmr $\delta(\text{d}^6\text{-DMSO})$, ppm) 18.85, 21.00 ($\text{C}^{11}, \text{C}^{19}$), 92.60 ($\text{C}^{10}, \text{C}^{18}$), 110.80 ($\text{C}^{12}, \text{C}^{17}$), 117.63, 119.84 ($\text{C}^9, \text{C}^{21}$), 123.94 (C^{15}), 127.45, 128.49, 129.01, 130.12 (Ph), 136.04, 136.49 ($\text{C}^1, \text{C}^{23}$), 157.30, 159.19 ($\text{C}^{14}, \text{C}^{16}$), 161.72, 162.37 ($\text{C}^8, \text{C}^{20}$), 164.24, 165.82, 169.59, 172.00 ($\text{C}^7, \text{C}^{13}, \text{C}^{22}, \text{C}^{29}$); i.r. 3070 (O-H), 2220 ($\text{C}\equiv\text{N}$), 1660 ($\text{C}=\text{O}$) 1460 ($\text{C}=\text{C}$, Ph), 1350 ($\text{C}-\text{N}$) cm^{-1} ; u.v/visible λ_{max} (H_2O) 591 (ϵ_{max} , 3.56×10^4), 548 nm (sh, $1.12 \times 10^4 \text{ mol}^{-1} \text{ dm}^3 \text{ cm}^{-1}$); poor analysis.

10.1.61. HPT (330)



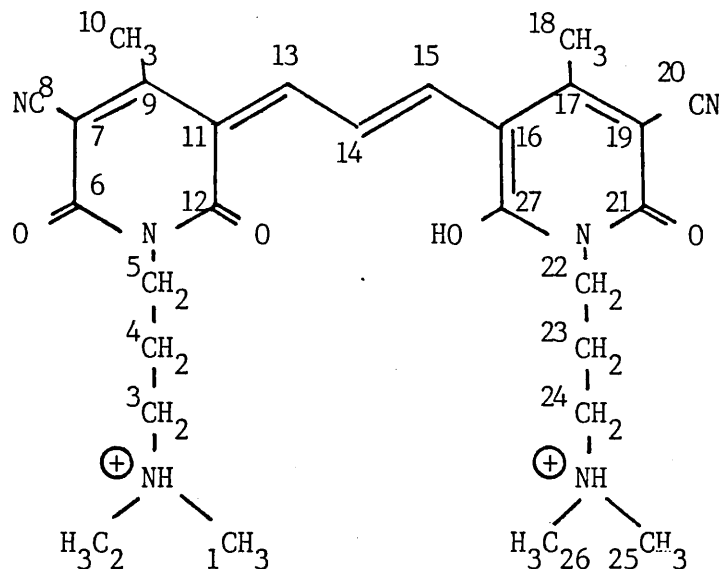
A mixture of 1-(p-tolyl)-3-cyano-6-hydroxy-4-methyl pyrid-2-one (1.0 g, 0.004 mol), 1,1',3,3'-tetramethoxypropane (0.34 g, 0.002 mol) and calcium hydroxide (0.08 g, 0.001 mol) in 20 ml 9:1 ethanol:acetic acid was refluxed for 1 hr. The product was precipitated out with diethyl ether, filtered and dried, yielding 0.7 g (65%) (recryst. methanol (pale blue precipitate), m.p. 317.0-320.0°; ^1H n.m.r. $\delta(\text{d}^6\text{-DMSO, ppm})$ 2.17 (s) C^{12}H_3 , 2.35 (s) C^5H_3 , 7.13 (m) Ar, 7.85 (d) C^{15}H , 8.80 (t) C^{16}H ; ^{13}C nmr $\delta(\text{d}^6\text{-DMSO, ppm})$ 18.79 ($\text{C}^{12}, \text{C}^{20}$), 20.61 ($\text{C}^5, \text{C}^{28}$), 94.10 ($\text{C}^{11}, \text{C}^{19}$), 110.67 ($\text{C}^{13}, \text{C}^{18}$), 118.53 ($\text{C}^{10}, \text{C}^{22}$), 120.81 (C^{16}), 128.23, 128.69, 129.14 (Ar), 133.43, 133.76 ($\text{C}^4, \text{C}^{27}$), 136.62, 137.01 ($\text{C}^1, \text{C}^{24}$), 157.24 ($\text{C}^{15}, \text{C}^{17}$), 158.99 ($\text{C}^9, \text{C}^{21}$), 161.66, 162.31 ($\text{C}^8, \text{C}^{14}, \text{C}^{23}, \text{C}^{31}$), i.r. 3080 (C-H), 3025 (C-H), 2210 ($\text{C}\equiv\text{N}$), 1650 (C=O), 1608 ($\text{C}=\text{C}$) cm^{-1} ; u.v./visible λ_{max} (EtOH) 605 (ϵ_{max} , 3.76×10^4), 560 nm (sh, $9.68 \times 10^3 \text{ mol}^{-1} \text{ dm}^3 \text{ cm}^{-1}$); poor analysis.

10.1.62. HPT (331)



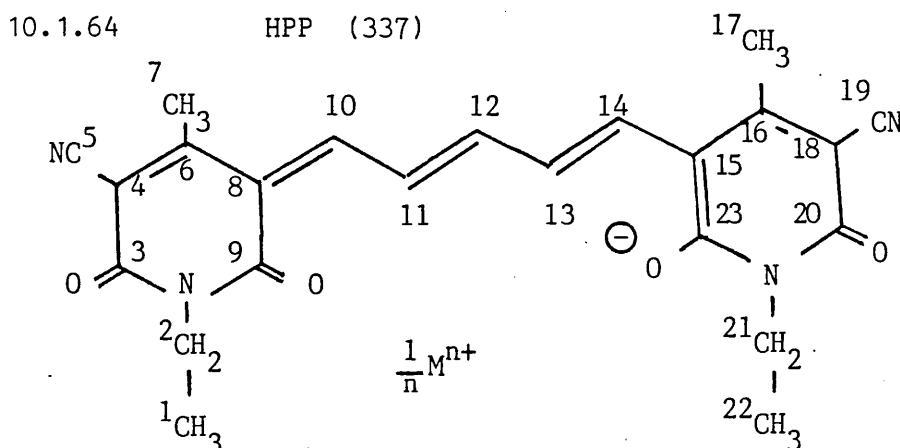
A mixture of 1-(p-anisyl)-3-cyano-6-hydroxy-4-methyl pyrid-2-one (1.0 g, 0.004 mol), 1,1',3,3'-tetramethoxypropane (0.32 ml, 0.002 mol) and calcium hydroxide (0.07, 0.001 mol) in 20 ml 9:1 ethanol:acetic acid was refluxed for 1 hr. The product was precipitated out with diethyl ether, filtered and dried yielding 0.7 g (60%) (recryst. methanol (pale blue powder); m.p. > 360.0°; ¹H nmr δ(d⁶-DMSO, ppm) 2.26 (s) C¹²H₃, 3.82 (s) OC⁵H₃, 7.02 (m) Ar, 7.85 (d) C¹⁵H, 8.90 (t) C¹⁶H; i.r. 3070 (C-H), 3025 (C-H), 2210 (C≡N) 1660 (C=O), 1608 (C=C) cm⁻¹; u.v./visible λ_{max} (EtOH) 605 (ε_{max}, 2.53 x 10⁴), 560 nm (sh, 6.53 x 10³ mol⁻¹dm³ cm⁻¹); poor analysis

10.1.63. HPT (325)



A mixture of 1-(dimethylaminopropyl)-3-cyano-6-hydroxy-4-methyl pyrid-2-one (2.5 g, 0.01 mol), 1,1',3,3'-tetramethoxypropane (0.9 g, 0.006 mol), hydroiodic acid (2.54 g, 0.02 mol) and iodine (2.87 g, 0.01 mol) was refluxed for 5 hrs in 50 ml ethanol. On cooling a dark green microcrystalline material precipitated out. After filtering and drying

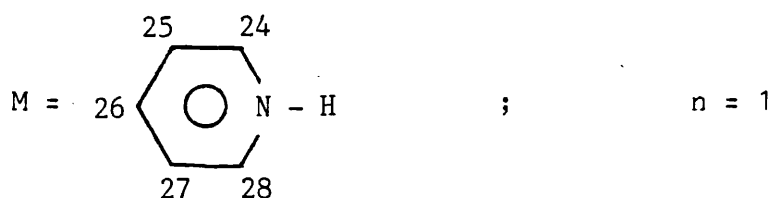
it weighed 3.95 g (52%) (recryst. ethanol (green cubes); m.p. 227.0-229.0° (decomp); ^1H n.m.r. δ (d^6 -DMSO, ppm) 1.44 (m) C^4H_2 , 1.90 (s) C^{10}H_3 , 2.27 (s) C^1H_3 , C^2H_3 , 2.35 (m) C^5H_2 , 3.40 (m) C^3H_2 , 3.49 (s) NH, 7.25 (d) C^{13}H 8.47 (t) C^{14}H ; ^{13}C nmr δ (d^6 -DMSO, ppm) 18.67 ($\text{C}^{10}, \text{C}^{18}$), 23.02 ($\text{C}^4, \text{C}^{23}$), 36.03 ($\text{C}^5, \text{C}^{22}$), 42.34 ($\text{C}^1, \text{C}^2, \text{C}^{25}, \text{C}^{26}$), 54.76 ($\text{C}^3, \text{C}^{24}$), 92.28 ($\text{C}^9, \text{C}^{17}$), 110.42 ($\text{C}^{11}, \text{C}^{16}$), 117.51 ($\text{C}^8, \text{C}^{20}$), 121.15 (C^{14}), 157.64 ($\text{C}^{13}, \text{C}^{15}$), 158.55 ($\text{C}^7, \text{C}^{19}$), 161.80, 162.25 ($\text{C}^6, \text{C}^{12}, \text{C}^{21}, \text{C}^{27}$); Found: C, 38.96; H, 5.19; N, 10.22, I, 39.02.



A mixture of 1-ethyl-3-cyano-6-hydroxy-4-methyl pyrid-2-one (3.0 g, 0.02 mol) and glutaconic dialdehyde dianil hydrochloride (2.4 g, 0.01 mol) ^{in 20ml acetic anhydride} was gently warmed (30-40°) with stirring until the solid starting materials had dissolved. Triethylamine (2.3 ml, 0.216 mol) was then added dropwise and the reaction mixture was heated to 95°C and maintained at this temperature for 30 mins. On cooling a dark green precipitate was

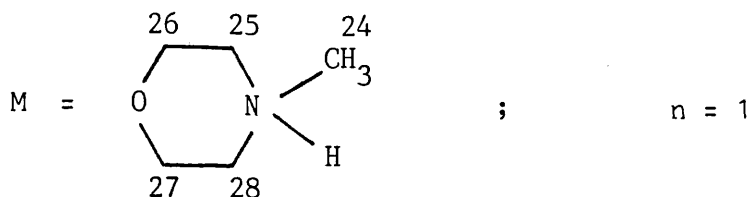
obtained. On filtering and drying it weighed 1.5 g (37%) (recryst. acetonitrile (metallic green microcrystalline); m.p. = 138.0-139.0°; ^1H nmr $\delta(\text{d}^6\text{-DMSO, ppm})$ 1.21 (m) C^1H_3 , C^{25}H_3 , 2.39 (s) C^7H_3 , 3.81 (m) C^2H_2 , C^{24}H_2 , 7.75 (m) $\text{C}^{10}, \text{C}^{11}\text{H}$, 8.92 (m) C^{12}H ; ^{13}C nmr $\delta(\text{d}^6\text{-DMSO, ppm})$ 8.51 (C^{25}), 12.93 ($\text{C}^1, \text{C}^{22}$), 18.46 ($\text{C}^7, \text{C}^{17}$), 33.74 ($\text{C}^2, \text{C}^{21}$), 45.90 (C^{24}), 91.88 ($\text{C}^6, \text{C}^{16}$), 110.41 ($\text{C}^8, \text{C}^{15}$), 117.63 ($\text{C}^5, \text{C}^{19}$), 123.50 (C^{12}) 146.13 ($\text{C}^{11}, \text{C}^{13}$), 156.92 ($\text{C}^{10}, \text{C}^{14}$), 157.89 ($\text{C}^4, \text{C}^{18}$), 161.21, 162.12 ($\text{C}^3, \text{C}^9, \text{C}^{20}, \text{C}^{23}$); u.v./visible λ_{max} (H_2O) 680 nm (ϵ_{max} , $8.42 \times 10^4 \text{ mol}^{-1} \text{ dm}^3 \text{ cm}^{-1}$); Calcd. for $\text{C}_{29}\text{H}_{37}\text{N}_5\text{O}_4$: C, 67.02; H, 7.19; N, 13.48: Found C, 66.70; H, 6.98; N, 13.38.

10.1.65. HPP (323)



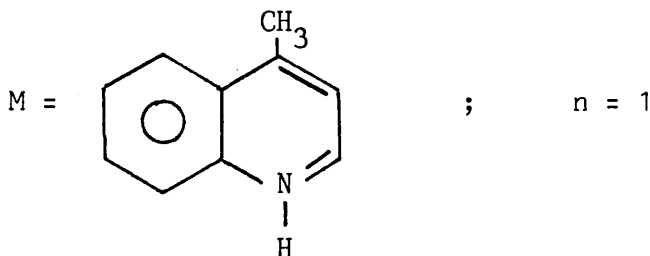
Procedure as for 10.1.64 however using pyridine (2.0 g, 0.025 mol) in place of triethylamine. Yield = 0.8 g (21%) (recryst. ethanol (green powder); m.p. 209.0-211.0°; ^{13}C nmr $\delta(\text{d}^6\text{-DMSO, ppm})$ 127.01 (C^{25}), 142.03 (C^{26}), 150.61 (C^{24}); u.v./visible λ_{max} (H_2O) 682 (ϵ_{max} , 1.04×10^5 , 605 nm (sh, $4.46 \times 10^3 \text{ mol}^{-1} \text{ dm}^3 \text{ cm}^{-1}$); Calcd. for $\text{C}_{28}\text{H}_{27}\text{N}_5\text{O}_4$: C, 67.59; H, 5.48; N, 14.08: Found C, 67.60; H, 5.48; N, 14.06.

10.1.66. HPP (322)



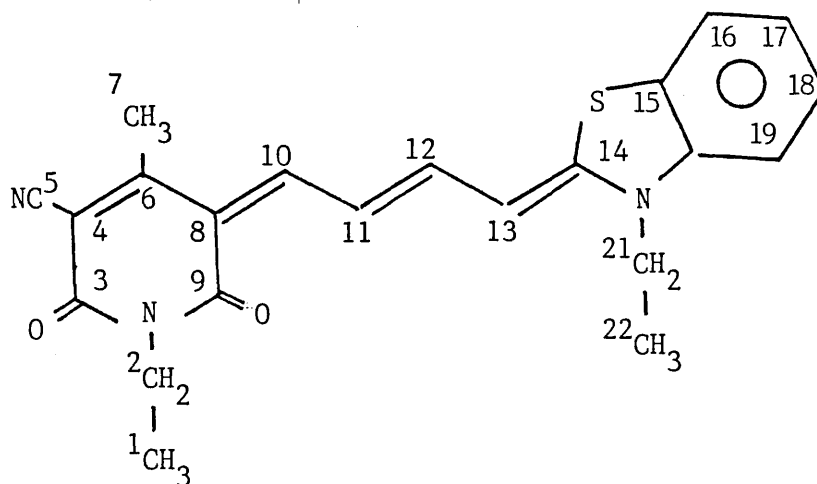
Procedure as for 10.1.64 however replacing the triethylamine with N-methylmorpholine (2.8 ml, 0.025 mol). Yield = 2.85 g (70%) (recryst. methanol (metallic green cubes); m.p. = 205.0-208.0°; ¹³C nmr δ(d⁶-DMSO, ppm) 42.42 (C²⁴), 53.00 (C²⁶), 63.31 (C²⁵); u.v./visible λ_{max}(H₂O) 679 nm ε_{max}, 7.81 x 10⁴ mol⁻¹dm³cm⁻¹); Calcd. for C₂₈H₃₃N₅O₅: C, 64.71; H, 6.41; N, 13.48; Found C, 64.37; H, 6.39; N, 13.17.

10.1.67. HPP (321)

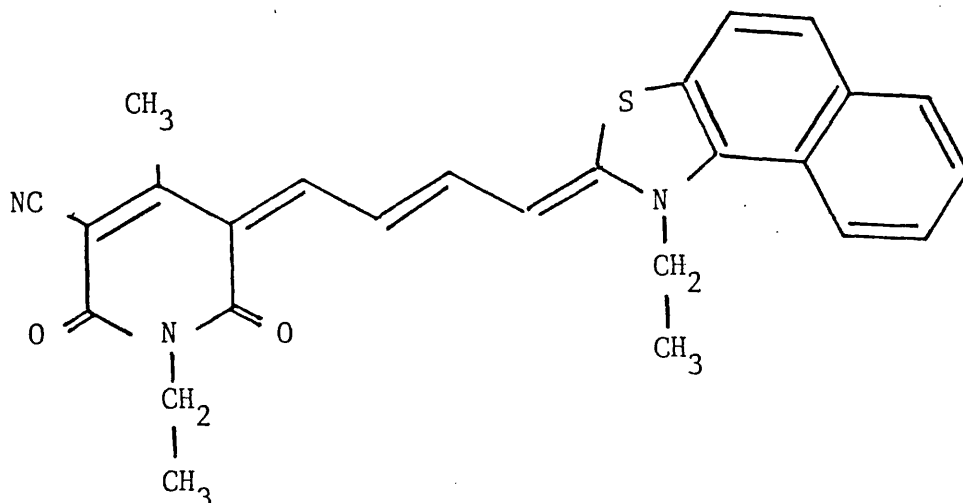


Procedure as for 10.1.64 however replacing the triethylamine with lepidine (3.3 ml, 0.025 mol). Yield = 2.1 g (48%) (recryst. methanol (dark green powder); m.p. = 211.0-212.0° (decomp); u.v./visible λ_{max} (EtOH) 678 (ε_{max}, 1.33 x 10⁵) 630 nm (sh, 2.50 x 10⁴ mol⁻¹dm³cm Calcd. for C₃₃H₃₁N₅O₄: C, 70.57; H, 5.57; N, 12.47; Found: C, 70.77; H, 5.49; N, 12.51.

10.1.68. HPT (320)



A mixture of 3-(3'-acetanilidoallylidene)-1-ethyl-4-methyl-5-cyanopyrid-2,6-dione (2.5 g, 0.007 mol), 1-ethyl-2-methylbenzothiazolium iodide (2.2 g, 0.007 mol) and triethylamine (1.0 ml, 0.007 mol) in 9.0 ml pyridine was heated to 100° and was maintained at this temperature for 30 mins. After cooling, filtering and drying the green precipitate weighed 1.6 g (58%) (recryst. acetonitrile (green cubes); m.p. = 193.0-194.5° (decomp); ¹H nmr δ(d⁶-DMSO, ppm) 1.22 (m) C¹H₃, C²²H₃, 2.39 (s) C⁷H₃; 3.47 (m) C²H₂, 4.15 (m) C²¹H₂, 6.79 (d) C¹⁰H, 7.49 (m) C¹⁶⁻¹⁹H, C¹³H, 7.89 (m) C¹¹H, C¹²H; ¹³C nmr δ(d⁶-DMSO, ppm) 12.41 (C²²), 12.93 (C¹), 18.91 (C⁷), 34.52 (C²), 36.73 (C²¹), 92.87 (C⁶), 112.75 (C⁸), 117.24 (C⁵), 122.64 (C¹¹, C¹²), 124.46 (C¹⁶⁻¹⁹), 125.05 (C¹¹, C¹²), 127.58, 128.04, 129.34 (C¹⁶⁻¹⁹), 138.31 (C¹⁵), 140.52 (C²⁰), 149.95 (C¹³), 157.52 (C⁴), 161.07, 162.49 (C³, C⁹); uv/visible λ_{max} (H₂O) 646 nm (ε_{max}, 4.53 x 10⁴ mol⁻¹ dm³ cm⁻¹: Calcd for C₂₂H₂₁N₃O₂S: C, 67.49; H, 5.42; N, 10.74: Found C, 66.76; H, 6.02; N, 11.01.



A mixture of 3-(3'-acetanilidoallylidene)-1-ethyl-4-methyl-5-cyanopyrid-2,6-dione (1.0 g, 0.003 mol), 1-ethyl-2-methyl- β -naphthothiazolium tosylate (1.2 g, 0.003 mol) and triethylamine (0.5 g, 0.004 mol) in 5.0 ml pyridine was heated to 100 ° and maintained at this temperature for 30 mins. After cooling, filtering and drying the precipitate weighed 0.54 g (41%) (recryst. acetonitrile (dark purple powder) m.p. = 181.0-183.0° (decomp); u.v./visible λ_{\max} (H₂O) 665 nm (ϵ_{\max} , $8.27 \times 10^3 \text{ mol}^{-1} \text{ dm}^3 \text{ cm}^{-1}$); poor analysis.

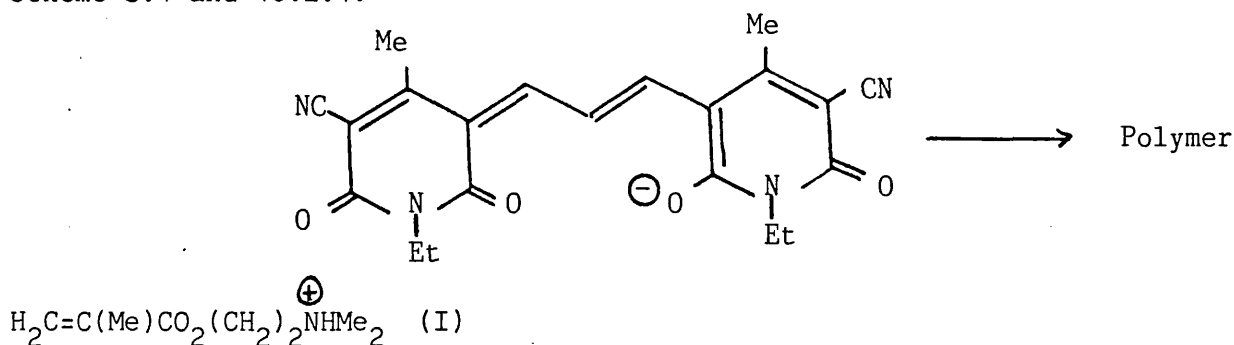
10.2. Polymeric Dye Systems as Bleachable Antihalation Underlayers

10.2.1. Instrumentation

A 35 ml dilatometer, a high pressure mercury photolysis lamp, Bruker WM-250 MHz and WH-400 MHz n.m.r. spectrometers and a Perkin-Elmer 550S u.v./visible spectrophotometer.

10.2.2. Chain-growth polymerisation : hydroxypyridone oxonol salts of polymerisable cation.

The following attempts were made to polymerise the oxonol dye (I), scheme 3.1 and 10.2.1.



Scheme 10.2.1.

- a) Dye (I) (0.3 g, 0.55 mmol) and 4,4'-azobis(4-cyanopentanoic acid) (ABCPA) (1.6 mg, 0.003 mmol) in 3 ml water were heated to 60° under nitrogen overnight.
- b) Dye (I) (2.0 g, 3.6 mmol) and azobisisobutyronitrile (AIBN) (3.0 mg, 0.021 mmol) in 10.0 g absolute ethanol was heated at 60°, under nitrogen overnight.
- c) Dye (I) (0.5 g, 0.9 mmol) and AIBN (1.5 mg, 0.01 mmol) in 5.0 g dimethylformamide, DMF, was heated at 60°, under nitrogen, overnight.

d) Dye (I) (2.0 g, 3.6 mmol) and AIBN (3.0 mg, 0.02 mmol) in 10.0 g DMF was heated at 60°, under nitrogen, overnight.

e) Dye (I) (0.3 g, 0.55 mmol) heated at 160°, for 8 hours.

f) Dye (I) (0.3 g, 0.55 mmol) exposed to ultra-violet light

($\lambda = 207 \text{ nm}$) over a weekend.

In each case ^1H nmr analyses revealed that no polymerisation had taken place.

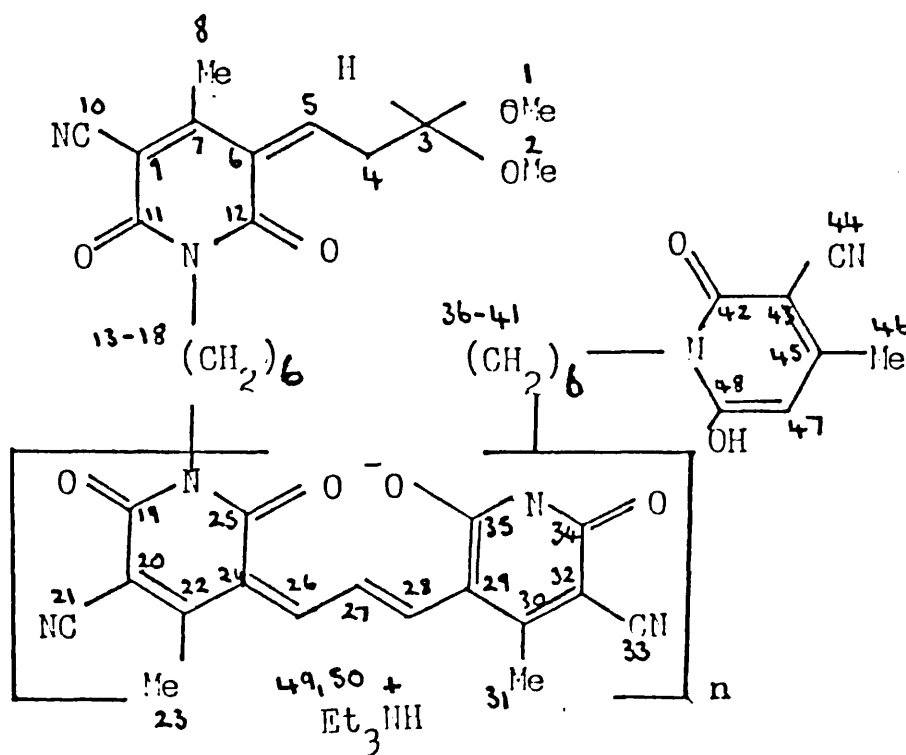
Dilatometric measurements were then undertaken to establish whether or not dye (I) was an inhibitor to free-radical polymerisation^{23,24}. A stock solution of pre-distilled (38°, 79 mmHg) methyl methacrylate (70.0 g, 0.7 mol) and AIBN (0.2 g, 1.2 mmol) in 200 g methyl ethyl ketone was prepared. A portion of this stock solution (35 ml) was placed in a dilatometer which itself was placed in a water bath at 60°. The contraction in volume over a period of 1 hr was recorded. To a second portion of the stock solution (135 g) was added dye (I) (0.1 g, 0.2 mmol) and 35 ml of this solution was placed in a dilatometer, in a water bath at 60°, and the contraction in volume measured over the same time period. The results are shown in figure 3.3, Chapter 3.

10.2.3. Step-growth polymerisation

N,N'-Hexamethylene-bis-(3-cyano-6-hydroxy-4-methyl pyrid-2-one) (20.0 g, 0.05 mol) was dissolved in 50.0 g DMF to yield a 40% w/w solution. 1,1',3,3'-Tetramethoxypropane (8.6 g, 0.05 mol) and

triethylamine (6.8 g, 0.06 mol) were then added and the mixture heated at 130° for 48 hrs. Aliquots (5.0 ml) were taken from the reaction mixture every 4 hrs. These aliquots were diluted to 10 ml with DMF and were individually added dropwise to a vigorously stirred ethyl acetate (750 ml) solution. The precipitates were filtered off and dried.

Each of the samples was then characterised using ^1H nmr and uv/visible spectroscopy. Table 10.2.1 shows the assignment of the ^1H nmr spectrum for the 4 hour aliquot (III, $x = 6$, $M = \text{Et}_3\text{NH}$, $m = 1$, scheme 3.3).



III

Table 10.2.1

$\delta(d^6\text{-DMSO, ppm})$	Assignment
1.19 (t)	$C^{49}H_3$
1.30 (s, broad) }	$C^{13-18}H_2, C^{36-41}H_2$
1.47 (s, broad) }	
2.00 (s)	Unreacted hydroxypyridone
2.44 (s)	$C^{23,31}H_3$
2.51 (s)	$C^{46}H_3$
3.10 (s)	Unreacted TMP
3.26 (s)	$C^{1,2}H_3$
3.60 (s, broad) }	$C^{13-18}H_2, C^{36-41}H_2$
3.80 (s, broad) }	
4.35 (m)	C^4H_2
5.11 (s)	$C^{47}H$
5.43 (t)	C^3H
6.97 (t)	C^5H
7.76 (d)	$C^{26,27}H$
8.43 (s)	$C^{48}\text{-OH}$
9.28 (t)	$C^{27}H$

The peaks selected for molecular weight distribution analyses ("end-group" analyses) were those at 7.7 (repeating unit) and 5.4 ppm (end-group). The ratio of their relative integrals for each of the aliquots is shown in table 3.1, Chapter 3. The uv/visible spectra of each of the aliquots (1 mg in 100 ml H₂O) are represented in figure 3.4, Chapter 3.

The most promising material was that formed after 4 hrs. Gelatin coatings containing this material were made up on triacetate base. That is, this sample (80 mg) was dissolved in 10 ml water. A portion of this solution (0.5 ml) was then added to a solution of 10% DIB gelatin (3.0 ml) and 1% saponin (surfactant) (1.0 ml) which was made up to 10 ml with water. This mixture was then coated on to triacetate base¹⁷. The coating then underwent a number of standard evaluation tests¹⁷.

i) Substantivity; the visible spectrum of the coating is recorded, it is then immersed in water for 30 mins after which time the spectrum is re-recorded. The dye was 88.7% substantive.

ii) Bleachability; again the visible spectrum of the coating is recorded before and after, (a) being immersed in a 0.5 M Na₂SO₃ solution for 2 mins. The dye was 100% bleachable; and (b) being immersed in a solution of ID11 (standard Ilford developer) for 2 mins. Here dye was 97.8% bleachable.

The results of these tests are illustrated in figure 3.5, Chapter 3.

10.3. The Bleaching Reaction

The dye chosen for the investigation was HPT261, figure 10.3.1.

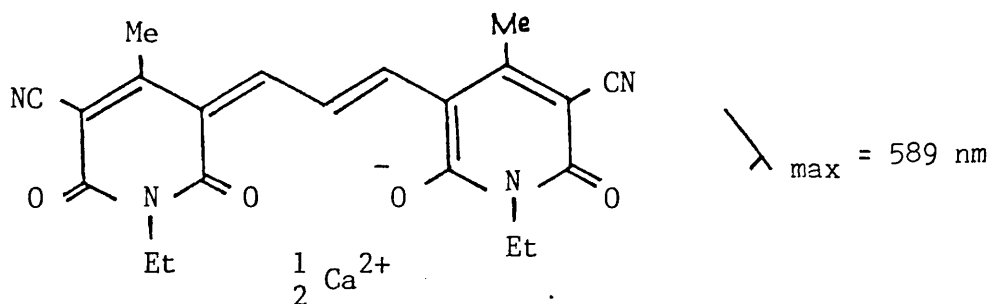


Figure 10.3.1.

10.3.1. Instrumentation.

Bruker WM-250 MHz and WH-400 MHz n.m.r. spectrometers, a Jeol FX-90Q n.m.r. spectrometer and a Varian SuperScan 3 u.v./visible spectrophotometer.

10.3.2. Kinetic studies of sulphite bleaching.

Two standard solutions were prepared, a 10^{-6} M aqueous solution of HPT 261 and a 10^{-2} M aqueous solution of sodium sulphite. 15 ml Aliquots of the standard dye solution were pipetted into a 16 ml quartz cell and varying amounts of the standard sulphite solution ranging from 0.05 - 0.4 ml were added, in each case the contents of the cell being made up to 16 ml with water. The change in absorbance with time on the addition of the sulphite solution was then measured. The results thus obtained are shown in section 4.2.1, Chapter 4.

The effect of pH on the rate of sulphite bleaching was also investigated. A citric acid/sodium hydroxide buffer was used,⁹⁴ thus for:

a) pH = 2.1, 1.4 g citric acid was dissolved in 100 ml 10^{-6} M standard dye solution (0.06 M citric acid); 6 ml of this solution was then made up to 16 ml in the cell with 10 ml 10^{-2} M standard sulphite solution.

b) pH = 3.2, 1.4 g citric acid was dissolved in 80 ml 10^{-6} M dye solution and was made up to 100 ml with 20 ml 0.2 M sodium hydroxide solution; 6 ml of this solution was then made up to 16 ml with 10 ml 10^{-2} M sulphite solution.

c) pH = 4.1, 1.4 g citric acid was dissolved in 60/40 ml solution of 10^{-6} M dye/0.2 M sodium hydroxide solution. 6 ml of this solution was then diluted to 16ml with 10 ml 10^{-2} M sulphite solution. Absorbance vs time plots and the pseudo-first order rate constants, thus obtained, for each of the pH values, can be seen in table 4.4. and figure 4.4., Chapter 4.

10.3.3. Qualitative studies

All studies were carried out in 0.2 mmol dimethyl sulphoxide solutions of HPT 261 with the addition of 4 molar excess of the bleaching agent. Where necessary a few drops of water were added to aid in solubilising the bleachant. The potential bleaching reagents investigated were potassium cyanide, sodium methoxide, sodium sulphide, ammonia, triethylamine, sodium hydroxide, potassium thiol, ethylamine, sodium azide, aniline, potassium thiocyanate, triphenylphosphine, sodium

thiosulphate and of course sodium sulphite. To test for reversibility of the reaction, molar equivalents of hydrochloric acid to bleachant were added. Excess acid resulted in protonation of the dye species.

10.3.4. NMR studies

0.2 mmol Solutions of HPT 261 were made up in either 50/50 D_2O/d^6 -DMSO (NH_3 , CN^- , S^{2-}), 50/50 d^4 -MeOH/ d^6 -DMSO (CD_3O^-) or d^6 -DMSO ($EtNH_2$), 4 Molar excesses of the nucleophiles were again used.

10.3.5. Trapping a bleached adduct

HPT 298 (2.0 g, 4.2 mmol) (II, scheme 4.4) and o-phenylene-diamine (2.3 g, 0.02 mol) were refluxed in absolute ethanol (50 ml) for 2 hrs. A pale blue solid had precipitated almost immediately on refluxing. This solid was filtered off from the hot ethanolic solution (1.3 g (55%); m.p. $312.0 - 314.0^\circ$ (decomp) calcd for $C_{33}H_{33}N_6O_4$: C, 67.25; H, 6.01; N, 15.18; found C, 67.63, H, 6.19, N, 15.47). This materials insolubility in all of the common solvents made both recrystallisation and solution nmr spectroscopy studies impossible. The accurate top mass obtained from mass spectrometry was 544. Solid state ^{13}C nmr spectra of both the dye HPT 298 and its o-phenylenediamine bleached adduct were recorded.

10.4. Structural Studies in the Solid State

10.4.1. X-ray crystal structure analyses

10.4.1.1. Instrumentation

The radiation used was either Ni-filtered copper K_{α} radiation or Zr-filtered molybdenum K_{α} radiation. The diffractometer used was a CAD4-F instrument (ENRAF NONIUS DELFT) controlled by a PDP8-A mini-computer. All subsequent computational work was done on either an ICL 298 computer or an ICL 1906A machine using the "Crystals" series of programmes^{95,96,97,98}.

10.4.1.2. The structure of tetraphenylphosphonium 1-ethyl-3-cyano-6-hydroxy-4-methyl pyrid-2-one trimethine oxonol.

Crystal data - $C_{45}H_{39}N_4O_4P$, Monoclinic, $M_w = 730$, $a = 12.634(6)$, $b = 11.802(0)$, $c = 12.875(9)$ Å, $\beta = 95.69(3)^{\circ}$, $U = 1909.1$ Å³, $D_m = 1.3$ gcm⁻³, $D_c = 1.3$ gcm⁻³ for $z = 4$, $C_u K_{\alpha}$ radiation, $\lambda = 1.5418$ Å, Space group P2/c.

A selected crystal (octahedra with a gold metallic lustre) was mounted on an Enraf-Nonius CAD-4F diffractometer. The orientation routine and unit cell parameters were optimised by a least squares refinement using the angular coordinates of 25 reflections. An inspection of the intensities of reflections from the three zero-level zones (hk0, h0l, 0kl) revealed systematic absences consistent with the space group P2/c. Automatic data collection was implemented in the range $0 < \theta < 75^{\circ}$. The angular coordinates of three reflections and the intensities of a further three were monitored throughout data collection to provide a check on variation in crystal orientation and intensity. In all, 5478 distinct reflections were measured with a net intensity greater

than zero. Lorentz and polarisation corrections were applied and the data merged to give 2679 independent structure amplitudes with $I > 3 \sigma(I)$, where I is the final observed intensity and $\sigma(I)$ the standard deviation derived from counting statistics. The structure was solved by direct methods using MULTAN. Full matrix least-squares techniques were employed for the refinement. Hydrogen atoms were found from an electron density difference Fourier synthesis. In the final refinement the coordinates and anisotropic temperature factors of the carbon, oxygen, nitrogen and phosphorus atoms were refined with the coordinates and isotropic temperature factors of the hydrogen atoms. A three-term Chebyshev series was used as a weighting scheme. A final R-value of 6.1% was reached. The atom coordinates anisotropic temperature factors, bond lengths and bond angles are listed in Chapter 6. The hydrogen atom isotropic temperature factors and the structure factors are listed in appendix 1B.

10.4.1.3. The structure of tetrabutylammonium 1-ethyl-3-cyano-6-hydroxy-4-methyl pyrid-2-one trimethine oxonol.

Crystal data - $C_{37}H_{55}N_5O_4$, Monoclinic, $M_w = 633$, $a = 8.399(5)$, $b = 10.445(5)$, $c = 21.265(7)$ Å, $\beta = 83.34(2)$ U = 1853.2 Å³, $D_m = 1.3$ gcm⁻³, $D_c = 1.3$ gcm⁻³ for $z = 4$, Cu - K $_{\alpha}$ radiation, $\lambda = 1.5418$ Å, Space group P2/n.

A selected crystal (needles with a metallic green reflex) was mounted on the diffractometer. The orientation matrix and unit cell parameters were optimised by a least squares refinement using the angular coordinates of 25 reflections, as before. The systematic absences observed were consistent with the space group P2/n. 4723 reflections

with a net intensity greater than zero were measured in the range $0 < \theta < 70^\circ$. The data was merged to give 1677 independent reflections having $I > 3 \sigma(I)$. The structure was solved by direct methods. The hydrogen atoms were placed geometrically. In the final refinement, the coordinates and anisotropic temperature factors of the carbon, nitrogen and oxygen atoms were refined with the fixed coordinates and isotropic temperature factors of the hydrogen atoms. A three-term Chebyshev series was used as a weighting scheme. A final R-value of 8.3% was reached. The atom coordinates, anisotropic temperature factors, bond lengths and bond angles are listed in Chapter 6. The structure factors are listed in Appendix 1B.

10.4.1.4. The structure of dimethylammonium ethyl methacrylate
1-ethyl-3-cyano-6-hydroxy-4-methyl pyrid-2-one
trimethine oxonol.

Crystal data - $C_{29}H_{35}N_5O_6$, Monoclinic, $M_w = 549$, $a = 31.313(5)$, $b = 7.436(3)$, $c = 25.495(4)$, $\beta = 100.63(7)^\circ$
 $U = 5834.7 \text{ \AA}^3$, $D_m = 1.3 \text{ gcm}^{-3}$, $D_c = 1.3 \text{ gcm}^{-3}$ for $z = 8$,
Cu - K_α radiation, $\lambda = 1.5418 \text{ \AA}$, Space group C2/c.

A selected crystal (dark blue needles) was mounted on the diffractometer. The systematic absences observed were consistent with the space group C2/c. 4141 reflections with a net intensity greater than zero were measured in the range $0 < \theta < 45^\circ$. The data was merged to give 1065 independent reflections having $I > 3 \sigma(I)$. The structure was solved by direct methods. The hydrogen atoms were placed geometrically. In the final refinement, the coordinates and anisotropic temperature factors of the carbon, nitrogen and oxygen atoms were refined with the

fixed coordinates and isotropic temperature factors of the hydrogen atoms. A three-term Chebyshev series was used as a weighting scheme. A final R-value of 6.5% was obtained. The atom coordinates, anisotropic temperature factors, bond lengths and bond angles are listed in Chapter 6. The structure factors are listed in Appendix 1B.

10.4.1.5. N-Methyl morpholinium 1-butyl-3-cyano-6-hydroxy-4-methyl pyrid-2-one trimethine oxonol.

On recrystallisation from ethanol two crsytalline forms of this dye were obtained, a needle-like form (which crystallised out after a few hours) and a cuboid form (which crystallised after a few days), the needles being dark blue in colour and the cubes having a bright green metallic lustre.

An attempt was made to collect a data set on the cuboid form. However, preliminary photographs taken on the CAD4-F diffractometer revealed a diffraction pattern very similar to that one might observe for a powder, figure 10.4.1. This suggested a high degree of disorder at the data collection temperature (room temperature). Obtaining a solution would have been impossible from this standard of data.

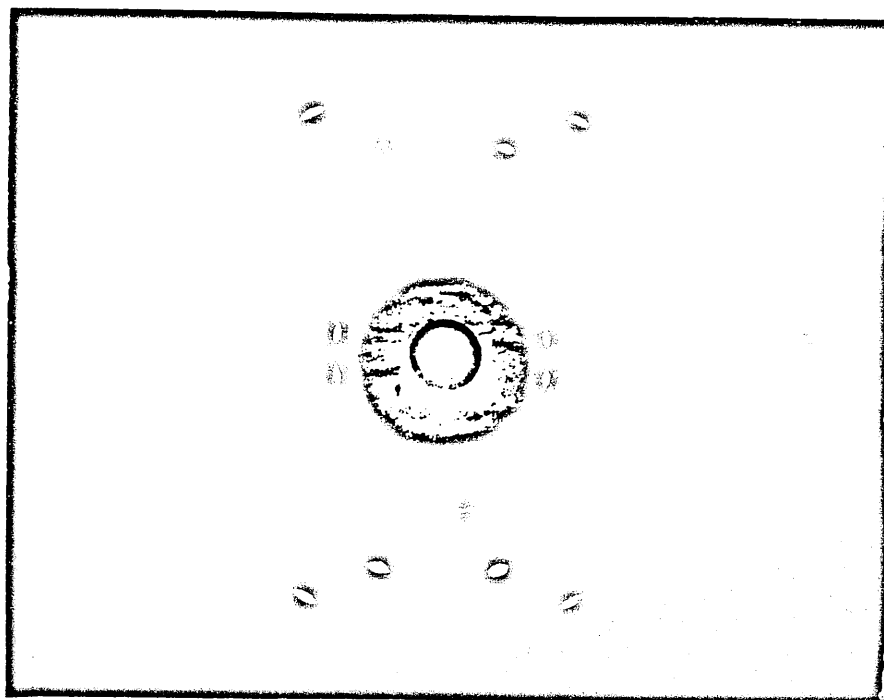


Figure 10.4.1

10.4.1.6. Methyl triphenylphosphonium 1-ethyl-3-cyano-6-hydroxy-4-methyl pyrid-2-one trimethine oxonol.

An attempt to collect a data set on the blue needles of this key material was undertaken. The small size of the crystal led to very few high intensity spots in the diffraction pattern, figure 10.4.2.

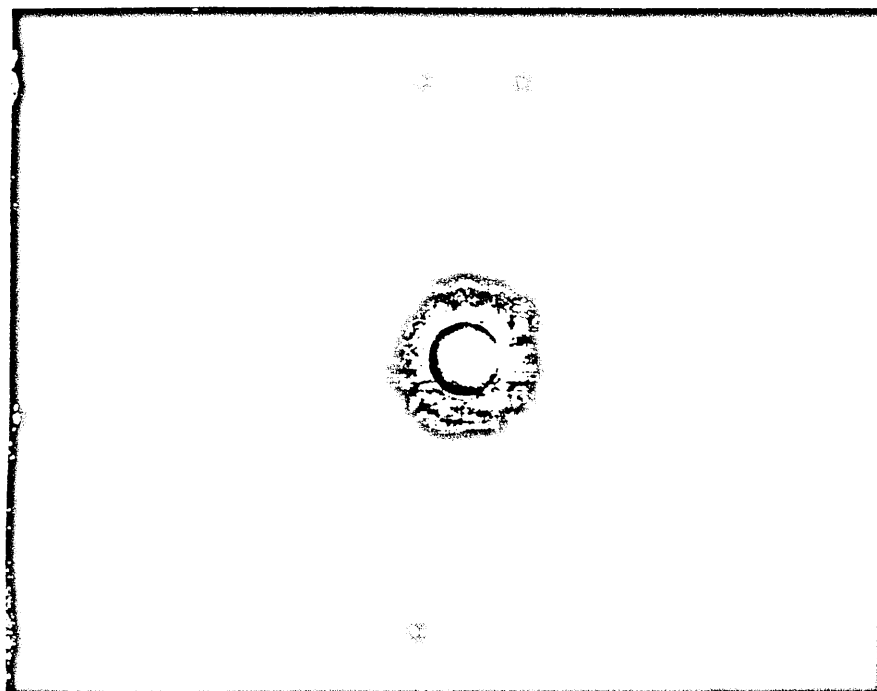


Figure 10.4.2

Obtaining a satisfactory solution from so few strong reflections would have been practically impossible.

10.4.2. Solid state nmr spectroscopic studies

The high resolution ^{13}C nmr experiments were performed on Bruker CXP 200 and 300 spectrometers. High-power proton decoupling was used to eliminate ^{13}CH dipolar broadening along with high-speed "magic angle" spinning in a Delrin rotor to eliminate broadening from the carbon chemical shift anisotropy. In addition, matched spin-lock cross-polarisation was used to enhance the sensitivity.

10.5. Electrochemical Investigations: The Design of a Radical Cation-Dye Complex

10.5.1. Instrumentation

Varian E4 EPR spectrometer. Figure 10.5.1 shows a circuit diagram of the CV set up used (where AE = auxiliary electrode (platinum), RE = reference electrode (S.C.E.), WE = working electrode (platinum) and X and Y are the terminals of the XY-plotter (JJ Instruments, PL51). The potentiostat used was a Thompson Associates ministat and the ramp generator a Thompson Associates "16 bit" ramp generator (Model DRG 16).

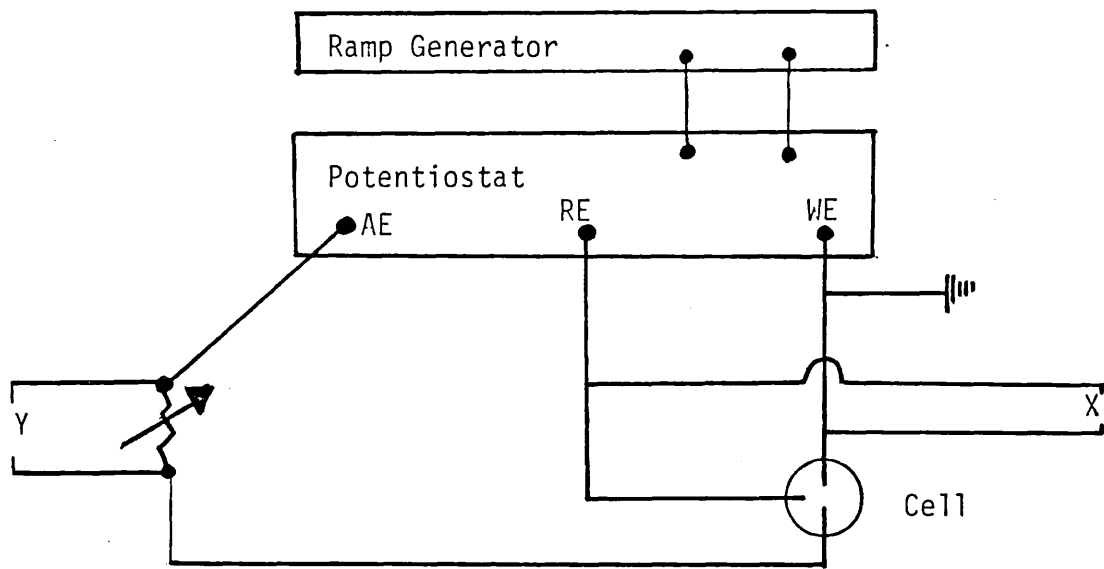


Figure 10.5.1

10.5.2. Experimental

For all CV samples 1.0 mmol solutions were made up in acetonitrile with 10.0 mmol tetrabutylammonium perchlorate as supporting electrolyte. The voltage was scanned between -2.0 and 2.0 V at a rate of 1000 mV/s. A saturated calomel electrode was used as a reference. Platinum electrodes were used for both auxiliary and working electrodes.

10.5.3. The preparation of the TTF-oxonol dye complex.

The complex was prepared by the electrolysis (2mA, 4 hr, Pt electrodes) of tetrabutylammonium 1-ethyl-3-cyano-6-hydroxy-4-methylpyrid-2-one trimethine oxonol (0.32 g, 5.0×10^{-4} mol) and tetrathiafulvalene (0.10 g, 5.0×10^{-4} mol) in acetonitrile (100 ml) and tetrabutylammonium perchlorate (1.5 g, 4.4×10^{-3} mol). The black crystalline material formed at the anode (m.p. = 230.0° (decomp.); uv/visible, λ_{\max} (EtOH) 597 (ϵ_{\max} , 4.72×10^4), 552 nm (sh, $1.16 \times 10^4 \text{ mol}^{-1} \text{ dm}^3 \text{ cm}^{-1}$); Calcd. for $\text{C}_{27}\text{H}_{23}\text{O}_4\text{N}_4\text{S}_2$: C, 54.43; H, 3.90; N, 9.41; S, 21.53: Found: C, 54.61; H, 4.00; N, 9.44; S, 21.73).

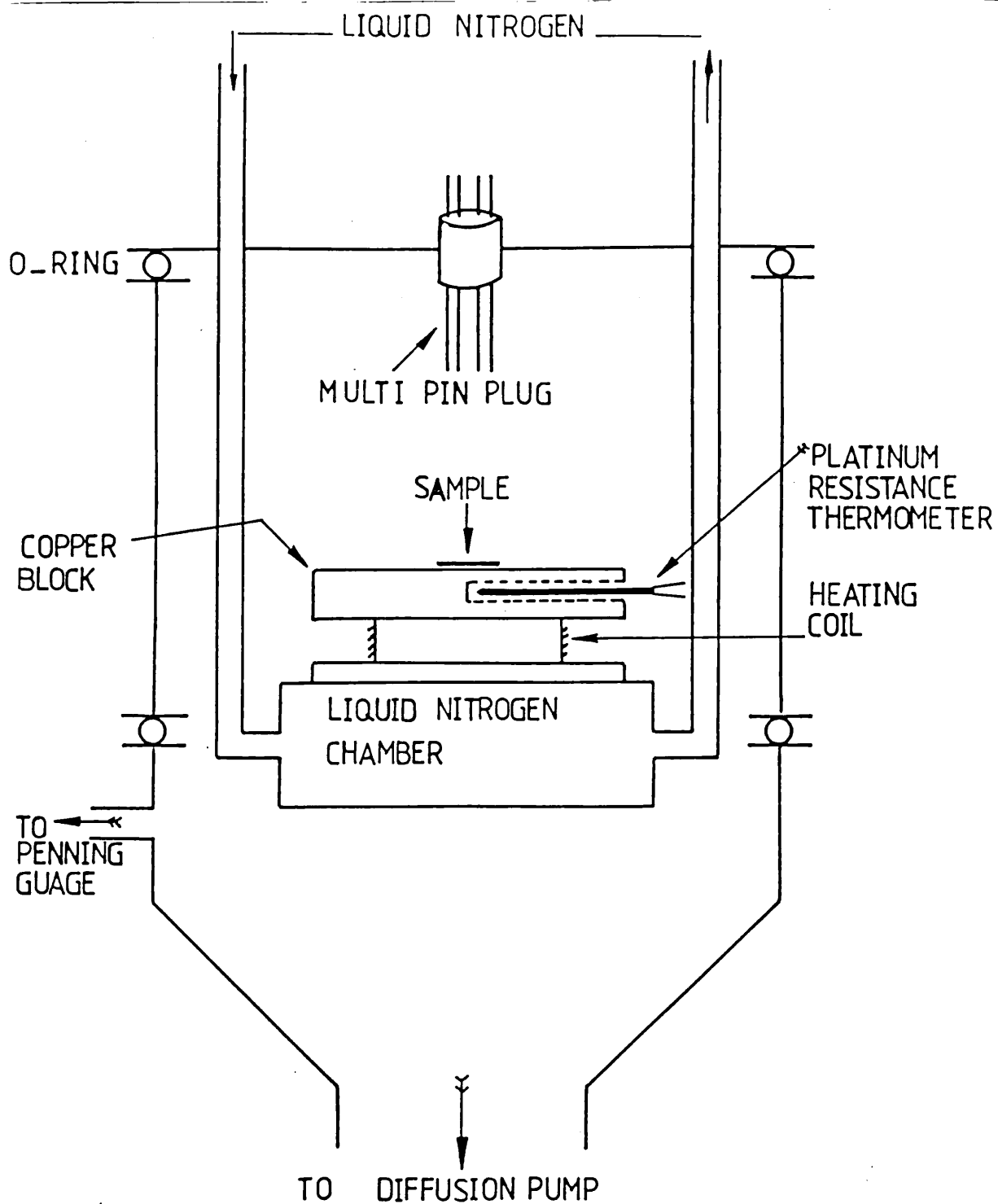


FIGURE. 10.6.2

SCHEMATIC DIAGRAM OF THE CRYOSTAT

10.6. D.c. Conductivity and Dielectric Spectroscopic Measurements

10.6.1. Sample preparation

All of the electrical measurements were carried out on samples in the form of compressed discs. For silver dag contacts, two paper reinforcers were placed on either side of the disc; two copper wires were then connected on either side by the silver dag, which filled the centre hole of the reinforcer figure 10.6.1.

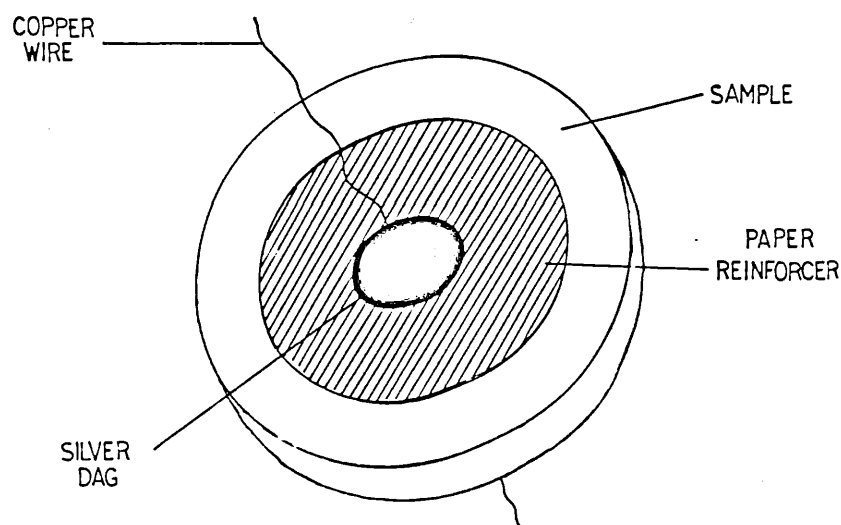


Figure 10.6.1

Of the other contacts used, the aluminium and indium were vacuum deposited on to an accurately defined area on either side of the sample discs, and the pressure contacts involved sandwiching the sample discs between two copper discs of known area. Each of these contacts was then connected to the external circuit via copper wire silver daged to their surfaces.

10.6.2. Low temperature measurements

Measurements below room temperature were made in a liquid nitrogen cryostat system, figure 10.6.2. This system consists of a temperature

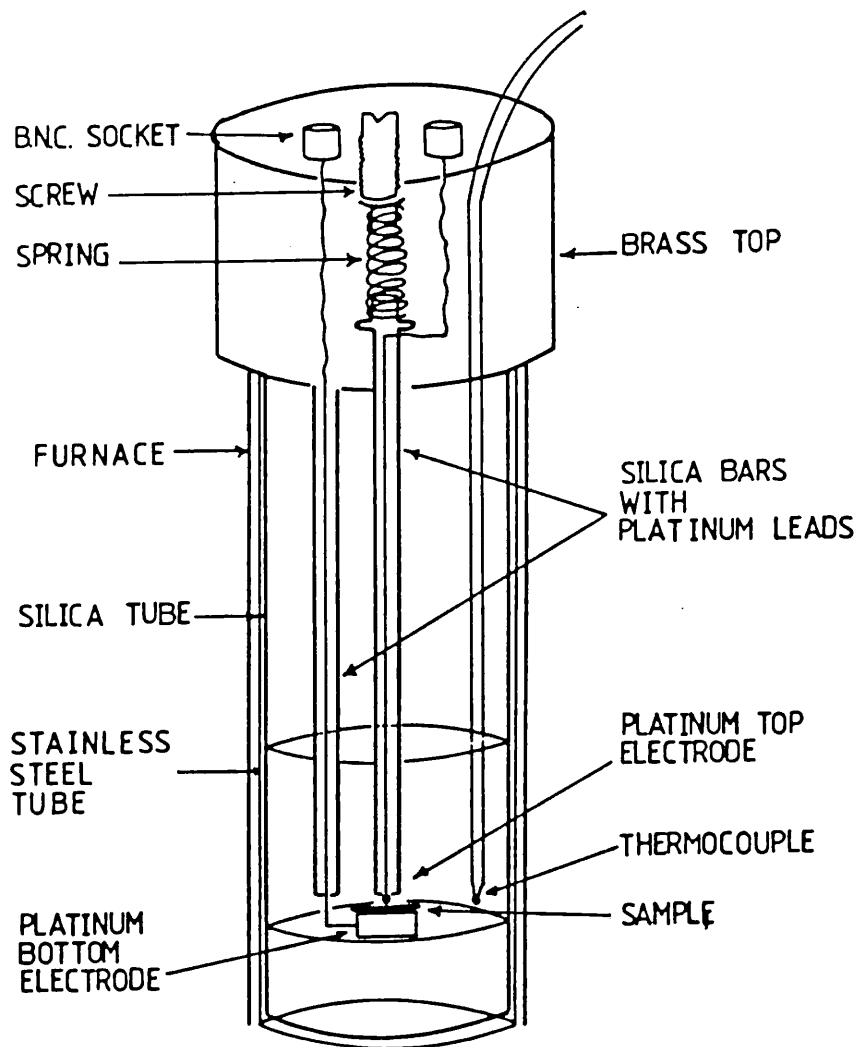


FIGURE 10.6.3
 HIGH TEMPERATURE SAMPLE HOLDER

controller and cooling-heating arrangement. The system used a vacuum of 5×10^{-2} mbar in order to avoid moisture condensation on the sample during measurements. Temperature was controlled by balancing the heat flow from the liquid nitrogen reservoir to the cold finger (a copper block) by supplying the required amount of heat through a heating coil wound around the latter. A Eurotherm model 070/008/010 controlled the heating current and a platinum resistance thermometer was used to sense the temperature of the copper block. To ensure that the temperature of the sample was as close as possible to that of the copper-block, good thermal contact was obtained by applying a thin coating of heat-sink compound between the copper and a thin mica sheet which was used as an electrical insulator.

10.6.3. High temperature measurements

High temperature work (above 373 K) was carried out by keeping the sample in a non-inductive Severn Science vertical furnace.

The cylindrical core, which was fitted with a 30 cm long, 5.4 cm diameter stainless steel cylinder, was wired to give a heat plateau at the centre of the furnace tube. The metallic cylinder was earthed to shield the sample from any electrical noise. The sample was placed in the stainless steel cylinder as shown in figure 10.6.3. A Chromel-Alumel thermocouple connected to the Eurotherm controller and hung between the stainless steel cylinder and the furnace core at the central position was used to control the temperature. The actual temperature was measured by another Chromel-Alumel thermocouple attached to the sample holder near the sample. There was always a slight

difference between the temperature set on the Eurotherm and that measured by the thermocouple. The thermo-emf of the measuring thermocouple, with reference to the ice point maintained by an Mk-11 ICEL unit, was monitored by a SOLARTRON digital voltmeter having a reading accuracy of $\pm 0.02\%$. Standard calibration tables were used to record the temperature sensed by the thermocouple.

10.6.4. D.c. conductivity measurements

10.6.4.1. Instrumentation

A Kingshill stabilised power supply (MODEL 36V2C), two 610C solid state electrometers (Keithley Instruments), a variable resistance box ($100\ \Omega - 1\ \text{M}\Omega$), a non-inductive Severn Science vertical furnace, two Chromel-Alumel thermocouples, a Eurotherm controller, an MK-11 ICEL unit, a SOLARTRON digital voltmeter, and a liquid nitrogen cryostat system.

10.6.4.2. Experimental

Figure 10.6.4 shows the circuit used for all of the measurements.

V_1 measured the applied voltage and V_2 the voltage drop across a

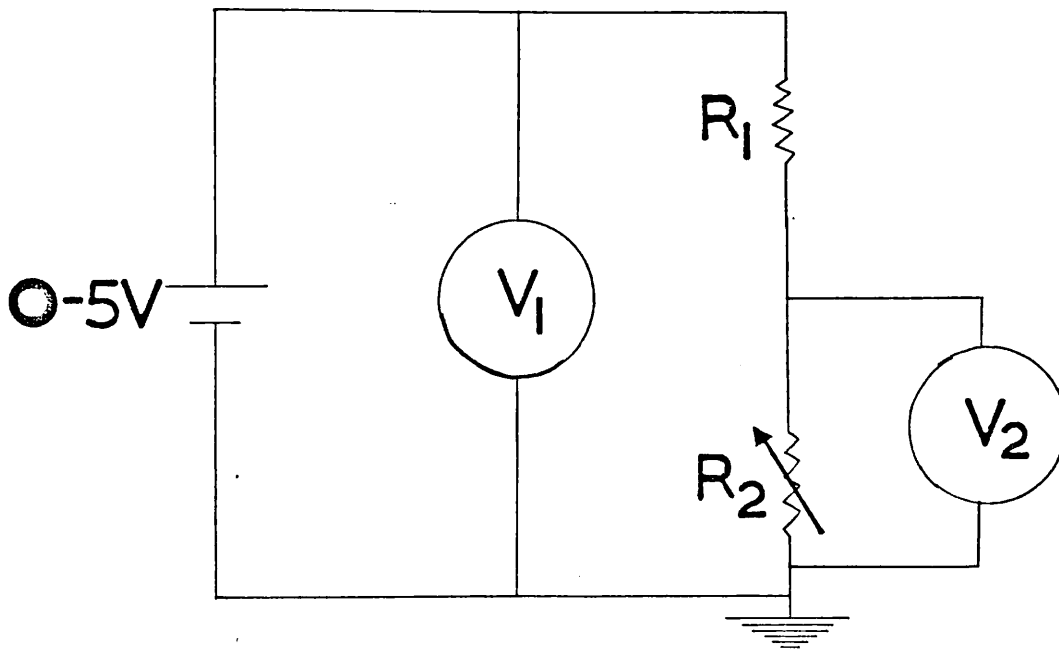


Figure 10.6.4

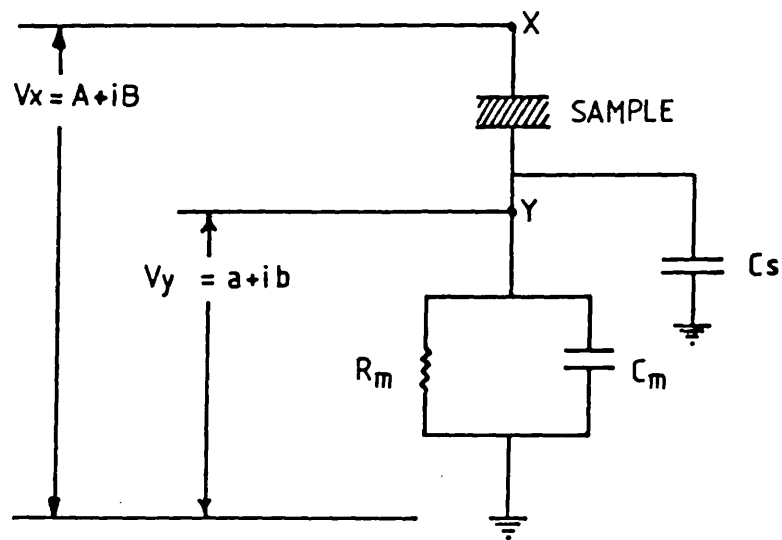
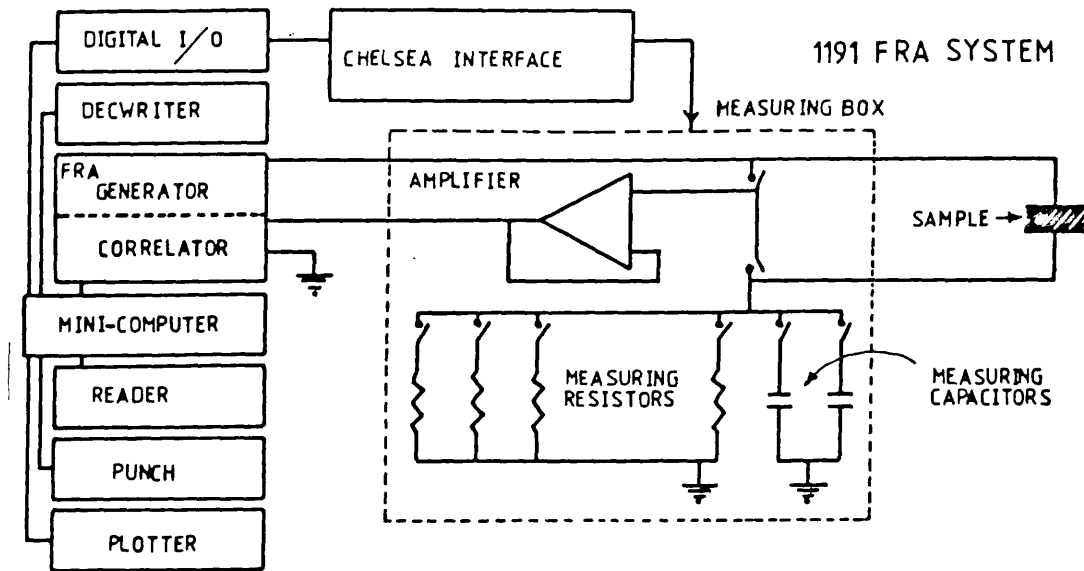


FIGURE 10.6.5
 THE BLOCK DIAGRAM OF FRA SYSTEM WITH EQUIVALENT
 CIRCUIT OF SAMPLE AND MEASURING RESISTOR/CAPACITOR
 COMBINATION.

known resistance in series with our sample. The known resistance was kept small compared to the sample resistance to maintain as large a voltage drop across the sample as possible. From Ohms Law,

$$I_2 = \frac{V_2}{R_2} \quad \text{and} \quad 10.6.1.$$

$$I_1 = \frac{V_1}{R_1} \quad 10.6.2.$$

where I_1 and I_2 are the currents flowing through resistances R_1 (sample) and R_2 (known), respectively. As these resistances are in series ($I_1 = I_2$) and as R_2 is known and V_2 measured, I_2 and hence I_1 can be obtained. Measurements similar to these were made for a range of temperatures.

10.6.5. Dielectric measurements^{99,100,101}.

10.6.5.1. Instrumentation (Frequency Response Analyser) The basic component of the system is a SOLARTRON 1191-FRA. The full system consists of a generator, a correlator, a measuring box together with its interface and a PDP- 11/04 computer. The block diagram together with an equivalent circuit is shown in figure 10.6.5. A digitally synthesised sine wave signal which is produced by the generator in the form of a stair-case with 2000 steps per cycle is applied to the dielectric sample. The correlator measures directly the in-phase and quadrature components

of the received signals in comparison to the generator output. If the generator output is proportional to $\sin \omega t$ and the input to the correlator is $V \sin(\omega t + \Phi)$ then the in-phase and quadrature components of V are given by:

$$A = \frac{2}{NT} \int_0^{NT} V \sin(\omega t + \Phi) \sin \omega t dt \quad 10.6.3.$$

$$B = \frac{2}{NT} \int_0^{NT} V \sin(\omega t + \Phi) \cos \omega t dt \quad 10.6.4.$$

where $V = A + iB$, $\text{Arg } V = \Phi$, and N is the number of complete cycles, each of time $T = 2\pi/\omega$, over which integration takes place. If P is an integer greater than unity, then

$$\frac{1}{NT} \int_0^{NT} \sin(P\omega t + \Phi) \sin \omega t dt = 0 \quad 10.6.5.$$

so that the system will not only reject the harmonics completely but also the noise.

The measuring box consists of 34 resistors in the range 10 to 10^{12} ohms. Each decade has three resistors of values 1, 2 and 5×10^n ohms where n is the decade. To overcome any possible problem arising from the presence of stray capacitance (C_s), four measuring capacitances (C_m) are included in the measuring box.

The box also contains all the relays that are required to switch the signal to the sample and to choose the required measuring resistor and capacitor. An interface controls the relays in the measuring box using digital outputs from the computer. The signal received into the measuring box is fed via the relays to a high impedance buffer amplifier before being transmitted back to the correlator.

10.6.5.2. Experimental

All the variables are controlled by the computer via the interface unit and the capacitance and conductance of the sample under investigation are calculated. $V_x (= A + iB)$ is the value of the applied signal with the generator connected to the sample and the measuring resistor R_m . If the impedance of the sample is low it will reduce the amplitude of the applied signal. This can be overcome by modifying the program so that the amplitude of the signal actually applied to the sample is within 2% of the nominal value. In the second measurement $V_y = (a + ib)$ is measured across the measuring resistor (R_m) only. In the third measurement the amplifier output V_z is then subtracted from both V_x and V_y . It is desirable to make V_y small compared to V_x so that most of the signal is dropped across the sample and not across the measuring resistor. The values of C and G/ω are then obtained from V_x and V_y measurements by means of the relationships:

$$C = \frac{1}{\omega R_m} \frac{Ab - aB}{(A-a)^2 + (B-b)^2} + C_m \frac{a(A-a) + b(B-b)}{(A-a)^2 + (B-b)^2} \quad 10.6.6.$$

$$G/\omega = \frac{1}{\omega R_m} \frac{a(A-a) + b(B-b)}{(A-a)^2 + (B-b)^2} - C_m \frac{Ab - aB}{(A-a)^2 + (B-b)^2} \quad 10.6.7.$$

where $\omega = 2\pi f$.

The loss tangent is given by

$$\tan \delta = G/\omega C = \epsilon''/\epsilon \quad 10.6.8.$$

In the case of low loss materials, $\tan \delta \ll 1$, the capacitance is recorded with higher accuracy than the conductance. For high loss materials, $\tan \delta \gg 1$, the reverse is true.

APPENDIX 1A

X-Ray Structure Determination¹⁰²1.1. The CAD4-F diffractometer

This instrument is employed to collect accurate X-ray diffraction intensity data for a crystal. It consists of a goniometer and X-ray counter controlled by a PDP8-A mini-computer¹⁰³. The instrument uses either copper K_{α} or molybdenum K_{α} radiation. The sequence of operations leading up to data collection will be outlined below.

First the crystal is placed at the intersection of the four rotation axes of the instrument and the X-ray beam, where it can be accurately viewed through a telescope, figure 1.2(A). Having aligned the crystal the instrument is instructed to measure the setting angles of 25 reflections. These reflections can be obtained either from a Polaroid rotation photograph of the crystal about the Φ axis or from a random search of reciprocal space. The instrument indexes these reflections and from them calculates the cell parameters and orientation matrix. The values of the cell parameters are then compared with the values derived from the photographic techniques. Any necessary transformations are performed at this stage (for example the instrument may have chosen the incorrect axis to be the unique axis in a monoclinic cell). Next a rapid data collection (probably from 10 to 12 or 13 degrees in theta) is initiated with the object of measuring some strong reflections from which to refine the cell parameters and orientation matrix. 25 such reflections are chosen from those collected and stored in the computer (in the "Ref dump"). They are all accurately recentered and a routine in the computer checks for zero-error in the detector position and outputs an accurate value of theta. The cell parameters and the orientation matrix are

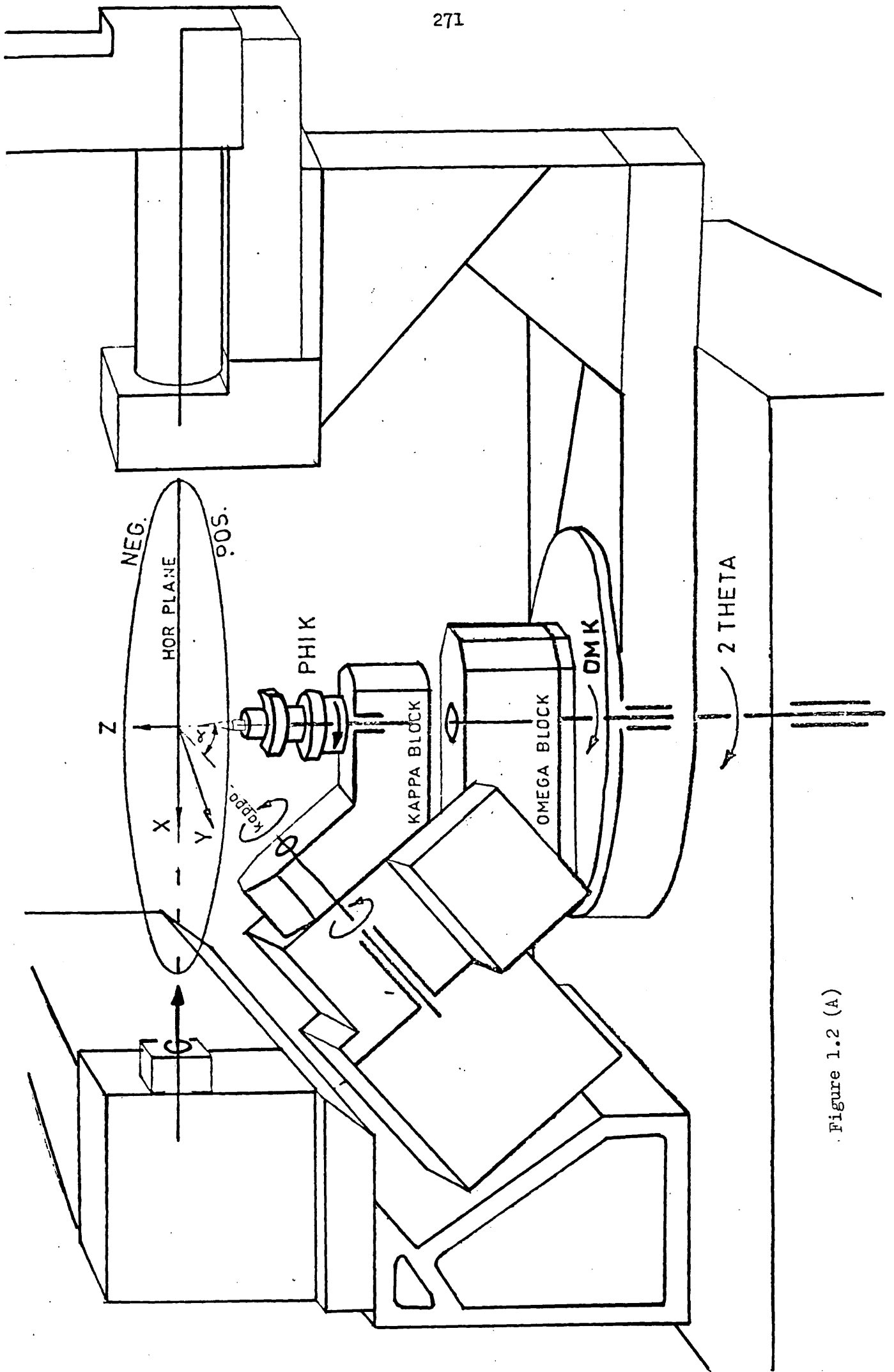


Figure 1.2 (A)

refined by a least squares calculation and accurate values are output to the terminal. Following this, the intensity profiles of a few reflections are examined in detail to determine the optimum intensity collection parameters for the detector (i.e. the aperture size, scan angle and the ratio of various motor drives during the scan). From the 25 reflections in the "Ref dump" a few are chosen as intensity and orientation standards to provide checks for crystal decay and change in alignment during data collection. At this stage a final review of the data collection parameters is made before initiating the full automatic data collection. The data so collected is stored on a magnetic disc in the computer and at the end of data collection it is transferred to, and stored on, 7-track magnetic tape from whence it can be read onto another computer (in Oxford, either the ICL 1906A or the ICL 2980) for data reduction and subsequent analysis.

1.2. Data reduction

The data reduction program takes the raw diffractometer data and outputs a set of sorted, scaled and merged structure factor amplitudes, $|F_{\text{obs}}|$. The structure factor is related to the observed intensity by the equation

$$|F_{\text{hkl}}| = \sqrt{\frac{K \cdot I_{\text{hkl}}}{L \cdot p}} \quad 1.1(A)$$

p is the polarisation factor which allows for partial polarisation of the X-ray beam of reflection. L is the Lorentz factor and arises because of the variation in time t for reciprocal lattice (r.l.) points to pass through the sphere of reflection. It depends on the position of the point in the r.l. and the direction from which it approaches the limiting

sphere, and is therefore also dependent on the method of intensity measurement. K is normally a constant for any given set of measurements. This term is normally omitted from further calculation and becomes integrated into the scale factor used to relate the observed structure factor amplitude to the absolute structure factor modulus, thus

$$|F_{\text{relative}}| = k'|F_{\text{observed}}| = \sqrt{I_{\text{hkl}}/L.p} \quad 1.2(A)$$

After the above corrections have been applied the data is sorted, so that the reflections are placed in a pre-determined order with reflections having the same indices adjacent in the list. The systematic absences are checked for consistency with the space-group symmetry operators and are removed. Equivalent reflections for the space-group in question are merged to produce a single mean structure factor amplitude and the final list of reflections is stored in the computer. The cell parameters, symmetry elements and the atomic scattering curves are also entered to be on hand when required⁹⁵.

1.3. Fourier synthesis

At this stage in the structure determination the crystal data consists of a set of observed structure factor amplitudes. The structure factor (F_{hkl}) is the resultant of the j waves scattered in the direction of the hkl reflections by the j atoms of the unit cell.

$$F_{\text{hkl}} = \sum_j f_j \exp 2\pi i (hx_j + ky_j + lz_j) \quad 1.3(A)$$

Alternatively the structure factor may be expressed in terms of the electron density in the unit cell as

$$F_{hkl} = \int_V \rho(x,y,z) \exp 2\pi i(hx + ky + lz) dv \quad 1.4(A)$$

A relationship exists between the electron density and the structure factor in as much as each is the Fourier transform of the other.

$$\rho(x,y,z) = \frac{1}{V} \sum_h \sum_k \sum_l F_{hkl} / \exp -2\pi i(hx + hy + lz - \alpha'_{hkl}) \quad 1.5(A)$$

The expression for the electron density above is a three-dimensional Fourier series using the structure factor amplitudes as coefficients and requires the phase α' of each reflection. The intensity measurements, however, only provide information on the amplitude of the structure factor and not on its phase. This is because the structure factor is proportional to the square-root of the intensity and not the intensity itself (which has been measured). This lack of any direct experimental measurement of the phase of a reflection is referred to as the phase problem. In order to overcome this problem a final structure can be used as a phasing model to calculate structure factors in a Fourier synthesis. These structure factors together with their signs are compared with the observed structure factors and, from the success of the comparison, adjustments are made to the model and the "adjusted" model used in a subsequent structure factor calculation. The two main approaches in use today to obtain the phasing model are the Patterson or heavy atom method and the Direct Method approach.

1.4. The Patterson Function and the Heavy Atom Method

The Patterson Function is a three-dimensional Fourier series using $|F_{hkl}|^2$ as coefficients which gives rise to peaks corresponding to all the interatomic vectors.

$$P(x,y,z) = \frac{1}{V} \sum_h \sum_k \sum_l |F_{hkl}|^2 \cos 2\pi(x,y,z) \quad 1.6(A)$$

Thus for a molecule with N atoms in the unit cell the Patterson map will show N^2 peaks. Of these, N will be vectors of zero length from each atom to itself and will be concentrated as a very large peak at the origin, while the remaining $N^2 - N$ will be vectors distributed throughout the cell. There is generally a great deal of overlapping in the Patterson map, caused by both the increased number of peaks and their increased width (compared to Fourier peaks). This can be corrected for in a "sharpened" Patterson map by modifying the observed structure factor amplitudes to those $|F_{hkl}|$'s expected for point atoms. The weight or height of a Patterson peak is proportional to the product of the atomic numbers of the atoms giving rise to it. If only one or two heavy atoms are present in a molecule the small number of large Patterson peaks so produced enables a solution of the map and positioning of these heavy atoms in the unit cell. The heavy atoms also contribute a large percentage to the structure factors (i.e. the scattering of X-rays by the electrons and so a phasing model based on the heavy atom positions can usually give a reasonable correlation between observed and calculated structure factors. The remaining non-hydrogen atoms can then usually be detected from a normal or difference Fourier.

1.5. Direct Methods

This approach attempts to obtain a phasing model directly from the observed structure factor amplitudes¹⁰⁴. Sayre¹⁰⁵ showed that subject to certain restrictions where Φ_{hkl} is simply a scaling term.

$$F_{hkl} = \Phi_{hkl} \sum_h \sum_k \sum_l F_{h'k'l'} F_{h-h'k-k'l-l'} \quad 1.7(A)$$

This implies that any structure factor F_{hkl} is determined by the products of all the pairs of structure factors whose indices add to give (hkl). If F_{hkl} above is large then the series summation above must have tended strongly in one direction (+ or -) which can be determined by the parity agreement between products with large values for F. Thus for large values of F where S means "the sign of". The probability of the

$$S(F_{hkl}) \cong S(F_{h'k'l'}) S(F_{h-h'k-k'l-l'}) \quad 1.8(A)$$

equation above being true is an important consideration of the Direct Methods approach. This probability is given by the tangent formula below

$$P = \frac{1}{2} + \frac{1}{2} \tan h \left\{ \frac{1}{\sqrt{N}} / E_{hkl} E_{h'k'l'} E_{h-h'k-k'l-l'} \right\} \quad 1.9(A)$$

which contains the normalised structure factor amplitudes or E-values and where N is the number of atoms in the unit cell. In a determination by direct methods a small number of reflections are assigned phases and then used with equation 1.8(A) to build up a large enough set of phases which, when used in a Fourier synthesis, give a reasonable representation of the structure.

1.6. Completion of the Structure

When a phasing model has been obtained, by one of the methods described, the phases are used in combination with the observed (phaseless) structure factors as coefficients in a Fourier synthesis. The atomic positions so found may be used to calculate a more accurate set of phases which may then be used to calculate a more accurate set of atomic positions and so on.

A "difference" Fourier is often useful for locating atoms not found in the phasing model. This uses the quantities as coefficients in a

$$\Delta F = /F_{\text{obs}}/ - /F_{\text{calc}}/ \quad 1.10(\text{A})$$

Fourier synthesis.

The last stages of a structure determination involve "least squares" refinement of the atomic parameters. The function minimised in

$$D = \sum W_{\text{hkl}} (/F_{\text{obs}}/ - /kF_{\text{calc}}./)^2 \quad 1.11(\text{A})$$

where W is the weight assigned to the observation.

The agreement between observed and calculated structure factors is expressed in terms of the residual index or 'R-value', given by

$$R = \frac{\sum / /F_{\text{obs}}/ - /F_{\text{calc}}./ /}{\sum /F_{\text{obs}}/} \quad 1.12(\text{A})$$

This may be used during refinement as a guide to the correctness of the model.

APPENDIX 1B

X-Ray Structure Data

1.1. The isotropic temperature factors for the hydrogen atoms of I(b), with estimated standard deviations in parentheses.

Atom	U[iso]		
H(1)	0.089(24)	H(20)	0.084(19)
H(2)	0.101(24)	H(21)	0.078(19)
H(3)	0.089(26)	H(22)	0.099(21)
H(4)	0.092(18)	H(23)	0.121(21)
H(5)	0.057(16)	H(24)	0.052(15)
H(6)	0.074(18)	H(25)	0.042(14)
H(7)	0.108(22)	H(26)	0.049(17)
H(8)	0.131(24)	H(27)	0.064(21)
H(9)	0.047(13)	H(28)	0.150(28)
H(10)	0.054(19)	H(29)	0.082(21)

1.2. Structure Factors for I(b)

H / F07 / F07 / F01				H / F07 / F07 / F01				H / F07 / F07 / F01				H / F07 / F07 / F01			
** K= 0 L= 0 **				** K= 10 L= 0 **				** K= 0 L= 1 **				** K= 1 L= 0 **			
1	36	29	346	10	40	99	182	-10	41	40	182	0	124	121	357
2	242	243	2	11	36	99	182	-11	37	40	182	1	483	787	1
3	822	849	181	12	41	89	184	-12	182	182	182	2	214	210	182
4	212	215	2	13	82	78	177	-13	182	182	182	3	360	363	180
5	147	182	357	14	205	194	182	-14	96	89	182	4	31	32	190
6	113	109	3	15	79	78	178	-15	34	34	182	5	85	72	176
7	110	110	184	16	12	69	184	-16	92	96	182	6	151	143	2
8	102	99	183	17	13	67	183	-17	60	64	182	7	328	319	181
9	102	99	183	18	14	66	184	-18	60	64	182	8	116	49	3
10	295	294	1	19	15	66	184	-19	63	66	182	9	221	214	181
11	214	202	182	20	16	51	3	-20	44	47	353	10	213	227	1
12	41	36	3	21	17	41	7	-21	73	80	0	11	42	11	177
13	41	36	3	22	18	41	7	-22	113	109	1	12	51	33	183
14	41	36	3	23	19	41	7	-23	104	94	180	13	36	41	3
15	70	67	182	24	20	41	7	-24	66	63	180	14	37	35	183
16	42	40	4	25	21	41	7	-25	31	27	360	15	37	35	183
** K= 1 L= 0 **				** K= 5 L= 0 **				** K= 11 L= 0 **				** K= 12 L= 0 **			
0	124	121	357	0	324	321	1	0	73	80	0	0	184	132	181
1	483	787	1	1	178	172	178	1	113	109	1	1	52	53	182
2	214	210	182	2	349	347	181	2	104	94	180	2	124	117	181
3	360	363	180	3	210	208	2	3	66	63	180	3	35	40	3
4	31	32	190	4	46	47	166	4	66	63	180	4	99	94	1
5	85	72	176	5	107	100	182	5	31	27	360	5	35	40	3
6	151	143	2	6	268	232	180	6	184	132	181	6	124	117	181
7	328	319	181	7	156	148	181	7	52	53	182	7	35	40	3
8	116	49	3	8	131	116	179	8	124	117	181	8	99	94	1
9	221	214	181	9	156	148	181	9	35	40	3	9	99	94	1
10	213	227	1	10	131	116	179	10	35	40	3	10	35	40	3
11	42	11	177	11	123	108	359	11	99	94	1	11	201	187	182
12	51	33	183	12	39	34	3	12	99	94	1	12	188	181	2
13	36	41	3	13	75	66	182	13	99	94	1	13	94	70	182
14	37	35	183	14	179	80	181	14	99	94	1	14	37	30	5
15	37	35	183	15	33	38	3	15	105	99	182	15	35	33	185
16	37	35	183	16	31	33	182	16	29	18	8	16	35	33	185
** K= 2 L= 0 **				** K= 6 L= 0 **				** K= 12 L= 0 **				** K= 13 L= 0 **			
0	103	104	180	0	233	223	181	0	93	84	2	0	93	84	2
1	188	192	359	1	178	150	179	1	105	99	182	1	105	99	182
2	794	828	180	2	225	214	0	2	29	18	8	2	29	18	8
3	605	603	0	3	83	75	339	3	82	80	182	3	82	80	182
4	91	96	1	4	48	53	1	4	70	64	3	4	70	64	3
5	98	74	359	5	48	53	1	5	76	64	183	5	76	64	183
6	214	208	1	6	93	91	339	6	44	43	3	6	44	43	3
7	32	48	1	7	179	80	181	7	44	43	3	7	44	43	3
8	131	127	181	8	178	150	179	8	44	43	3	8	44	43	3
9	90	64	360	9	83	75	339	9	44	43	3	9	44	43	3
10	48	45	180	10	48	53	1	10	44	43	3	10	44	43	3
11	48	45	180	11	93	91	339	11	44	43	3	11	44	43	3
12	48	45	180	12	174	158	181	12	44	43	3	12	44	43	3
13	48	45	180	13	44	42	339	13	44	43	3	13	44	43	3
14	48	45	180	14	44	42	339	14	44	43	3	14	44	43	3
** K= 3 L= 0 **				** K= 7 L= 0 **				** K= 14 L= 0 **				** K= 1 L= 1 **			
0	134	134	2	0	233	223	181	0	70	70	181	0	460	457	359
1	396	397	360	1	178	150	179	1	82	80	182	1	364	339	181
2	112	107	3	2	225	214	0	2	70	64	3	2	631	628	181
3	261	262	359	3	83	75	339	3	76	64	183	3	297	305	181
4	210	197	1	4	48	53	1	4	44	43	3	4	43	44	353
5	344	329	181	5	48	53	1	5	44	43	3	5	141	141	3
6	112	100	2	6	93	91	339	6	44	43	3	6	208	207	181
7	48	36	355	7	179	80	181	7	44	43	3	7	185	181	181
8	120	120	2	8	178	150	179	8	44	43	3	8	197	181	181
9	241	223	181	9	83	75	339	9	44	43	3	9	197	181	181
10	35	37	177	10	48	53	1	10	44	43	3	10	94	70	308
11	190	181	181	11	93	91	339	11	44	43	3	11	267	255	179
12	85	64	2	12	174	158	181	12	44	43	3	12	301	305	183
13	117	109	181	13	44	42	339	13	44	43	3	13	364	360	179
14	75	74	-1	14	44	42	339	14	44	43	3	14	460	457	359
** K= 4 L= 0 **				** K= 8 L= 0 **				** K= 14 L= 0 **				** K= 1 L= 1 **			
0	30	21	196	0	118	114	2	-16	70	70	181	0	460	457	359
1	132	136	3	1	43	51	355	-15	55	57	2	1	364	339	181
2	319	312	181	2	30	33	8	-14	188	180	181	2	631	628	181
3	284	282	2	3	128	122	182	-13	163	184	1	3	297	305	181
4	30	21	196	4	38	19	12	-12	93	84	183	4	43	44	353
5	132	136	3	5	86	78	183	-11	163	142	1	5	141	141	3
6	319	312	181	6	110	103	2	-10	64	59	183	6	208	207	181
7	284	282	2	7	158	151	359	-9	64	59	183	7	185	181	181
8	30	21	196	8	193	179	1	-8	166	142	182	8	197	181	181
9	132	136	3	9	86	78	183	-7	125	126	178	9	94	70	308
10	319	312	181	10	110	103	2	-6	177	175	182	10	267	255	179
11	284	282	2	11	158	151	359	-5	106	109	178	11	301	305	183
12	30	21	196	12	86	78	183	-4	99	88	183	12	364	360	179
13	132	136	3	13	110	103	2	-3	1332	1540	0	13	460	457	359
14	284	282	2	14	158	151	359	-2	478	486	360	14	364	339	181
15	30	21	196	15	86	78	183	-1	864	1006	0	15	205	205	182
16	132	136	3	16	110	103	2	0	366	375	181	16	788	846	180
17	284	282	2	17	158	151	359	1	205	205	182	17	69	67	5
18	30	21	196	18	86	78	183	2	788	846	180	18	137	127	178
19	132	136	3	19	110	103	2	3	205	205	182	19	137	127	178
20	284	282	2	20	158	151	359	4	397	393	181	20	297	283	181
21	30	21	196	21	86	78	183	5	257	240	1	21	257	240	1
22	132	136	3	22	110	103	2	6	257	240	1	22	257	240	1
23	284	282	2	23	158	151	359	7	257	240	1	23	257	240	1
24	30	21	196	24	86	78	183	8	257	240	1	24	257	240	1
25	132	136	3	25	110	103	2	9	257	240	1	25	257	240	1
26	284	282	2	26	158	151	359	10	257	240	1	26	257	240	1
27	30	21	196	27	86	78	183	11	257	240	1	27	257	240	1
28	132	136	3	28	110	103	2	12	257	240	1	28	257	240	1
29	284	282	2	29	158	151	359	13	257	240	1	29	257	240	1
30	30	21	196	30	86	78	183	14	257	240	1	30	257	240	1
31	132	136	3	31	110	103	2	15	257	240	1	31	257	240	1
32	284	282	2	32	158	151	359	16	257	240	1	32	257	240	1
33	30	21	196	33	86	78	183	17	257	240	1	33	257	240	1
34	132	136	3	34	110	103	2	18	257	240	1</				

H	/FO/	/FC/	PHI	H	/FO/	/FC/	PHI	H	/FO/	/FC/	PHI	H	/FO/	/FC/	PHI
-4	79	88	2	-3	197	184	182	-10	80	73	182	-1	462	1049	181
-3	677	660	360	-2	178	183	2	-9	86	87	182	0	183	104	184
-2	298	297	180	-1	76	68	355	-8	75	70	183	1	210	229	177
-1	314	302	360	1	58	65	185	-7	77	23	182	2	728	812	360
0	613	621	0	2	88	96	4	-6	48	43	184	3	48	35	187
1	43	46	358	4	322	311	1	-5	98	84	3	4	508	581	181
3	71	67	182	5	224	214	182	-1	38	39	355	5	385	488	1
4	142	135	1	7	229	213	181	-3	47	47	5	6	187	148	183
5	257	279	181	8	117	113	2	-2	105	105	182	7	621	598	4
6	30	25	4	11	67	64	183	-1	168	162	2	8	217	211	181
7	82	84	358	12	84	38	3	0	168	148	182	10	174	187	180
8	239	226	180	13	66	65	183	1	243	237	1	11	47	40	5
9	80	80	359	** K= 8 L= 1 **				2	102	93	182	13	48	43	178
10	63	56	179					4	114	111	182	14	37	41	374
13	85	49	359					5	47	48	4	** K= 1 L= 0 **			
** K= 5 L= 1 **				-12	120	116	181	6	106	103	182	-13	80	78	182
				-11	46	34	178	7	62	51	3	-13	61	57	358
-13	102	99	181	-10	150	138	181	8	44	38	184	-11	99	94	182
-9	88	80	182	-7	262	258	1	9	69	51	3	-11	149	149	2
-3	74	71	2	-6	48	53	183	10	52	49	183	-9	208	200	181
-7	73	59	182	-5	111	108	2	** K= 12 L= 1 **			-8	70	64	4	
-5	46	14	357	-4	136	134	181	-9	44	40	183	-7	115	114	182
-3	165	153	359	-3	95	92	2	-8	58	49	3	-6	249	261	1
-2	358	348	0	-2	72	58	183	-4	86	82	2	-5	40	38	188
-1	432	405	360	0	94	79	358	-3	45	42	357	-4	335	321	179
0	255	252	1	3	167	154	1	-2	102	92	2	-3	1499	1705	180
1	178	186	181	4	95	96	182	-1	97	84	182	-1	322	349	181
2	61	61	177	5	71	71	2	0	167	161	1	0	892	1015	0
3	110	105	182	6	247	232	181	1	83	44	183	1	548	379	181
5	84	71	182	7	199	188	180	2	35	33	5	2	132	124	177
6	79	79	179	8	191	179	181	4	27	24	6	3	109	108	357
7	138	134	181	9	52	48	178	6	47	48	3	4	65	62	174
9	77	71	182	10	39	34	183	7	40	35	184	5	107	96	357
10	79	77	179	13	37	34	3	8	76	69	2	6	24	24	12
12	62	60	2	** K= 9 L= 1 **				9	48	46	183	7	277	242	181
** K= 6 L= 1 **				-12	34	34	181	** K= 13 L= 1 **				8	158	140	2
-14	58	38	184	-11	54	55	180	10	102	97	2	11	102	97	2
-13	53	47	3	-10	31	32	181	-7	25	25	1	11	45	38	185
-12	47	35	186	-9	84	78	1	-6	38	40	181	12	35	30	6
-9	38	59	177	-7	75	69	180	-4	31	26	182	13	63	65	358
-8	136	126	182	-5	56	54	180	-2	30	31	182	14	33	30	1
-7	140	134	2	-4	122	112	0	0	38	31	181	15	62	31	182
-3	106	104	183	-3	78	72	180	2	33	46	359	** K= 2 L= 2 **			
-5	388	362	180	2	113	110	181	3	69	69	180	-15	29	26	180
-4	223	209	182	3	103	91	180	4	94	91	0	-14	44	43	360
-3	355	345	1	4	257	251	0	5	94	91	0	-13	29	22	182
-2	158	132	358	5	171	151	1	6	34	37	360	-12	111	107	280
-1	140	126	3	6	39	33	181	** K= 14 L= 1 **				-11	40	40	1
0	183	186	182	7	75	74	180	-4	46	45	182	-10	123	127	181
1	365	328	179	8	120	113	181	-3	50	43	2	-9	48	47	1
2	477	447	181	9	59	57	180	-2	33	35	182	-8	37	30	180
3	260	253	2	10	75	75	181	2	80	73	181	-7	112	98	180
4	41	43	187	12	43	43	0	** K= 0 L= 2 **				-6	375	357	0
5	60	61	5	** K= 10 L= 1 **				-16	46	48	183	-5	374	381	0
7	117	108	3	-10	82	83	2	-15	54	50	3	-4	158	161	0
8	101	93	183	-9	97	95	182	-14	141	133	182	-3	173	167	180
12	72	64	183	-8	123	118	1	-12	66	59	357	-2	525	585	180
13	47	45	3	-7	65	56	183	-11	325	304	1	-1	360	309	1
14	99	93	182	-6	62	60	3	-10	233	223	181	0	937	1004	140
** K= 7 L= 1 **				-5	34	49	184	-9	122	115	3	1	491	491	0
-12	33	36	5	-3	54	51	184	-8	35	34	190	2	38	35	357
-11	114	100	182	-1	138	138	182	-7	312	301	1	3	744	712	180
-10	186	149	179	0	61	53	3	-6	131	136	183	4	237	201	360
-9	229	93	183	1	64	50	184	-5	618	617	180	5	98	95	180
-8	139	129	2	6	118	107	2	-4	1500	1602	180	6	144	109	354
-6	170	161	2	9	93	78	182	-3	1410	1600	180	8	91	85	181
-5	157	146	182	10	28	36	3	-2	847	915	360	9	69	66	1
-4	56	55	179	** K= 11 L= 1 **				11	100	147	181	11	100	147	181

H	/FO/	/FC/	FBI	H	/FO/	/FC/	FBI	H	/FO/	/FC/	FBI	H	/FO/	/FC/	FBI
** K=	3	L=	2 **	-1	544	534	1	-13	78	74	4	0	45	41	183
-15	64	63	1	0	238	226	122	-12	47	41	193	1	51	47	183
-13	111	109	1	1	126	113	177	-10	82	80	182	2	57	54	183
-12	49	43	183	2	246	233	182	-9	85	81	182	3	52	50	183
-10	77	72	358	3	397	391	1	-8	71	67	183	4	51	50	183
-9	97	92	182	4	403	387	181	-7	80	77	183	5	50	46	181
-7	53	46	4	5	58	53	175	-6	81	80	183	6	43	39	181
-6	481	453	181	6	66	69	183	-5	106	93	2	7	47	46	180
-5	600	587	1	7	266	236	1	-1	164	149	222	8	49	48	182
-4	328	335	181	8	67	70	184	0	121	81	357	** K=	12	L=	2 **
-3	190	198	1	9	57	47	5	1	113	113	1	-3	64	64	2
-2	344	354	181	10	35	34	187	2	216	218	181	-3	63	49	182
-1	625	651	0	11	67	58	4	4	364	344	181	-5	26	20	358
0	34	30	185	12	54	53	183	6	209	199	359	-4	70	49	2
1	319	308	179	13	117	107	2	7	206	194	1	0	110	106	1
2	21	28	352	14	40	33	184	8	86	83	182	1	69	64	182
3	244	234	1	** K=	6	L=	2 **	9	35	41	176	3	110	105	182
4	174	167	181	-14	41	35	2	10	154	154	181	5	52	48	182
5	409	378	1	-13	47	45	359	12	41	41	183	7	77	71	182
6	363	328	360	-12	75	73	1	13	80	75	2	** K=	9	L=	2 **
7	195	178	1	-11	44	52	182	** K=	9	L=	2 **	** K=	13	L=	2 **
8	92	81	353	-9	96	96	181	-11	85	83	182	-7	71	70	2
10	38	30	183	-7	88	83	182	-10	32	30	5	-6	64	24	180
11	83	80	179	-6	138	128	1	-9	91	71	3	-5	80	75	183
12	39	32	184	-4	261	244	1	-7	63	56	184	-4	87	80	183
13	42	35	3	-3	47	48	183	-6	121	116	2	-3	74	68	3
14	28	31	183	-2	244	229	1	-5	41	42	186	-2	81	45	357
** K=	4	L=	2 **	-1	64	65	183	-4	78	77	4	-1	36	35	5
-14	92	85	2	1	336	319	181	-3	68	64	184	1	44	37	4
-13	103	83	2	2	100	102	2	-2	87	87	5	4	70	67	183
-11	126	115	182	3	113	97	182	-1	77	73	184	6	61	58	183
-10	40	34	7	4	110	103	2	0	132	131	2	7	24	24	5
-9	49	30	6	5	130	123	181	2	94	92	3	** K=	14	L=	2 **
-7	92	99	183	6	137	124	1	3	253	238	181	-4	53	53	0
-6	48	45	7	8	80	36	177	4	227	217	179	-3	55	54	182
-5	233	229	182	9	76	68	369	5	180	167	182	-2	44	42	182
-4	167	153	178	13	44	34	182	6	64	59	4	0	36	38	3
-3	318	322	181	14	65	62	1	7	29	18	347	2	92	82	2
-2	180	174	2	** K=	7	L=	2 **	8	40	37	175	2	82	82	2
-1	140	142	183	-14	51	45	1	9	184	173	181	3	38	39	355
0	37	48	172	-13	104	98	0	10	37	41	4	12	109	106	2
1	244	232	358	-12	33	29	2	12	109	106	2	** K=	10	L=	2 **
2	129	125	3	-11	98	89	181	** K=	10	L=	2 **	-10	37	34	183
3	86	86	354	-10	87	86	180	-10	40	45	183	-12	81	43	183
4	231	226	2	-9	43	31	182	-9	34	38	2	-10	144	103	0
5	338	317	1	-8	54	58	179	-8	51	39	184	-9	205	212	181
6	96	78	357	-7	82	74	181	-7	51	44	3	-8	81	71	183
7	183	178	2	-6	86	76	1	-6	71	69	2	-6	687	622	181
8	203	198	182	-5	92	89	359	-4	84	88	182	-5	470	459	180
9	147	138	2	-4	110	107	1	-3	66	61	3	-3	383	373	181
10	102	99	182	-3	70	46	358	-2	182	178	181	-4	274	279	1
11	85	58	3	-2	190	175	180	-1	86	75	2	-4	479	481	360
12	72	63	183	-1	230	223	181	0	82	48	184	-2	397	301	179
13	108	111	2	0	279	267	1	1	196	195	1	-1	85	68	356
14	30	33	184	1	74	71	181	3	149	144	2	0	252	268	179
15				2	103	87	1	4	123	121	182	1	205	226	181
** K=	5	L=	2 **	3	139	130	181	5	96	90	179	2	709	707	1
-14	23	20	187	4	229	217	1	6	119	77	182	3	289	291	181
-13	102	102	2	5	58	56	360	8	129	123	181	4	89	60	5
-11	87	83	3	6	164	156	1	9	27	34	177	5	193	182	181
-10	80	52	184	7	88	84	359	10	89	22	185	6	107	104	181
-9	79	76	3	8	64	70	180	11	30	32	3	7	213	177	181
-8	81	44	355	9	66	62	181	** K=	11	L=	2 **	8	87	86	181
-7	139	179	2	10	30	21	3	-9	28	25	181	11	80	77	181
-6	190	176	359	11	64	60	181	-5	42	34	181	12	82	83	181
-5	84	87	175	12	50	50	180	-4	66	64	180	13	67	67	181
-4	134	136	182	** K=	8	L=	2 **	-1	54	57	360	** K=	2	L=	3 **
-3	190	189	2	-14	41	35	2	** K=	2	L=	3 **	2	64	64	2
-2	376	355	359	-13	47	45	359	-11	85	83	182	-7	71	70	2
				-12	75	73	1	-10	32	30	5	-6	64	24	180
				-11	44	52	182	-9	91	71	3	-5	80	75	183
				-9	96	96	181	-7	63	56	184	-4	87	80	183
				-7	88	83	182	-6	121	116	2	-3	74	68	3
				-6	138	128	1	-5	41	42	186	-2	81	45	357
				-4	261	244	1	-4	78	77	4	-1	36	35	5
				-3	47	48	183	-3	68	64	184	1	44	37	4
				-2	244	229	1	-2	87	87	5	4	70	67	183
				-1	64	65	183	-1	77	73	184	6	61	58	183
				1	336	319	181	0	132	131	2	7	24	24	5
				2	100	102	2	2	94	92	3	** K=	14	L=	2 **
				3	113	97	182	3	253	238	181	-4	53	53	0
				4	110	103	2	4	227	217	179	-3	55	54	182
				5	130	123	181	5	180	167	182	-2	44	42	182
				6	137	124	1	6	64	59	4	0	36	38	3
				8	80	36	177	7	29	18	347	2	92	82	2
				9	76	68	369	8	40	37	175	3	38	39	355
				13	44	34	182	9	184	173	181	10	37	41	4
				14	65	62	1	10	37	41	4	12	109	106	2
				** K=	7	L=	2 **	12	109	106	2	** K=	1	L=	3 **
				-14	51	45	1	** K=	10	L=	2 **	-10	37	34	183
				-13	104	98	0	-10	40	45	183	-12	81	43	183
				-12	33	29	2	-9	34	38	2	-10	144	103	0
				-11	98	89	181	-8	51	39	184	-9	205	212	181
				-10	87	86	180	-7	51	44	3	-8	81	71	183
				-9	43	31	182	-6	71	69	2	-6	687	622	181
				-8	54	58	179	-4	84	88	182	-5	470	459	180
				-7	82	74	181	-3	66	61	3	-3	383	373	181
				-6	86	76	1	-2	182	178	181	-4	274	279	1
				-5	92	89	359	-1	86	75	2	-4	479	481	360
				-4	110	107	1	0	82	48	184	-2	397	301	179
				-3	70	46	358	1	196	195	1	-1	85	68	356
				-2	190	175	180	3	149	144	2	0	252	268	179

H	/FO/	/FC/	PHI	H	/FO/	/FC/	PHI	H	/FO/	/FC/	PHI	H	/FO/	/FC/	PHI
** K= 1	L= 4	**													
-14	47	50	183	2	343	320	180	-2	38	40	3	2	42	40	186
-13	31	23	6	3	709	693	180	-4	22	77	182	3	31	21	170
-11	79	77	2	4	174	166	1	-3	247	243	1	4	135	101	181
-10	185	180	181	5	27	21	351	-2	44	20	187	5	47	32	336
-9	99	98	2	6	121	105	2	-1	34	36	5	6	94	90	182
-8	95	89	358	7	86	73	358	2	192	177	360	10	61	66	183
-7	484	447	1	11	35	30	184	3	129	119	179	11	49	45	3
-6	335	313	360	12	31	27	4	4	131	119	181	** K= 10	L= 4	**	
-5	201	175	179	13	38	35	183	6	101	102	1	-10	30	34	3
-4	83	84	134	14	46	47	2	7	199	200	181	-9	43	44	180
-3	320	319	1	** K= 4	L= 4	**	8	38	38	183	-8	36	49	180	
-2	52	50	187	-15	37	29	4	9	137	127	1	-6	63	70	358
-1	121	112	177	-14	40	30	185	10	106	102	181	-5	38	26	358
0	202	190	359	-13	36	36	4	12	43	45	182	-4	63	71	170
1	729	708	1	-12	108	102	182	** K= 7	L= 4	**	-3	62	66	183	
2	34	38	352	-11	97	87	3	-13	41	45	1	-2	230	235	180
3	161	148	2	-10	38	31	354	-11	64	61	1	0	38	37	2
4	142	134	182	-9	52	50	5	-11	64	61	1	1	209	198	360
5	69	68	176	-7	355	344	1	-10	40	40	181	2	141	135	184
6	109	100	185	-6	218	221	182	-8	135	130	181	3	51	44	184
7	235	226	1	-5	91	95	3	-7	124	115	1	4	42	35	2
8	169	157	182	-4	438	422	181	-4	35	27	184	5	34	34	357
9	56	57	4	-3	178	172	2	-3	212	208	180	6	37	36	3
10	37	40	185	-2	200	216	182	-2	44	37	358	7	70	69	182
11	67	60	3	-1	329	320	1	0	111	117	181	9	48	47	182
12	77	73	358	0	173	164	182	2	45	43	182	10	59	59	2
13	189	180	1	3	439	415	181	3	29	16	175	** K= 11	L= 4	**	
14	36	37	357	5	156	169	2	4	172	163	181	-3	45	51	180
** K= 2	L= 4	**	4	331	314	181	5	83	81	1	-2	64	61	181	
-14	43	36	1	5	274	258	2	7	232	217	1	-1	35	32	180
-9	270	233	181	6	35	41	354	9	177	171	1	0	36	27	181
-8	140	136	180	9	65	60	4	10	110	109	181	4	49	49	0
-7	283	275	0	13	118	106	2	11	41	40	2	5	76	72	0
-6	417	414	0	14	93	96	182	13	37	38	180	6	76	72	0
-5	149	141	350	** K= 5	L= 4	**	** K= 6	L= 4	**	6	53	50	0		
-4	92	88	181	-14	71	67	2	-12	37	33	4	8	36	40	0
-3	313	297	0	-13	66	65	182	-9	66	57	183	** K= 12	L= 4	**	
-2	60	56	360	-12	65	69	3	-7	156	150	181	-8	99	93	184
-1	303	337	0	-11	158	148	182	-6	61	54	4	-7	49	46	180
0	384	368	180	-10	39	39	5	-5	128	120	182	-6	37	40	358
1	112	83	1	-9	43	36	189	-4	94	92	2	-5	69	65	180
2	59	58	360	-8	123	118	2	-3	139	134	180	-4	69	65	180
3	139	133	180	-7	208	229	181	-2	235	230	1	-3	36	41	180
4	455	424	180	-5	403	379	181	-1	165	164	182	0	37	34	184
5	39	39	180	-4	289	284	1	0	244	244	1	7	37	31	184
6	184	170	181	-3	131	134	182	1	24	24	183	8	20	23	184
7	106	98	1	-2	292	267	1	3	343	338	181	** K= 13	L= 4	**	
10	65	59	180	-1	157	155	182	5	206	196	309	-5	47	45	184
11	57	54	181	0	132	133	3	6	212	194	1	-3	40	35	184
12	104	98	1	1	174	163	358	7	58	45	184	0	49	44	180
13	48	47	360	2	80	65	175	8	99	94	2	1	63	61	181
14	24	20	180	3	573	539	181	9	174	169	181	4	59	57	180
** K= 3	L= 4	**	4	113	106	3	11	60	64	182	11	29	28	4	
-15	34	28	183	5	136	127	182	12	29	28	4	** K= 9	L= 4	**	
-12	114	107	1	6	133	133	2	** K= 9	L= 4	**	** K= 14	L= 4	**		
-10	72	77	179	7	452	428	181	-12	35	33	184	-3	49	45	185
-9	37	26	186	8	99	92	3	-11	45	42	3	-1	23	20	176
-8	92	89	179	9	140	132	182	-8	78	74	183	0	64	59	182
-7	69	59	358	10	68	43	5	-7	67	64	3	1	92	88	180
-6	173	154	1	11	134	130	182	-6	35	39	186	2	30	32	182
-5	45	43	356	13	33	29	185	-5	148	141	2	** K= 7	L= 5	**	
-4	348	340	180	14	59	60	2	-4	60	58	184	-14	35	25	184
-3	291	295	359	** K= 6	L= 4	**	-3	29	25	10	-12	46	37	187	
-2	50	46	176	-13	62	78	1	-2	125	119	182	-11	99	94	3
-1	174	181	181	-10	67	64	182	-1	276	261	1				
0	358	329	180	-9	103	102	179	0	103	103	358				
1	130	131	182	-7	87	78	179	1	362	360	1				

H	/FO/	/FO/	PHI	H	/FO/	/FO/	PHI	H	/FO/	/FO/	PHI	H	/FO/	/FO/	PHI
-7	102	95	181	1	134	134	181	** K= 11	L= 8 **	-11	107	94	181		
-6	57	54	181	2	94	94	182	-10	107	94	181				
-5	134	133	181	3	51	53	182	-9	107	94	181				
-4	34	52	181	4	69	69	1	-8	107	94	181				
-3	33	43	183	5	9	9	1	-7	48	47	0				
-2	50	44	357	** K= 7	L= 9 **	-6	52	35	0						
0	61	68	3	-8	38	34	182	-5	99	97	0				
1	102	102	182	-7	33	47	179	-4	69	43	182				
2	133	148	1	-6	131	123	0	-3	171	134	182				
3	169	164	181	-5	67	69	179	-2	143	129	182				
4	133	133	1	-4	87	78	181	-1	132	103	184				
5	228	314	181	-3	71	74	179	0	67	56	184				
6	231	220	1	-2	144	137	0	1	43	39	184				
7	115	105	181	-1	340	318	1	2	42	24	184				
8	32	47	181	0	32	17	357	3	94	81	184				
9	33	60	182	1	79	78	181	4	204	204	184				
10	44	46	182	2	69	70	180	5	103	111	182				
11	39	40	182	3	91	95	181	6	152	170	182				
** K= 4	L= 8 **	4	131	5	139	130	180	7	150	126	182				
-12	50	50	183	6	89	92	181	8	130	131	182				
-10	31	53	183	7	38	41	350	9	72	51	182				
-9	32	73	183	8	31	22	183	10	47	53	164				
-8	32	77	183	** K= 8	L= 8 **	-12	41	38	183						
-7	33	85	183	-11	29	27	184	-11	36	34	3				
-6	174	164	182	-10	32	28	4	-9	83	83	2				
-5	34	35	183	-9	60	57	182	-7	175	162	1				
-4	194	196	181	-8	49	42	3	-6	64	64	358				
-3	32	39	183	-7	74	60	3	-5	89	94	2				
-2	139	130	38	-6	130	142	2	-4	34	26	186				
-1	133	136	182	-5	62	62	3	-3	99	95	182				
0	59	49	173	-4	63	71	353	-2	146	131	2				
1	137	171	182	-3	60	68	178	-1	132	123	182				
2	66	81	182	-2	68	96	182	0	152	145	1				
3	103	101	182	-1	58	53	3	1	111	102	182				
4	64	62	184	0	58	40	183	2	374	363	1				
5	33	32	184	1	58	53	3	3	153	147	181				
** K= 5	L= 8 **	5	30	6	67	75	179	4	73	75	179				
-13	32	33	183	7	284	264	181	5	67	67	359				
-12	27	30	4	8	86	84	2	6	86	84	2				
-11	39	52	182	9	10	38	358	7	38	40	358				
-10	61	58	182	10	12	28	25	183	8	67	67	359			
-9	133	137	183	** K= 9	L= 8 **	9	86	84	2						
-8	40	31	173	-10	30	36	182	10	38	40	358				
-7	133	240	181	-9	36	36	4	12	28	25	183				
-6	56	52	174	-8	31	35	184	** K= 2	L= 9 **	-13	46	38	183		
-5	126	123	182	-7	87	92	2	-12	59	53	3				
-4	34	36	186	-6	71	58	3	-11	106	103	182				
-3	83	82	3	-5	84	87	182	-10	113	108	2				
-2	47	47	185	-4	60	57	184	-9	117	106	182				
-1	79	71	3	-3	66	63	3	-8	119	116	2				
0	133	127	359	-2	150	153	182	-7	150	136	182				
1	111	103	3	-1	57	40	4	-6	154	144	2				
2	45	46	184	0	31	46	357	-5	70	70	184				
3	131	139	179	1	32	27	7	-4	127	124	182				
4	33	22	354	2	35	38	4	-3	116	112	3				
5	65	70	3	3	74	74	2	-2	116	112	3				
** K= 6	L= 8 **	6	33	4	33	35	183	-1	197	190	182				
-13	32	33	2	5	33	35	183	0	0	70	59	5			
-12	60	57	179	6	36	37	3	1	170	159	182				
-11	39	78	359	7	30	25	357	2	190	186	2				
-10	68	60	2	8	97	94	1	3	181	170	359				
-9	37	28	4	9	31	29	357	4	400	383	1				
-8	242	235	181	10	31	47	3	5	76	77	183				
-7	184	144	180	11	71	58	2	6	90	90	182				
-6	81	74	182	12	40	40	183	7	95	90	182				
-5	148	141	1	13	138	134	1	8	117	112	2				
1	44	41	3	14	68	62	182	9	67	64	183				
				15	73	75	2	10	40	41	4				
				16	125	119	181	11	77	75	182				
				17	47	44	2	12	24	35	4				
				18	48	50	182	** K= 3	L= 9 **	-12	35	36	183		
				19	89	91	1	-12	35	36	183				

H	/FO/	/FC/	PHI	H	/FO/	/FC/	PHI	H	/FO/	/FC/	PHI	H	/FO/	/FC/	PHI
-10	106	97	2	-9	141	133	2	-1	103	95	183	-1	103	95	183
-9	45	66	357	-4	43	47	336	0	103	95	183	-1	103	95	183
-8	143	135	182	-2	176	163	182	-1	103	95	183	-1	103	95	183
-4	64	88	2	-1	312	300	1	-2	103	95	183	-1	103	95	183
0	43	41	184	0	244	231	181	3	103	95	183	-1	103	95	183
6	95	100	2	1	223	209	1	4	103	95	183	-1	103	95	183
** K= 8	L= 9	**		2	307	337	181	4	103	95	183	-1	103	95	183
				3	221	202	2	5	103	95	183	-1	103	95	183
				5	144	132	2	6	103	95	183	-1	103	95	183
				6	142	133	182	7	103	95	183	-1	103	95	183
				7	79	83	176	8	103	95	183	-1	103	95	183
				9	106	102	2	9	103	95	183	-1	103	95	183
				10	131	130	182	-10	39	31	185	-7	39	31	185
				11	23	29	176	-9	37	22	6	-4	39	31	185
				** K= 1	L= 10	**		-8	31	22	35	-3	39	31	185
								-7	197	185	1	-1	39	31	185
								-6	62	63	358	5	39	31	185
								-3	97	91	2	** K= 11	L= 10	**	
								-4	111	108	182	-4	38	35	180
								-2	33	38	335	0	42	43	1
								0	56	46	185	2	22	24	1
								2	101	96	182	** K= 1	L= 11	**	
								3	151	148	2	-11	92	88	181
								5	147	150	1	-8	55	51	181
								6	142	137	182	-4	61	58	181
								7	40	38	4	-3	67	65	18
								9	30	34	4	-2	69	68	181
								** K= 6	L= 10	**		-1	153	140	13
												1	93	92	359
												2	97	92	1
												4	140	138	16
												5	95	93	180
												7	73	71	16
												8	48	43	18
												9	102	97	16
												10	30	26	187
												** K= 2	L= 11	**	
												-12	44	46	182
												-10	53	55	182
												-7	71	71	181
												-5	81	84	18
												-3	90	90	180
												-1	104	104	181
												1	117	117	181
												3	144	144	181
												5	177	177	181
												7	217	217	181
												9	257	257	181
												11	297	297	181
												13	337	337	181
												15	377	377	181
												17	417	417	181
												19	457	457	181
												21	497	497	181
												23	537	537	181
												25	577	577	181
												27	617	617	181
												29	657	657	181
												31	697	697	181
												33	737	737	181
												35	777	777	181
												37	817	817	181
												39	857	857	181
												41	897	897	181
												43	937	937	181
												45	977	977	181
												47	1017	1017	181
												49	1057	1057	181
												51	1097	1097	181
												53	1137	1137	181
												55	1177	1177	181
												57	1217	1217	181
												59	1257	1257	181
												61	1297	1297	181
												63	1337	1337	181
												65	1377	1377	181
												67	1417	1417	181
												69	1457	1457	181
												71	1497	1497	181
												73	1537	1537	181
												75	1577	1577	181
												77	1617	1617	181
												79	1657	1657	181
												81	1697	1697	181
												83	1737	1737	181
												85	1777	1777	181
												87	1817	1817	181
												89	1857	1857	181
												91	1897	1897	181
												93	1937	1937	181
												95	1977	1977	181
												97	2017	2017	181
												99	2057	2057	181
												101	2097	2097	181
												103	2137	2137	181
												105	2177	2177	181
												107	2217	2217	181
												109	2257	2257	181

H / F0 / /FC/ PHI	H / F0 / /FC/ PHI	H / F0 / /FC/ PHI	H / F0 / /FC/ PHI
** K= 4 L= 11 **	-1 64 63 180	8 40 39 178	** K= 2 L= 13 **
-11 42 41 1	-1 24 16 182	** K= 4 L= 12 **	-3 40 39 183
-10 37 30 181	-1 34 31 0	-10 85 70 181	-7 30 30 184
-9 32 26 179	-1 29 27 0	-8 56 30 184	-10 30 30 184
-8 28 23 181	3 54 49 180	-7 45 42 3	-10 30 30 184
-7 23 18 181	** K= 10 L= 11 **	-5 67 58 3	-10 30 30 184
-6 18 13 181	-4 31 27 183	-4 85 79 182	-10 30 30 184
-5 13 8 181	-2 40 43 182	-2 85 73 183	-10 30 30 184
-4 8 3 181	0 47 37 183	0 82 78 182	-10 30 30 184
-3 3 0 181	1 38 36 3	2 81 43 183	-10 30 30 184
-2 0 0 181	2 32 26 184	3 103 105 2	-10 30 30 184
-1 0 0 181	** K= 0 L= 12 **	4 84 85 2	-10 30 30 184
0 0 0 181	-9 88 85 182	5 69 69 2	-10 30 30 184
1 0 0 181	-8 46 43 3	8 66 75 182	-10 30 30 184
2 0 0 181	-7 64 55 183	** K= 5 L= 12 **	-10 30 30 184
3 0 0 181	-6 73 67 2	-10 27 26 177	-10 30 30 184
4 0 0 181	-5 84 73 183	-9 47 48 182	-10 30 30 184
5 0 0 181	-4 94 84 183	-8 79 73 2	-10 30 30 184
6 0 0 181	-3 104 94 183	-6 71 62 2	-10 30 30 184
7 0 0 181	-2 114 104 183	-5 40 29 185	-10 30 30 184
8 0 0 181	-1 124 114 183	-4 85 77 2	-10 30 30 184
9 0 0 181	0 134 124 183	-1 60 60 183	-10 30 30 184
	1 144 134 183	1 108 100 182	-10 30 30 184
	2 154 144 183	2 71 67 3	-10 30 30 184
	3 164 154 183	3 83 80 182	-10 30 30 184
	4 174 164 183	4 71 78 182	-10 30 30 184
	5 184 174 183	6 64 71 2	-10 30 30 184
	6 194 184 183	7 36 43 183	-10 30 30 184
	7 204 194 183	** K= 6 L= 12 **	-10 30 30 184
	8 214 204 183	-9 29 26 2	-10 30 30 184
	9 224 214 183	-8 25 30 309	-10 30 30 184
		-7 45 46 1	-10 30 30 184
		-6 69 61 181	-10 30 30 184
		-4 41 42 182	-10 30 30 184
		-2 36 37 182	-10 30 30 184
		-1 36 31 3	-10 30 30 184
		2 72 69 181	-10 30 30 184
		3 79 82 181	-10 30 30 184
		** K= 7 L= 12 **	-10 30 30 184
		-4 65 49 181	-10 30 30 184
		-3 45 41 180	-10 30 30 184
		-2 85 82 181	-10 30 30 184
		-1 82 46 1	-10 30 30 184
		3 69 71 1	-10 30 30 184
		5 48 53 1	-10 30 30 184
		** K= 8 L= 12 **	-10 30 30 184
		-6 38 29 3	-10 30 30 184
		-4 43 42 3	-10 30 30 184
		-3 104 98 181	-10 30 30 184
		-1 44 46 182	-10 30 30 184
		0 63 61 2	-10 30 30 184
		2 52 52 2	-10 30 30 184
		3 39 42 182	-10 30 30 184
		** K= 9 L= 12 **	-10 30 30 184
		-3 67 33 4	-10 30 30 184
		-2 34 33 183	-10 30 30 184
		-1 23 18 6	-10 30 30 184
		0 52 54 184	-10 30 30 184
		1 24 29 4	-10 30 30 184
		2 30 50 184	-10 30 30 184
		** K= 10 L= 11 **	-10 30 30 184
		-5 31 27 183	-10 30 30 184
		-2 40 43 182	-10 30 30 184
		0 47 37 183	-10 30 30 184
		1 38 36 3	-10 30 30 184
		2 32 26 184	-10 30 30 184
		** K= 11 L= 11 **	-10 30 30 184
		-9 88 85 182	-10 30 30 184
		-8 46 43 3	-10 30 30 184
		-7 64 55 183	-10 30 30 184
		-6 73 67 2	-10 30 30 184
		-5 84 73 183	-10 30 30 184
		-4 94 84 183	-10 30 30 184
		-3 104 94 183	-10 30 30 184
		-2 114 104 183	-10 30 30 184
		-1 124 114 183	-10 30 30 184
		0 134 124 183	-10 30 30 184
		1 144 134 183	-10 30 30 184
		2 154 144 183	-10 30 30 184
		3 164 154 183	-10 30 30 184
		4 174 164 183	-10 30 30 184
		5 184 174 183	-10 30 30 184
		6 194 184 183	-10 30 30 184
		7 204 194 183	-10 30 30 184
		8 214 204 183	-10 30 30 184
		9 224 214 183	-10 30 30 184

1.3. Structure Factors for I(c)

H /FO/ /FC/ PHI	H /FO/ /FC/ PHI	H /FO/ /FC/ PHI	H /FO/ /FC/ PHI
** K= 0 L= 0 **	2 42 45 0	-2 80 74 0	-2 48 41 0
2 2436 2230 180	3 49 58 180	-1 400 406 0	0 126 93 180
4 388 378 0	** K= 11 L= 0 **	0 147 138 0	1 37 43 0
** K= 1 L= 0 **	3 35 27 0	1 196 191 180	2 32 45 0
0 1137 1519 180	5 37 33 180	2 242 241 180	3 45 39 180
1 758 790 0	** K= 12 L= 0 **	3 148 164 180	4 34 29 180
2 1300 1274 0	0 39 24 180	4 246 249 0	** K= 0 L= 2 **
3 354 343 180	** K= 0 L= 1 **	** K= 5 L= 1 **	-8 197 251 180
4 307 307 180	-7 169 187 180	-7 45 49 0	-6 382 409 0
6 129 146 0	-5 899 887 0	-6 148 154 180	-4 678 669 180
** K= 2 L= 0 **	-3 1837 1672 180	-4 246 253 0	-2 134 79 180
0 295 358 180	-1 430 424 0	-3 37 48 0	0 13 27 180
1 122 65 0	1 288 198 0	-2 131 117 180	2 1043 1054 180
2 203 202 180	3 390 370 180	-1 174 139 180	4 62 60 0
4 181 182 0	5 207 232 0	0 167 167 0	6 48 46 0
5 130 122 180	7 166 147 180	1 159 166 0	8 43 55 180
7 46 45 0	** K= 1 L= 1 **	3 116 123 180	** K= 1 L= 2 **
** K= 3 L= 0 **	-7 131 140 0	4 129 121 180	-9 84 106 0
0 437 450 180	-6 141 166 180	6 78 85 0	-8 87 80 0
2 212 190 0	-5 368 392 180	** K= 6 L= 1 **	-7 270 279 180
3 101 73 0	-4 628 588 0	-6 50 54 0	-6 128 123 180
4 231 241 180	-3 581 563 0	-4 111 96 180	-5 335 342 0
6 65 75 180	-2 1995 1851 180	-3 82 105 0	-4 66 47 180
** K= 4 L= 0 **	-1 94 59 180	-2 95 79 0	-2 137 157 180
0 165 148 0	0 223 251 0	-1 85 95 180	0 47 44 180
1 101 161 180	1 63 115 180	1 98 108 180	1 343 284 0
2 562 577 180	2 133 125 180	2 48 81 180	2 143 186 180
4 319 333 0	3 49 34 180	3 129 111 0	3 87 30 180
5 82 93 0	4 51 66 180	5 91 120 180	4 91 70 180
6 51 72 180	5 204 180 180	7 38 46 0	6 85 95 180
** K= 5 L= 0 **	7 55 72 0	** K= 7 L= 1 **	7 104 120 0
0 284 308 180	** K= 2 L= 1 **	-1 63 37 180	** K= 2 L= 2 **
1 478 467 0	-5 67 68 180	1 112 76 0	-9 36 66 180
2 234 243 0	-4 219 210 180	2 105 96 0	-7 107 119 0
3 146 135 180	-2 199 210 180	4 61 59 180	-6 54 71 180
4 97 93 180	-1 216 249 0	** K= 8 L= 1 **	-4 257 247 0
7 54 54 0	0 176 228 180	-4 75 69 0	-3 168 133 180
** K= 6 L= 0 **	1 149 140 0	0 45 30 0	-2 230 234 180
1 193 176 180	2 66 103 0	2 49 51 180	-1 404 471 180
2 56 79 0	3 117 109 180	3 39 41 0	0 45 15 180
3 91 92 0	4 213 257 180	4 91 100 0	1 198 197 0
4 52 62 180	5 91 88 0	6 34 30 180	2 107 142 0
** K= 7 L= 0 **	6 122 129 180	7 29 22 180	3 423 425 0
0 43 46 180	** K= 3 L= 1 **	** K= 9 L= 1 **	4 94 87 180
3 71 72 180	-8 47 47 180	-6 50 53 0	5 181 163 0
4 41 47 180	-6 117 95 0	-4 49 42 180	7 108 112 180
5 50 46 0	-4 113 90 180	-3 62 74 0	** K= 3 L= 2 **
** K= 8 L= 0 **	-3 156 192 0	-2 56 81 0	-4 87 91 0
3 45 27 0	-2 51 114 180	2 57 71 0	-3 301 304 0
** K= 9 L= 0 **	-1 235 247 180	3 73 61 180	-2 350 359 0
1 125 106 180	0 279 270 180	7 29 24 0	-1 450 462 180
3 53 53 0	1 257 280 180	** K= 10 L= 1 **	0 65 84 180
** K= 10 L= 0 **	2 253 262 0	-3 62 64 180	1 144 92 0
3 126 109 180	3 426 411 0	-2 59 52 180	2 124 96 180
	4 212 242 180	-1 57 44 0	3 42 1 0
	6 83 71 0	0 56 87 0	4 348 354 0
	** K= 4 L= 1 **	1 46 33 180	** K= 4 L= 2 **
	-5 79 93 0	2 44 47 180	-8 64 67 180
	-3 126 109 180	4 39 51 0	-7 42 55 0
		** K= 11 L= 1 **	-6 95 94 0
			-5 92 90 180
			-4 101 77 180
			-3 158 146 180

H	/FO/	/FC/	PHI	H	/FO/	/FC/	PHI	H	/FO/	/FC/	PHI	H	/FO/	/FC/	PHI
-2	158	166	0												
-1	519	530	0												
0	43	68	180												
1	373	374	180												
2	189	227	0												
3	93	103	180												
4	90	70	180												
5	62	63	180												
6	54	53	0												
** K= 5 L= 2 **															
-9	45	62	0												
-7	72	85	180												
-5	136	141	0												
-4	139	140	0												
-3	167	188	180												
-2	196	201	180												
-1	127	130	180												
0	128	88	0												
1	471	466	0												
2	70	50	180												
3	323	320	180												
4	55	44	0												
5	69	67	0												
** K= 6 L= 2 **															
-7	43	47	0												
-5	37	42	180												
-4	51	24	180												
-3	56	42	0												
-2	77	56	0												
-1	141	136	0												
1	87	93	180												
2	143	146	0												
3	66	38	0												
4	65	59	180												
5	56	36	180												
8	36	36	0												
** K= 7 L= 2 **															
-4	53	51	0												
-3	48	48	0												
-1	65	56	180												
1	95	103	0												
2	76	96	0												
4	85	83	180												
6	66	67	0												
** K= 8 L= 2 **															
-4	34	40	0												
-1	36	59	0												
1	89	91	180												
4	70	73	0												
** K= 9 L= 2 **															
-4	61	54	180												
-1	54	47	180												
1	58	48	180												
2	74	92	0												
3	76	57	0												
4	86	69	180												
** K= 10 L= 2 **															
-6	25	15	0												
-2	64	47	180												
2	85	82	180												
** K= 12 L= 2 **															
3	35	25	0												
** K= 0 L= 3 **															
-9	112	128	180												
-7	93	80	0												
-5	225	249	0												
-3	739	729	180												
-1	1439	1369	0												
1	125	41	0												
3	110	104	180												
5	40	27	0												
7	120	115	0												
** K= 1 L= 3 **															
-7	69	87	0												
-6	103	98	0												
-5	171	156	180												
-4	153	166	0												
-3	225	191	0												
-2	312	286	180												
-1	626	667	180												
0	495	523	0												
1	698	780	0												
2	384	400	0												
3	220	224	0												
6	59	71	180												
7	68	81	180												
** K= 2 L= 3 **															
-9	48	73	0												
-7	131	135	180												
-6	44	63	0												
-5	166	177	0												
-4	154	168	0												
-3	196	195	180												
-2	111	107	0												
-1	204	157	0												
0	383	485	0												
1	588	595	180												
2	232	301	180												
3	321	329	0												
4	133	150	0												
5	188	196	180												
6	73	94	0												
** K= 3 L= 3 **															
-8	72	88	0												
-6	142	147	180												
-5	133	139	180												
-4	62	69	0												
-3	275	267	0												
-2	157	192	0												
-1	99	94	0												
0	52	80	0												
1	394	442	180												
2	150	136	0												
3	504	474	180												
5	169	154	0												
** K= 4 L= 3 **															
-8	36	42	180												
-7	71	64	0												
-6	165	164	0												
-5	55	71	180												
-4	283	280	180												
-2	131	89	0												
-1	117	118	0												
0	46	20	0												
1	125	151	180												
2	160	168	180												
3	124	134	0												
4	135	152	0												
** K= 5 L= 3 **															
-6	86	82	180												
-5	70	60	0												
-4	248	258	0												
-3	34	34	0												
-2	343	370	180												
0	360	345	0												
1	117	135	0												
2	64	53	180												
3	61	44	180												
4	108	106	180												
5	56	67	0												
** K= 6 L= 3 **															
-5	73	71	0												
-4	158	130	180												
-3	47	52	180												
-2	143	155	0												
1	34	18	0												
2	59	57	180												
3	65	80	0												
4	47	48	180												
5	35	18	180												
** K= 7 L= 3 **															
-5	62	54	180												
-4	88	92	0												
-2	91	98	180												
-1	162	137	180												
0	72	67	180												
1	183	175	0												
3	45	30	180												
4	67	76	0												
5	74	59	180												
6	52	51	180												
7	34	45	0												
** K= 8 L= 3 **															
-4	58	66	180												
-3	52	61	180												
2	50	60	0												
3	66	77	180												
4	102	91	180												
5	50	56	0												
** K= 9 L= 3 **															
-6	31	34	180												
-1	60	73	180												
0	36	49	180												
2	48	41	180												
3	82	77	0												
** K= 10 L= 3 **															
-1	87	66	0												
0	54	65	180												
4	30	28	0												
** K= 11 L= 3 **															
-1	39	27	0												
2	52	15	0												
** K= 12 L= 3 **															
-3	33	22	0												
-1	43	31	180												
0	33	26	180												
2	45	35	0												
3	33	24	180												
** K= 0 L= 4 **															
-8	49	69	180												
-6	271	294	0												
-4	341	348	180												
-2	186	197	0												
0	260	253	0												
2	775	763	0												
6	190	174	180												
** K= 1 L= 4 **															
-9	41	31	180												
-7	39	58	180												
-6	81	81	180												
-5	93	71	0												
-4	216	211	0												
-3	94	89	0												
-2	173	212	0												
-1	664	756	180												
0	391	432	180												
1	83	72	0												
2	104	134	0												
3	71	67	180												
4	107	122	0												
6	48	35	0												
** K= 2 L= 4 **															
-8	41	53	180												
-5	67	55	0												
-3	34	64	180												
-2	179	191	0												
-1	60	75	180												
0	58	95	0												
1	406	419	180												
2	247	250	180												
3	77	55	180												
4	185	166	0												
5	58	60	0												
7	97	116	180												
8	52	47	0												
** K= 3 L= 4 **															
-8	34	45	0												
-6	95	103	180												
-2	163	167	180												
-1	51	38	0												
0	210	251	0												
1	51	48	180												
2	95	106	0												
3	248	252	0												
4	135	120	180												
5	100	89	180												
** K= 4 L= 4 **															
-6	94	84	0												
-4	127	149	180												
-3	103	127	180												
-2	198	220	0												
-1	521	574	0												

H /FO/ /FC/ PHI	H /FO/ /FC/ PHI	H /FO/ /FC/ PHI	H /FO/ /FC/ PHI
0 222 242 180	2 27 20 180	-8 42 42 180	** K= 1 L= 6 **
1 26 17 180	** K= 0 L= 5 **	-6 78 71 0	-6 59 51 180
2 135 117 180	-9 65 89 180	-5 66 81 0	-3 58 66 0
3 151 158 180	-7 75 73 0	-4 144 151 180	-2 159 147 0
4 64 67 180	-3 88 62 180	-3 301 320 180	-1 361 360 0
5 144 153 0	-1 156 145 180	0 159 159 0	0 567 603 180
6 49 56 0	1 522 586 180	2 33 42 180	2 234 278 0
** K= 3 L= 4 **	5 83 85 0	4 54 40 180	4 89 68 0
-3 57 75 0	7 95 100 180	5 74 66 180	5 75 72 180
-2 75 54 180	** K= 1 L= 5 **	** K= 6 L= 5 **	6 133 146 180
-1 115 131 180	-9 29 28 0	-4 77 67 0	7 55 52 0
0 180 188 0	-8 60 77 180	-3 100 104 0	8 59 64 0
1 76 88 0	-4 61 72 0	-2 90 75 180	** K= 2 L= 6 **
2 207 240 180	-2 201 207 0	-1 97 57 180	-5 49 47 0
4 82 96 180	-2 201 207 0	2 121 115 0	-4 136 134 0
** K= 6 L= 4 **	-1 82 34 0	5 46 35 180	-2 116 129 180
-6 39 44 180	0 852 869 180	7 52 44 0	-1 45 66 180
-4 63 57 0	1 260 240 180	** K= 7 L= 5 **	0 273 290 180
-3 205 218 180	2 123 114 0	-7 28 26 180	1 78 5 180
-2 124 123 180	3 224 172 0	-5 69 77 0	2 61 75 0
-1 96 86 0	4 59 35 0	0 46 51 0	3 128 91 0
0 59 55 180	5 234 210 180	-2 42 31 0	4 154 128 180
2 58 52 0	6 99 91 0	0 46 51 0	5 215 222 0
3 75 48 180	7 65 64 0	1 185 170 0	7 88 114 180
6 70 59 180	** K= 2 L= 5 **	3 161 167 180	8 38 41 180
7 37 29 180	-4 92 97 180	4 115 100 0	9 34 42 0
8 40 46 0	-3 115 115 0	5 142 121 0	** K= 3 L= 6 **
** K= 7 L= 4 **	-2 83 93 0	6 111 121 180	-5 63 53 180
-5 51 41 180	-1 327 306 180	8 56 74 0	-4 201 209 180
-4 44 38 0	0 257 267 0	** K= 8 L= 5 **	-3 68 88 0
-2 104 125 180	1 665 676 0	-7 26 14 0	-2 199 191 0
1 67 75 180	2 527 554 180	-5 46 50 0	-1 310 332 0
2 54 59 0	3 224 246 180	-4 49 62 0	0 138 145 0
4 52 56 180	4 184 217 0	-3 63 65 180	1 520 526 180
5 50 40 180	5 79 89 0	-2 55 38 0	2 249 238 180
6 93 83 0	** K= 3 L= 5 **	-1 121 118 0	3 133 130 0
7 31 7 180	-9 41 32 0	1 103 92 180	5 66 73 180
8 57 74 180	-3 100 120 0	3 115 106 0	6 54 64 0
** K= 8 L= 4 **	-2 102 91 0	4 134 124 180	7 74 71 0
-1 71 57 180	-1 345 346 0	6 113 123 0	8 57 76 180
3 115 97 0	0 489 526 180	7 42 58 180	** K= 4 L= 6 **
4 62 43 0	1 541 580 180	** K= 9 L= 5 **	-3 36 40 0
7 40 52 0	2 206 229 180	-3 78 71 0	-7 57 70 0
** K= 9 L= 4 **	3 311 316 0	3 42 25 180	-6 45 41 180
-5 31 26 180	4 118 153 0	5 42 42 180	-5 112 104 180
-4 30 42 0	5 97 102 0	** K= 11 L= 5 **	-4 42 35 180
-3 97 92 0	6 74 81 180	2 31 31 180	-3 36 15 180
-1 67 69 180	** K= 4 L= 5 **	3 33 44 180	-2 83 70 0
1 107 94 0	-8 35 30 0	** K= 12 L= 5 **	-1 137 126 180
2 60 60 0	-5 75 72 180	-1 51 36 0	0 274 291 0
3 47 45 180	-4 37 44 180	0 30 34 180	1 191 212 0
** K= 10 L= 4 **	-3 86 102 0	2 63 56 0	2 87 89 180
-1 75 77 0	-2 146 149 180	** K= 0 L= 6 **	3 191 214 180
0 56 41 0	-1 77 104 180	-6 80 94 0	8 42 59 0
1 54 58 180	0 113 95 0	-2 460 437 180	** K= 5 L= 6 **
** K= 11 L= 4 **	1 103 100 0	0 33 90 180	-6 48 68 0
-1 46 44 180	2 83 89 180	2 146 200 0	-5 126 144 0
** K= 12 L= 4 **	3 168 151 180	6 73 45 0	-4 72 56 0
	4 98 99 180		-3 144 168 180
	5 60 59 0		-1 99 115 0
	6 50 48 0		0 64 59 0
	** K= 5 L= 5 **		1 88 88 180
			2 70 31 0
			3 120 127 0

H /FO/ /FC/ PHI	H /FO/ /FC/ PHI	H /FO/ /FC/ PHI	H /FO/ /FC/ PHI
4 62 75 0	-3 177 181 0	-2 34 28 0	0 310 241 180
6 45 60 0	-1 107 103 180	0 38 46 180	2 415 386 0
** K= 6 L= 6 **	1 55 32 0	1 118 135 0	6 160 132 180
-6 41 39 0	3 235 257 0	2 45 49 0	** K= 1 L= 8 **
-5 46 38 180	5 220 255 180	3 146 151 180	-5 90 88 180
-3 172 168 0	7 159 161 0	4 55 78 0	-4 83 84 0
1 47 31 0	** K= 1 L= 7 **	6 60 55 180	-3 122 111 0
2 112 105 0	-8 33 20 180	** K= 6 L= 7 **	-2 65 64 180
3 70 67 180	-7 41 43 0	-4 107 104 180	0 122 141 0
5 64 67 0	-5 52 45 180	-2 44 30 180	1 57 31 0
7 55 48 180	-4 65 53 0	1 58 52 180	2 39 55 180
** K= 7 L= 6 **	-3 66 69 0	2 31 33 180	3 37 40 180
-5 45 44 0	-2 77 101 0	4 67 43 180	4 78 64 180
-4 95 94 0	-1 162 153 180	6 94 100 180	6 133 134 0
-3 83 90 180	0 430 449 180	** K= 7 L= 7 **	** K= 2 L= 8 **
-2 113 92 180	1 58 54 0	-3 56 53 180	-3 134 130 180
-1 111 112 0	2 154 175 0	0 224 228 180	-2 203 201 0
0 83 73 0	3 34 58 0	1 46 62 0	-1 627 656 0
1 151 166 180	4 33 44 180	3 141 137 180	1 653 681 180
2 75 36 180	5 146 125 0	5 190 180 0	2 288 265 0
3 245 274 0	7 68 90 180	7 98 108 180	3 135 165 0
4 34 42 180	8 61 73 180	** K= 8 L= 7 **	4 118 137 180
5 137 124 180	** K= 2 L= 7 **	-6 41 45 180	5 80 61 180
6 64 74 0	-3 85 81 0	-4 64 59 0	8 56 56 0
8 56 74 180	-2 280 285 0	-3 87 101 180	** K= 3 L= 8 **
** K= 8 L= 6 **	-1 167 185 180	-2 116 122 180	-7 57 65 0
-6 60 61 0	0 69 85 180	-1 198 194 0	-6 53 63 0
-4 69 59 180	2 392 374 180	0 83 59 0	-5 121 136 180
-3 49 64 0	3 137 138 0	1 287 297 180	-4 88 91 180
-2 50 42 0	4 360 340 0	2 38 40 0	-3 287 310 0
-1 203 199 180	5 94 96 180	3 185 178 0	-1 500 509 180
1 256 269 0	6 179 172 180	4 83 90 180	0 297 290 0
2 176 159 180	7 54 52 0	5 81 78 180	1 291 256 0
3 225 205 180	8 75 99 0	6 40 53 0	2 349 331 180
4 172 175 0	** K= 3 L= 7 **	7 48 46 0	3 110 106 180
6 98 97 180	-8 44 40 0	** K= 9 L= 7 **	4 313 289 0
7 48 49 0	-6 51 41 180	-3 105 102 0	5 59 70 0
** K= 9 L= 6 **	-4 52 86 180	-1 171 169 180	6 84 98 180
-6 45 53 180	-3 64 47 180	0 83 84 0	7 59 50 180
-3 69 70 180	-2 189 227 0	1 128 120 0	** K= 4 L= 8 **
-2 49 69 180	-1 72 41 0	2 72 79 180	-5 58 57 0
-1 86 70 0	0 124 105 0	4 46 32 0	-4 46 53 0
0 44 29 180	1 150 172 0	** K= 10 L= 7 **	-3 107 112 180
1 102 88 180	2 292 334 0	-3 34 16 180	-2 35 45 180
2 129 121 0	3 349 357 180	-1 48 24 0	-1 132 128 0
4 100 87 180	4 109 84 180	** K= 11 L= 7 **	0 201 234 180
** K= 10 L= 6 **	5 160 159 0	1 32 25 0	1 98 81 0
-2 34 31 0	6 62 50 0	2 39 38 0	2 70 81 0
** K= 11 L= 6 **	7 92 101 180	4 27 17 180	3 153 173 180
3 44 37 0	9 34 55 0	** K= 12 L= 7 **	4 89 82 180
4 40 20 180	** K= 4 L= 7 **	-1 31 24 0	** K= 5 L= 8 **
** K= 12 L= 6 **	-6 81 73 0	1 34 25 180	-4 104 97 180
-1 57 53 180	-5 38 23 0	** K= 0 L= 8 **	-2 89 80 180
1 56 53 0	-3 175 176 180	-8 38 30 0	0 47 57 0
** K= 0 L= 7 **	-1 195 170 0	-6 60 60 180	1 196 171 180
-7 65 45 180	0 73 93 0	-4 95 104 0	2 31 39 180
-5 87 91 0	1 48 17 0	-2 69 76 180	3 170 142 0
	2 31 36 0		4 169 168 180
	3 228 188 0		** K= 6 L= 8 **
	5 216 210 180		-5 50 48 0
	6 118 128 0		-3 76 81 180
	** K= 5 L= 7 **		
	-3 74 56 0		

H	/FO/	/FC/	PHI	H	/FO/	/FC/	PHI	H	/FO/	/FC/	PHI	H	/FO/	/FC/	PHI
-1	82	85	180	4	126	135	180	-1	113	108	180	** K=	4	L=	10 **
0	131	103	180	5	144	151	180	0	210	206	0	-8	34	42	0
1	46	68	180	6	71	70	180	1	43	53	0	-5	110	115	0
2	39	12	0	** K=	3	L=	9 **	2	57	64	180	-3	164	145	180
3	252	264	0	-6	55	61	180	4	62	53	180	1	204	198	0
5	89	96	180	-5	56	57	0	5	43	61	0	2	234	247	0
6	38	46	180	-3	289	313	180	6	57	63	0	4	49	56	180
** K=	7	L=	8 **	-2	101	113	0	** K=	9	L=	9 **	6	41	44	180
-5	118	111	180	-1	473	473	0	-5	30	24	0	** K=	5	L=	10 **
-3	153	116	0	0	369	391	180	-4	93	97	180	-7	33	39	0
-2	37	54	180	1	200	203	180	-2	83	95	0	-4	164	155	0
-1	99	104	180	3	99	96	180	0	59	60	180	-3	86	101	0
0	147	140	0	4	74	83	180	5	31	30	180	-2	81	72	180
1	127	143	0	5	67	92	0	** K=	10	L=	9 **	-1	68	57	180
2	209	219	180	** K=	4	L=	9 **	-3	48	43	180	0	157	156	0
3	95	92	180	-5	141	131	180	-2	33	37	180	1	62	54	180
4	172	180	0	-3	172	183	0	0	46	50	0	2	70	55	180
** K=	8	L=	8 **	-2	263	234	180	2	51	45	180	3	96	114	0
-6	28	46	0	-1	197	208	180	3	45	30	0	4	90	88	0
-5	82	83	0	0	242	224	0	** K=	0	L=	10 **	** K=	6	L=	10 **
-4	113	116	180	1	209	209	0	-8	60	67	180	-5	66	69	180
-3	90	74	180	2	233	220	180	-6	91	93	0	-4	52	41	180
-2	195	198	0	3	77	96	180	-4	42	22	180	-3	147	169	0
-1	55	38	0	** K=	5	L=	9 **	-2	109	80	0	-2	126	122	0
0	68	81	180	-5	65	68	0	0	287	276	180	-1	150	168	180
1	62	73	0	-4	72	78	180	2	234	228	0	0	161	147	180
2	72	54	0	-3	75	66	180	4	153	166	180	1	138	139	0
3	119	116	180	-2	101	96	0	6	81	80	0	2	255	259	0
5	81	66	0	-1	138	145	180	** K=	1	L=	10 **	3	146	154	180
7	33	7	0	0	123	121	180	-7	33	22	180	4	114	113	180
** K=	9	L=	8 **	1	148	147	0	-6	91	109	180	** K=	7	L=	10 **
-6	32	44	180	2	129	128	0	-4	111	130	0	-4	110	117	180
-4	80	90	0	3	68	57	0	-2	244	280	180	-3	84	73	180
-2	45	37	180	4	72	72	180	-2	244	280	180	-2	60	49	0
-1	102	91	0	** K=	6	L=	9 **	-1	79	79	180	-1	115	108	0
1	57	64	180	-4	94	90	0	0	426	426	0	0	91	93	0
3	42	43	0	-2	73	67	0	1	124	117	0	1	208	205	180
** K=	11	L=	8 **	-1	90	85	0	2	406	396	180	2	211	190	180
-1	45	37	180	0	106	116	180	3	176	162	180	3	171	174	0
** K=	0	L=	9 **	1	104	85	180	4	79	97	0	4	116	130	0
-3	114	94	0	2	61	78	0	** K=	2	L=	10 **	5	55	58	180
1	118	108	180	3	67	53	0	-5	105	109	180	6	67	69	180
5	47	39	0	4	87	72	0	-4	60	60	180	7	35	35	180
** K=	1	L=	9 **	5	78	76	180	-3	169	165	0	** K=	8	L=	10 **
-7	58	54	180	7	64	67	0	-2	180	168	0	-6	53	46	180
-4	98	95	0	** K=	7	L=	9 **	-1	200	204	180	-5	53	60	0
-3	125	139	0	-3	57	53	180	0	406	402	180	-2	45	45	0
-1	210	203	180	-2	82	80	0	2	90	97	0	0	89	69	180
0	62	35	180	-1	192	211	0	3	131	130	0	1	62	60	0
1	187	178	0	0	46	59	180	4	115	113	180	2	41	52	180
3	177	182	180	1	206	217	180	5	62	81	180	3	78	73	180
6	50	33	0	2	75	72	0	6	55	59	0	** K=	9	L=	10 **
** K=	2	L=	9 **	4	93	109	0	** K=	3	L=	10 **	-5	55	60	180
-4	124	138	180	5	49	36	0	-6	54	64	0	-2	36	49	180
-2	64	62	0	6	78	87	180	-4	62	59	180	3	43	56	180
-1	148	146	180	7	53	46	180	-2	115	116	180	** K=	10	L=	10 **
1	60	86	180	** K=	8	L=	9 **	-1	196	202	0	0	34	47	180
2	171	150	0	-5	69	73	180	0	78	90	0	** K=	11	L=	10 **
3	208	225	0	-4	59	69	0	2	63	79	180				
				-3	101	97	0	4	106	97	0				
				-2	171	174	180	6	58	57	180				
								7	60	58	0				

H /FO/ /FC/ PHI	H /FO/ /FC/ PHI	H /FO/ /FC/ PHI	H /FO/ /FC/ PHI
1 38 24 180	4 208 207 0	5 46 35 0	1 128 128 180
** K= 0 L= 11 **	5 52 73 180	** K= 2 L= 12 **	3 133 128 0
-7 37 27 180	6 53 50 180	-8 44 51 0	4 35 32 180
-5 43 55 180	** K= 6 L= 11 **	-6 79 89 180	** K= 8 L= 12 **
-3 129 125 0	-6 73 89 180	-4 135 140 0	-5 34 38 0
-1 82 62 180	-5 82 95 180	-3 118 115 0	-4 33 39 180
3 103 110 180	-4 53 57 0	-2 149 154 180	-3 49 54 180
** K= 1 L= 11 **	-3 137 112 0	-1 82 79 180	0 68 59 0
-6 64 68 180	-2 47 55 180	0 162 146 0	1 45 51 0
-5 96 107 0	-1 182 181 180	1 88 94 0	** K= 9 L= 12 **
-4 82 75 0	0 198 186 180	5 67 67 180	-4 29 29 0
-3 193 205 180	1 95 86 0	7 45 59 0	** K= 10 L= 12 **
-2 117 101 180	2 253 273 0	** K= 3 L= 12 **	** K= 11 L= 12 **
-1 127 140 0	4 169 173 180	-6 81 82 0	0 54 44 0
0 194 167 0	5 54 42 180	-5 66 53 0	** K= 11 L= 12 **
1 65 49 180	6 38 40 0	-4 129 130 180	0 35 26 180
2 142 131 180	** K= 7 L= 11 **	-3 93 83 180	2 35 20 0
5 60 49 0	-3 41 50 180	-2 103 109 0	** K= 0 L= 13 **
** K= 2 L= 11 **	-3 64 53 180	-1 42 43 180	-7 51 78 0
-5 35 37 180	-2 91 79 0	0 81 67 180	-5 71 71 180
-4 42 20 180	-1 104 93 0	1 52 51 180	-3 49 35 0
-3 100 116 0	0 97 98 180	** K= 4 L= 12 **	1 81 55 0
-2 68 48 0	1 104 93 180	-7 43 43 0	** K= 1 L= 13 **
-1 62 58 180	2 122 103 180	-5 53 60 180	-7 34 55 180
0 76 67 180	3 110 85 0	-4 69 90 0	-6 42 42 0
1 210 231 0	4 113 110 0	0 122 111 180	-5 79 91 0
2 233 228 0	6 58 68 180	1 99 97 0	-3 153 150 180
3 54 44 180	** K= 8 L= 11 **	3 118 101 180	-1 210 217 0
4 146 137 180	-1 37 46 0	5 74 75 180	2 75 51 180
7 55 53 0	0 62 69 0	** K= 5 L= 12 **	3 76 74 180
** K= 3 L= 11 **	4 48 39 180	-7 34 46 180	4 35 26 180
-7 54 67 0	** K= 9 L= 11 **	-6 45 46 0	6 82 79 0
-5 80 75 180	-2 51 52 180	-5 56 50 0	8 53 72 180
-2 63 75 180	0 85 84 0	-4 76 81 180	** K= 2 L= 13 **
-1 224 258 0	4 33 22 0	-3 102 110 180	-5 55 53 180
0 269 280 0	** K= 10 L= 11 **	-2 45 23 180	-3 107 113 0
1 192 169 180	-2 43 33 0	-1 126 130 0	-2 42 40 180
2 55 50 0	0 39 30 180	0 49 50 180	-1 167 182 180
3 84 75 0	3 35 35 180	1 53 64 180	1 85 97 180
6 53 55 180	** K= 11 L= 11 **	2 122 124 0	2 67 67 0
** K= 4 L= 11 **	-2 26 21 0	3 88 75 180	6 86 101 180
-5 61 61 0	3 52 39 0	4 60 75 180	** K= 3 L= 13 **
-4 38 22 0	** K= 0 L= 12 **	5 62 45 0	-3 58 53 180
-2 101 109 0	-2 49 49 180	6 38 39 180	-2 78 93 180
-1 219 212 180	-2 92 83 0	** K= 6 L= 12 **	0 54 41 0
0 88 87 180	4 36 34 0	-7 25 16 180	2 79 48 180
1 90 86 0	6 46 55 0	-6 66 74 180	3 53 64 180
2 101 100 0	8 55 62 180	-4 120 120 0	6 63 69 0
3 44 39 0	** K= 1 L= 12 **	-3 147 154 0	** K= 4 L= 13 **
4 120 129 180	-2 47 46 180	-2 129 114 180	-3 44 35 0
6 122 133 0	-2 92 83 0	-1 168 174 180	-2 98 101 180
** K= 5 L= 11 **	4 36 34 0	0 51 41 0	0 91 82 0
-7 34 58 180	6 122 133 0	1 71 70 0	1 48 46 180
-5 58 58 0	** K= 11 L= 11 **	2 62 56 180	2 51 56 180
-4 45 42 0	-2 26 21 0	5 106 98 0	3 97 90 0
-3 97 89 180	3 52 39 0	** K= 7 L= 12 **	4 39 40 0
-2 68 57 180	** K= 0 L= 12 **	-5 49 52 180	
-1 71 66 0	-4 49 49 180	-4 57 64 180	
0 142 126 0	-2 92 83 0	-2 177 161 0	
1 63 80 180	4 36 34 0	-1 116 95 0	
2 256 259 180	6 46 55 0	0 131 124 180	
	8 55 62 180		

H /FO/ /FC/ PHI	H /FO/ /FC/ PHI	H /FO/ /FC/ PHI	H /FO/ /FC/ PHI
** K= 5 L= 13 **	4 58 61 180	5 104 103 180	2 131 145 180
-5 68 78 0	6 64 55 0	6 86 88 0	4 258 255 0
-4 78 64 180	7 55 50 180	7 62 67 0	6 162 162 180
-2 78 77 0	** K= 3 L= 14 **	8 53 70 180	8 44 66 0
-1 55 62 180	-4 38 24 0	** K= 2 L= 15 **	** K= 1 L= 16 **
0 100 90 180	1 112 137 0	-5 42 46 0	-5 63 65 0
2 102 90 0	4 38 81 0	-4 61 51 0	-3 98 87 180
3 128 133 0	** K= 4 L= 14 **	-3 41 42 180	-2 106 113 0
4 86 89 180	1 69 84 0	-1 60 69 0	0 140 140 180
5 47 45 0	2 50 61 0	0 40 35 180	1 79 106 0
** K= 6 L= 13 **	3 41 26 180	4 100 88 0	2 186 173 0
-4 126 127 0	** K= 5 L= 14 **	** K= 3 L= 15 **	3 115 109 180
-3 44 47 0	-2 50 36 0	-5 43 40 180	4 100 95 180
-2 77 79 180	-1 121 120 0	-3 53 49 0	5 172 179 0
-1 66 66 180	1 117 99 180	1 66 59 0	7 121 135 180
0 104 110 0	2 67 71 180	3 110 107 180	** K= 2 L= 16 **
1 169 155 0	6 32 27 180	4 48 43 0	-5 43 42 180
2 131 127 180	** K= 6 L= 14 **	5 42 53 0	-3 60 56 0
3 69 51 180	-4 58 59 0	6 64 60 180	-1 79 80 0
4 51 41 0	-2 59 47 180	** K= 4 L= 15 **	1 165 158 180
5 47 36 180	2 134 129 0	-5 38 30 0	3 128 139 0
7 33 44 0	3 100 103 180	1 144 136 180	4 38 52 180
** K= 7 L= 13 **	4 50 68 180	3 100 94 0	5 106 104 180
-5 73 74 180	7 43 41 180	4 76 73 180	6 65 61 0
-4 54 51 180	** K= 7 L= 14 **	7 45 41 180	7 43 52 0
-2 118 121 0	-3 34 43 0	** K= 5 L= 15 **	8 55 63 180
0 77 85 180	-1 40 49 180	-6 31 36 0	** K= 3 L= 16 **
2 45 57 0	1 64 61 180	-4 60 55 180	-1 61 54 180
** K= 8 L= 13 **	3 68 77 0	0 62 57 0	2 59 47 180
-5 25 18 0	5 38 41 180	4 54 57 180	3 51 55 180
-3 34 31 180	** K= 8 L= 14 **	5 41 41 180	5 71 53 0
0 41 32 0	0 50 34 0	6 59 73 0	** K= 4 L= 16 **
4 52 41 0	6 46 37 0	** K= 6 L= 15 **	-2 46 52 0
** K= 9 L= 13 **	** K= 9 L= 14 **	-1 56 60 180	2 138 130 180
-4 34 32 180	3 51 31 0	0 71 80 0	3 83 69 0
-3 28 22 0	5 34 26 180	1 68 62 0	4 94 104 0
-2 36 30 0	** K= 10 L= 14 **	2 60 67 180	5 85 75 180
2 39 26 0	-2 43 46 180	4 75 92 0	** K= 5 L= 16 **
** K= 10 L= 13 **	2 49 37 180	** K= 7 L= 15 **	1 48 50 0
-3 26 21 180	** K= 0 L= 15 **	-2 91 90 0	2 63 67 0
** K= 0 L= 14 **	-5 45 35 180	0 87 96 180	3 117 123 180
-2 127 144 0	-3 74 77 180	** K= 8 L= 15 **	5 72 69 0
0 266 245 180	-1 220 191 0	1 45 37 0	** K= 6 L= 16 **
4 73 74 0	1 117 99 180	3 39 30 180	-4 42 48 0
8 67 67 180	3 74 70 180	** K= 9 L= 15 **	-2 34 31 180
** K= 1 L= 14 **	5 131 124 0	0 48 36 180	-1 84 86 0
-2 132 140 180	7 126 148 180	** K= 10 L= 15 **	0 40 43 180
0 148 161 0	** K= 1 L= 15 **	0 31 31 180	1 93 100 180
2 54 58 180	-1 109 116 180	2 39 39 0	2 56 59 0
3 51 44 180	0 96 117 0	** K= 0 L= 16 **	3 69 60 0
6 55 62 180	1 36 45 0	-4 44 29 0	4 45 52 180
8 38 42 0	2 45 44 180	-2 109 93 180	5 36 21 180
** K= 2 L= 14 **	3 110 91 0	0 218 199 0	6 39 46 0
-3 58 62 180	0 109 116 180	** K= 7 L= 16 **	** K= 7 L= 16 **
-2 100 90 0	1 36 45 0	-3 50 58 0	-3 50 58 0
-1 40 22 180	2 45 44 180	-2 41 41 180	0 75 75 0
	3 110 91 0	1 56 55 0	1 56 55 0
		2 62 68 180	2 62 68 180

H /FD/ /FC/ PHI	H /FD/ /FC/ PHI	H /FD/ /FC/ PHI	H /FD/ /FC/ PHI
3 53 49 180	-2 75 73 0	1 68 67 180	-5 30 35 180
6 29 28 180	0 89 66 180	3 109 105 0	-4 49 52 180
** K= 8 L= 16 **	1 30 65 0	5 60 59 180	-2 62 53 0
3 53 49 0	3 37 27 180	** K= 5 L= 18 **	0 90 37 180
4 44 50 180	4 36 31 180	1 96 94 180	2 53 41 0
** K= 9 L= 16 **	** K= 7 L= 17 **	3 57 60 0	** K= 5 L= 19 **
2 37 33 180	-3 47 60 180	-5 44 45 0	5 39 26 0
** K= 0 L= 17 **	-1 38 45 0	-3 62 67 180	** K= 6 L= 19 **
1 110 96 180	3 45 48 0	-1 41 44 0	5 39 26 0
3 156 153 0	** K= 8 L= 17 **	3 56 66 180	** K= 6 L= 19 **
7 98 102 180	-1 34 41 180	** K= 6 L= 18 **	-4 30 28 180
** K= 1 L= 17 **	0 34 30 180	-3 33 29 0	** K= 7 L= 19 **
-4 80 78 0	1 45 39 0	0 64 61 0	1 40 30 180
-2 108 115 180	3 42 34 180	2 46 47 180	** K= 0 L= 20 **
0 137 140 0	5 42 33 0	** K= 7 L= 18 **	4 105 104 0
2 311 310 180	** K= 9 L= 17 **	-2 38 37 0	6 54 62 180
3 70 68 0	-1 25 16 0	2 37 31 0	** K= 1 L= 20 **
4 170 158 0	** K= 0 L= 18 **	** K= 8 L= 18 **	-5 26 20 180
5 118 120 180	-6 28 39 0	-2 38 35 180	-4 70 76 0
7 74 80 0	-4 82 92 180	0 47 51 0	0 55 49 180
** K= 2 L= 17 **	-2 168 177 0	** K= 9 L= 18 **	1 83 82 180
-4 114 107 180	0 191 200 180	0 36 20 180	2 95 101 0
-2 117 129 0	2 82 87 180	1 25 18 180	4 79 83 180
-1 60 63 180	4 109 121 0	2 31 33 0	6 47 55 0
0 209 203 180	** K= 1 L= 18 **	** K= 0 L= 19 **	** K= 2 L= 20 **
1 131 120 0	-6 33 38 180	-5 50 55 180	-5 47 60 180
2 121 109 0	-4 43 38 0	-1 96 111 0	-4 75 76 180
3 211 208 180	-3 104 110 180	1 82 98 180	-3 48 48 0
5 150 159 0	-2 69 59 180	3 123 110 0	0 86 73 0
6 53 64 180	-1 214 196 0	5 51 64 180	2 102 107 180
** K= 3 L= 17 **	0 75 76 180	** K= 1 L= 19 **	4 57 55 0
-4 37 46 0	1 158 140 180	-4 98 106 180	** K= 3 L= 20 **
-3 63 65 180	2 195 192 0	-3 109 111 0	-5 53 64 0
-2 47 55 180	4 143 141 180	-2 60 62 0	-4 29 26 0
-1 63 51 0	5 45 48 0	-1 218 206 180	-3 39 47 180
1 62 70 180	** K= 2 L= 18 **	0 46 53 0	-2 51 58 180
3 78 85 0	-5 56 65 180	3 44 42 180	2 46 49 0
4 65 66 180	-3 96 90 0	** K= 2 L= 19 **	4 45 51 180
5 72 71 180	-2 127 126 180	-5 86 93 0	** K= 4 L= 20 **
6 58 57 0	-1 54 69 180	-3 156 155 180	-3 44 41 0
7 54 41 0	0 221 228 0	-2 98 106 0	-1 53 57 180
** K= 4 L= 17 **	1 60 50 180	-1 185 188 0	3 52 50 0
-2 49 42 0	2 148 140 180	0 107 117 180	** K= 5 L= 20 **
0 61 61 180	3 73 69 0	1 154 161 180	-4 23 19 180
2 60 62 0	4 78 77 0	3 58 67 0	** K= 6 L= 20 **
6 39 38 180	** K= 3 L= 18 **	** K= 3 L= 19 **	3 35 9 0
** K= 5 L= 17 **	-6 26 15 0	-5 48 42 180	** K= 0 L= 21 **
-2 72 73 180	-2 72 61 0	-4 79 80 0	1 110 96 180
0 149 150 0	-1 63 61 180	-2 110 112 180	5 50 62 0
1 48 43 180	1 91 97 0	-1 60 75 180	** K= 1 L= 21 **
2 121 121 180	3 55 59 180	0 74 73 0	
4 44 58 0	4 43 32 180	1 158 171 0	
5 37 45 0	6 70 79 0	3 146 141 180	
** K= 6 L= 17 **	** K= 4 L= 18 **	** K= 4 L= 19 **	
-4 36 42 180	-4 37 44 180		
	-2 75 80 0		
	0 59 68 180		

H	/FD/	/FC/	PHI	H	/FD/	/FC/	PHI	H	/FD/	/FC/	PHI	H	/FD/	/FC/	PHI
-4	47	52	180	** K=	0	L= 24	**								
-3	47	51	0	0	37	38	0								
-2	87	88	0	2	94	100	180								
-1	70	68	180	4	84	88	0								
1	50	37	0	** K=	1	L= 24	**								
2	51	55	180	4	46	45	180								
** K=	2	L= 21	**	** K=	2	L= 24	**								
-3	54	55	180	-1	43	34	0								
-1	54	58	0	0	36	38	0								
5	37	26	0	** K=	3	L= 24	**								
** K=	6	L= 21	**	-1	39	45	180								
3	31	13	0	1	47	44	0								
** K=	0	L= 22	**	** K=	4	L= 24	**								
-2	46	40	0	-1	34	36	0								
2	55	60	180	1	45	53	180								
6	46	51	0	** K=	0	L= 25	**								
** K=	1	L= 22	**	-1	51	50	0								
-1	52	55	0	1	61	56	180								
** K=	2	L= 22	**	** K=	1	L= 25	**								
-4	32	43	180	0	44	42	0								
-3	45	44	0												
4	29	27	180												
** K=	3	L= 22	**												
-2	35	39	180												
0	56	63	0												
2	46	51	180												
3	46	36	180												
** K=	4	L= 22	**												
2	58	56	0												
5	37	30	0												
** K=	5	L= 22	**												
1	30	20	0												
2	28	28	180												
4	29	31	0												
** K=	2	L= 23	**												
-2	31	36	0												
2	47	43	180												
** K=	3	L= 23	**												
-2	42	36	180												
0	42	29	0												
3	37	30	0												
4	30	38	180												
5	29	33	180												
** K=	4	L= 23	**												
-2	35	26	0												
-1	45	38	180												
0	32	31	180												
** K=	5	L= 23	**												
-1	26	30	0												

1.4. Structure Factors for I(d)

H /FO/ /FC/ PHI	H /FO/ /FC/ PHI	H /FO/ /FC/ PHI	H /FO/ /FC/ PHI
** K= 0 L= 0 **	-13 628 625 0	** K= 5 L= 1 **	-2 1961 1754 0
2 212 229 181	-11 622 631 0	-11 656 711 0	0 2661 2392 180
4 2721 2943 180	-9 641 692 180	-9 340 330 181	2 5410 4642 180
8 1494 1521 180	-7 224 255 181	-7 424 439 0	4 1941 1801 0
10 1113 1194 180	-5 576 535 0	1 279 249 181	8 294 324 180
12 530 557 0	-3 709 695 0	21 259 276 181	12 219 244 181
14 1961 1877 0	-1 518 480 0	** K= 6 L= 1 **	20 294 329 360
16 549 501 181	1 708 618 180	10 347 394 0	24 274 227 180
18 238 171 180	3 1392 1332 0	18 315 336 180	26 248 277 180
20 254 259 1	5 480 510 360	20 356 421 180	** K= 3 L= 2 **
24 250 273 180	7 305 309 180	** K= 0 L= 2 **	-23 336 346 180
** K= 1 L= 0 **	9 1079 1092 0	-30 315 312 1	-19 201 235 0
1 1466 1291 0	13 1424 1562 180	-28 311 286 0	-13 556 528 0
3 611 627 0	15 306 313 180	-22 221 191 1	-9 453 408 180
7 1183 1184 180	17 600 558 0	-20 201 231 0	-7 168 152 180
9 1434 1519 0	23 495 498 180	-16 555 536 1	-3 599 548 180
11 621 609 180	** K= 2 L= 1 **	-14 2037 2011 180	-1 1287 1238 0
13 470 430 0	-24 297 275 180	-12 733 791 180	1 1429 1349 180
17 829 865 0	-22 231 250 0	-10 3042 3072 0	3 537 479 0
19 382 416 180	-16 477 472 0	-8 1538 1652 0	7 279 279 180
21 422 363 180	-14 239 214 0	-6 635 671 0	9 611 630 0
23 446 443 0	-12 201 275 181	-4 809 857 0	11 624 626 0
** K= 2 L= 0 **	-10 450 475 180	-2 3273 3577 0	15 731 744 180
0 1483 1317 0	-6 1254 1238 180	0 963 1096 0	19 281 300 180
2 1744 1547 180	-4 695 556 180	2 649 647 180	21 513 500 0
4 1341 1218 180	-2 2649 2416 180	4 2055 2315 180	25 259 231 180
6 432 430 0	0 2756 2574 0	6 1337 1529 360	** K= 4 L= 2 **
8 465 488 180	2 5656 4700 0	8 1265 1303 180	-16 254 267 180
10 955 881 180	4 1191 1095 0	10 1422 1532 0	-12 590 594 180
12 498 475 180	6 554 494 180	12 301 312 181	-10 597 555 0
14 1308 1261 0	10 727 689 180	14 781 828 180	-8 255 145 1
20 259 215 180	16 1062 1092 0	18 581 595 180	-6 435 385 0
28 216 184 180	20 279 297 0	26 250 234 181	2 456 399 180
30 266 216 180	24 286 298 180	** K= 1 L= 2 **	4 2477 2255 0
** K= 3 L= 0 **	** K= 3 L= 1 **	-29 362 370 1	6 252 234 180
1 270 334 0	-19 640 615 180	-23 516 474 1	12 597 591 0
3 273 197 180	-15 205 132 181	-19 544 561 0	14 425 370 180
5 1361 1310 180	-13 613 599 180	-17 761 807 0	22 434 461 0
7 223 213 0	-11 204 196 180	-15 463 441 180	** K= 5 L= 2 **
11 271 241 360	-9 434 455 0	-13 550 533 180	-25 205 249 0
13 355 372 0	-7 332 339 0	-9 335 292 0	-23 215 216 0
17 403 438 180	-5 573 582 180	-7 1114 1219 0	-21 336 357 180
19 286 312 180	-3 243 259 180	-5 357 413 180	-17 227 279 180
25 342 319 180	-1 613 685 180	-3 2125 2216 0	-11 316 284 180
27 301 317 1	3 1522 1419 0	-1 1731 1763 180	-5 464 442 0
** K= 4 L= 0 **	7 486 455 360	1 746 714 180	1 983 987 180
0 450 482 180	9 502 423 0	3 476 415 180	3 450 408 0
6 354 358 360	11 233 251 0	5 460 510 180	5 331 370 0
10 824 851 0	13 463 493 0	7 1077 1100 0	7 306 326 0
12 346 304 180	17 333 336 0	9 486 499 180	9 353 317 1
18 696 701 180	21 330 317 0	11 492 516 180	15 280 264 180
22 481 487 0	29 236 220 0	13 321 315 180	21 629 615 0
** K= 5 L= 0 **	** K= 4 L= 1 **	17 295 257 180	23 349 375 0
3 296 303 180	-28 226 242 180	23 331 326 180	** K= 6 L= 2 **
9 578 580 180	-26 480 455 180	29 247 250 181	-20 248 302 180
25 232 208 0	-19 213 249 180	** K= 2 L= 2 **	-8 286 274 180
** K= 1 L= 1 **	-14 466 446 0	-24 434 492 0	16 305 318 180
-21 243 304 0	-10 331 333 0	-16 1161 1134 0	18 191 151 180
-19 558 543 181	-2 296 258 0	-14 495 500 180	** K= 7 L= 2 **
-17 934 939 0	2 294 285 0	-12 460 496 180	-15 207 181 180
	4 631 564 180	-10 345 404 0	** K= 1 L= 3 **
	6 331 257 180	-8 503 458 180	
	8 422 359 180	-6 469 469 180	
	14 332 326 181	-4 333 323 180	
	16 373 346 0		
	18 209 203 0		
	24 302 358 0		

H	/FO/	/FC/	PHI	H	/FO/	/FC/	PHI	H	/FO/	/FC/	PHI	H	/FO/	/FC/	PHI	
-23	230	235	0	0	1123	1073	0	8	744	724	0	5	1343	1408	180	
-21	666	656	0	2	1468	1239	180	10	402	357	181	7	535	524	180	
-17	232	210	0	4	1402	1267	180	12	190	203	181	9	281	265	360	
-15	1370	1360	0	10	320	329	180					11	213	208	180	
-9	447	510	0	14	402	395	0	** K= 3	L= 4 **			13	616	602	180	
-7	1113	1193	0	20	694	719	0									
-5	623	641	180	** K= 5	L= 3 **			-23	228	220	180	** K= 2	L= 5 **			
-3	2882	3140	0					-17	348	291	180					
-1	1228	1162	0	-13	378	394	0	-15	379	388	0	-26	541	517	0	
1	2209	2165	180	3	246	194	181	-13	336	365	0	-22	285	287	180	
3	840	887	180	7	525	497	1	-7	783	724	0	-20	218	220	1	
5	322	272	0	15	232	233	180	-5	479	530	180	-14	442	491	0	
7	356	321	360	21	402	405	0	-3	373	382	180	-12	700	709	180	
9	960	881	0	** K= 6	L= 3 **			1	1205	1083	0	-10	454	458	180	
11	373	374	0					5	567	553	0	-8	260	280	0	
13	1356	1342	180	-12	413	428	180	7	396	399	180	-4	558	521	180	
15	1232	1248	180	6	724	794	0	9	570	583	180	-2	1543	1512	0	
17	405	424	0	8	336	313	0	** K= 4	L= 4 **			0	548	574	360	
25	289	354	181	18	320	339	180					2	2161	2104	180	
27	345	393	0	** K= 0	L= 4 **			-28	225	268	181	6	843	817	180	
** K= 2	L= 3 **							-22	350	375	180	8	515	546	180	
-26	519	533	0	-32	277	249	1	-18	385	373	1	10	428	405	0	
-24	300	260	0	-28	311	311	1	-16	270	279	180	12	763	697	0	
-22	320	325	180	-24	574	581	180	-14	317	336	180	26	262	270	181	
-20	553	531	0	-22	351	362	180	-12	1039	975	0	28	312	355	0	
-16	438	412	0	-14	1637	1706	180	-6	354	332	1	** K= 3	L= 5 **			
-12	192	223	0	-10	519	532	0	-4	291	254	0					
-10	288	256	180	-6	1090	1187	0	-2	717	647	180	-25	212	164	180	
-8	568	511	180	-4	134	106	358	0	0	558	593	0	-21	456	445	180
-6	1446	1439	0	-2	1821	2263	0	2	2279	2215	0	-17	243	201	0	
-4	506	479	180	0	2549	2854	180	4	845	842	0	-13	424	423	180	
-2	290	275	180	2	303	339	180	6	282	257	180	-11	536	525	180	
0	2374	2194	0	4	652	642	0	8	650	597	180	-7	358	387	180	
2	2622	2487	0	6	1304	1299	180	12	276	273	180	-5	460	453	0	
4	1810	1601	180	8	1123	1227	0	18	559	511	0	-3	398	411	180	
6	279	232	180	10	871	887	180	20	260	277	0	-1	1431	1339	180	
8	903	927	0	12	1011	1031	0	22	250	247	180	3	225	225	180	
12	832	824	180	14	711	684	180	** K= 5	L= 4 **			7	333	297	180	
14	649	596	0	28	465	501	0					25	246	191	1	
18	326	329	181	** K= 1	L= 4 **			-13	438	454	0	** K= 4	L= 5 **			
24	502	483	180					-11	585	587	180					
26	382	359	180	-27	431	409	180	-7	489	519	0	-22	221	258	1	
** K= 3	L= 3 **			-19	417	393	0	-3	422	404	0	-14	278	245	180	
-29	257	285	0	-17	652	669	180	3	516	454	0	-10	731	720	0	
-27	369	338	1	-11	179	155	180	5	353	315	0	-8	720	694	0	
-25	504	461	180	-9	469	503	180	7	282	242	180	-6	214	226	180	
-23	408	403	180	-5	841	962	180	19	568	632	0	-2	669	679	0	
-21	287	271	0	-3	1010	1046	180	** K= 6	L= 4 **			0	1288	1110	180	
-17	293	302	0	-1	545	562	181					2	2019	1836	180	
-15	275	290	0	1	245	279	180	-10	399	446	180	6	320	268	0	
-13	566	525	180	3	2372	2507	0	0	504	491	0	8	520	502	180	
-11	1125	1114	180	5	1567	1680	180	2	464	524	0	10	422	398	0	
-7	1397	1267	0	7	682	680	0	4	432	425	180	** K= 5	L= 5 **			
-5	527	494	180	9	974	990	180	6	478	513	180					
-3	511	541	0	11	1042	1027	180	** K= 1	L= 5 **			-11	274	339	0	
1	559	531	180	13	329	299	181					-9	475	477	0	
3	601	486	0	** K= 2	L= 4 **			-29	283	286	0	-1	375	433	180	
7	617	589	180					-27	466	462	180	1	609	548	0	
9	179	197	360	-24	286	294	0	-23	526	556	0	3	231	211	0	
11	309	285	0	-20	421	375	0	-21	344	360	0	21	245	240	0	
** K= 4	L= 3 **			-16	419	366	180	-19	519	499	0	** K= 6	L= 5 **			
-26	271	282	180	-12	931	913	0	-13	787	823	0					
-18	325	261	0	-8	1087	1020	180	-11	212	235	180	-14	330	317	180	
-12	294	283	0	-6	441	465	0	-7	353	323	180	-8	259	262	0	
-8	235	262	181	-4	400	318	180	-5	686	762	180	2	309	331	0	
-6	542	531	0	-2	1903	1944	180	-3	266	252	180	4	992	1034	0	
-2	365	332	360	0	3116	3018	180	-1	2940	3160	0	6	269	321	0	
				2	920	832	0	1	189	208	0	16	408	401	180	
								3	512	478	180					

H /FO/ /FC/ PHI	H /FO/ /FC/ PHI	H /FO/ /FC/ PHI	H /FO/ /FC/ PHI
** K= 7 L= 5 **	-14 247 217 181	5 317 240 180	-22 301 312 0
-11 213 282 180	-10 536 554 0	25 356 339 1	-20 264 309 180
1 313 328 180	0 525 490 0	** K= 4 L= 7 **	-16 359 329 0
** K= 0 L= 6 **	** K= 5 L= 6 **	-12 787 764 0	-10 225 26 2
-24 1289 1300 180	-13 295 305 180	-10 253 232 0	-8 780 769 180
-18 899 949 180	-7 350 310 0	-8 313 328 180	-6 890 920 180
-14 879 873 0	5 270 229 180	-6 612 574 180	-4 969 947 0
-12 1319 1511 180	9 273 262 180	0 1372 1281 180	-2 405 378 180
-10 1076 1092 180	13 257 255 180	24 183 118 0	0 364 373 180
-8 2006 2092 0	15 239 253 0	** K= 5 L= 7 **	2 469 516 0
-6 241 208 181	17 415 420 0	6 728 689 0	8 359 305 1
-2 991 1121 0	19 205 185 0	24 599 626 180	** K= 3 L= 8 **
0 2349 2581 0	** K= 6 L= 6 **	-25 234 204 0	-27 344 328 0
2 1552 1627 180	-2 324 342 0	-23 271 261 180	-25 545 567 180
4 623 625 180	4 826 881 180	-13 318 276 0	-21 247 231 0
6 2131 2216 0	** K= 1 L= 7 **	1 725 701 0	-17 322 283 0
8 342 414 181	-27 379 381 181	3 349 324 0	-15 297 282 180
10 677 628 0	-23 643 623 0	5 455 462 180	-13 337 339 180
12 955 854 1	-19 214 202 0	7 356 338 180	-11 376 306 0
26 333 354 0	-17 198 157 180	15 420 429 0	-9 354 356 180
30 264 258 181	-15 1089 1077 180	** K= 6 L= 7 **	-5 344 352 0
** K= 1 L= 6 **	-13 272 289 180	-10 281 279 0	-3 323 368 180
-29 485 519 180	-11 1285 1274 0	2 681 732 0	-1 238 227 181
-27 234 239 180	-9 201 171 0	4 456 506 0	1 211 240 180
-25 507 515 0	-5 386 394 0	6 281 310 181	3 274 279 180
-19 660 657 180	-3 1091 1254 180	** K= 0 L= 8 **	25 200 196 180
-15 385 394 180	1 1160 1167 0	-32 296 251 180	** K= 4 L= 8 **
-13 506 537 180	3 626 623 180	-26 590 602 180	-28 208 196 1
-9 704 703 0	5 487 536 0	-18 340 350 1	-24 362 398 180
-7 578 547 180	7 527 461 180	-16 267 293 0	-16 332 304 180
-5 360 395 360	9 1077 1158 0	-12 615 691 180	-14 250 281 0
-3 985 1047 0	11 307 345 0	-10 1015 1007 0	-12 328 330 181
-1 198 165 180	25 724 745 0	-8 499 435 0	-6 254 278 180
1 675 778 180	** K= 2 L= 7 **	-4 1680 1755 0	-2 467 493 180
3 1256 1321 180	-26 191 153 0	-2 952 954 180	22 336 356 1
5 802 799 0	-24 205 215 180	0 1923 2074 0	** K= 5 L= 8 **
7 386 385 181	-22 259 264 180	2 2019 2199 0	-21 205 156 181
9 1803 1841 0	-20 243 306 180	4 894 946 180	-9 263 295 0
11 369 345 1	-16 381 387 180	6 748 726 0	-7 760 782 180
27 389 359 180	-12 271 332 0	8 1202 1165 180	-5 301 317 0
** K= 2 L= 6 **	-10 824 848 180	10 575 585 180	-1 348 312 180
-16 238 227 180	-8 827 808 180	12 521 534 180	11 428 426 180
-14 1197 1182 0	-6 186 155 1	26 542 555 180	15 477 422 0
-10 1571 1543 180	-4 351 412 180	** K= 1 L= 8 **	17 236 260 0
-6 1577 1544 180	-2 386 384 180	-29 266 270 180	21 220 210 1
-4 515 568 0	0 693 718 0	-25 510 488 0	** K= 6 L= 8 **
-2 593 534 180	2 477 499 0	-23 426 422 180	-10 283 356 0
0 820 771 180	4 267 295 180	-13 926 1025 0	2 1151 1169 180
2 829 770 0	6 488 418 0	-11 724 758 0	6 294 305 0
4 652 655 180	8 935 888 0	-9 1156 1212 180	12 231 257 0
8 289 272 0	26 458 428 0	-7 502 506 0	14 359 335 180
** K= 3 L= 6 **	** K= 3 L= 7 **	-5 520 506 0	16 362 426 180
-25 201 156 180	-27 398 416 180	-3 377 397 180	** K= 7 L= 8 **
-17 593 540 0	-25 292 275 0	-1 1238 1370 0	-3 279 294 180
-15 228 236 0	-21 413 459 181	3 456 474 180	** K= 1 L= 9 **
-11 262 258 180	-19 209 202 180	5 1175 1159 0	-27 335 286 180
-7 338 327 180	-17 198 195 180	11 243 277 180	-23 249 305 0
-5 172 176 180	-15 419 397 180	25 671 683 180	-21 275 285 0
-1 587 599 0	-7 1263 1200 180	27 378 375 180	-17 368 404 0
1 796 794 0	-3 303 351 180	29 289 330 0	** K= 2 L= 8 **
3 711 668 180	-1 455 395 180	** K= 2 L= 8 **	-24 362 355 0
5 894 887 180	1 308 343 0	-24 362 355 0	
** K= 4 L= 6 **	3 575 513 180		

H	/FO/	/FC/	PHI	H	/FO/	/FC/	PHI	H	/FO/	/FC/	PHI	H	/FO/	/FC/	PHI
-13	317	304	181	2	1513	1595	180	** K= 1	L= 11	**	-21	310	341	180	
-11	371	390	0	4	197	153	180	-23	376	373	0	-19	352	350	180
-9	921	947	0	6	220	233	180	-11	637	632	0	-17	535	538	0
-7	228	279	180	8	1303	1288	180	-7	1173	1280	0	-15	423	413	180
-5	681	670	0	26	635	630	1	-5	451	440	180	-9	558	574	0
-3	637	614	0	28	290	284	181	1	479	505	180	-7	654	642	180
-1	226	233	0	** K= 1	L= 10	**	3	302	292	1	-5	781	813	180	
3	407	415	0	-23	336	326	0	5	492	437	0	-3	294	296	1
5	545	518	0	-15	250	208	360	23	226	229	0	-1	902	1016	180
7	501	499	0	-9	358	387	180	27	227	224	181	3	928	910	0
** K= 2	L= 9	**	-7	833	772	0	** K= 2	L= 11	**	** K= 2	L= 12	**			
-24	418	388	180	-5	235	269	180	-22	573	544	0	-24	373	349	0
-14	310	230	0	-3	1191	1240	180	-18	362	343	180	-16	341	298	180
-12	299	249	180	-1	502	531	0	-16	322	358	0	-12	338	376	0
-10	943	911	180	1	639	552	180	-12	1002	967	180	-10	186	137	1
-8	150	222	0	3	1069	1122	0	-10	295	244	1	-8	379	371	360
-6	556	528	0	5	147	139	181	-8	1379	1329	0	-6	493	468	180
-4	695	646	0	7	413	451	180	-6	298	305	360	-4	467	519	180
-2	182	235	180	23	748	719	180	-4	478	468	0	24	275	312	0
0	778	759	0	27	240	232	1	-2	415	370	0	** K= 3	L= 12	**	
2	1611	1607	0	** K= 2	L= 10	**	0	582	568	180	-27	229	253	180	
6	811	803	0	-24	568	550	0	2	448	466	0	-23	334	354	0
** K= 3	L= 9	**	-22	369	340	0	22	299	261	0	-11	329	323	0	
-19	399	376	181	-20	357	379	0	** K= 3	L= 11	**	-7	370	370	0	
-17	285	298	180	-16	308	283	180	-9	510	470	180	-3	278	300	0
-15	196	270	1	-14	498	450	0	-7	183	201	0	1	194	149	180
-13	406	376	180	-12	510	482	180	-5	471	444	0	** K= 4	L= 12	**	
-5	246	311	0	-10	302	249	0	-1	331	342	180	-24	257	247	1
-1	363	318	0	-8	230	202	180	1	276	276	180	-6	435	421	0
1	362	347	180	-6	212	221	0	** K= 4	L= 11	**	-2	266	235	0	
** K= 4	L= 9	**	-4	647	632	180	-22	477	473	0	0	285	272	180	
-20	284	312	0	-2	281	297	0	-18	246	218	1	16	326	331	0
-14	254	251	0	0	1066	1044	0	-12	318	339	180	** K= 5	L= 12	**	
-12	385	340	0	22	313	284	181	-2	419	364	180	-17	200	189	180
-10	436	396	180	24	360	381	180	0	331	350	180	-9	293	287	180
-4	421	441	180	** K= 3	L= 10	**	** K= 5	L= 11	**	-1	253	234	1		
-2	236	244	180	-25	510	507	180	-1	282	300	0	5	229	235	180
0	590	578	180	-21	683	670	0	11	322	349	0	** K= 6	L= 12	**	
** K= 5	L= 9	**	-13	264	227	180	13	384	393	0	-2	296	296	0	
-23	320	365	180	-11	498	532	180	19	306	288	0	2	353	343	0
-19	293	299	0	-7	666	649	0	** K= 6	L= 11	**	** K= 1	L= 13	**		
-15	345	399	0	-1	1089	1147	0	0	338	324	0	-3	834	902	180
-1	399	426	0	1	749	723	180	** K= 0	L= 12	**	-1	341	315	360	
13	433	442	0	21	325	303	180	-28	199	242	180	23	365	326	1
** K= 6	L= 9	**	** K= 4	L= 10	**	-28	297	347	0	** K= 2	L= 13	**			
-14	282	333	1	-24	360	406	180	-24	331	326	180	-26	322	271	1
-2	261	283	1	-22	359	305	181	-22	332	363	180	-20	250	277	180
0	327	343	0	-10	667	665	180	-16	615	602	0	-18	238	218	180
14	344	382	181	-6	467	462	0	-14	213	222	180	-14	232	273	1
** K= 0	L= 10	**	-4	308	300	0	-12	201	249	181	-12	292	278	180	
-26	528	502	180	0	277	260	180	-20	834	847	180	-8	210	207	0
-24	604	563	0	** K= 5	L= 10	**	-16	615	602	0	-4	751	715	180	
-18	278	240	0	-7	280	306	0	-14	213	222	180	0	947	915	0
-16	227	242	180	-5	362	334	180	-12	201	249	181	20	338	334	0
-14	753	734	180	3	321	302	180	-10	1048	1033	0	** K= 3	L= 13	**	
-12	1167	1180	180	13	448	481	0	-6	1585	1571	180	-21	272	203	180
-10	1793	1769	0	17	234	220	180	-2	149	137	360	-11	401	397	180
-8	1212	1203	0	** K= 6	L= 10	**	0	824	890	180					
-6	1532	1632	0	10	340	311	0	2	1252	1237	180				
-4	429	470	180	12	253	255	180	4	241	255	180				
-2	935	1013	180	14	317	326	180	** K= 1	L= 12	**					

H /FO/ /FC/ PHI	H /FO/ /FC/ PHI	H /FO/ /FC/ PHI	H /FO/ /FC/ PHI
-5 380 405 180	1 322 322 0	** K= 1 L= 17 **	-20 242 234 0
-3 319 292 0	** K= 2 L= 15 **	-21 396 352 180	10 192 172 180
-1 231 148 180	18 267 275 1	-17 355 338 0	** K= 4 L= 19 **
1 517 513 180	20 297 324 0	** K= 2 L= 17 **	-10 423 431 180
** K= 4 L= 13 **	** K= 3 L= 15 **	18 195 193 0	-2 321 360 0
-24 359 420 0	15 213 188 181	20 224 252 0	** K= 0 L= 20 **
-12 319 351 0	** K= 4 L= 15 **	** K= 3 L= 17 **	14 267 264 181
-2 413 403 180	-12 291 267 0	-19 253 226 0	** K= 1 L= 20 **
14 404 388 0	-8 674 703 180	** K= 4 L= 17 **	-9 440 414 180
18 297 318 181	0 439 435 180	-12 278 291 0	-7 398 392 0
** K= 5 L= 13 **	** K= 5 L= 15 **	-10 295 284 180	-3 303 289 0
-21 224 252 0	-13 246 204 180	-8 402 347 180	-1 465 497 180
-7 254 283 0	-11 294 291 181	-2 310 311 180	1 530 560 180
1 358 342 0	-3 215 188 1	8 239 268 1	** K= 2 L= 20 **
5 217 219 181	-1 333 304 180	12 234 228 180	8 237 211 181
11 287 263 0	1 308 298 180	** K= 5 L= 17 **	12 246 258 0
13 266 265 1	11 271 279 0	-3 229 215 180	** K= 4 L= 20 **
** K= 6 L= 13 **	** K= 6 L= 15 **	5 252 261 1	-10 228 220 180
-10 216 227 1	-4 322 349 0	** K= 6 L= 17 **	-2 344 338 0
-4 243 258 0	** K= 0 L= 16 **	-6 222 270 0	2 621 614 180
-2 338 342 0	-26 211 272 180	-2 295 311 180	** K= 1 L= 21 **
** K= 0 L= 14 **	18 881 845 0	** K= 0 L= 18 **	-9 592 571 180
20 491 473 0	20 722 729 181	-24 215 209 1	1 233 274 180
** K= 1 L= 14 **	** K= 1 L= 16 **	16 315 297 0	** K= 0 L= 22 **
-23 703 665 180	-11 294 311 0	18 266 277 180	6 701 722 180
-19 257 243 0	-7 345 337 180	** K= 1 L= 18 **	14 323 305 180
-11 319 288 181	-5 543 524 0	-9 328 318 180	** K= 1 L= 22 **
-9 316 289 180	-3 692 631 180	-7 359 378 180	14 323 305 180
-7 250 291 0	-1 537 563 0	-1 307 302 0	** K= 1 L= 22 **
-3 768 798 0	1 271 270 0	17 399 396 181	-13 231 170 0
-1 252 300 180	17 333 344 180	** K= 2 L= 18 **	-11 330 352 180
1 507 500 0	** K= 2 L= 16 **	14 615 611 0	-7 255 285 0
** K= 2 L= 14 **	20 386 347 181	18 469 498 181	-3 305 299 180
-26 215 224 0	** K= 3 L= 16 **	** K= 4 L= 18 **	** K= 2 L= 22 **
22 279 261 180	-21 340 322 0	-16 211 236 0	2 362 403 0
** K= 4 L= 14 **	13 412 407 180	-10 217 152 180	4 314 324 0
-16 294 245 180	17 331 322 0	-8 251 308 180	** K= 3 L= 22 **
-14 304 302 0	** K= 4 L= 16 **	-4 351 361 180	1 446 453 0
-2 345 357 180	-2 769 744 180	-2 337 333 0	3 212 155 180
14 260 259 0	12 280 288 180	4 248 328 180	5 296 320 180
** K= 5 L= 14 **	** K= 5 L= 16 **	** K= 5 L= 18 **	** K= 4 L= 22 **
-7 276 306 180	-11 415 422 180	3 303 293 0	4 355 374 180
-5 404 390 0	-1 348 358 180	** K= 1 L= 19 **	** K= 1 L= 23 **
-1 358 347 180	5 336 336 0	-19 242 248 180	1 366 329 180
13 434 413 0	11 216 219 0	-7 321 305 180	7 260 246 1
** K= 6 L= 14 **	** K= 6 L= 16 **	15 391 367 0	** K= 2 L= 23 **
-10 283 316 0	-10 310 348 0	** K= 2 L= 19 **	-10 331 374 0
-8 290 299 0	-2 265 290 180	-24 197 210 180	4 357 358 0
2 301 293 180			
** K= 1 L= 15 **			
-21 377 398 180			
-9 200 179 360			
-1 586 606 180			

H /FO/ /FC/ PHI

H /FO/ /FC/ PHI

H /FO/ /FC/ PHI

H /FO/ /FC/ PHI

** K= 4 L= 23 **

-8 199 212 180

** K= 0 L= 24 **

-12 284 322 1

-10 274 243 180

-8 428 413 180

0 661 642 0

4 468 476 180

6 266 263 180

** K= 1 L= 24 **

-9 252 227 0

3 236 222 181

5 234 242 0

** K= 2 L= 24 **

-10 241 247 180

-6 280 322 0

** K= 2 L= 25 **

-10 193 186 0

2 206 240 0

** K= 3 L= 25 **

-7 272 254 0

** K= 0 L= 26 **

-4 205 218 180

APPENDIX 2

Dielectrics

2.1. Basic Definitions

Any medium subjected to a steady external electric field E may show a finite amount of charge transport by either electrons or ions resulting in a current i , but the magnitude of the resulting direct current (dc) conductivity, $\sigma_0 = i/E_0$, may vary in very wide limits. In cases where σ_0 is very small in comparison to any polarisation displacement currents the medium may be regarded as an insulator, in which dielectric phenomena are important. In the opposite case where σ_0 dominates, the medium is a conductor of electricity. The term dielectric refers to the presence of relaxation in a predominantly insulating medium, which may show a finite amount of dc conductivity.

The application on an external field, E , to a dielectric medium placed between two electrodes induces two component charges. The first Q_0 , which would be present even in the absence of the material medium and which is due to the free space between the electrodes, is given by

$$Q_0 = \epsilon_0 E \quad 2.1(A)$$

where ϵ_0 is the permittivity of free space ($8.854 \times 10^{-12} \text{ F m}^{-1}$).

The second, Q_s , which appears on the surface of the material, arises from the re-arrangement of internal charges of the dielectric medium.

The total charge appearing on the electrodes, D , given by

$$D = Q_0 + Q_s \quad 2.2(A)$$

is termed the "dielectric induction" or the "dielectric displacement". The surface charge per unit area normal to the plane of the electrodes is termed the "dielectric polarisation" (P).

There are several distinct physical mechanisms of polarisation which are characterised by very different response rates:

(1) At the atomic level the application of an external field to a dielectric medium shifts the centres of the electron clouds with respect to the centres of the positive nuclei. This effect produces induced dipoles and "electronic polarisation" is said to occur. This type of polarisation is found in all materials and occurs very rapidly with typical response times of the order of 10^{-15} seconds.

(2) There are many materials which contain permanent dipoles in the absence of an electric field. The permanent dipoles, which arise from the asymmetric charge distribution between the unlike partners of a molecule develop "orientational (or dipole) polarisation" in the presence of the applied field, E.

(3) In ionic materials, the external field displaces the ions with respect to each other and induces a second type of polarisation, "ionic polarisation", which has a response time of the order of 10^{-13} seconds.

In addition to the bound charges, some mobile charges (electrons or ions) are also found in dielectrics. Although "free carrier conduction" is uncommon, electronic carriers may move by hopping between localised sites, in which case their effective mobility becomes low and they then make a distinctive contribution to dielectric dispersion.

For a linear system polarisation, P , is proportional to the applied field E ,

$$P = \epsilon_0 \chi E \quad 2.3(A)$$

or

$$D = \epsilon_0 E + P \quad 2.4(A)$$

where χ is called the "dielectric susceptibility" and is defined by

$$\chi = P/\epsilon_0 E = Q_s/Q_0 \quad 2.5(A)$$

The dielectric induction per unit field is called the "dielectric permittivity", and from equations 2.3(A) and 2.4(A) it can be written

$$D/E = \epsilon = \epsilon_0 (1 + \chi) \quad 2.6(A)$$

here ϵ consists of the free space contribution and that due to the charges in the medium. Re-writing equation 2.6(A)

$$D/\epsilon_0 E = \epsilon/\epsilon_0 = \epsilon_r = 1 + \chi \quad 2.7(A)$$

where ϵ_r is defined as the "relative permittivity" or the "dielectric constant" of the material.

2.2. Time Dependent Dielectric Behaviour

The variation of the dielectric response corresponding to a time varying electric field $E(t)$ can be described in a manner similar to the static field response of equation 2.4(A)

$$D(t) = \epsilon_0 E(t) + P(t) \quad 2.8(A)$$

where $P(t)$ is a time dependent polarisation. The polarisation can be related to a response function $f(t)$ by the equation:

$$P(t) = \epsilon_0 (E\Delta t)f(t) \quad 2.9(A)$$

where E is the applied field strength for a time interval Δt . The term $E\Delta t$ is referred to as a delta function excitation.

The response function has two important properties

$$(i) \quad f(t) = 0 \quad \text{for } t < 0 \quad 2.10(A)$$

i.e. there can be no response before the application of an exciting force.

$$(ii) \quad f(t) = 0 \quad \text{for } t \longrightarrow \infty \quad 2.11(A)$$

i.e. response should vanish as the time tends to infinity because there can be no permanent polarisation as a result of a delta excitation. If it is assumed¹⁰⁶ that (a) the dielectric system is linear, (b) the response to individual excitations can be added to evaluate the total response and (c) the time dependent $E(t)$ is a summation of a series of

delta function excitations each of strength $E(t)dt$ then at any time t

$$P(t) = \epsilon_0 \int_0^{\infty} f(\tau)E(t - \tau)d\tau \quad 2.12(A)$$

In practice the time domain study of dielectrics is based on step function excitation $E(t) = E_0 l(t)$ which has the following properties:

$$E(t) = 0 \quad \text{for } t < 0 \quad 2.13(A)$$

$$E(t) = E_0 \quad \text{for } t > 0 \quad 2.14(A)$$

In which case equation 2.9(A) becomes

$$P(t) = \epsilon_0 E_0 \int_0^t f(\tau)d\tau \quad 2.15(A)$$

giving the dielectric induction as

$$D(t) = \epsilon_0 E_0 \left\{ l(t) + \int_0^t f(\tau) d\tau \right\} \quad 2.16(A)$$

Differentiating w.r.t. time now gives the charging current

$$\begin{aligned} i_c &= dD(t)/dt \\ &= \epsilon_0 E_0 \{ \delta(t) + f(t) \} \end{aligned} \quad 2.17(A)$$

The delta function describing the instantaneous reaction to the step function represents the response of free space which is equivalent to the volume of the dielectric material. The response function $f(t)$ describes the polarisation arising from the material medium which is not instantaneous.

If the dielectric system has any dc conductivity σ_0 , this should also be taken into account while considering the charging current, although it does not contribute to the polarisation. At finite times the dc current has a steady value and therefore the charging current can be written as

$$i_c(t) = \epsilon_0 E_0 \{ \delta(t) + f(t) \} + \sigma_0 E_0 \quad 2.18(A)$$

The polarisation after an infinite charging time under a steady electric field E_0 is given by

$$P(\infty) = \epsilon_0 E_0 \int_0^{\infty} f(t) dt \quad 2.19(A)$$

which means that the integral of the function $f(t)$ must be finite otherwise the steady state polarisation will not be finite. Using equation 2.3(A) which defines the polarisation, equation 2.9(A) can be written in the form

$$P(\infty) = \epsilon_0 \chi(0) E_0 \quad 2.20(A)$$

where $\chi(0)$ relates to the static (zero frequency) susceptibility. If, after achieving the steady state polarisation, the field is removed abruptly, then the depolarisation (discharging) current results from the return of the partially oriented polarising species to their initial equilibrium orientations or positions which they have in the absence of a field. The depolarisation current¹⁰⁷ does not include the direct

current (because there is no driving force) and therefore it offers a more convenient form of measuring $f(t)$ in comparison to the charging current.

2.3. Frequency Dependent Dielectric Behaviour

The dielectric behaviour as a function of frequency is known as the frequency domain response. It is linked to the time domain response through Fourier transformations by the relation

$$\begin{aligned} \mathcal{F}\{\chi(t)\} &= K(\omega) \\ &= (2\pi)^{-\frac{1}{2}} \int_{-\infty}^{+\infty} K(t) \exp(-i\omega t) dt \end{aligned} \quad 2.21(A)$$

where $K(t)$ is a time dependent function and $K(\omega)$ is its frequency dependent transform which provides all the information concerning the amplitude, phase, and frequency of the sinusoidal waves which make up the time dependent signal. It can be shown that the Fourier transform of the convolution integral of equation 2.12(A) gives¹⁰⁷,

$$P(\omega) = \epsilon_0 \chi(\omega) \xi(\omega) \quad 2.22(A)$$

where $P(\omega)$ and $\xi(\omega)$ are the Fourier transforms of the time dependent polarisation and the field respectively. The function $\chi(\omega)$ is called the frequency dependent susceptibility and is a Fourier transform of the response function $f(t)$. This function is defined by

$$\begin{aligned}\chi(\omega) &= \chi'(\omega) - i\chi''(\omega) \\ &= \int_0^{\infty} f(t)\exp(-i\omega t)dt\end{aligned}\quad 2.23(A)$$

$$\text{or } \chi'(\omega) = \int_0^{\infty} f(t) \cos \omega t \, dt \quad 2.24(A)$$

$$\chi''(\omega) = \int_0^{\infty} f(t) \sin \omega t \, dt \quad 2.25(A)$$

The real component $\chi'(\omega)$ is an even function of frequency and gives the amplitude of polarisation in phase with the harmonic driving frequency. On the other hand the imaginary component $\chi''(\omega)$ is an odd function of frequency and is in quadrature with the field. It should be noted that one half ($t < 0$) of the integral limits is being ignored, in describing the real and imaginary parts of the complex susceptibility, because $f(t) = 0$ for $t < 0$ for the step field. For zero frequency equations 2.24(A) and 2.25(A) can be expressed as

$$\chi'(0) = \int_0^{\infty} f(t)dt \quad 2.26(A)$$

which is the static values of susceptibility, and

$$\chi''(0) = 0 \quad 2.27(A)$$

Consequently the real part has a finite value at zero frequency and the imaginary part becomes zero as the frequency vanishes.

The real part of the complex susceptibility contributes to that

component of the frequency dependent displacement current which is in quadrature with the driving field, and therefore does not give rise to power loss. In contrast, the imaginary part $\chi''(\omega)$ appears as the component of the displacement current which is in phase with the driving field, and therefore does contribute to the power loss. Because of this behaviour the imaginary component of the dielectric susceptibility $\chi''(\omega)$ is known as the "dielectric loss". Correspondingly the frequency dependent complex capacitance and hence the complex relative permittivity can be described by

$$\begin{aligned} C(\omega) &= C'(\omega) - iC''(\omega) & 2.28(A) \\ &= C'(\omega) - iG(\omega)/\omega \end{aligned}$$

where $G(\omega)$ is the frequency dependent conductance and

$$\epsilon_r(\omega) = \epsilon_r'(\omega) - i\epsilon_r''(\omega) \quad 2.29(A)$$

If A is the area and d is the thickness of the sample then

$$C(\omega) = \epsilon_0 \epsilon_r(\omega) A/d \quad 2.30(A)$$

Therefore the parameters which describe the complex dielectric behaviour can be described by the relationships:

$$\chi'(\omega) = \{ \epsilon_r'(\omega) - 1 \} \propto C'(\omega) \quad 2.31(A)$$

$$C''(\omega) = G(\omega)/\omega \propto \epsilon_r''(\omega) \propto \chi''(\omega) \quad 2.32(A)$$

2.4. Time Dependence of Relaxation

The application of a time dependent electric field to a dielectric medium disturbs its equilibrium. The time dependent response of the medium is then described by a relationship equivalent to the one given in equation 2.3(A) for a time independent response. The process of recovery of the equilibrium within the system after the removal of the perturbing field is called "relaxation". The first model which was proposed by Debye¹⁰⁸ to describe the relaxation processes deals with non-interacting permanent dipoles embedded in a viscous medium. In the absence of an exciting field, thermal motions randomise the dipole which compose the system. Debye's classical model of relaxation starts from the rate equation for the polarisation^{109,110} of a single dipole floating in a viscous medium, i.e.

$$\frac{dp(t)}{dt} = - \frac{P(t)}{\tau} \quad 2.33(A)$$

where τ is a viscosity dependent relaxation time. The solution of equation 2.33(A) can be described in terms of an exponential decay function $\exp(-t/\tau)$ as

$$\begin{aligned} P(t) &= P_0 \exp(-t/\tau) \\ &= \chi(0)E \exp(-t/\tau) \end{aligned} \quad 2.34(A)$$

which can be transformed to the frequency domain using equation 2.21(A).

thus

$$\begin{aligned}\chi(\omega) &= \chi(0) (1 + i\omega\tau)^{-1} \\ &= \chi'(\omega) - i\chi''(\omega)\end{aligned}\quad 2.35(A)$$

which affords

$$\chi'(\omega) = \chi(0) (1 + \omega^2\tau^2)^{-1} \quad 2.36(A)$$

$$\chi''(\omega) = \chi(0) (1 + \omega^2\tau^2)^{-1} \omega \tau \quad 2.37(A)$$

where $\chi(0)$ is the magnitude of the real part of the susceptibility at zero frequency.

The dielectric loss curve for the Debye system is symmetric in the logarithmic frequency plot about the loss peak frequency ω_p . The half-height width of the loss peak covers 1.144 decades and the loss curve slope is ± 1 on either side of the peak on a log/log scale. The dielectric process is usually activated with an energy ω , in which case the loss peak frequency moves towards high frequencies with temperature such that

$$\omega = 1/\tau = \omega_0 \exp(-\omega/kT) \quad 2.38(A)$$

here ω_0 is a pre-exponential frequency factor. The ratio of the imaginary to the real part of the susceptibility for the Debye model is given by:

$$\chi''(\omega)/\chi'(\omega) = \omega \tau \quad 2.39(A)$$

However, evidence for the Debye response is very rare in solids^{107,111}.

In many materials where polarisation and conduction is caused by hopping charge carriers a peak in the loss cannot be readily observed, due to the onset of dc conduction¹⁰⁷. It was proposed by Jonscher¹¹² that the loss due to conduction by the hopping charges obeys a "universal" power law of the type:

$$\chi''(\omega) \propto \omega^{n-1} \quad 2.40(A)$$

which corresponds to a frequency dependent ac conductivity

$$\sigma(\omega) \propto \omega^{n-1} \text{ with } 0 < n < 1 \quad 2.41(A)$$

over several decades of frequency. Sometimes n approaches unity implying an almost frequency independent loss¹⁰⁷.

It can be proved¹⁰⁷ that the ratio of the imaginary to the real part of the susceptibility for the power law response of equation 2.40(A) does not depend on frequency, i.e.

$$\begin{aligned} \chi''(\omega)/\chi'(\omega) &= \cot n \pi/2 \\ &= \tan (n-1)\pi/2 = \text{constant} \end{aligned} \quad 2.42(A)$$

which means the ratio of the energy lost to the energy stored, per cycle, is independent of frequency, a marked contrast to the Debye mechanism for which it is equal to $\omega\tau$.

Power law behaviour has been observed in dipolar materials as well. The dielectric response of dipolar systems which have non-Debye loss peaks has been described^{107,110,111} by power laws of the form

$$\chi'(\omega) \propto \chi''(\omega) \propto \omega^{-1(n-1)} ; \omega \gg \omega_p \quad 2.43(A)$$

$$\chi''(\omega) \propto \{ \chi(0) - \chi'(\omega) \} \propto \omega^m ; \omega \ll \omega_p \quad 2.44(A)$$

having $0 < m < 1$, $0 < n < 1$. The frequency corresponding to the maximum loss is given by ω_p , see figure 2.1(A).

2.5. Low Frequency Dispersion

The frequency dependence of conductivity in low conductivity materials can be expressed in the form

$$\sigma(\omega) = \sigma_o + \sigma_{ac}(\omega) \quad 2.45(A)$$

where σ_o is the frequency independent d.c conductivity. The ac conductivity, $\sigma_{ac}(\omega)$, which is due to the in-phase response of current can be expressed as the dielectric loss and can usually be described by the relationship¹¹².

$$\sigma_{ac}(\omega) \propto \omega \chi''(\omega) \propto \omega^n \quad 2.46(A)$$

In many materials at low frequencies $\sigma_{ac}(\omega)$ becomes nearly frequency independent yet it cannot be described as a dc conductivity. This slowly varying $\sigma_{ac}(\omega)$ introduces a completely different response which was identified by Jonscher¹¹³ as low frequency dispersion (LFD) or quasi-dc conductivity.

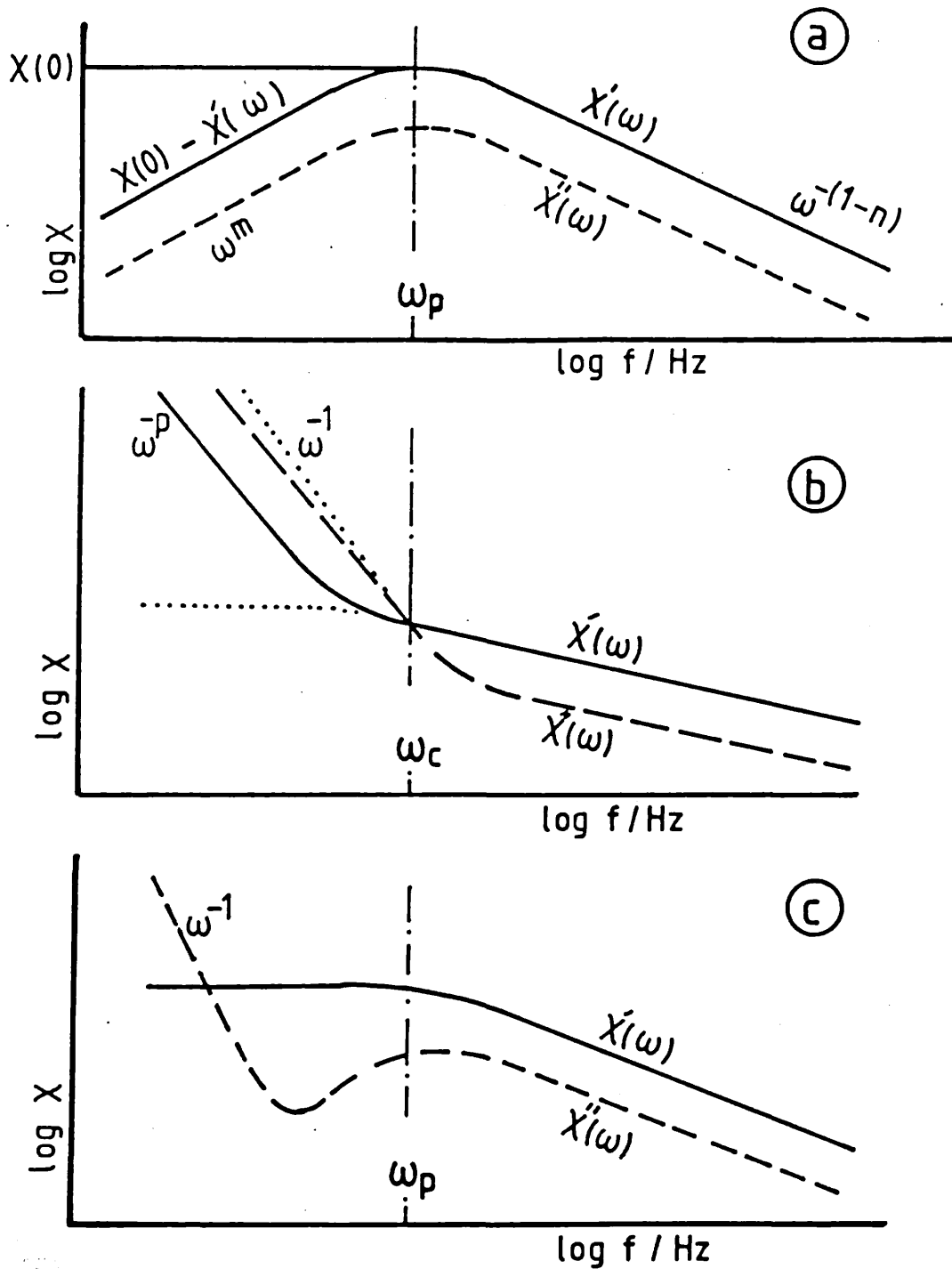


Figure 2.1(A)

Schematic diagrams to show the power law for

- a) non-Debye dipolar response below and above ω_p
- b) carrier dominated response with two power laws below and above ω_c .
For lower frequencies ($\omega < \omega_c$) the full lines represent the LFD and the dotted lines show the dc case
- c) two components of susceptibility in the presence of dc and a loss peak.

It has been observed¹⁰⁷ that the response of dipolar materials for $\omega > \omega_p$ and the response of the charge carrier systems for $\omega > \omega_c$ obeys the same form of power law. However in the case of carrier dominated systems the dielectric response is represented by two power laws and the frequency ω_c defines the transition frequency where one form of power law gives way to the other. This behaviour is shown schematically in figure 2.1(A) and mathematically can be written

$$\chi''(\omega) \propto \omega^{-(1-n)} \quad \text{for } \omega > \omega_c$$

2.47(A)

$$\chi'(\omega) \propto \omega^{-p} \quad \text{for } \omega < \omega_c$$

The value of the exponent $(1-n)$ for the high frequency process has been observed to be less than the exponent p which refers to the low frequency process. In fact both the $(n-1)$ law (for $\omega > \omega_c$) and the $-p$ law (for $\omega < \omega_c$) are special cases of the "universal response, and they characterise two processes which exist together at the same time.

The phenomena of LFD or quasi-dc conduction has been observed in a large variety of materials in which a polarisation process is dominated by hopping charge carriers of either electronic or ionic nature, e.g. at a liquid electrolyte-electrode interface¹¹⁴, in a solid nickel suspension¹¹⁵, for wetted proteins¹¹³, and with stearic acid¹¹⁶.

It is important to realise that LFD or quasi-dc conductivity is completely different from dc conductivity since $\chi'(\omega)$ remains constant under dc conditions and the imaginary part has the frequency dependence of ω^{-1} at low frequencies¹¹³. On the other hand in the case of LFD both the real and the imaginary parts of the dielectric susceptibility behave in a Kramers-Kronig compatible fashion with the same power law exponent and their ratio is constant. It has been observed that this behaviour is general to materials which contain high concentrations¹¹³ of low mobility charge carriers. It has been proposed that movement of charge carriers over "limited" paths can give rise to LFD, in contrast to dc conduction in which case charges move from one electrode to the other¹¹⁴.

2.6. Dielectrics of Semiconductors (DSS)

In addition to the dielectric effects observed in insulating materials it is also possible to study delayed electronic transitions between deep levels in the forbidden gap as well as between deep levels and free bands in semiconductors. The former normally involve "horizontal" thermally assisted transitions in the volume of the sample with relatively small changes in energy, the latter are termed "vertical" transitions with energy changes of the order of half the band gap and take place mainly in interfacial space charge regions and at the interfaces between semiconductors and metals. These various transitions have well recognisable spectral "signatures". Figure 2.2(A) shows schematically the various electronic processes giving rise to dielectric effects in semi-conducting and semi-insulating materials. The conduction

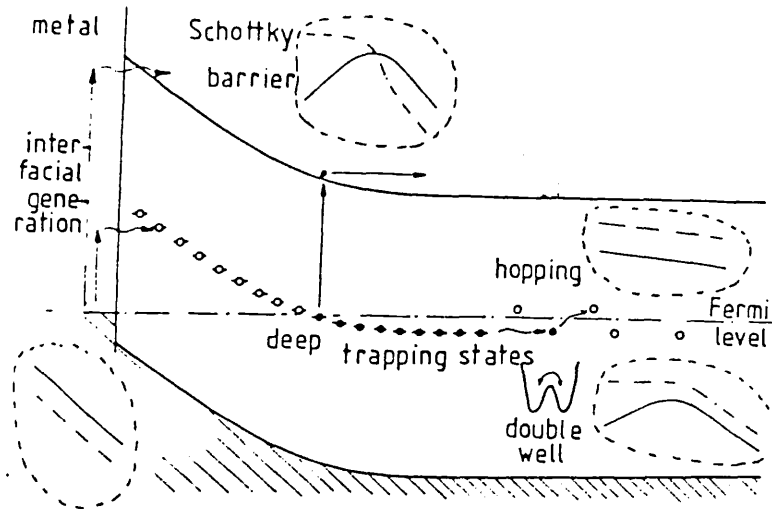


Figure 2.2(A)

and valence bands are shown with a Schottky barrier near the metal contact and a set of deep trapping states is shown in the vicinity of the Fermi level. The vertical arrow shows the release of an electron from a deep trap near the crossing-over position with the Fermi level, the resulting free electron is then driven into the neutral semiconductor. Hopping transitions are indicated between filled and empty states near the Fermi level. A potential double well is shown representing a localised defect around which an electron or an ion may execute hopping transitions of a dipole-like nature. Various interfacial generation processes are indicated. Inserts within dotted contours show the expected characteristic frequency "signatures" of the real (chain-dotted lines) and imaginary (continuous lines) components of the complex susceptibility, plotted logarithmically against the logarithm of frequency.

REFERENCES

1. S.R. Postle, Ilford Ltd., Report, "Bleachable Dyes".
2. O. Johnson, Part II Thesis, Oxford University.
3. Brit. Pat. 1,538,943.
4. J. Griffiths, "Colour and Constitution of Organic Molecules," (Academic Press, 1976).
5. A. Vystr and R. Prokes, Chem. Listy, 1952, 46, 670.
6. D.G. Duff and G.H. Giles in "Water - A Comprehensive Treatise", ed. F. Franks, vol. 4, ch. 3 Plenum, 1975.
7. T.H. James, "The Theory of the Photographic Process", Macmillan, 4th Edn., 1977.
8. D. Sturmer in "The Chemistry of Heterocyclic Compounds", ed. A. Weissburger and E.C. Taylor, vol. 30, Interscience, 1978.
9. D.G. Duff, D.J. Kirkwood and D.M. Stevenson, J. Soc. Dyers. Col., 1977, 93, 303.
10. B.B. Carson, R.W. Scott and C.E. Vose, Org. Synth., Vol.1, 179.
11. J.M. Bobbitt and D.A. Scola, J. Org. Chem., 1959, 25, 560
12. Lund, Ber., 1937, 70, 1520.
13. R.H. Still, A.L. Mansell and P.B. James, Chem. and Ind., 1967, 279
14. C.L. Arcus and R.E. Schauffer, J. Chem. Soc., 1958, 2428.
15. I.C.I. Report D76585C, Ilford Ltd., 1971.
16. I.C.I. Report D76607C, Ilford Ltd., 1971.
17. Ilford Ltd., personal communication.
18. J. Nakayama, Synthesis, 1975, 3, 168.
19. B.P. 1,278,621.
20. B.P. 1,512,863.
21. B.P. 1,521,083.
22. D. Kilcast, C.R.F. No. 3543, Ilford Ltd., 1976.
23. H.W. Starkweather and G.B. Taylor, J. Am. Chem. Soc., 1930, 52, 4708.
24. R.J. Young, "Introduction to Polymer Science", Chapman and Hall, London, 1981.
25. McGawan and Page, Chem and Ind., 1957, 1648.

26. Stolle and Bach, J. Signal AM, 1981, 9, 31.
27. F.J.Hyde, "Semiconductors", Macdonald and Co. (Publishers) Ltd., London, 1965.
28. F.Gutmann and L.E. Lyons, "Organic Semiconductors", John Wiley and Sons Inc., N.York, 1967.
29. H. Meier, "Topics in Current Chemistry", Springer-Verlag, N. York, 1976, 61, 85.
30. J.J. O'Dwyer, "The Theory of Electrical Conduction Breakdown in Solid Dielectrics" Clarendon Press, Oxford, 1973.
31. R.H. Tredgold, "Space Charge Limited Conduction in Solids" Elsevier Publ. Co., London, Amsterdam, N. York, 1967.
32. D.R. Lamb, "Electrical Conduction Mechanisms in Thin Films", Methuen and Co. Ltd., London 1967.
33. J.G. Simmons, J. Appl. Phys., 1963, 34, 1793.
34. R.M. Hill, Phil. Mag., 1971, 23, 59.
35. R.M. Hill, Thin Solid Films, 1971, 8, R21.
36. P. Walley and A.K. Jonscher, Thin Solid Films, 1967, 1, 367.
37. J.H. Perstein, Angew. Chem. Int. Ed. Engl., 1977, 16, 519.
38. J.B. Torrance, Acc. Chem, Res., 1979, 12, 79.
39. K. Bechgaard and D. Jerome, Sci. Am., 1982, 247, 5
40. P. Day, Chem. in Brit., 1983, 19, 306.
41. D. Bloor, Chem. in Brit., 1984, 20, 8.
42. F. Wudl, Acc. Chem. Res., 1984, 17, 227.
43. M. Pope and C.E. Swenberg, "Electronic Processes in Organic Crystals", Clarendon Press, Oxford, 1982.
44. J.J. Andre and A. Bieber, J. Chem. Phys., 1975, 7, 137.
45. L.R. Melby et.al., J. Am. Chem. Soc., 1962, 84, 3374.
46. J. Ferraris, D.O. Cavan, V.V. Walatka Jr., and J.H. Perlstein, J. Am. Chem. Soc., 1973, 95, 948.
47. A.J. Heeger et.al., Solid State Comm ., 1973, 12, 1125.
48. R.C. Wheland and J.L. Gillson, J. Am. Chem. Soc., 1976, 98, 3916
49. J. Bardeen, L.N. Cooper and J.R. Schneffer, Phys. Rev., 1957 108, 1175..
50. F.J. London, J. Phys. Radium, 1937, 8, 397.
51. W.A. Little, Phys. Rev. A., 1964, 134, 1416.
52. R. Liepins, C. Walker, H.A. Fairbank, P. Lawless and C. Moeller, Am. Chem. Soc. Polymer Preprints, 1970, 11, 1048.

53. Z.G. Soos, *Ann. Rev. Phys. Chem.*, 1974, 25, 121.
54. R.P. Shibaeva and L.O. Atomyan, *J. Struct. Chem.*, 1972, 13, 514
55. M. Kano, T. Ishii and Y. Saito, *Acta Crystallogr. B*, 1977, 33, 763.
56. C.J. Fritchie Jr., *Acta. Crystallogr.*, 1966, 20, 892.
57. O.H. Le Blanc, *J. Chem. Phys.*, 1965, 42, 4307.
58. D. Davis, H. Gutfreund and W.A. Little, *Phys. Rev. B.*, 1976, 13, 4766.
59. J.B. Torrance, B.A. Scott and F.B. Kaufman, *Solid State Commun.*, 1975, 17, 1369.
60. M. Heider, P. Lochan, and J. Neel, *Compt. Rend. Acad. Sci. Paris*, 1968, 267C, 797.
61. M. Heider and J. Neel, *J. Chem. Phys.*, 1973, 3, 547.
62. M.C. Etter, R.B. Kress, J. Bernstein and D.J. Cash, *J. Am. Chem. Soc.*, 1984, 106, 6921.
63. D.L. Smith, *Photogr. Sci. Eng.*, 1974, 18, 309.
64. K. Nakatsu, and H. Yoshioka, *Chem. Phys. Lett.*, 1971, 11, 255.
65. R.P. Shibaeva, L.O. Atovmyan, V.I. Panomarjev, O.S. Philipenko and L.P. Rozenberg, *Tet. Lett.*, 1973, 185.
66. R. Allmann, *Chem. Ber.*, 1966, 99, 1332.
67. D.L. Smith and H.R. Luss, *Acta Crystallogr.*, 1972, 28, 2793.
68. D.L. Smith and H.R. Luss, *Acta Crystallogr.*, 1975, 31, 402.
69. D.L. Smith and E.K. Barrett, *Acta Crystallogr.*, 1971, 27, 969
70. B. Dammeier and W. Hoppe, *Acta Crystallogr.*, 1971, 27, 2364.
71. J. Potenza and D. Mastropaolo, *Acta Crystallogr.*, 1974, 30, 2353
72. P.J. Wheatley, *J. Chem. Soc.*, 1959, 3245.
73. P.J. Wheatley, *J. Chem. Soc.*, 1959, 4096.
74. B.H. Klanderma and D.C. Hoesterey, *J. Chem. Phys.*, 1969, 51, 377.
75. G.E. Maciel, *Science*, 1984, 226, 282.
76. G.E. Maciel, "Magnetic Resonance: Introduction to Advanced Topics and Applications to Fossil Energy", NATO ASI Series, Reidel, Boston, 1984.
77. R.K. Harris, "Nuclear Magnetic Resonance", Pittman, London, 1983.

78. B.P. 1,177,037
79. A.J. Bard and L.R. Faulkner, "Electrochemical Methods: Fundamentals and Applications", J. Wiley and Sons, N. York, 1980.
80. D.D. MacDonald, "Transient Techniques in Electrochemistry", Plenum Press, N. York, 1977.
81. Z. Galus, "Fundamentals of Electrochemical Analysis", J. Wiley and Sons, N. York, 1976.
82. (a) R.M. Hill, Nature, 1978, 275, 96.
(b) H.A. Pohl, "The Behaviour of Matter in Non-Uniform Electric Fields: Dielectrophoresis", Cambridge University Press, London, 1978.
83. E.P. application No. 86810569.3
84. U.S.P. 2,734,900.
85. U.S.P. 2,756,227.
86. U.S.P. 2,887,479.
87. U.S.P. 2,882,158.
88. U.S.P. 3,253,925.
89. (a) B.P. application No. 29352.
(b) B.P. application No. 30455.
90. G. Wittig, H. Eggers and P. Duffner, Ann., 1958, 619, 10.
91. L. Horner, P. Beck and H. Hoffmann, Chem. Ber., 1959, 92, 2088.
92. J. Nakayama, J. Chem. Soc. Chem. Comm., 1974, 5, 166.
93. J. Nakayama, Synthesis, 1975, 1, 38.
94. H.J.S. Britton and G. Welford, J. Chem. Soc., 1937, 1848.
95. D.J. Watkins, J.R. Carruthers and P.W. Betteridge, "Crystals User Guide" Chem. Cryst. Lab., University of Oxford, 1985.
96. P. Main et.al., "MULTAN80; A System of Computer Programs for the Automatic Solution of Crystal Structures from X-ray Diffraction Data", Dept. of Physics, University of York, 1980.
97. Scattering Factors; International Tables for X-ray Crystallography, Vol. IV, 202 Kynoch Press, Birmingham, 1974.
98. J.R. Carruthers and D.W. Watkins, "Chebyshev Weighting Scheme, Acta Cryst., 1979, A35, 698.

99. C.T. Morse, J. Phys. E7, 1974, 657.
100. J. Pugh and J.T. Ryan, I.E.E. Conference Reports on Dielectric Measurements and Applications, Aston, 1979, 1104.
101. J. Pugh, Phys. Bulletin, 1979, 29, 469.
102. G.H. Stout and L.H. Jensen "X-Ray Structure Determination: A Practical Guide", Macmillan, 1968.
103. CAD4-F Diffractometer User Handbook, Enraf-Nonius, 1977.
104. B.P. Hitchcock and R. Mason, Chem. in Brit., 1971,7, 511.
105. D. Sayre, Acta. Cryst., 1952, 5, 60.
106. A.K. Jonscher, Physics of Thin Films, 1980, 11, 205.
107. A.K. Jonscher, "Dielectric Relaxation in Solids", Chelsea Dielectrics Press, London, 1983.
108. P. Debye, "Polar Molecules", Dover Publications, N. York, 1945.
109. R.M. Hill, Thin Solid Films 1983, 100, 319.
110. R.M. Hill and A.K. Jonscher, Contempt. Phys., 1983, 24, 75.
111. A.K. Jonscher, Colloidal and Polymer Sci., 1975, 253, 231.
112. A.K. Jonscher, J. Phys. C, 1973, 6, L235.
113. A.K. Jonscher, Phil. Mag. B, 38, 1978, 6, 587.
114. A.K. Jonscher, CEIDP Conference, U.S.A., 1983.
115. T. Ramdeen, L.A. Dissado and R.M. Hill, J. Chem Soc., Farad Trans 1, 1984, 80, 325.
116. A.K. Jonscher, F. Meca, and H.M. Millany, J. Phys. C, 1979, 12, L293.